Investigation of molecular mechanisms of cell death in human oligodendrocytes under metabolic stress

Milton Guilherme Forestieri Fernandes

Integrated Program in Neuroscience
Department of Neurology and Neurosurgery
Montreal Neurological Institute
McGill University
Montreal, Quebec, Canada

September 2023

A thesis submitted to McGill University
in partial fulfillment of the requirements for
the degree of Doctor of Philosophy

Table of contents

Abstract

Oligodendrocyte (OL) injury and loss is a feature of multiple sclerosis (MS) lesions and other CNS disorders across the age spectrum. MS is known as an immune-mediated disease and all current treatments target the immune system. These treatments are effective in attenuating relapses associated with this disease but have not shown a significant effect on its progressive course. The probable reason for this ineffectiveness is that multiple factors, not only immune-mediated insults, may cause OL degeneration. Metabolic stress is among these potential insults. This stress can be caused by cerebral blood hypoperfusion, which has been consistently identified in imaging studies as an early feature of MS. Metabolic stress also consistently causes significant cell death in human (h)OLs cultured *in vitro*.

Metabolic stress can inflict sub-lethal injuries to hOLs, characterized mainly by process retraction, or cell death. In response to stress, cells can activate survival mechanisms, but in some cases, regulated cell death (RCD) pathways are triggered. Many RCD pathways are currently recognized and may be involved in OL death in demyelinating disorders.

The main aim of this study was to understand how metabolic stress causes hOL death *in vitro*. The role of autophagy, a process closely associated with cell death and survival, in response to metabolic stress was also analysed. Finally, an *in situ* investigation of signs of metabolic stress based on features observed *in vitro* was conducted.

We identified age-related differences in the injury response of hOLs to metabolic stress. Adult hOLs are more resistant to death than pediatric hOLs. Adult hOLs are also less prone to trigger apoptosis. This resistance is supported by a simultaneous upregulation of anti-apoptotic molecules and downregulation of pro-apoptotic molecules of the BCL-2 family in adult hOLs.

The inhibition of autophagy in hOLs under metabolic stress accelerated cell death, indicating that this process plays a pro-survival role. Sustained metabolic stress (4 days of glucose deprivation *in vitro*) led to a failure in autophagic flux, characterized by the accumulation of autophagosomes that were unable to fuse with lysosomes. The impairment of autophagy was linked to a reduction in processes extension and release of myelin fragments. *In situ* studies indicated signs of autophagy failure in MS lesions and normal appearing white matter in MS patients.

Besides apoptosis, the RCD pathways ferroptosis and mitochondrial permeability transition (MPT)-driven necrosis, which are potentially activated by metabolic stress, were also investigated. Although an increase in the production of reactive oxygen species in hOLs under metabolic stress was detected, which could lead to lipid peroxidation and cell death by ferroptosis, treatment with the ferroptosis inhibitor ferrostatin-1 was unable to reduce hOL loss in response to metabolic stress. Similarly, treatment with the MPT-driven necrosis inhibitor cyclosporin A did not affect the level of hOL death caused by metabolic stress. These results indicate that hOL death induced by metabolic stress is not an RCD.

Prolonged metabolic stress resulted in a strong reduction of intracellular adenosine triphosphate (ATP) levels and cleavage of spectrin, a target of Ca^{2+}-dependent proteases. When hOLs under metabolic stress were treated with the Ca^{2+} chelator ethylene glycol-bis(β-aminoethyl ether)-N,N,N',N'-tetraacetic acid (EGTA), cleavage of spectrin was reduced. These results indicate that Ca^{2+} plays an important role in the injury and demise of hOLs under metabolic stress.

In conclusion, our findings indicate that hOL death in response to metabolic stress is a long process and is not associated with any known regulated cell death. The demise of cells occurs due to a decrease in ATP availability, which potentially causes autophagy failure and an increase in intracellular Ca^{2+} concentration, resulting in degeneration of cellular structural integrity. These findings contribute to the understanding of disease-associated hOL injury and provide guidance for developing neuroprotective therapies.

Résumé

Des dommages sous-létaux et létaux aux oligodendrocytes (OLs) sont des caractéristiques de la sclérose en plaques (SP) et d'autres troubles du SNC. La SP est connue comme étant une maladie immuno-médiée et tous les traitements actuels ciblent le système immunitaire. Ces traitements atténuent les rechutes associées à la SP, mais ne sont pas si efficaces contre son aspect progressif. Plusieurs facteurs, autres que des agressions immuno-médiées, peuvent causer la dégénérescence des Ols. Le stress métabolique (SM) causé par une hypoperfusion sanguine cérébrale, régulièrement identifiée dans des études d'imagerie comme une caractéristique précoce de la SP, en est un exemple.

Le SM peut infliger des lésions sous-létales aux OLHs, caractérisées par la rétraction des processus, ou la mort cellulaire. En réponse au stress, les cellules peuvent activer soit des mécanismes de survie, soit des voies de mort cellulaire régulée (MCR). De nombreuses voies de MCR sont actuellement reconnues et pourraient être impliquées dans la mort des Ols dans les troubles de la démyélinisation tels que la SP.

L'objectif principal de cette étude était de comprendre les mécanismes derrière la mort des OLHs provoquée par le SM *in vitro*. Le rôle de l'autophagie, qui est associé tant qu'à la mort qu'à la survie cellulaire en réponse au SM, a également été étudié. Enfin, une enquête *in situ* sur les signes de SM a été réalisée en se basant sur les caractéristiques observées *in vitro*.

Nous avons identifié des différences liées à l'âge dans la réponse des OLHs au SM. Les OLHs adultes sont plus résistants à la mort cellulaire induite par le SM que les OLHs pédiatriques. Les OLHs adultes sont également moins enclins à déclencher l'apoptose. Cette résistance est soutenue par une plus grande expression des molécules anti-apoptotiques et une expression plus faible des molécules pro-apoptotiques de la famille BCL-2 chez les OLHs adultes comparés aux OLHs pédiatriques.

L'inhibition de l'autophagie chez les OLHs sous un SM a accéléré la mort cellulaire, indiquant que ce processus soutient la survie des OLHs. Un SM soutenu a conduit à un échec du flux autophagique, caractérisé par l'accumulation d'autophagosomes non fusionnés avec les lysosomes. Une rétraction des processus et une perte de fragments de myéline ont été observées. *In situ*, des signes de défaillance de l'autophagie ont été observés dans des lésions de la SP et dans la matière blanche d'apparence normale chez les patients atteints de SP.

Outre l'apoptose, la ferroptose et la nécrose induite par la transition de perméabilité mitochondriale (NTPM) sont également des voies de MCR. Une augmentation de la production d'espèces réactives de l'oxygène a été détectée chez les OLHs sous un SM, ce qui pourrait conduire à la peroxydation lipidique et à la mort cellulaire par la ferroptose. Cependant, un traitement avec la ferrostatine-1 (inhibiteur de la ferroptosis) n'a pas réduit la perte de OLHs en réponse au SM. Le traitement avec la cyclosporine A, un inhibiteur de la NTPM, n'a eu aucun effet sur la perte des OLHs non plus. Ces résultats indiquent que la mort des OLHs induite par le SM n'est pas une MCR.

Un SM prolongé a entraîné une forte réduction des niveaux d'adénosine triphosphate (ATP) intracellulaire et le clivage de la spectrine, une cible des protéases dépendantes du Ca^{2+}. Lorsque les OLHs sous un SM ont été traités avec l'ethylene glycol-bis(β-aminoethyl ether)-N,N,N',N'-tetraacetic acid (EGTA) (chélateur de Ca^{2+}), le clivage de la spectrine a été réduit. Ces résultats indiquent que le Ca^{2+} joue un rôle important dans la mort des OLHs sous un SM.

En conclusion, la mort des OLHs en réponse au SM est un processus long et n'est associée à aucune MCR connue. La mort des OLHs survient d'une diminution des niveaux d'ATP, la défaillance de l'autophagie et une augmentation de la concentration intracellulaire de Ca^{2+}, entraînant la dégénérescence cellulaire. Ces résultats contribuent à la compréhension des lésions des OLHs associées à la SP et orientent le développement de thérapies neuroprotectrices.

Acknowledgments

It was a great honor to be directed by two of the most prestigious scientists in Canada and the world, Jack Antel and Tim Kennedy. I could not have made a better choice of mentors. They were able to harness my strongest abilities in the best way possible and keep me highly motivated in these last four years.

I am equally honored to have the opportunity to work with the extremely competent professionals Manon Blain and Qiao-Ling, without whom I would not be able to accomplish my research. Also of inestimable value was the help of my talented colleagues Julia Luo, Florian Pernin, Caroline Hodgins, Marie-France Dorion, Tiger Xu and Daryan Chitsaz. I am sure they will be great professionals in whichever pathway they choose for their lives.

I would like to acknowledge my appreciation for the valuable advice received from Maziar Divangahi and Eric Shoubridge during the Advisory Committee Meetings. I am equally thankful for the support of the bioinformaticians Abdulshakour Mohammadnia, Moein Yaqubi and Kelly Perlman for lending their magic skills and collaborating with my work.

I would also like to show my appreciation for the advice I received from Luke Healy and Jo Anne Stratton, it was a true privilege to work alongside scientists of such high expertise.

Finally, I would like to express my gratitude for the valuable collaboration of Jeffery Hall, Roy Dudley, Myriam Srour, Charles Couturier, Kevin Petrecca, Catherine Larochelle, Stephanie Zandee, Laura Schmitz-Gielsdorf, Wendy Klement, Alexandre Prat, Moses Rodriguez, Tanja Kuhlmann, Wayne Moore and for the help of Heidi McBride and Mai Nguyen with the luminescence assays.

Contribution to original knowledge

The following findings presented in this thesis constitute contribution to original knowledge:

1. Injury response of human oligodendrocytes to metabolic stress varies according to age, as resistance to cell death is increased in adults.
2. The expression of BCL-2 family genes in human oligodendrocytes, important components of the intrinsic apoptotic pathway, varies according to age and differential stage of oligodendrocyte-lineage cells toward a profile that supports resistance to apoptosis.
3. Some BH3-only molecules, responsible for stress detection by the cell, are activated under metabolic stress.
4. Inhibition of anti-apoptotic molecules of the BCL-2 family increases hOL susceptibility to apoptosis.
5. Inhibition of autophagy causes an increase in human oligodendrocyte death, indicating that this process supports the survival of these cells.
6. Expression of lysosome-related genes is lower in fetal oligodendrocyte-lineage cells, indicating that the autophagy capacity of oligodendrocytes increases with age and cell differentiation.
7. Metabolic stress causes rapid reduction of ATP levels in human oligodendrocytes.
8. Prolonged metabolic stress leads to autophagy failure.
9. Modulation of autophagy does not affect ATP levels in human oligodendrocytes.
10. Increased expression of autophagy failure markers is present in MS lesions and normal appearing white matter of MS patients.

11. Inhibition of autophagy causes processes reduction and loss of myelin fragments in human oligodendrocytes.
12. Metabolic stress causes reduction of nuclear size of human oligodendrocytes in MS lesions, indicating that cells are undergoing necrosis or apoptosis.
13. Metabolic stress increases the levels of reactive oxygen species in human oligodendrocytes.
14. The intrinsic oxidative stress generated by metabolic stress causes limited injury to human oligodendrocytes.
15. Metabolic stress does not induce ferroptosis or mitochondrial permeability transition-driven necrosis, regulated cell death pathways that can be potentially activated in response to this stress.
16. Expression of voltage-dependent anion channel 1 and 2 genes are downregulated in human oligodendrocytes. The low expression of these channels, which are responsible for the transfer of energetic substrates between the cytosol and the mitochondria, is a potential cause of the low level of mitochondrial respiration and reactive oxygen species generation in human oligodendrocytes.
17. Metabolic stress causes spectrin cleavage, a major component of the cytoskeleton and a target of Ca^{2+}-dependent proteases, indicating an increase in cytosolic Ca^{2+}. This increase is a hallmark of cell death in human oligodendrocytes in response to metabolic stress.

Contribution of Authors

Chapters 1 and 2, the bridge between chapters 3 and 4, and the discussion were written by Milton Guilherme Forestieri Fernandes.

Chapter 3:

Milton Guilherme Forestieri Fernandes designed and performed studies related to BCL-2 and autophagy regulation of cell injury.

Julia Luo designed and analyzed the single-cell sequencing studies.

Qiao-Ling Cui contributed to the design and performance of in vitro functional studies; responsible for cell isolation and culture.

Kelly Perlman participated in the design and analysis of the single-cell sequencing studies.

Florian Pernin contributed to the design and performance of in vitro functional studies.

Moein Yaqubi participated in the design and analysis of the single-cell sequencing studies.

Jeffery Hall designed the protocol to provide adult surgical specimens.

Roy Dudley designed the protocol to provide pediatric surgical specimens.

Myriam Srour participated in the design of pediatric studies and the writing of the manuscript.

Charles Couturier participated in the design and analysis of the single-cell sequencing studies.

Kevin Petrecca designed the protocol to provide adult surgical specimens and participated in the design and analysis of the single-cell sequencing studies.

Catherine Larochelle participated in the characterization of oligodendrocyte populations.

Luke Healy participated in the design and analysis of the single-cell sequencing studies and the preparation of the manuscript.

Jo Anne Stratton participated in the design and analysis of the single-cell sequencing studies and preparation of the manuscript.

Timothy E. Kennedy contributed to the design of the overall study and preparation of the manuscript.

Jack P. Antel coordinated the design of the study and the preparation of the manuscript.

Chapter 4:

Milton Guilherme Forestieri Fernandes designed the study and performed the functional and biochemical assays.

Abdulshakour Mohammadnia and Moein Yaqubi designed and performed the bioinformatics analysis.

Florian Pernin and Laura Eleonora Schimitz-Gielsdorf performed the immunohistochemical analysis.

Caroline Hodgins performed ATP functional assays.

Qiao-Ling Cui performed cell isolation and culture.

Manon Blain performed some of the biochemical assays.

Jeffery Hall designed the protocol to provide adult surgical specimens.

Roy Dudley designed the protocol to provide pediatric surgical specimens.

Myrian Srour participated in the design of pediatric studies.

Stephanie E. J. Zandee, Wendy Klement and Alexandre Prat provided tissue samples for immunohistochemical analysis.

Jo Anne Stratton and Tanja Kuhlmann contributed to the design of the overall study and preparation of the manuscript.

Moses Rodrigues, Tanja Kuhlmann and Wayne Moore contributed to the pathological analysis.

Timothy E. Kennedy contributed to the design of the overall study and preparation of the manuscript.

Jack P. Antel coordinated the design of the study and the preparation of the manuscript.

List of Figures and Tables

Supplementary Figure 4.2 - Loss of hOL is intensified in the center of MS lesions.

List of Abbreviations

4E-BP1 – 4E-binding protein 1

ACC1 – Acetyl-CoA carboxylase 1

ACD – Accidental cell death

AD – Alzheimer's disease

ADCD – Autophagy-dependent cell death

AIF – apoptosis-inducing factor

AIM – Absent in melanoma

AMPK – AMP-activated protein kinase

ANXA1 – Annexin A1

APAF1 – Apoptotic protease activating factor 1

APC – Antigen-presenting cells

ARE – antioxidant response elements

AST – Astrocyte

ATF – Activating factor

ATM – Ataxia telangiectasia mutated

ATP – Adenosine triphosphate

ATR – ATM-Rad3-related

BAK - BCL2 antagonist/killer

BAX - BCL2-associated X protein

BBB – Blood-brain barrier

BCAS – Bilateral carotid artery stenosis

BCL-2 – B-cell lymphoma 2

BDNF – Brain-derived neurotrophic factor

BID – BH3 interacting domain death agonist

BID – BH3 interacting-domain

BIM - BCL-2 interacting mediation

BOK - BCL-2 related ovarian killer

BSO – Buthionine Sulfoximine

CARD – Caspase recruitment domain

CASP – Caspase

CASPR – Contactin-associated protein at the side of the neuron

CCA – Canonical correlation analysis

Cdk5 – Cyclin-dependent kinase 5

Chk – Checkpoint kinase

CHOP - C/EBP homologous protein

CMA – Chaperone-mediated autophagy

CNP - 2', 3'-Cyclic nucleotide-3'-phosphohydrolase

CNS – Central nervous system

CQ – Chloroquine

CRCHUM – Centre Hospitalier de l'Université de Montréal

CXCL10 – CXC-chemokine ligand 10

CYLD – cylindromatosis

DAMP – Damage-associated molecular pattern

DDR – DNA damage repair

DE – Differential expression

DIABLO - direct inhibitor of apoptosis-binding protein with low pI

DIF-1 – Differentiation-inducing factor

DISC – death-induced signaling complex

DIV – Days in vitro

DSB – Double-strand breaks

DSC-MRI – Dynamic susceptibility contrast-enhanced perfusion magnetic resonance imaging

EAE – Experimental autoimmune encephalomyelitis

EBV – Epstein-Barr virus

EGTA – ethylene glycol-bis(β-aminoethyl ether)-N,N,N',N'-tetraacetic acid

eIF2α – Eukaryotic initiation factor 2 α

ER – Endoplasmic reticulum

ERK – extracellular signal-regulated kinase

ESCRT – Endosomal sorting complex required for transport

ET-1 - Endothelin-1

ETC – Electron transport chain

Fe^{2+} - Ferrous iron

FIH1 – Factor-inhibiting HIF-1α

FOXO – Forkhead box O

FWER – Familywise error rate

GA – Glatiramer acetate

GABARAP - γ-aminobutyric acid receptor-associated protein

GADD34 – Growth arrest and DNA-damage-inducible protein

GalC – Galactosylceramide

GCN2 – General control non-depressible protein 2

GEO – Gene expression omnibus

GLUT1 – Glucose transporter 1

GPX4 – Glutathione peroxidase 4

GR – Glutathione reductase

GSDMD – Gasdermin D

GSEA – Gene set enrichment analysis

GSH – Glutathione

GSSG – Glutathione disulfide

H_2O_2 – Hydrogen peroxide

HIF – Hypoxia inducible factor 1

HLA – human leukocyte antigen

HMGB1 – High-mobility group box 1

HMOX1 – Heme oxygenase 1

HNE – Hydroxynononal

hOL – Human oligodendrocyte

HR – Homologous recombination

HRI – Heme-regulated eIF2α

HSF1 – Heat shock factor 1

HSP – Heat shock proteins

HXK – Hexokinase

IAP – inhibitors of apoptosis

ICD – Immunogenic cell death

IFN – Interferon

IL-10 – Interleukin 10

iPSC – Induced pluripotent stem cells

IRE1α – Inositol requiring enzyme-1α

ISR – Integrated stress response

LAMP2A – lysosome-associated membrane protein 2A

LC3 – Microtubule-associated protein light chain 3

LDCD – Lysosome-dependent cell death

LDH – Lactate dehydrogenase

LDHA – Lactate dehydrogenase A

LG – low glucose

LMP – Lysosome membrane permeabilization

MAG – Myelin-associated glycoprotein

MAMP – Microorganism-associated molecular patterns

MCR – Mort cellulaire régulée

MCT1 – monocarboxylate transporter 1

MDA – Malondialdehyde

MHC – major histocompatibility complex

MHC II – Major histocompatibility complex class II

MLKL - mixed lineage kinase domain like pseudokinase

MNI - Montreal Neurological Institute

MOG – Myelin oligodendrocyte glycoprotein

MOM – Mitochondria outer membrane

MPB – Myelin basic protein

MPTP - Mitochondrial permeability transition pores

mPTP – mitochondrial permeability transition pores

MRN - Mre11-Rad50-Nbs1

MS – Multiple sclerosis

mTOR – mammalian target of rapamycin

NAA – N-acetyl aspartate

NAWM – Normal-apparent white matter

NCKX - Na^+/Ca^{2+}-exchanger

NCV – neurovascular coupling

NCX - Na^+/Ca^{2+}-exchanger

NET – Neutrophil extracellular trap

NF155 – Neuropascin 155

NF-κB - Nuclear factor kappa-light-chain-enhancer of activated B cells

NG – no glucose

NHEJ – Nonhomologous end joining

NLRP - NACHT, LRR, FIIND, CARD domain, and PYD domains-containing proteins

NMDA - N-methyl-D-aspartate

NO – nitric oxide

NP – Neural precursors

NPC – Neural progenitor cells

NRF2 – Nuclear factor-like

NTPM – Nécrose induite par la transition de perméabilité mitochondriale

NVU – neurovascular unit

OH^- - Hydroxyl radical

OL – Oligodendrocyte

OPC – Oligodendrocyte progenitor cells

OXPHOS – oxidative phosphorylation

PAD4 – Peptidyl-arginine deaminase 4

PAMP – pathogen-associated molecular pattern

PAR – poly (ADP-ribose)

PARP – Poly (ADP-ribose) polymerase (PARP)

PARP – poly (ADP-ribose) polymerase 1

PBR – Peripheral benzodiazepine receptor

PCA – principal component analysis

PCD – Programmed cell death

PDGFR – Platelet derived growth factor-receptor α

PDH – Pyruvate dehydrogenase

PDIA3 – Protein disulfide isomerase family A member 3

PDK1 – Pyruvate dehydrogenase kinase 1

PE – pericytes

PERK – Protein kinase R (PKR)-like endoplasmic reticulum kinase

PHC/SLC25A3 - F_1F_0-ATPase, inorganic phosphate carrier

PHD – Prolyl hydroxylase domain-containing

PI – propidium iodide

PI3P – Phosphatidylinositol-3-phosphate

PKC – Protein kinase C

PKR – Double-stranded RNA-dependent protein kinase

PKR – Protein kinare R

PLP – Proteolipic protein

PMCA – Plasma membrane calcium ATPase transporter

PMD – Pelizaeous-Merzbacher disease

PP1 – Protein phosphatase 1

PPARγ - Proliferator-activated receptor γ

PPIF – Peptidylprolyl isomerase F

PPMS – Primary progressive MS

PPP – Pentose phosphate pathway

PRK2 – Phosphorylating phosphofructokinase-2

PRKCE – Protein kinase Cε

PRR – Pattern recognition receptors

PUFA – Polyunsaturated fatty acid

pVHL – Hippel-Linday protein

RA – Retinoic acid

RCD – Regulated cell death

RIPK1 – receptor-interacting serine/threonine-protein kinase 1

RNS - Reactive nitrogen species

RNS – reactive nitrogen species

ROCK I/II – Rho-kinase I and II

ROS – reactive oxygen species

RRMS – Relapsing-remitting MS

S6K - S6 kinase

SCG10 – superior cervical ganglia protein 10

scRNAseq

SIRT1 – Sirtuin 1

SM – Stress métabolique

SMAC - second mitochondrion-derived activator of caspase

SOD – Enzyme superoxide dismutase

SOD – Superoxide dismutase

SP – Sclérose en plaques

SPMS – Secondary progressive MS

SQSTM1 – Sequestrosome-1

SREBP1c – Sterol regulatory element-binding protein 1 c

SSA – Single-stranded annealing

SSB – Single strand breaks

STAT3 – Signal transducer and activator of transcription 3

TCA – tricarboxylic acid cycle

TFEB – Transcription factor EB

TLR – Toll-like receptor

TMEV – Theiler's murine encephalomyelitis virus

TRADD – TNFR-associated death domain

TRAIL – TNF-related apoptosis-inducing ligand

TSPO – 18kDa translocator protein

TUNEL - terminal deoxynucleotidyl transferase dUTP nick end labeling

ULK1 - Unc-51-like autophagy-activating kinase 1

UMAP – uniform manifold approximation and projection

UPR – Unfolded protein response

VDAC - voltage-dependent anion channel

VEGF – Vascular endothelial growth factor

VSMC – vascular smooth muscle cells

WIPI2 – Phosphoinositide-interacting protein 2

XBP1 - Factor X-box-binding protein 1

CHAPTER 1 – Introduction

1.1 Rationale

Oligodendrocytes (OLs), the cells responsible for myelin production in the CNS, are essential components for the healthy functioning of the brain, allowing rapid transmission of neural impulses (Skoff and Benjamins, 2014). Injury and loss of OLs are the main pathological features of multiple sclerosis (MS) and other demyelinating diseases (Love, 2006). The process and causes for these insults are not completely characterized in MS.

MS is classified into three types, according to the evolution of disabilities. The most common type is relapsing-remitting MS (RRMS), characterized by neurologic deficits followed by a recovery period. In some cases, RRMS patients can develop progressive disabilities, called secondary progressive MS (SPMS). The disease can also progress gradually without relapse episodes, known as primary progressive MS (PPMS) (Marcus, 2022). Many treatments are available today and are efficient in reducing the number and intensity of relapses, but there is no treatment capable of halting the progression of this disease.

MS is known as an immune-mediated disease, and all treatments developed so far target the immune system (Yang et al., 2022). However, other pathological features are observed in this disease, including energy deficiency (Lassmann and van Horssen, 2011). Hypoperfusion is a feature that is present early in the course of MS, which can impose metabolic stress on OLs, causing injury and cell death (D'Haeseleer et al., 2015). Moreover, as MS progresses, evidence of immune-mediated injury diminishes, while the importance of energetic failure consequences increases (Lassmann et al., 2012). Metabolic stress consistently causes (h)OL death *in vitro* (Rone et al., 2016, Cui et al., 2017, Rao et al., 2017). Therefore, metabolic stress is a relevant

component of injury in MS, and its impact on hOL is critical for the understanding of this disease.

Research on cell death pathways has advanced considerably in recent years and many regulated cell death (RCD) pathways are currently described in the literature (Galluzzi et al., 2018). The activation of these RCD pathways depends on the cell micro-environment, stresses that may be imposed upon them, and their intrinsic susceptibility to triggering these pathways (Galluzzi et al., 2018). Exploring the mechanisms responsible for hOL death in response to metabolic stress can provide valuable knowledge about the etiology of MS and support the development of new treatments.

1.2 Objectives

The main aim of this study was to investigate the molecular mechanisms that cause hOL death in response to metabolic stress *in vitro*. For this purpose, mechanisms involved in the main RCD pathways were taken into account. The investigation was focused on pathways that are more likely to be mobilized in response to metabolic stress.

Another aim of this study was to understand the resistance of hOL to apoptosis, which may be activated in response to metabolic stress. We also assessed the differences in this resistance according to age of individuals and differentiation stage of OL lineage cells.

In the literature, autophagy is considered an essential process for cell survival, but sometimes it is associated with cell death. We aimed to understand the role of autophagy in cell death and survival of hOLs in response to metabolic stress. We also aimed to explore the potential benefits of autophagy modulation to support hOL survival.

Another aim of this study was to examine *in situ* tissue samples of MS patients in search of molecular evidence of induction of the same mechanisms that induce hOL death in response to metabolic stress *in vitro*.

CHAPTER 2: Literature review

2.1 Oligodendrocytes

OLs are the cells in the CNS responsible for producing myelin sheaths, which support neuronal conduction of action potentials (Skoff and Benjamins, 2014). Compared to astrocytes (AST), the other macroglia of the CNS, OLs are smaller and have denser soma. They present fewer intermediate filaments and a great number of microtubules in their processes (Peters, 1991, Lunn et al., 1997). OLs possess long processes that vary in number depending on the area of the CNS. The same axon may be ensheathed by different OLs (Peters, 1991).

During development, oligodendrocyte progenitor cells (OPCs) arise from neuroepithelial cells. OPCs proliferate and migrate inside the CNS. These cells eventually differentiate into mature OLs following strict regulation (Elbaz and Popko, 2019). This process of proliferation and differentiation results in an overproduction of OPCs. OPCs produced in excess are eliminated by programmed cell death, mainly apoptosis (Hughes and Stockton, 2021b). However, after development in humans, the quantity of OLs is consolidated in early childhood and remains stable for the rest of the individual life. Little turnover is observed, indicating that OLs are a long-living type of cell (Yeung et al., 2019a).

During differentiation, OL processes start to form, scanning for the presence of axons. In most cases, contact with axons causes process retraction, but in some situations, an association is started. This association is followed by the wrapping of the axon. The distal part of the process forms the inner tongue, which moves around the axon always in contact with it and entering underneath the previously deposited myelin membrane, resulting in the formation of a multilayer sheath. This sheath also extends laterally, forming coiling structures in the sides of the nodes of

Ranvier known as paranodes. Adhesion and scaffold proteins localized at the paranodes increase the stability of the connection between axons and OLs (Snaidero and Simons, 2017).

It is possible to classify the OL lineage cells into neural precursors (NP), OPCs, pre-OLs, and myelinating OLs (Antel et al., 2019). A2B5, a monoclonal antibody for several gangliosides, is an early marker for NP and OPCs (Fredman et al., 1984). The expression of PDGFRα indicates differentiation into OPCs (Antel et al., 2019). The monoclonal antibody O4 is capable of marking OPCs and mature OLs (Armstrong et al., 1992). Galactosylceramide (GalC) identifies immature and mature OLs (Pfeiffer et al., 1993). The specific myelin protein 2', 3'-Cyclic nucleotide-3'-phosphohydrolase (CNP), myelin basic protein (MBP), and PLP are markers of mature OLs., while myelin-associated glycoprotein (MAG) and myelin oligodendrocyte glycoprotein (MOG) identify myelinating mature OLs (Baumann and Pham-Dinh, 2001).

2.2 Myelin structure

Myelin sheaths are composed of compact multilayer stacks with a periodicity of 12 nm on average (Hildebrand et al., 1993). To create the compact structure of myelin, the membranes of the layers composing the sheaths are sealed together by adhesion molecules. MBP is responsible for the connexion between plasma membranes at the cytoplasmic side and PLP, a transmembrane molecule, closely attaches the layers between them (Readhead et al., 1987, Roach et al., 1983, Roach et al., 1985, Boison et al., 1995). Cytoplasmic channels are necessary for the trafficking of metabolites and trophic molecules within myelin (Stadelmann et al., 2019).

The paranodes are located at the edges of each myelin sheath segment and consist of a sequence of compact loops. The paranode has an average length of 4 μm comprising around 40 loops (Hildebrand et al., 1993). Regions of 10-15 μm adjacent to paranodes are called juxtaparanodes.

The rest of the ensheathed segment is called the internode. The nodal region has 0.8 to 1.1 μm of length, in which the axon is constricted by 30-50% compared to the internode (Stadelmann et al., 2019). Paranode loops are connected to axons by tight junctions, formed by neurofascin 155 (NF155) at the side of the OL and contactin and contactin-associated protein (CASPR) at the side of the neuron (Gow et al., 1999, Yermakov et al., 2019). These complexes are connected to the scaffolding proteins of the cytoskeleton in the submembrane region, ankyrin G in the OL and 4.1B, αII spectrin, and βII spectrin in the axon (Chang et al., 2014, Ogawa et al., 2006, Zhang et al., 2013). These tight junctions are essential for saltatory conduction, as it prevents the leaking of current and avoids diffusion of ion channels (Rosenbluth, 2009). Paranodes are attached between them by gap junctions formed by connexins (Abrams and Scherer, 2012). These gap junctions are necessary for electrical coupling and metabolite transport through the loops of paranodes (Stadelmann et al., 2019). Paranodes separate voltage-gated sodium channels that localize at the node of Ranvier from K^+ channels at the juxtaparanodes (Rasband et al., 2001).

The axon-glial internodal domain is a space of about 10 nm between the axon and the myelin sheath (Stadelmann et al., 2019). MAG expressed by OLs localizes to this region in the membrane of the inner tongue of the myelin sheath and interacts with neuronal gangliosides (Schnaar and Lopez, 2009). MAG signaling through Cyclin-dependent kinase 5 (Cdk5) and extracellular signal-regulated kinase 1/2 (ERK1/2) modulates axonal cytoskeleton maturation and diameter size (Yin et al., 1998).

2.3 Multiple sclerosis

Many diseases involve the degeneration of myelin. A demyelinating disease is characterized by the loss of myelin with primary preservation of axons. Therefore, diseases that present

demyelination following neuronal injury are not included in this category. Also, disorders in which myelin fails to form are not considered, denoted as dysmyelinating diseases (Love, 2006). Demyelinating diseases can be classified according to their pathogenesis: inflammation, viral infection, metabolic derangement, hypoxia/ischemia, and focal compression (Love, 2006).

Among demyelinating diseases, multiple sclerosis is the most prevalent. Multiple sclerosis is a chronic autoimmune disease in which the main hallmark is demyelination. About 900,000 people are afflicted with MS in the US. MS is frequently diagnosed between 20 and 30 years old and is three times more common in women than men. The main risk factors for MS are genetics, low vitamin D levels, Epstein-Barr virus (EBV) infection, and smoking. (Marcus, 2022).

2.3.1 Progressive MS

The most common type of MS is RRMS. A considerable number of patients with RRMS develop SPMS. There is also a minority of patients who have PPMS. Most of the MS treatments currently available are effective for RRMS, as they reduce the occurrence of relapses. However, there are no treatments for the progressive forms of MS with consistent effectiveness (Cree et al., 2021).

From a pathologic point of view, the key difference between RRMS and SPMS is that in RRMS the immune-mediated damage is more accentuated, while in SPMS neurodegeneration becomes more relevant and the immune contribution to injury is reduced (Lassmann et al., 2012). RRMS and SPMS seem to be intertwined with pathological features in common (Lassmann, 2018). A differential feature is that cortical demyelination and diffuse white matter damage evolve during the transition from RRMS and SPMS (Bevan et al., 2018). OL loss is more frequently detected in lesions in SPMS patients (Lucchinetti et al., 2004).

During the early stages of MS, and when RRMS is prevalent, peripheral immune responses toward the CNS are the main cause of injury. As the disease passes to its progressive form, immune reactions within the CNS are the most relevant (Correale et al., 2016). A reduction in blood-brain barrier (BBB) permeability has been detected during the transition from RRMS to SPMS (Correale et al., 2017). However, BBB permeability is higher in patients with SPMS compared to normal white matter due to the accumulation of fibrin in the perivascular area (Cree et al., 2021).

The formation of lymphocytic aggregates and tertiary lymphoid structures is observed in patients with SPMS. These structures are close to chronic inflammation sites and subpial cortical lesions. Meningeal lymphoid aggregates are associated with progression independent of relapse activity (Ransohoff, 2023).

Brain atrophy is observed in SPMS. Neuroaxonal loss is present in both white and gray matter and may be the cause of atrophy along with loss of myelin (Chard and Miller, 2016, Bergsland et al., 2018).

MRI, histologic studies, and PET indicate that macrophages and microglia present a higher level of activation in SPMS patients compared to healthy controls, suggesting that microglia activation may be the cause of diffuse inflammation in SPMS (Matthews, 2019, Rissanen et al., 2014).

Iron accumulation is observed by MRI in patients with SPMS, especially in deep gray matter (Stankiewicz et al., 2007). Iron staining was observed around demyelinated plaques, within blood vessels near lesions at gray matter, and perilesional white matter near lesions (Craelius et al., 1982). Iron accumulation may be an effect of neurodegeneration and also can underlie further

damage (Zecca et al., 2004). Iron can cause toxicity when combined with reactive oxygen species (ROS) leading to lipid peroxidation and cell death (Halliwell, 2006).

Mitochondrial dysfunction contributes to neurodegeneration in MS (Su et al., 2009). Mitochondria potentiate the production of ATP, an important property, especially for neurons due to their high energetic demand (Witte et al., 2014). Mitochondria also produce ROS, that can cause oxidative stress (Lin and Beal, 2006). In some acute MS lesions, defects in the respiratory chain of mitochondria are present in OLs, ASTs, and neurons (Witte et al., 2014). Mitochondrial injury is associated with oxidative bursts caused by the release of ROS and reactive nitrogen species (RNS) by microglia and macrophages (Fischer et al., 2012, Witte et al., 2010).

Demyelination causes an increase in mitochondrial activity in axons, which may underlie further damage. An elevation in the activity of sodium channels increases the energy demand, overwhelming mitochondria respiration and causing virtual hypoxia (Trapp and Stys, 2009). This virtual hypoxia reduces mitochondrial respiratory capacity and shortage of ATP, leading to axon degeneration (Trapp and Stys, 2009).

2.3.2 Potential treatments for progressive MS

The development of therapies for progressive MS is the ultimate challenge in the treatment of the disease. Up to now, only ocrelizumab was approved for the treatment of PPMS(Lamb, 2022). Other drugs targeting the immune system have shown some positive effects in the treatment of progressive MS, but only in the active mode of the disease (Kappos et al., 2018, Hartung et al., 2002, Sorensen et al., 2020, Kuhle et al., 2016).

The supplementation with some co-factors has shown some positive effects, especially lipoic acid, an iron chelator and co-factor for pyruvate dehydrogenase and alpha-ketoglutarate dehydrogenase, N-acetylcysteine, which increase the anti-oxidative system of cells, and vitamin D (Spain et al., 2017, Monti et al., 2020, Ascherio et al., 2014).

All treatments for RRMS target the immune system. However, these treatments have limited effects on progressive MS. The pathological features of progressive MS, showing increased mitochondrial dysfunction and oxidative stress, along with the positive effect of anti-oxidants and co-factors involved in energetic metabolism, point that treatments aiming to reduce oxidation and restore proper metabolic functions may constitute promising strategies for the treatment of this type of the disease.

2.4 Potential contribution of metabolic stress to MS

2.4.1 Brain energy supply

The brain is by far the most demanding human organ in terms of caloric consumption (Raichle and Gusnard, 2002). To meet this high energetic demand, the brain is equipped with a vast vascular network of arteries, arterioles, capillaries, venules, and veins that need to be dynamically regulated to supply a proper and constant blood flow to the brain (Fouda et al., 2019). Due to the importance of this constant supply, it is not surprising that impairments in blood flow are linked to dementia and neurodegenerative diseases (Iadecola et al., 2019, Wardlaw et al., 2019, Gorelick et al., 2016, Chabriat et al., 2009, Sweeney et al., 2018, Cortes-Canteli and Iadecola, 2020, Paul and Elabi, 2022).

The blood flow needs also to be locally regulated to deliver nutrients and oxygen to meet the demands of specific brain regions (Muoio et al., 2014). This regulation is executed at the level of

the microvasculature by the neurovascular unit (NVU) which is composed of endothelial cells, vascular smooth muscle cells (VSMC), pericytes (PE), and ASTs (Schaeffer and Iadecola, 2021). There is an active communication, known as neurovascular coupling (NVC), between the NVU and cells from the CNS parenchyma to coordinate the regional blood flow in the CNS (Kaplan et al., 2020).

VSMCs are capable of contractions and can alter the blood vessel diameter providing a regulatory mechanism by which it modulates the cerebral blood flow. Changing oxygen and nutrient levels trigger a signaling cascade that induces contractions of VSMCs by the modulation of Ca^{2+} concentration and interaction between myosin and actin (Hayes et al., 2022). VSMCs also respond to mechanical forces and circumference pressure, a reaction that is faster than chemical signaling (Na et al., 2008, Liu and Lin, 2022). VSMCs can change their phenotype in response to several stimuli. Instead of their most common state in which their main function is contraction and regulation of blood flow, they can adopt phenotypes involved in inflammation and matrix remodeling. Dysfunction of this dynamic regulation can lead to impaired cerebral blood flow (Starke et al., 2014).

Brain capillaries are not surrounded by VSMCs. In this case, PEs are present in contact with the endothelial cells. PEs are also capable of contraction and, therefore, implicated in the regulation of blood flow in the exchange zone of nutrients and other signaling molecules between the brain parenchyma and the circulating blood (Armulik et al., 2011). Neural activity and the release of glutamate elicit PE relaxation, increasing blood flow in the neighboring areas (Hall et al., 2014). Aging can lead to loss of PEs and cause vascular-mediated neurodegeneration (Bell et al., 2010). PE dysfunction and loss are also observed in the early stages of Alzheimer's disease (AD) (Nortley et al., 2019, Shi et al., 2020, Apátiga-Pérez et al., 2022). PEs can also be responsible for

neurodegeneration through excessive capillary constriction, immune system regulation, and participating in glial scar formation (Cheng et al., 2018).

Endothelial cells are also surrounded by AST end-feet. This structure creates an interface between the circulating blood and the brain parenchyma in a way that ASTs are responsible for the interchange of nutrients, signaling molecules, and other substances between these two elements in the brain (Abbott et al., 2006). ASTs are also implicated in changes in the BBB phenotype (Davson and Oldendorf, 1967). These changes involve the upregulation of tight junctions and a change in the expression of transporter molecules and enzymes (Dehouck et al., 1990, Rubin et al., 1991, Schinkel, 1999, McAllister et al., 2001, Hayashi et al., 1997, Sobue et al., 1999, Haseloff et al., 2005). ASTs give metabolic support to neurons by executing glycolysis and transferring lactate to neurons which are used to produce high volumes of ATP by OXPHOS, supplying the energy necessary for neural function (Bonvento and Bolaños, 2021, Bélanger et al., 2011, Alberini et al., 2018). Impairments in the metabolic relation between ASTs and neurons can be implicated in neurologic disorders such as stroke, migraines, edema, and encephalopathy (Benarroch, 2005). Expression of ApoE4 by ASTs was shown to cause dysfunction in the BBB causing loss of selective permeability. As ApoE4 is a gene associated with AD, ASTs may contribute to this disease via disruption of the BBB (Jackson et al., 2022).

The NVU and the BBB are delicate structures essential for the supply of elements necessary for the survival and proper function of the cells of the brain parenchyma. Many possible conditions can lead to impairments in these structures causing a shortage of nutrients and neurodegeneration (Yu et al., 2020, Cai et al., 2017, Iadecola, 2017, Kugler et al., 2021).

At the level of the brain parenchyma, neurons, ASTs, and OLs consume glucose and other energetic substrates in a shared manner (Dienel, 2019). Glucose is the main energy source in the

brain (Mergenthaler et al., 2013). The most energetic demanding cells in the brain are neurons, consuming much more than glial cells to execute their functions (Li and Sheng, 2022). To support this energy demand, ASTs share part of their energetic resources with neurons. This is accomplished by the execution of oxidative glycolysis, a low-efficient mechanism for the production of ATP, and lactate is shuttled to neurons where it is used for mitochondrial respiration, a more productive mechanism of ATP synthesis (Dienel, 2019, Bélanger et al., 2011, Bonvento and Bolaños, 2021). Besides, ASTs also store glycogen, providing an energy buffer that can be used to guarantee a constant supply (Alberini et al., 2018, Brown and Ransom, 2015, Falkowska et al., 2015).

The metabolic relationship between OLs and neurons is less understood, but some studies suggest that OLs also support neurons in their metabolic needs (Fünfschilling et al., 2012, Bastian et al., 2019). OLs switch their metabolism during development, importing glucose and lactate in the myelinating stage to produce lipids, but become mainly glycolytic after maturation (Rinholm et al., 2011, Fünfschilling et al., 2012). Due to this glycolytic phenotype, OLs release lactate in the periaxonal space via MCT-1 and transfer it to neurons, which is essential for their physiological activities (Lee et al., 2012b).

ASTs and OLs are also connected metabolically and share energetic substrates. This exchange is allowed by gap junctions formed between ASTs and OLs via connexin47 and connexin30 (Tress et al., 2012). This junction supports OLs in their development during myelination (Nave, 2010). This pan-glial network is possibly the main source of glucose and energetic metabolites to neurons (Saab et al., 2013).

Impairments in the metabolic support of neurons by ASTs and OLs can cause neurodegeneration, which can induce dysregulation in the NVC, leading to disruption of the energy metabolism in local brain areas (Griffiths et al., 1998, Saab et al., 2013, Mot et al., 2018).

2.4.2 Cerebral hypoperfusion in MS

The immune-related aspects of MS are well characterized and all current treatments target this feature of the disease. These treatments are effective for RRMS. However, progressive MS continues to be resistant to current systemic immune therapies (Doshi and Chataway, 2016).

Many observations indicate that auto-immune reaction is not the only cause of the disease. The self-antigen that characterizes auto-immune disease has not yet been discovered. Some focal MS lesions evolve without a prior inflammatory response. The causes of axonal degeneration, a major aspect of progressive MS, are not known and seem not related to inflammation. After 30 years of development of treatments based on immune suppression, none of them can effectively reduce disabilities linked to progressive MS (D'Haeseleer et al., 2015).

Many studies with different techniques that range from single-photon emission computed tomography and positron emission tomography to dynamic susceptibility contrast-enhanced perfusion magnetic resonance imaging (DSC-MRI) indicate a reduction in CNS perfusion (Swank et al., 1983, Brooks et al., 1984, Lycke et al., 1993, Sun et al., 1998, Law et al., 2004a, Adhya et al., 2006, Varga et al., 2009). Hypoperfusion was diffusely detected in gray matter and normal-apparent white matter (NAWM) in progressive MS, RRMS, and clinically isolated syndrome patients, showing that cerebral hypoperfusion is an early event in MS (Papadaki et al., 2012, Law et al., 2004a, Varga et al., 2009). In a longitudinal study, altered local perfusion was detected before inflammation, BBB leakage, and plaque formation (Wuerfel et al., 2004). A

recent study using 3-T MRI demonstrated a correlation between gray matter hypoperfusion and white matter damage in MS patients (Mascali et al., 2023). An association between low cerebral artery flow and increased neurofilament light chain in the blood was also identified in patients with MS, indicating an implication of hypoperfusion on axonal pathology (Jakimovski et al., 2022).

Imaging studies revealed a general decrease in perfusion in the CNS of MS patients in both RRMS and progressive forms of MS, which is not caused by metabolic impairments due to axonal degeneration (D'Haeseleer et al., 2011). Hypoperfusion in NAWM in MS patients seems to be primarily caused by vascular impairment and not as a consequence of axonal degeneration induced by metabolic demand decrease (De Keyser et al., 2008).

Some MS lesions are gadolinium-enhancing, which may be caused by vasodilation induced by inflammation, as well as actual disruption of the BBB (Ge et al., 2005). However, in some lesions, it is possible to observe that the increase in enhancement forms a ring in the border of the lesion, with a center with low perfusion (Wuerfel et al., 2004).

MS lesions preferentially form in areas of the brain with low blood perfusion (Narayana et al., 2014). An area of the brain that is particularly susceptible to the formation of MS lesions is the periventricular white matter (Martinez Sosa and Smith, 2017). This area of the brain possesses particularly long and thin arterioles and poor vascularization. Besides, these are end-arterioles that supply exclusive fields, meaning that they lack compensatory supply (Martinez Sosa and Smith, 2017). Moreover, long and narrow arteries tend to lose more oxygen through their walls and this loss is exacerbated in tissues that are hypoxic, which is observed in MS (Martinez Sosa and Smith, 2017).

Hypoperfusion was also observed in animals with experimental autoimmune encephalomyelitis (EAE), with hypoxia being observed in conjunction with clinical effects and demyelination (Davies et al., 2013). Treatments with nimodipine, a CNS-specific vasodilator, were able to restore oxygen levels in the lesioned area of EAE-affected mice, with a reduction in demyelination (Desai et al., 2020). Chen et al., using the bilateral carotid artery stenosis (BCAS) model, which mimics chronic cerebral hypoperfusion, identified an increase in expression of the immunoproteasome in reactive microglia and ASTs contributing to demyelination (Chen et al., 2021b). These findings indicate that hypoperfusion may be also secondarily caused by inflammation, causing a spiral increase in damage.

Another indicator of hypoperfusion is the expression of hypoxia inducible factor 1 (HIF-1). HIF-1 is a transcription factor activated in response to hypoxia and ischemia. HIF-1 is composed of two subunits (HIF-1α and HIF-1β). While HIF-1β is constitutively expressed, HIF-1α is regulated by oxygen availability. In normal conditions, HIF-1α is degraded by hydroxylation. In hypoxic conditions, HIF-1α accumulates, translocates to the nucleus, and forms a complex with HIF-1β, which interacts with its target genes promoting cell survival (Correia and Moreira, 2010, Benarroch, 2009). HIF-1α upregulation was detected in white matter pre-demyelinating lesions in MS patients (Graumann et al., 2003, Zeis et al., 2008). Overexpression of HIF-1α is associated with inflammatory responses and vascular permeability (Peyssonnaux et al., 2007, Thiel et al., 2007, Weidemann et al., 2009). A high expression of HIF-1α was detected in MS lesions with OLs presenting dying-back oligodendropathy (Lassmann, 2003).

Possible causes of cerebral hypoperfusion are edema and disturbance of microcirculation (Lassmann, 2003). BBB damage and edema are found in MS lesions (Kwon and Prineas, 1994). A breakdown of the BBB occurs before the formation of a new MS lesion, according to MRI

studies (Kermode et al., 1990). This breakdown causes leakage of serum proteins into the CNS parenchyma, which may result in swelling of the tissue and edema, consequently leading to disturbances of microcirculation and ischemia (Lassmann, 2003).

Inflammation of the vessel wall is another potential cause of hypoxia-like conditions in MS lesions (Lassmann, 2003). Inflammation can induce the clotting cascade, microvascular thrombosis, and impairment of microcirculation (Lassmann, 2003). Inflammation can be caused by antibodies that react against antigens present in the vessel or cytokines released by leukocytes (Lassmann, 2003). For example, monocytes can stimulate endothelial cells to express adhesion molecules, which can lead to coagulation activation and thrombosis (Mosevoll et al., 2018). Endothelial cell activation can also cause loss of thrombomodulin, which induces vascular thrombosis (Kopp et al., 1997). In a study using the EAE model, T-cells induced ischemic-like damages in the perivascular tissue (Huseby et al., 2001).

Excitotoxins can also induce ischemic-like conditions, especially glutamate, which is released by neurons, ASTs, and activated macrophages and microglia (Lipton, 1998). Altered glutamate homeostasis was detected in MS lesions and may cause excitotoxic damage to neurons and OLs and subsequently tissue damage (Werner et al., 2001).

Another possible cause for this decrease in hypoperfusion is impaired axonal metabolism. Axon degeneration in MS is related to mitochondria dysfunction and oxidative stress (Cambron et al., 2012). A decreased level of N-acetyl aspartate (NAA), which indicates a reduction in axon metabolism, was detected in NAWM of SPMS patients by quantitative magnetic resonance spectroscopy (Aboul-Enein et al., 2010). However, this decrease was comparable to control individuals who presented a milder decrease in hypoperfusion, suggesting that axonal metabolic failure is not the direct cause of hypoperfusion (Steen et al., 2013).

The diffused nature of hypoperfusion in MS indicates that the underlying causes are not local inflammation or microvessel thrombosis (De Keyser et al., 2008). Vascular pathologies cause regional cerebral defects, in contrast to the diffused impairment observed in MS (De Keyser et al., 2008). Moreover, structural vascular pathology is not present (Aboul-Enein and Lassmann, 2005). These observations suggest that hypoperfusion in MS may be linked to dysregulation of microcirculation in the CNS (De Keyser et al., 2008).

Endothelin-1 (ET-1), a potent vasoconstrictor, was found in elevated levels in the blood and cerebrospinal fluid of MS patients (Speciale et al., 2000, Haufschild et al., 2001). Patients with MS have presented impaired capacity in cerebral arterioles dilatation (Marshall et al., 2014). ET-1 is mainly released by endothelial cells (Piechota et al., 2010). However, some studies detected participation in the production of ET-1 by reactive ASTs in brain conditions such as Alzheimer's, stroke, and traumatic injury (Nie and Olsson, 1996, Ostrow et al., 2000). In MS plaques, ET-1 was detected in reactive ASTs (D'Haeseleer et al., 2013). High levels of serum ET-1 were detected in patients recovering from optic neuritis, which is linked to vascular hypoperfusion in MS patients (Castellazzi et al., 2019). Therefore, hypoperfusion could be caused by vasoconstriction induced by ET-1 released by reactive ASTs (D'Haeseleer et al., 2015).

ASTs also control vasodilation by K^+ signaling. ASTs release K^+ by its end-feet in the perivascular space that is captured by VSMC, causing hyperpolarization and closing voltage-dependent Ca^{2+} channels, which result in vasodilation (Butt and Kalsi, 2006, Knot and Nelson, 1998).

This regulation mediated by ASTs may also be impaired in MS and be a possible cause of hypoperfusion (De Keyser et al., 2008). A deficiency in β_2-adrenergic receptors in ASTs was

detected in MS (De Keyser et al., 1999, Zeinstra et al., 2000). The binding of norepinephrine to these receptors induces cAMP formation and release of trophic factors and lactate which are uptaken by neurons, supporting their energetic metabolism (De Keyser et al., 2004). A reduction in cAMP levels caused by the deficiency in β_2-adrenergic receptors in ASTs can reduce lactate shuttle to neurons and reduce the release of K^+ due to lower axonal activity (De Keyser et al., 2004). Also, the activity of Ca^{2+}-dependent K^+ channels can be reduced due to reduced levels of cAMP (Bolton et al., 2006). The reduced release of K^+ in the perivascular area would stimulate vasoconstriction (De Keyser et al., 2008).

2.5 OLs injury, demyelination, and remyelination in MS

2.5.1 Injury and demyelination in MS

OL injury is a major hallmark of MS and an underlying cause of disabilities. OLs injury is an early event in MS and may be sub-lethal, characterized by loss of processes, a phenomenon termed dying-back, or lethal, with permanent loss of OLs by cell death (RODRIGUEZ et al., 1993).

Sub-lethal injury is observed in the early onset of MS lesions. This type of injury leads to a loss of myelin sheets and is preceded by the widening of inner myelin lamellae and degeneration of internal glial loops (RODRIGUEZ et al., 1993). Alterations in myelin structure start at the inner cytoplasmic tongue in the distal region of processes, before demyelination and changes in OL cell bodies (Ludwin and Johnson, 1981).

Lethal injury is also observed, specifically in old and established plaques, suggesting a slow expansion of lesions. This expansion is not accompanied by signs of inflammation (Prineas et al., 2001). Changes in the microenvironment that may cause metabolic impairment in the cells are

recognized as a potential cause of OL injury (Fischer et al., 2012, Lassmann and van Horssen, 2011, Lassmann, 2003, Law et al., 2004b).

OPCs were shown to be more susceptible to cell death than mature OLs. The presence of OPCs in MS lesions is reduced compared to NAWM, while the reduction of mature OLs is less pronounced (Cui et al., 2013). *In vitro* studies demonstrated that OPCs are more susceptible to cell death under metabolic stress conditions compared to mature OLs and have a higher propensity to trigger apoptosis (Cui et al., 2013).

Injury response to metabolic and oligodendrogliopathy is associated with their distinct bioenergetic properties (Rone et al., 2016). *In vitro,* OPCs and mature OLs rely mainly on oxidative glycolysis for their energetic metabolism, which would redirect metabolites to protein and lipid synthesis necessary for myelin construction. Mature OLs are less metabolically active than OPCs and both OPCs and OLs are more active in rats than in humans. Under metabolic stress, a considerable retraction of OL processes, reduction in energy utilization, and ATP production are observed before any signs of cell death (Rone et al., 2016).

The maintenance of myelin requires a considerable amount of ATP, which may be provided by OXPHOS (Harris and Attwell, 2012). Concurrently, metabolites produced by glycolysis are necessary for the production of myelin (Sánchez-Abarca et al., 2001). Therefore, it is expected that the metabolic profile would be different between OPCs, which proliferate and differentiate, and mature OLs, which have less dynamic activity, in which energy is required to maintain their structure. Moreover, it is suggested that OLs support neurons by shuttling lactate (Philips and Rothstein, 2017). However, studies with rat OLs, indicated that adult OLs produce most of their ATP from glycolysis, while in OPCs, ATP is mainly produced by OXPHOS. Differentiation from OPC to OL leads to lower production of ATP. Seahorse analyses demonstrated a higher

level of extracellular acidification in adult OL compared with OPCs, which may indicate a higher release of lactate (Rao et al., 2017). Under metabolic stress, ECAR is reduced indicating a lower release of lactate as a consequence of less production of pyruvate by glycolysis. These findings suggest that OLs under metabolic stress are less capable of producing myelin, as observed by their processes retraction, and also less capable of releasing lactate that would be donated to neurons in the CNS (Rao et al., 2017).

2.5.2 Remyelination

Remyelination is traditionally attributed to OPCs, according to animal experiments (Zawadzka et al., 2010a). A stable and abundant population of OL progenitors is found in adult mice brains. This population is constantly renewed due to the mitotic capacity of these cells (Psachoulia et al., 2009). In the case of myelin injury in adult mice, OPCs are recruited to differentiate, proliferate and migrate to the injured region, where new myelin is formed, although the newly formed myelin sheaths are thinner and shorter (Zawadzka et al., 2010b). This process is subjected to a complex regulation, susceptible to inhibitors and dependent on pro-regenerative factors, and therefore susceptible to failure (Franklin and Ffrench-Constant, 2017a).

A significant number of OPCs are found in MS lesions. There are MS lesions that lack remyelination, despite the presence of OPCs, suggesting that these OPCs are not properly activated or lack an intrinsic capacity for remyelination (Wolswijk, 1998). *In vitro*, rodent OPCs are capable of myelinating nanofibers and the extension of myelination depends on the fiber diameter (Lee et al., 2012a, Franklin and ffrench-Constant, 2017b). Remyelination by OPCs is also modulated by action potentials (Wake et al., 2011).

Inhibition of remyelination by OPCs may be due to immune modulation and age (Cunniffe and Coles, 2021). The activity of macrophages and microglia seems to be important regulators of OPC activation (Rawji and Yong, 2013). Inhibitors of OPC differentiation are found in myelin debris (Robinson and Miller, 1999, Kotter et al., 2006). Therefore, myelin debris must be cleared by macrophages or microglia (Plemel et al., 2013). Microglia can assume two polarized phenotypes: proinflammatory (M1) and anti-inflammatory (M2). Studies in animal models have shown that microglia polarization to M2 promotes OPC differentiation (Miron et al., 2013).

Remyelination capacity also declines with age and duration of the disease (Goldschmidt et al., 2009, Franklin et al., 2012, Frischer et al., 2015). Clinical evidence indicates that age is a significant negative factor for remyelination, as the onset of progressive MS happens at similar ages (Confavreux and Vukusic, 2006). Remyelination is slower in older mice, attributed to an impairment of OPC recruitment and differentiation (Shields et al., 1999, Sim et al., 2002). Magnetization transfer ratio, which indicates remyelination, declines with age in MS lesions (Brown et al., 2013). OPC differentiation capacity is reduced with age (Woodruff et al., 2004). This decline is due both to extrinsic factors to OPCs, such as a reduction in the efficiency of the inflammatory response of macrophages (Zhao et al., 2006), and intrinsic factors, as OPCs are also less responsive to differentiation in aged individuals (Kuhlmann et al., 2008).

The capacity of OPCs to remyelination is also dependent on the location of the lesion, as remyelination of perivascular lesions is less extensive than in subcortical lesions (Patrikios et al., 2006). This difference indicates heterogeneity in OPC differentiation capacity due to intrinsic or extrinsic factors dependent on the brain region (Kitada and Rowitch, 2006).

However, a study investigating the dynamics of OL generation in MS, indicates that old OLs are present in shadow plaques, which are demarcated areas of remyelinated lesions, indicating that

mature OLs also contribute to the process of remyelination (Yeung et al., 2019b). New OLs were not detected in shadow plaques, possibly because they are incapable of surviving and integrating to form new myelin (Yeung et al., 2019b). A study using snRNA-sequencing analysis also indicated that the presence of OPCs is scarce and fully mature, and stable OLs are lost in MS lesions. This study also showed the upregulation of myelin genes in mature OLs in MS, suggesting that these cells play an important role in remyelination (Jäkel et al., 2019). Further supporting the importance of OLs for remyelination, *in vitro* studies indicate that OPCs are more susceptible to injury than OLs in MS lesions (Cui et al., 2013).

Mature OLs have the potential to restore myelin in MS lesions. *In situ* analysis indicates that OLs are preserved in MS lesions with active inflammatory demyelination, although with signs of process dysfunction (Cui et al., 2017). Changes in the inner tongue were observed, indicating that process degeneration starts at its distal part. Macrophages are mainly observed engulfing myelin debris, but not extracting myelin directly from OLs, indicating that processes fragmentation precedes phagocytosis by macrophages (Cui et al., 2017).

In situ observations of MS lesions suggest an overall cellular injury that is not dependent on cell-cell contact (Cui et al., 2017). These observations are coherent with the dying-back theory, supporting a gradual retraction of processes causing myelin loss (Ludwin and Johnson, 1981). These sub-lethal injuries do not necessarily lead to cell death as they can be reversed. In vitro studies have shown that mature OLs that had previously lost their processes in response to metabolic stress are capable of regrowing if optimal culture conditions are reestablished (Cui et al., 2017). *In vitro*, OLs have shown considerable resistance to metabolic stress, enduring up to 4 days without considerable levels of cell death. These cells have also presented resistance to trigger apoptosis (Cui et al., 2017).

2.6 Cell survival pathways

Cells will not always be in an optimal environment for their functions, growth, and replication and will be often challenged by stresses. To overcome stress, cells are equipped with a series of mechanisms that promote cell survival. These mechanisms are triggered in response to specific stresses, comprising ER stress, oxidative stress, hypoxia, DNA damage, nutrient stress, and heat shock (Twayana and Ravanan, 2018).

2.6.1 ER stress and unfolded protein response (UPR)

One of the functions of the ER is protein folding, which is a complex process that depends on specialized chaperone proteins. This process is frequently subjected to errors, so the

ER is also responsible for the quality control of protein folding. Polypeptides that are unproperly folded must be retained and destined for degradation by the proteasome (Twayana and Ravanan, 2018). ER stress can be triggered by nutrient deprivation, metabolic demand, infection, and chemical insults (Kaufman, 2002).

ER stress induces the unfolded protein response (UPR), a signal pathway that regulates the transcription and translation of genes, and post-translational modifications involved in protein folding (Hetz et al., 2020). Three proteins are responsible for initiating UPR: Protein kinase R (PKR)-like endoplasmic reticulum kinase (PERK), Inositol requiring enzyme-1α (IRE1α), and activating factor 6 (ATF6) (Figure 2.1) (Hetz et al., 2020).

When activated by ER stress, PERK phosphorylates eukaryotic initiation factor 2 α (eIF2α), reducing overall cellular protein translation. This response reduces the ER load and the accumulation of misfolded proteins. The phosphorylation of eIF2α also causes the selective translation of activating factor 4 (ATF4), a transcription factor that regulates genes involved in

amino acid metabolism, antioxidative response, autophagy, and ER protein folding. ATF4 is also indirectly responsible for the dephosphorylation of eIF2α by upregulating protein phosphatase 1 (PP1), which dephosphorylates eIF2α in association with growth arrest and DNA-damage-inducible protein (GADD34), returning protein synthesis to normal (Ron and Walter, 2007, Novoa et al., 2001).

IRE1α activation by ER stress induces its RNase activity, activating the transcription of factor X-box-binding protein 1 (XBP1), which upregulates genes involved in ER protein translocation, folding and secretion, and degradation of misfolded proteins (Hetz et al., 2020). IRE1α also cleaves a set of RNAs, which reduces the protein folding load in the ER (Hollien et al., 2009).

ER stress causes the translocation of ATF6 to the Golgi complex, where it is cleaved. A fragment of this cleavage translocates to the nucleus, where it is responsible for the upregulation of genes involved in ER protein translocation, folding and secretion, and degradation of misfolded proteins (Haze et al., 1999, Wu et al., 2007).

The effect of the UPR is an adjustment in ER folding capacity and proteostasis in response to ER stress. However, if the stress is too intense, UPR may lead to apoptosis by the activation of C/EBP homologous protein (CHOP) by ATF4, which induces the expression of the pro-apoptotic molecule BCL-2 interacting mediation (BIM) (Ohoka et al., 2005).

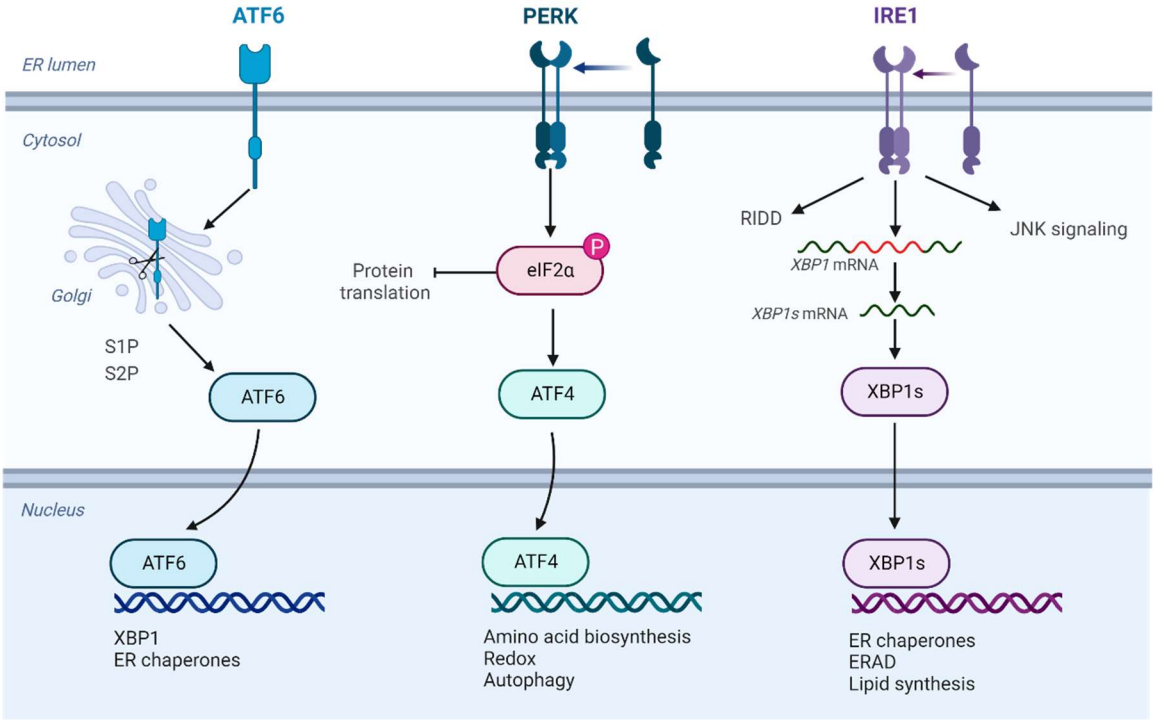

Figure 2.1 – Unfolded protein response pathways. ER Stress activates ATF6, PERK and IRE1, which induces the translocation to the nucleus of ATF6, ATF4 and XBP1, upregulating the expression of XBP1, ER chaperones, amino acid and lipid biosynthesis, autophagy and endoplasmic-reticulum associated degradation (ERAD). Obtained from Biorender under permission.

2.6.2 Integrated stress response (ISR)

The ISR is induced by hypoxia, glucose or amino acid deprivation, viral infection, ER and oncogene activation (Pakos-Zebrucka et al., 2016). It overlaps with the UPR, as PERK is also considered a trigger of the ISR. Also, the downstream pathway initiated by PERK in the ISR is the same: phosphorylation of eIF2α with reduction of protein synthesis, subsequent activation of ATF4, and regulatory negative feedback loop by GADD34 in association with PP1, which terminates the ISR by dephosphorylation of eIF2α (Ron and Walter, 2007, Novoa et al., 2001).

As in the UPR, the activation of ATF4 induces the transcription of autophagy-related genes and interaction with CHOP can lead to apoptosis (Ron and Walter, 2007, Ohoka et al., 2005).

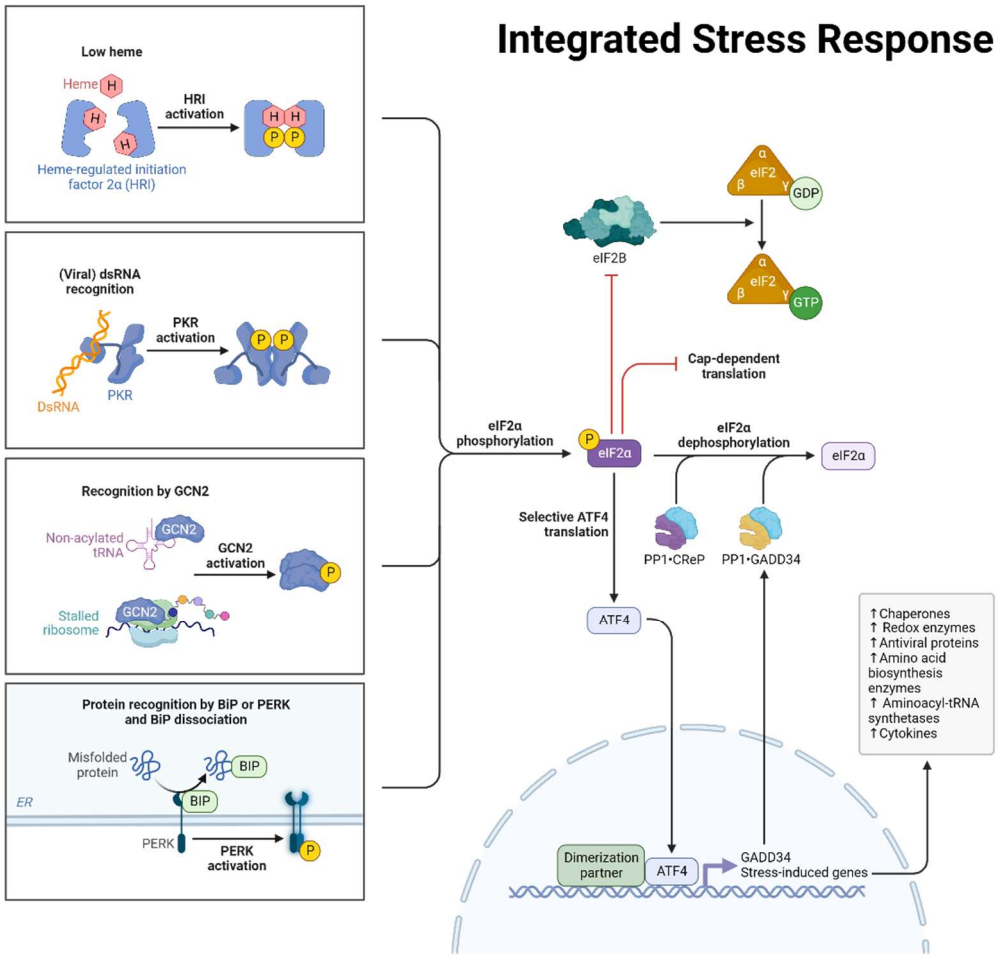

Figure 2.2 – Integrated stress response. The ISR is triggered by low heme, viral components and misfolded proteins respectively detected by HRI, PKR, GCN2 and PERK, causing the phosphorylation of eIF2α. This phosphorylation inhibits protein translation and activates ATF4, which induces the expression of genes associated with protective mechanisms. ATF4 also induces the expression of GADD34, which dephosphorylates eIF2α and terminates the ISR. Obtained from Biorender under permission.

However, the ISR can also be initiated in response to amino acid deprivation, viral infection, and heme deprivation (Figure 2.2). These stresses are respectively sensed by general control non-depressible protein 2 (GCN2), double-stranded RNA-dependent protein kinase (PKR), and heme-regulated eIF2α (HRI) (Donnelly et al., 2013). These kinases phosphorylate eIF2α and induce the same downstream mechanisms as PERK (Donnelly et al., 2013).

The outcome of the ISR is not always the same and depends on the duration, severity, and nature of the stress, and correspondent levels of eIFα phosphorylation and ATF4 translation (Dey et al., 2010, Guan et al., 2014). A mild and short ISR is regarded as pro-survival, while a longer activation may induce cell death (Rutkowski et al., 2006).

2.6.3 Antioxidant response

Eukaryotic cells are capable of efficiently produce energy for their functions by cellular respiration in their mitochondria, a process that requires oxygen to produce ATP. At the same time, oxygen can be toxic to the cell, as respiration also generates ROS as a subproduct, which at elevated levels can damage many cell components (Agrawal and Mabalirajan, 2016). This process is known as oxidative stress (Pizzino et al., 2017).

To keep ROS at homeostatic levels, cells are equipped with antioxidant mechanisms that counterbalance ROS production. During respiration, the uncoupling of electrons in the electron transport chain results in the generation of superoxide anion (Turrens, 2003). This ROS can be transformed into hydrogen peroxide (H_2O_2) by the enzyme superoxide dismutase (SOD) and H_2O_2 can be converted into water and oxygen by catalase (Karmakar et al., 2022, Glorieux and Calderon, 2017). However, H_2O_2 can also be converted into OH^- in the presence of ferrous iron (Fe^{2+}), which is known as the Fenton reaction (Winterbourn, 1995). Also involved in oxidative

stress are reactive nitrogen species (RNS), which are mainly nitric oxide (NO) and its derivate peroxynitrite (Adams et al., 2015). Oxidative stress can cause DNA damage resulting in cell cycle arrest or inducing apoptosis (Klein and Ackerman, 2003). ROS can cause lipid peroxidation, which not only damages membranes but also produces toxic subproducts 4-hydroxynonenal (HNE) and malondialdehyde (MDA) (Yang and Stockwell, 2016, Barrera, 2012, Bhat et al., 2015) (Figure 2.3).

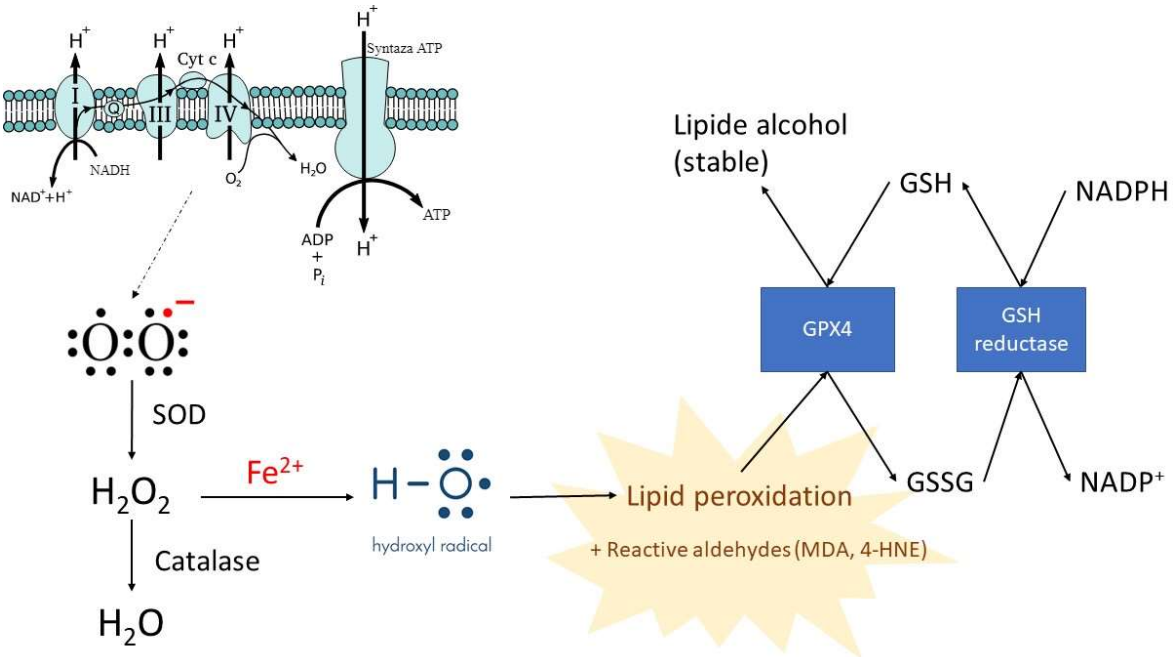

Figure 2.3 - Antioxidant system. ROS are generated as a by-product of the ETC and H_2O_2, which can react with Fe^{2+} generating OH^-, which causes lipid peroxidation and the formation of reactive aldehydes. Lipid peroxidation can be neutralized by the action of GSH and GPX4, which needs to be further restored by GSH reductase in the presence of NADPH.

The main cellular antioxidant system is performed by the neutralization of ROS/RNS by glutathione (GSH), yielding glutathione disulfide (GSSG), a process catalyzed by glutathione

peroxidase 4(GPX4). GSSG can be further converted back to GSH by glutathione reductase (GR) in exchange for the conversion of NADPH into NADP+, which is returned to its reduced form during the pentose phosphate pathway (Wu et al., 2004). Additional antioxidants are peptides such as thioredoxin, glutaredoxin, and peroxiredoxin (Lillig and Holmgren, 2007). Some nutrients such as tocopherol, ascorbic acid, and beta-carotene are important antioxidants (Lobo et al., 2010).

Some signaling pathways are activated under oxidative stress, which may lead to survival or cell death according to oxidative intensity. NRF2 is a transcription factor that stimulates the expression of antioxidant response elements (ARE) in response to the activation of MAP kinase pathways by mild oxidative stress (Koinzer et al., 2015). However, these signal pathways can also lead to apoptosis when oxidative stress is high (Ki et al., 2013). The PI3K/AKT pathway protects the cell under oxidative stress by inactivating proapoptotic molecules and upregulating antiapoptotic proteins (Choi et al., 2012). The tumor suppressor p53 is also involved in the transcriptional antioxidant response and may induce cell death when levels of oxidative stress are high (Liu and Xu, 2011).

2.6.4 Heat shock response

The conformation flexibility of proteins is an essential property for their functions and any temperature change can affect their activities. As cells are frequently subjected to changes in temperature, proteins alter their conformation, which can cause cytoskeleton disruption, Golgi system and ER breakdown, decrease in the number of lysosomes and mitochondria, protein aggregation, and impairment of nuclear processes, eventually resulting in cell cycle arrest or even cell death (Richter et al., 2010).

The response to heat stress is executed by heat shock proteins (HSP). There are seven classes of HSP (Richter et al., 2010): molecular chaperones, responsible for guiding protein conformation, are the most common (Ellis et al., 1989), components of the proteolytic system, which clear misfolded proteins and aggregates(Richter et al., 2010), nucleic acid modifiers are responsible to repair DNA and nuclear processes (Jantschitsch and Trautinger, 2003), metabolic enzymes are needed to modulate the cellular energy supply (Malmendal et al., 2006), regulatory proteins, which initiate stress responses and inhibit some gene expression, like those involved in ribosome biogenesis (Al Refaii and Alix, 2009). Other proteins are involved in the protection of the cytoskeleton and other cellular structures. The last class of heat proteins comprises those that are involved in transport, detoxification, and membrane stability (Richter et al., 2010).

The heat shock response is transcriptionally regulated by heat shock factor 1 (HSF1). HSF1 is kept inactive by forming a complex with HSP90, HSP70, and HSP40. When the level of unfolded proteins increases, these HSPs will let HSF1 free to translocate to the nucleus and bind to the heat shock element, inducing the overexpression of HSPs (Åkerfelt et al., 2010). HSF1 is also regulated by phosphorylation, oligomerization, and other post-translational modifications (Akerfelt et al., 2010, Prahlad and Morimoto, 2009, Hietakangas et al., 2003, Westerheide et al., 2009).

2.6.5 DNA damage repair (DDR)

DNA is constantly subjected to many types of stress, including oxidation, deamination, replication errors, radiation, and chemical agents (Helleday et al., 2014). These stresses cause single and double-strand breaks (SSB and DSB) that must be repaired. The DDR involves sensors, transducers, and effectors that are activated in response to damage. Sensor molecules including poly (ADP-ribose) polymerase (PARP) and DNA-dependent protein kinase detect

strand breaks and recruit the transducer molecules ataxia telangiectasia mutated (ATM) and ATM-Rad3-related (ATR) (Wei and Yu, 2016). These transducers activate checkpoint kinase (chk) 1 and 2, initiating the DDR, which includes cell cycle arrest, providing the necessary time for DNA repair, but can also lead to apoptosis or senescence (Wei and Yu, 2016, Zannini et al., 2014). The p38 MAPKs are also important stress sensor that induces cell cycle arrest by triggering G2/M cell cycle checkpoint (Wood et al., 2009).

SSB repair is initiated by PARP1 detection, followed by the insertion of nucleotide and ligation by specific enzymes (Caldecott, 2008). DSB can be repaired by homologous recombination (HR), nonhomologous end joining (NHEJ), and single-stranded annealing (SSA). DSB repair is initiated by the sensor molecules Ku70/80 and Mre11-Rad50-Nbs1(MRN) complex (Twayana and Ravanan, 2018).

2.6.6 Response to nutrient stress

Nutrients are not always available in the quantity and variety cells need to execute their functions, grow and proliferate. This availability may vary considerably from scarcity to excess, and cells need to modulate their consumption according to nutrient availability.

To cope with nutrient stress, cells are equipped with three main survival pathways mediated by mammalian target of rapamycin (mTOR), AMP-activated protein kinase (AMPK), and Sirtuin 1 (SIRT1).

The mTOR is a kinase and core component of two protein complexes, TORC1 and TORC2, which execute distinct but complementary functions in the regulation of protein synthesis, autophagy, metabolism, and organelle biogenesis (Lipton and Sahin, 2014). During fasting and starvation, nutrient levels in the blood decrease, resulting in a reduced level of insulin in

circulation. Also, the reduced availability of nutrients increases the AMP: ATP ratio (Zoncu et al., 2011). When these changes are sensed by the cell, mTOR in coordination with AMPK mediates a switch between anabolic and catabolic modes according to nutrient availability. mTORC1 activates ribosomal protein S6 kinase 1/2 (S6K1/2) and inhibits the eukaryotic translation initiation factor 4E-binding protein 1 (4E-BP1), which induces protein synthesis (Lipton and Sahin, 2014). mTORC1 also inhibits autophagy and indirectly activates mTORC2, which is involved in cell survival, proliferation, and maintenance of the actin cytoskeleton. Therefore, the inhibition of mTORC1 by AMPK or other pathways linked to nutrient or growth factors deprivation leads to a reduction in protein synthesis and activation of autophagy, switching the cell to a catabolic mode (Figure 2.4) (Lipton and Sahin, 2014).

Besides its role in regulating mTOR, AMPK also phosphorylates acetyl-CoA carboxylase 1 (ACC1) and sterol regulatory element-binding protein 1c (SREBP1c) and therefore regulates the metabolism of lipids (Jeon, 2016). AMPK is also implicated in promoting glucose uptake by inducing the translocation of glucose transporter 1 (GLUT1) to the cell membrane, glycolysis by phosphorylating phosphofructokinase-2 (PFK2), and autophagy by activating Unc-51-like autophagy-activating kinase 1 (ULK1) (Jeon, 2016).

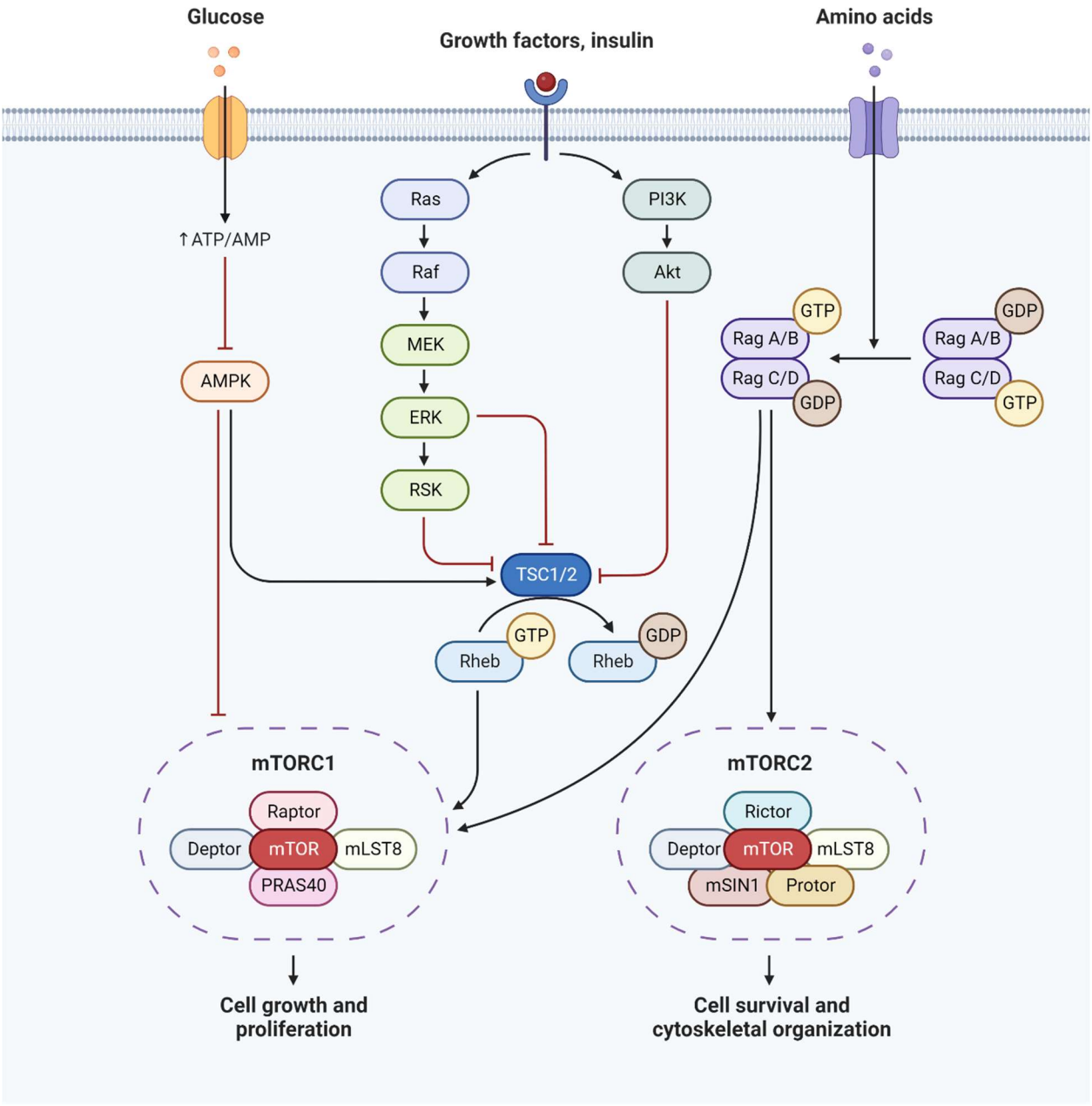

Figure 2.4 - AMPK/mTOR pathway. AMPK is activated when the ratio between ATP/AMP is low. AMPK inhibits mTORC1, causing a reduction in cell growth and proliferation, and inducing autophagy. Insulin withdrawal also leads to mTORC1 inhibition. Low levels of amino acids cause inhibition of mTORC1 and mTORC2, which is responsible for cell survival and cytoskeletal organization. Obtained from Biorender under permission.

SIRT1 is an NAD+-dependent deacetylase that localizes to the nucleus and cytoplasm (Lee, 2019). In the nucleus, it regulates gene expression by deacetylation of histones and signaling proteins (Chang and Guarente, 2014). In response to starvation, SIRT1 induces autophagy by deacetylating autophagic components and suppresses apoptosis by inhibiting p53 (Lee, 2019).

2.6.7 Response to hypoxia

Oxygen is an essential element for OXPHOS. Therefore, in the absence of oxygen, cells need to compensate for the lack of ATP production by OXPHOS and balance their energy consumption with its availability. To this end, the cell cycle is arrested, energy-consuming processes are slowed and a compensatory pathway for energy production, anaerobic glycolysis, is stimulated (Twayana and Ravanan, 2018).

The main mediators of the response to hypoxia in cells are the HIFs. HIFs are heterodimers consisting of an α and β units and have three isoforms. The α subunit is sensitive to oxygen and β is stable. HIF1α activation promotes a shift from OXPHOS to anaerobic glycolysis (Majmundar et al., 2010). This transcription factor induces the expression of glycolytic enzymes, glucose transporters, and lactate dehydrogenase A (LDHA), which converts pyruvate into lactate and increases the availability of NAD^+ for glycolysis (Gordan et al., 2007). HIF1α also upregulated pyruvate dehydrogenase kinase 1 (PDK1), which inhibits pyruvate dehydrogenase (PDH) and the conversion of pyruvate into acetyl-CoA, reducing the supply of this substrate of OXPHOS, and also reducing ROS generation (Majmundar et al., 2010). HIF1α also switches the pentose phosphate pathway (PPP) to a non-oxidative mode (Zhao et al., 2010) (Figure 2.5).

HIF2α induces the expression of anti-oxidant molecules, including SOD2 and heme oxygenase 1 (HMOX1). HIF2α is possibly implicated in stimulating a shift toward anaerobic glycolysis by

regulation of PPARα (Huang et al., 2002, Aragonés et al., 2008). HIF2α also modulates fatty acid metabolism, inhibiting β-oxidation and promoting the formation of lipid droplets (Rankin et al., 2009).

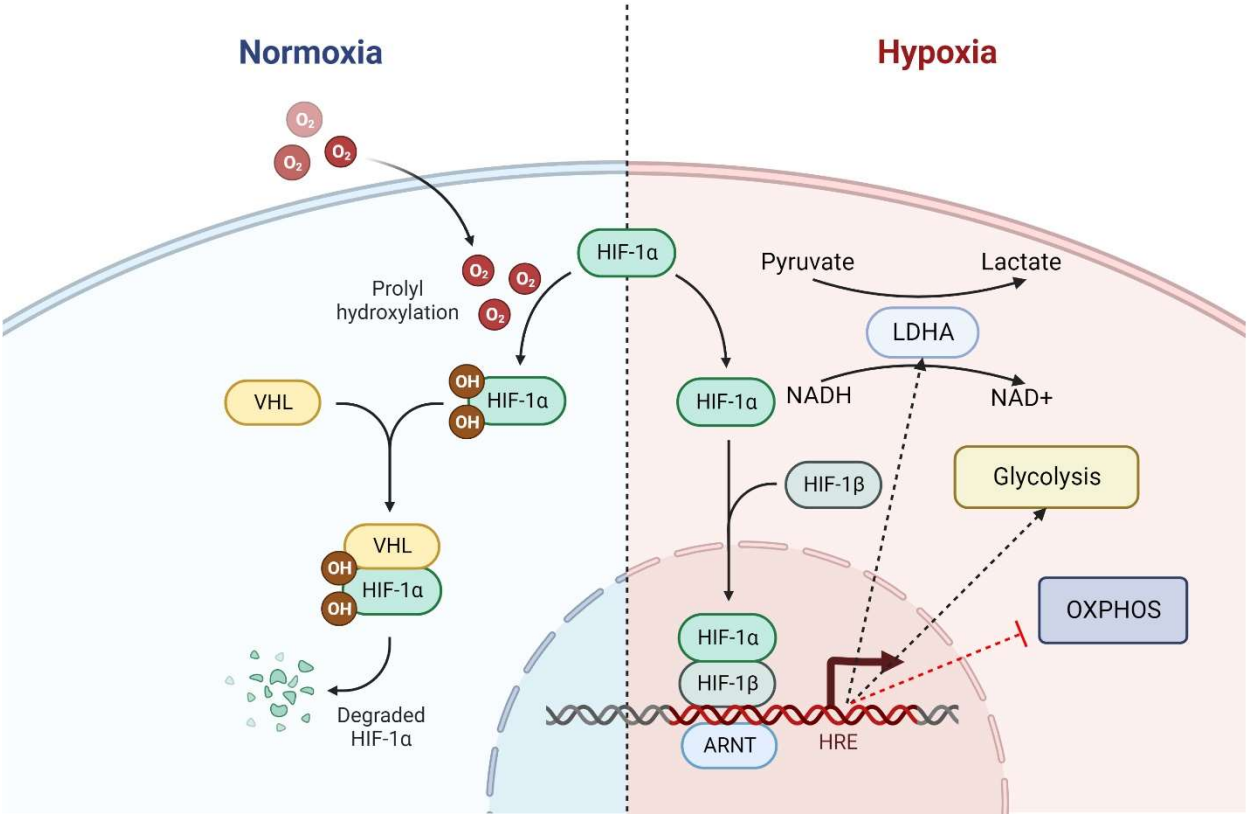

Figure 2.5 - HIF1 activation. In the presence of oxygen, VHL binds to HIF1α, leading to its degradation. In the absence of oxygen, HIF1α translocates to the nucleus, inducing the expression of Hypoxia-response elements (HRE), promoting glycolysis and lactate production, and inhibiting OXPHOS. Adapted from Biorender under permission.

Both HIF1α and HIF2α are involved in the modulation of cytochrome c oxidase, which increases the efficiency of the electron transport chain (ETC) (Gordan et al., 2007) and stimulates angiogenesis by promoting the expression of vascular endothelial growth factor (VEGF) (Manalo et al., 2005, Hu et al., 2003, Kelly et al., 2003).

Regulation of HIF is performed by oxygen availability. When O_2 is abundant, HIFs are hydroxylated by prolyl hydroxylase domain-containing (PHD) and consequently marked for degradation at the proteasome by von Hippel-Linday protein (pVHL). In the absence of O_2, PHD is inhibited and HIFs are stabilized for the execution of their functions (Kaelin and Ratcliffe, 2008). ROS, fumarate, and succinate also inhibit PHD activity (Klimova and Chandel, 2008, Kaelin, 2005, Sudarshan et al., 2009, Kaelin and Ratcliffe, 2008). Another regulator of HIFs is the hydroxylase factor-inhibiting HIF-1α (FIH1), which inhibits HIFs when O_2 is available (Webb et al., 2009, Mahon et al., 2001).

2.7 Autophagy

Autophagy is a major catabolic process in the cell, responsible for the degradation of intercellular components, including macromolecules, aggregates, and organelles (Dikic and Elazar, 2018). The biological functions of autophagy include providing nutrients to the cell during starvation, selectively eliminating potentially harmful cytosolic components, and secreting cytosolic components (Dikic and Elazar, 2018). Autophagy can be implicated in the modulation of neurodegeneration, cancer, infectious diseases, and other pathological conditions (Dikic and Elazar, 2018).

There are three types of autophagy: macroautophagy, characterized by the formation of vesicles called autophagosomes, microautophagy, which involves membrane internalization and chaperone-mediated autophagy (CMA), which selects materials from the cytosol and transports them to lysosomes (Yamamoto and Matsui, 2023). Macroautophagy and microautophagy can be both selective and non-selective (Figure 2.6) (Yamamoto and Matsui, 2023).

Macroautophagy is initiated by the activation of ULK complex, which in turn phosphorylates the class III PI3K complex I, starting the nucleation of autophagosomes by producing phosphatidylinositol-3-phosphate (PI3P). PI3P recruits WD repeat domain phosphoinositide-interacting protein 2 (WIPI2), which intermediates the binding with the ATG12-ATG5-ATG16L1 complex. This complex in association with ATG3 mediates the binding of microtubule-associated protein light chain 3 (LC3) and γ-aminobutyric acid receptor-associated protein (GABARAPs) to phosphatidylethanolamine (PE) in the autophagosome membrane. LC3 and GABARAP are responsible for cargo selection, elongation, and closure of the autophagosome membranes. After maturation, autophagosomes fuse with lysosomes forming autolysosomes, where the sequestered cytosolic components are degraded (Dikic and Elazar, 2018).

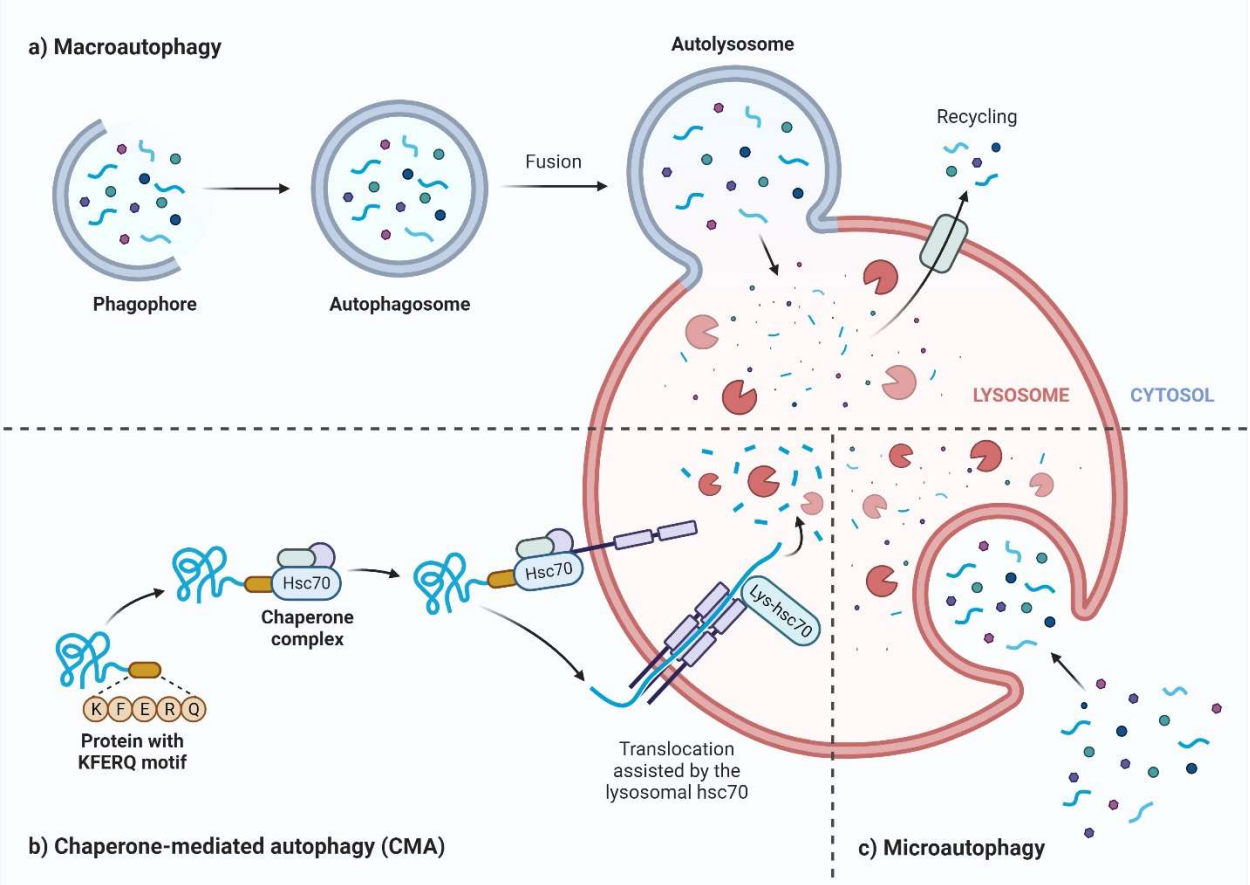

Figure 2.6 - The three types of autophagy. Macroautophagy is composed by the formation of autophagosomes, which capture components in the cytosol and transport them to lysosomes where these components are degraded. Chaperone-mediated autophagy depends on the recognition of the KFERQ motif in proteins by HSC70, which mediates their translocation to lysosomes. In microautophagy, components in the cytosol are absorbed directly by the lysosome. Obtained from Biorender under permission.

Microautophagy is executed at the surface of lysosomes, either by invagination or protrusion. Invagination requires an endosomal sorting complex required for transport (ESCRT) and protrusion requires SNARE proteins. In both cases, LC3 and GABARAP are recruited for cargo

selection. Microautophagy also occurs in endosomal membranes and requires either ESCRT or nSMase2 for invagination (Yamamoto and Matsui, 2023).

Important cargo receptor molecules for both macroautophagy and microautophagy are SQSTM1, NBR1, NDP52, TAX1BP1, and NCOA4, which are involved in the degradation of ferritin (Yamamoto and Matsui, 2023).

CMA is mediated by a complex formed by HSC70, HSP40, and CHIP, which binds to proteins containing KFERQ motives and is transported into the lysosome by lysosome-associated membrane protein 2A (LAMP2A) (Yamamoto and Matsui, 2023).

Autophagy is regulated in response to exposure to stresses such as nutrient starvation, hypoxia, oxidative stress, and growth factors deprivation (Pietrocola et al., 2013). An important sensor and regulator of autophagy is AMPK, which induces autophagy by inhibiting mTOR, a suppressor of autophagy (Egan et al., 2011, Inoki et al., 2003). The recognition of pathogen-associated molecular patterns (PAMPs) as a sign of infection by pattern recognition receptors (PRR) also activates autophagy (Nakamoto et al., 2012, Rasmussen et al., 2011). ER stress via PERK signaling can upregulate autophagy as well (Rouschop et al., 2010). As these mechanisms of regulation are based on post-translational modifications, activation of autophagy in these cases is fast.

Autophagy is also transcriptionally regulated. Transcription factors that regulate the expression of autophagy components include p53, nuclear factor kappa-light-chain-enhancer of activated B cells (NF-κB), HIF-1, HSF1, signal transducer and activator of transcription 3 (STAT3) and forkhead box O (FOXO) 1, 3 and 4 (Vousden and Prives, 2009, Karin, 2006, Semenza, 2007, Yu et al., 2009, Dansen, 2011). A strong driver of autophagy is transcription factor EB (TFEB),

which upregulates the expression of autophagy components and lysosomal biogenesis and is activated by nutrient deprivation (Settembre et al., 2011).

2.8 Cell Death

Cell death is a central feature in neurodegenerative diseases, and understanding its causes in each situation is an important requirement for the development of treatments (Moujalled et al., 2021).

In certain situations, cell death is a desirable event for the organism. During development, some cells must be eliminated, so an organ can acquire its proper shape and organization (Obeng, 2021). In some cases, cells must be destroyed as they represent a threat to the organism, as in the case of neoplasia and self-reactive lymphocytes (Nossal, 1994, Kroemer et al., 2013). Virus-infected cells are intentionally killed by cytotoxic cells from the immune system to avoid the spreading of the virus to other cells in the body (Tummers and Green, 2022).

Cells can also intentionally commit suicide when exposed to stress conditions like DNA damage, accumulation of misfolded proteins, oxidative stress, or metabolic stress (Tang et al., 2019). This behavior can be viewed as an altruistic attitude of the suicidal cells to avoid further damage that they can cause to other cells in the body. Therefore, cells are equipped with molecular mechanisms that trigger cell death when exposed to specific stress conditions. This is known as regulated cell death (RCD), in opposition to accidental cell death (ACD), in which cell death occurs as a failure to survive in harmful conditions (Tang et al., 2019).

In some cases, RCD is part of a physiological program, especially during development, but also in tissues with a high turnover of cells, as in the blood and skin. This type of RCD is called programmed cell death (PCD) (Obeng, 2021).

Cell death was initially classified by morphology into three types. Type I or apoptosis, in which the cell shrinks and forms extracellular vesicles known as apoptotic bodies, type II or autophagic cell death, in which a large number of intracellular vesicles are observed, and type III or necrosis, characterized by cell swelling, plasma membrane disruption and loss of organellar organization (Green and Llambi, 2015).

Currently, cell death is classified by its molecular mechanisms. Many signaling pathways have now been described, which characterizes cell death as a heterogeneous process (Galluzzi et al., 2018). The specific molecular pathway that causes the death of a cell depends on the type of signaling or stress this cell is subjected to (Kist and Vucic, 2021). Some pathways depend on the interaction between cells. Some are very specific to certain types of cells. Also, some types of cells are more prone to certain pathways than others (Kist and Vucic, 2021).

Detecting which pathways are involved in the death of cells in a disease helps in understanding its underlying pathology and eventually unveils potential therapeutical targets (Kist and Vucic, 2021). These pathways will be briefly described in this section.

2.8.1 Apoptosis

Apoptosis is a cell death pathway in which cell components disassemble in an organized fashion. Internal structures and molecules are degraded and packed in vesicles called apoptotic bodies that can easily be engulfed by phagocytic cells (Poon et al., 2014). This organized degradation of cells during apoptosis is orchestrated by a group of cysteine-aspartic proteases, simply called caspases (CASP). CASPs are divided into two groups: initiator CASPs, mainly CASP-8 and CASP-9, and executioner CASPs, mainly CASP-3, CASP-6, and CASP-7 (Elmore, 2007).

Cells express procaspases that, in response to stimuli, are cleaved and give origin to the activated CASPs. Activation of initiator CASPs triggers a cascade of molecular transformations resulting in the activation of executioner CASPs, which perform the events that cause DNA fragmentation, degradation of the cytoskeleton, expression of signaling molecules for phagocytic cells, and the formation of apoptotic bodies (Poon et al., 2014)

Apoptosis can be initiated by two distinct pathways, both dependent on CASPs. The intrinsic pathway is activated by the detection of intracellular signals, in many cases indicating damage or infection (Lockshin and Zakeri, 2004). The extrinsic pathway is activated by signaling molecules present in the microenvironment or expressed on the surface or near other cells (Oppenheim et al., 2001).

The initiation of the intrinsic apoptotic pathway is regulated by the interaction of molecules from the B-cell lymphoma 2 (BCL-2) family (Youle and Strasser, 2008). This family of molecules can be divided into three groups: pro-apoptotic, anti-apoptotic, and BH3-only molecules. Mainly pro-apoptotic molecules are BCL2-associated X protein (BAX), BCL2 antagonist/killer (BAK), and to a minor extent BCL-2 related ovarian killer (BOK). These molecules are located at the mitochondria outer membrane (MOM) and are capable of oligomerizing and forming pores in the MOM, causing the release of cytochrome c and DIABLO, which will cascade the downstream process of apoptosis (Youle and Strasser, 2008). To avoid this oligomerization, the anti-apoptotic molecules, BCL-2, BCL-X_L, MCL-1, BCL-W, BCL-B, and BCL-A1, bind to the pro-apoptotic molecules keeping them in an inactive complex (Youle and Strasser, 2008). The role of BH3-only is to disrupt this interaction between anti- and pro-apoptotic molecules and allow the oligomerization of pro-apoptotic molecules and the downstream process that leads to apoptosis. Many molecules can be classified as BH3-only and they are activated in response to

different triggers which can be DNA damage, oxidative stress, metabolic stress, and infection, among others (Figure 2.7) (Kønig et al., 2019).

In this way, a particular stress activates a BH3-only molecule that disrupts the interaction of anti-apoptotic and pro-apoptotic molecules, leading to the formation of pores by pro-apoptotic molecules and the release of cytochrome c and DIABLO (D'Arcy, 2019). These molecules bind to apoptotic protease activating factor 1 (APAF1), changing its conformation allowing for the binding to ATP and exposing their caspase recruitment domain (CARD). This change in conformation induces the oligomerization of APAF1 and the formation of the apoptosome (D'Arcy, 2019). The CARDs in the center of the apoptosome bind to procaspase 9 causing their activation. The activated CASP-9 then cleaves the executioner procaspase 3, which in its activated form will execute the proteolytic reactions that result in apoptosis and its typical characteristics (D'Arcy, 2019).

The extrinsic apoptotic pathway is initiated by signaling through the binding of extracellular ligands to cell membrane receptors from the TNF superfamily including TNF-related apoptosis-inducing ligand (TRAIL), Fas ligand and Fas receptor, and TNF and its receptor. The binding between ligand and receptor triggers the recruitment of Fas-associated death domain (FADD) or TNFR-associated death domain (TRADD) (Locksley et al., 2001, Hsu et al., 1995). These recruitments lead to the formation of signaling complexes called complex I in the case of Fas and death-induced signaling complex (DISC) in the case of TNF. These complexes include procaspase-8 which is cleaved and activated. CASP-8 then cleaves the executioner caspases, causing the subsequent catalytic reactions that lead to apoptosis (Hsu et al., 1995, Wajant, 2002).

The extrinsic apoptotic pathway can be inhibited by FLICE-like inhibitory protein (cFLIP). cFLIP has a similar structure to CASP-8, but without its enzymatic activity and it forms a

proteolytically inactive heterodimer with CASP-8 (Micheau et al., 2002). A protein called Toso also inhibits the biogenesis of CASP-8 and extrinsic apoptosis as a consequence (Hitoshi et al., 1998).

Inhibition of apoptosis is also performed by a series of proteins collectively known as inhibitors of apoptosis (IAP). These molecules are inhibited by second mitochondrion-derived activator of caspase/direct inhibitor of apoptosis-binding protein with low pI (SMAC/DIABLO), which is delivered in the cytosol after apoptosis is triggered and binds to IAPs, leading to their inactivation (Chai et al., 2000).

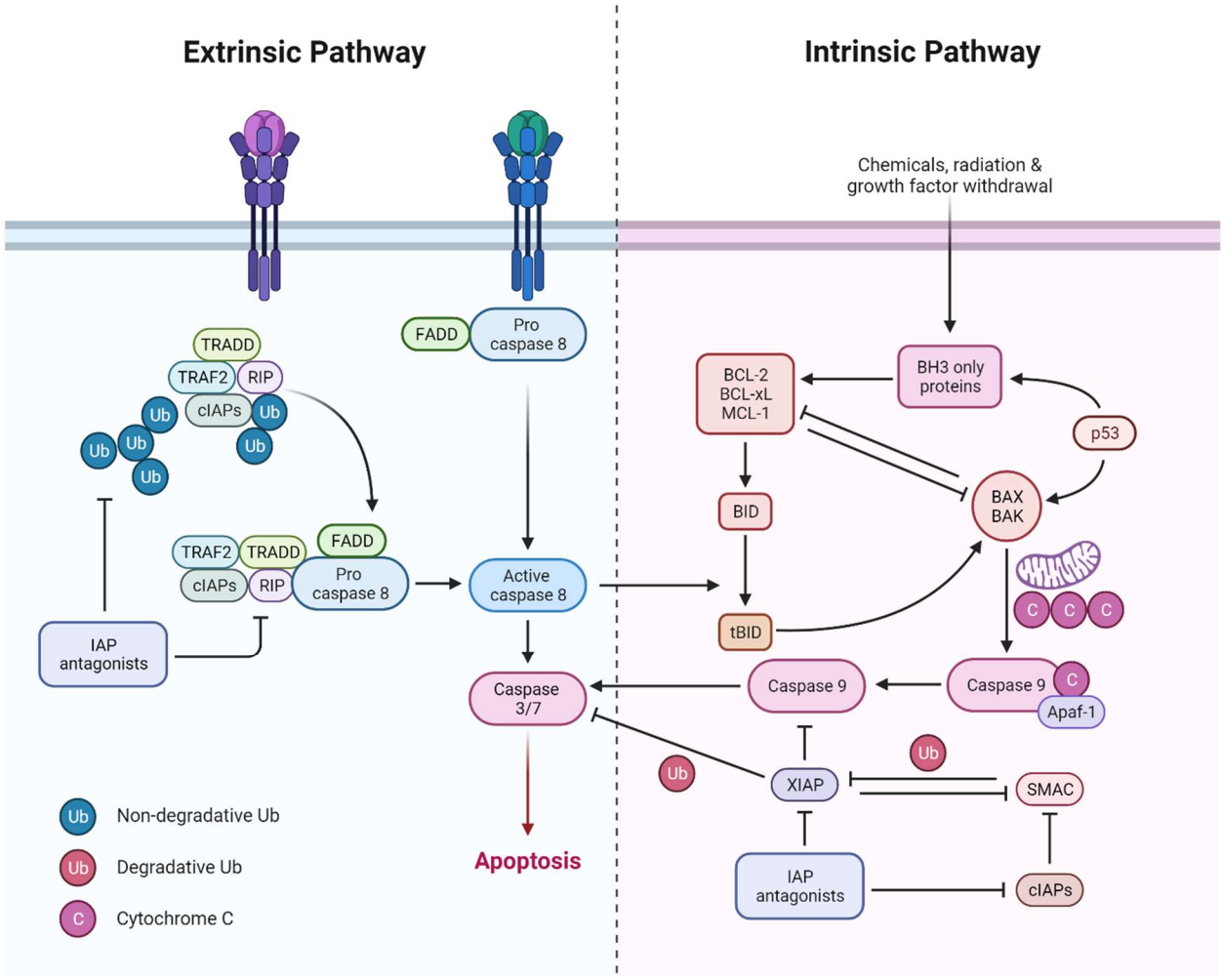

Figure 2.7 - Extrinsic and intrinsic pathway of apoptosis. The extrinsic apoptotic pathway is initiated by TNF, FasL or TRAIL binding to its receptors, inducing the activation of caspase 8, which activates caspase 3 and 7, leading to apoptosis. The intrinsic pathway is initiated by the recognition of stress signals by BH3-only molecules, inducing the formation of pores in the mitochondria by BAX and BAK, releasing cytochrome c in the cytosol and activating caspase 9, which activates caspase 3 and 7, leading to apoptosis. The anti-apoptotic molecules BCL-2, BLC-X_L and MCL-1 can inhibit the action of BAX and BAK, preventing apoptosis. XIAP can also prevent apoptosis by inhibiting caspase 9. Obtained from Biorender under permission.

2.8.2 Necroptosis

Necroptosis is a non-apoptotic form of RCD and, as in extrinsic apoptosis, is triggered by the binding of TNFα to TNFR1 or FasL to Fas (Laster et al., 1988, Holler et al., 2000). Necroptosis

can also be started by the binding of double-stranded DNA to Toll-like receptor (TLR) 3 and LPS to TLR4 (He et al., 2011). However, necroptosis is not mediated by CASP-8 activation. Inhibition of CASP-8, which may be caused by pathogens, induces necroptosis (Tummers and Green, 2017). Many pathogens have developed mechanisms to block apoptosis by targeting FADD, CASP-8, or cFLIP, which allow them to escape from their elimination from the organism by the immune system (Tummers and Green, 2017). Therefore, necroptosis is a counteraction against these pathogenic mechanisms. A key molecule in the pathway of necroptosis is receptor-interacting serine/threonine-protein kinase 1(RIPK1), which forms a complex with FADD/TRADD and CASP-8 or CASP-10 after activation of TNFR1 or Fas. RIPK1 recruits and phosphorylates RIPK3, forming a complex called ripoptosome (Bertheloot et al., 2021). This complex recruits and phosphorylates mixed lineage kinase domain like pseudokinase (MLKL). Phosphorylated MLKL induces the opening of Ca^{2+} and Na^{2+} channels and forms pores in the plasma membrane, causing cell swelling and membrane rupture, a morphology of necrosis (Figure 2.8) (Cai et al., 2014, Bertheloot et al., 2021).

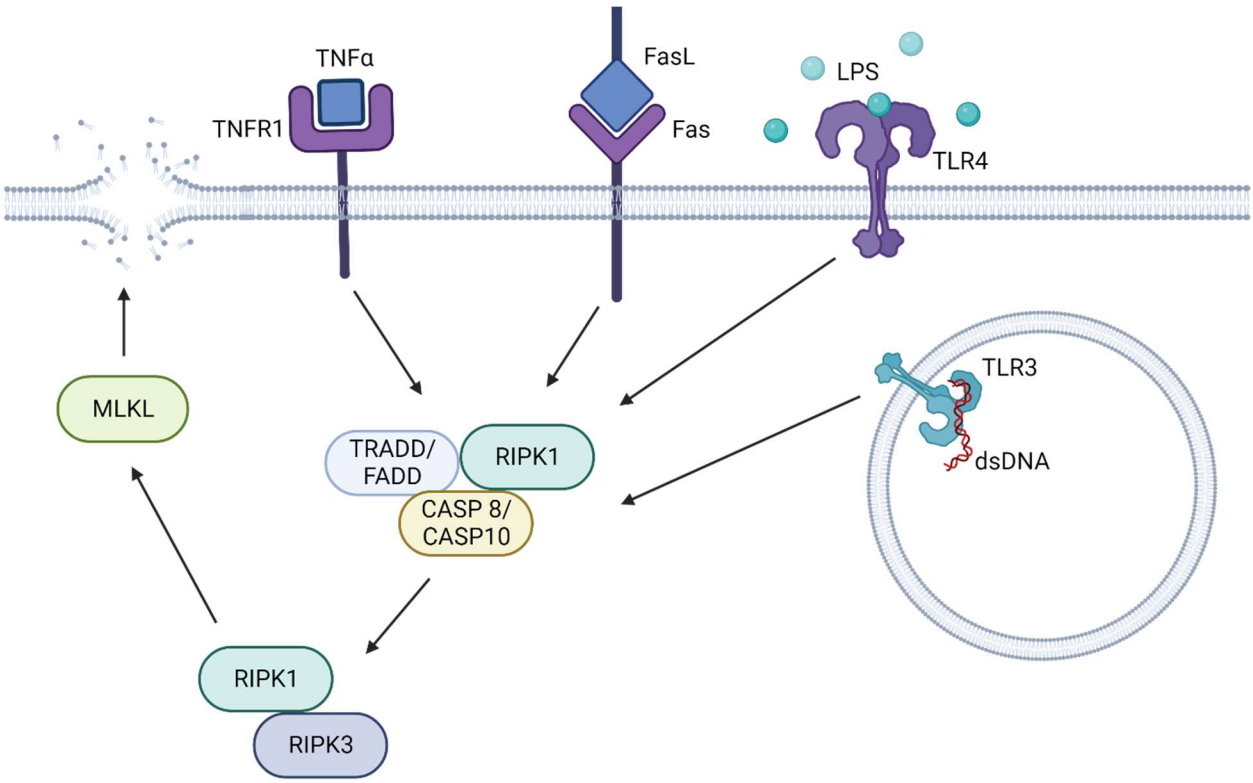

Figure 2.8 - Necroptosis pathway. TNFα, FasL and PAMPs can induce the binding of RIPK1 to TRADD/FADD and CASP8/10. RIPK1 then binds to RIPK3 activating MLKL which induces the degradation of the cell membrane. Created with Biorender.

RIPK1 can be inhibited by cIAP1/2 and XIAP, limiting the death effect of TNF by the necroptotic pathway (Mahoney et al., 2008). In opposition, cylindromatosis (CYLD) and Smac promote necroptosis by inhibiting cIAP1/2 and XIAP (Trompouki et al., 2003, Wang et al., 2008).

Necroptosis is an important pathway for the organism's defense against infection, as the release of damage-associated and pathogen-associated molecular patterns (DAMP, PAMP) and cytokines after the cell demise leads to a pro-inflammatory reaction. A similar reaction is induced in sterile inflammation, as in cancer, as the pro-inflammatory effects of necroptosis, in

special mediated by the activation of NFκB, is an efficient antitumor mechanism (Bertheloot et al., 2021).

2.8.3 Pyroptosis

Pyroptosis is another RCD pathway that has a necrotic morphology, presenting plasma membrane disruption instead of the formation of apoptotic bodies. Pyroptosis is mainly triggered by PAMPs and DAMPs, which are signs of microbial infection or breakdown of cells, possibly caused by pathogens (Bertheloot et al., 2021). Cells that undergo pyroptosis also release IL-1β and IL-18, therefore promoting a systemic inflammatory reaction, which includes fever. This reaction explains the name of this pathway, as pyros is the Greek word for fire (Fink and Cookson, 2005).

Pyroptosis is initiated by the recognition of pathogens linked molecules signs such as PAMPs, DAMPs, and microbial fragments like LPS, flagellin, or bacterial/viral genetic material (Wu et al., 2022). The detection of these signs is executed by a complex called inflammasome, which contains NACHT, LRR, FIIND, CARD domain, and PYD domains-containing proteins (NLRP) 1, 3, and 4 or absent in melanoma (AIM) 2. When the inflammasome recognizes a pathogen sign, it recruits and cleaves procaspase-1, activating CASP-1 (Rathinam and Fitzgerald, 2016). CASP-1 cleaves gasdermin D (GSDMD), causing its fragmentation and translocation to the plasma membrane, forming pores that lead to cell death. In parallel, CASP-1 also cleaves pro-IL-1-β and pro-IL-18. The active forms of IL-1β and IL-18 are then released through the pores formed in the plasma membrane (Figure 2.9) (Wu et al., 2022).

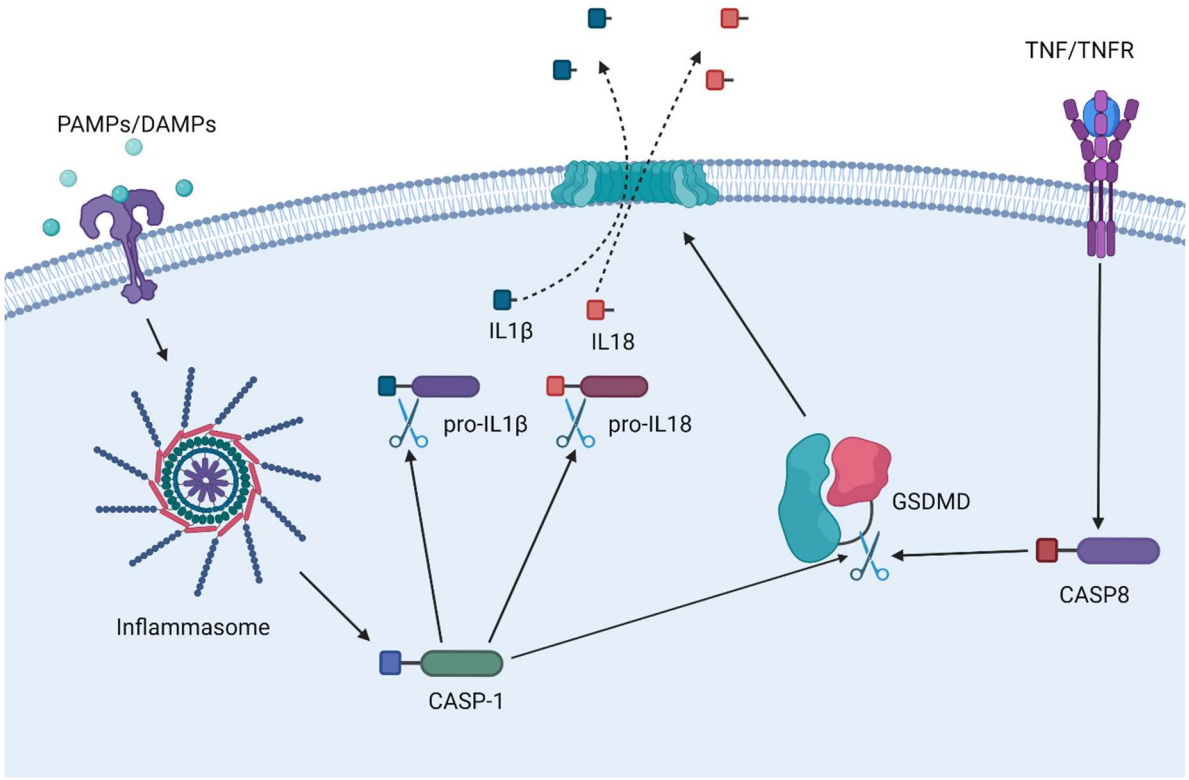

Figure 2.9 - Pyroptosis pathways. Pyroptosis is started by PAMPs, DAMPs, or TNF. These elements are recognized by the inflammasome, and activate caspase 1, which promotes the translocation of gasdermin D to the cell membrane, causing the opening of pores. Gasdermin D can also be activated by CASP-8, as a consequence of TNF binding to its receptor. IL-1β and IL-18 are also activated by caspase 1, and are released from the cell inducing inflammatory reactions. Created with Biorender.

Alternatively, GSDMD can be cleaved by CASP-4/5 or CASP-8. CASP-8 can also cleave GSDMC. Pores in the membrane can also be formed by GSDME, GSDMC, or GSDMB, which is activated upon cleavage by CASP-3 or granzyme B and granzyme A, respectively. Therefore, Pyroptosis can also be induced by TNF or granzyme-secreting cells such as CD8 T-cells (Wu et al., 2022).

Pyroptosis can be regulated by the action of ESCRT, which repairs the plasma membrane damaged by GSDMD (Rühl et al., 2018). However, the release of IL-1β and IL-18 can occur without the cell demise, as it only requires the formation of pores (Heilig et al., 2018). Pyroptosis is also regulated by ubiquitination and phosphorylation of NLRP1, NLRP3, and NLRP4 (Baker et al., 2017, Song et al., 2016).

2.8.4 Parthanatos

Parthanatos has morphological features similar both to apoptosis and necrosis. As in apoptosis, parthanatos presents DNA fragmentation, nuclei condensation, and shrinkage. However, the plasma membrane is disintegrated during parthanatos, but neither apoptotic bodies nor membrane blebbing is detected during this RCD pathway (Wang et al., 2009, Andrabi et al., 2008, David et al., 2009).

From the biochemical point of view, parthanatos is mediated by the activation of poly(ADP-ribose) polymerase 1 (PARP1) (Andrabi et al., 2008). PARP1 is located at the nucleus and is activated upon DNA damage (Yu et al., 2003, Szabó and Dawson, 1998). It has an important role in DNA repair (Oliver et al., 1999). However, in some cases when cells are subjected to significant injury, PARP1 activation leads to cell death (Andrabi et al., 2006). PARP1 activation causes the accumulation of poly (ADP-ribose) (PAR) polymers (Fatokun et al., 2014). These polymers or free PAR translocate from the nucleus to the mitochondria (David et al., 2009). The mitochondrial uptake of PAR leads to the release of apoptosis-inducing factor (AIF), which translocates from the mitochondria to the nucleus. Inside the nucleus, AIF induces chromatin condensation and DNA fragmentation, ultimately resulting in cell death (Loeffler et al., 2001) (Figure 2.10).

Parthanatos is triggered by diverse types of stress that lead to genomic stress and DNA damage that are common in conditions such as inflammation, ischemia-reperfusion, glutamate excitotoxicity, and myocardial infarction (David et al., 2009). Genomic stress may be caused by oxidative stress from ROS, nitrosative stress from NO or peroxynitrite, inflammation, hypoxia, hypoglycemia, and DNA-alkylating agents (Huang et al., 2022).

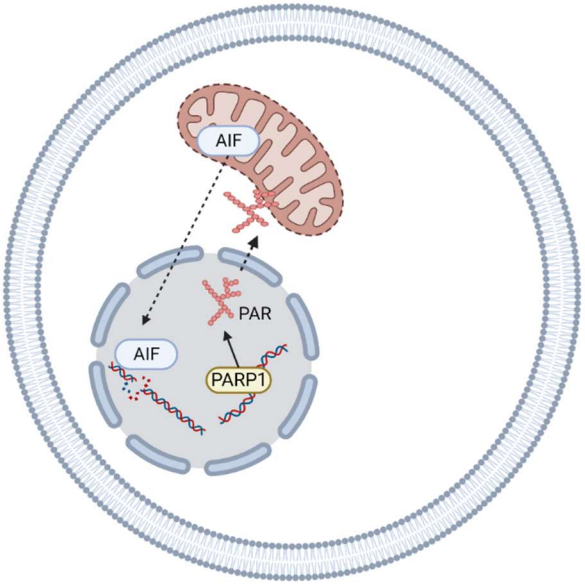

Figure 2.10 - Parthanatos pathway. Parthanatos is initiated by the recognition of DNA damage in the nucleus by PARP1, which produces PAR. In abundance, PAR translocates to mitochondria, inducing the translocation of AIF to the nucleus, where it promotes chromatin condensation and DNA fragmentation. Created with Biorender.

2.8.5 Lysosome-dependent cell death

The main hallmark of lysosome-dependent cell death (LDCD) is lysosome membrane permeabilization (LMP). LMP causes the release of lysosomal proteases, particularly cathepsins, which can cause uncontrolled cleavage of cellular components (Boya and Kroemer, 2008). Lysosomal proteases are functional under low pH, but high levels of LMP can lead to an increase

in cytosolic acidity, creating a favorable environment for lysosomal protease activity with cytotoxic effects (Wang et al., 2018).

LMP can be triggered by external and internal stimuli, including ROS, molecules from the pro-apoptotic BCL-2 family (BAX, BAK), DNA damage, some ATPase and kinase inhibitors, photodamage, some lipids, some antibiotics, some bacterial proteins, some viral infections and other lysosomotropic agents that can cause LMP (Boya, 2012) (Figure 2.11).

LMP can cause apoptosis by the cleavage of anti-apoptotic molecules from the BCL-2 family or IAPs (Galluzzi et al., 2018). LMP can also lead to ferroptosis due to the release of ROS from lysosomes, or pyroptosis, as some cathepsins may be involved in the activation of the inflammasome (Wang et al., 2018).

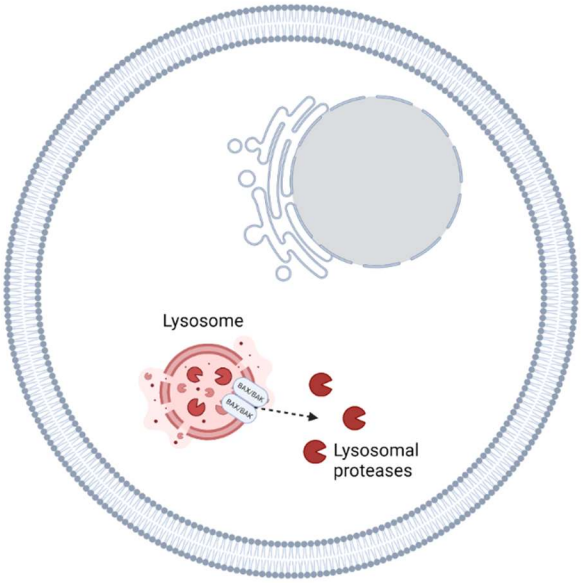

Figure 2.11 - Lysosome-dependent cell death. Lysosome membrane permeabilization can be caused by pores formed by BAX/BAK or ROS. This permeabilization causes the realise of lysosomal proteases in the cytosol, which can cause degradation of cellular components in the presence of a low pH. Created with Biorender

2.8.6 Immunogenic cell death

Immunogenic cell death (ICD) is a type of RCD executed by the organism's immune system in response to cellular signals (Kroemer et al., 2022). This RCD pathway is mediated by cells of the immune system, and its mechanisms are not contained in the cell that is dying, in contrast to other RCDs discussed so far. Cells subjected to certain stresses, mostly related to infection or tumorigenic mutations, may release antigens that are detected by the immune system, which interprets this release as a signal of a threat to the organism (Galluzzi et al., 2017b). The adaptive immune system is activated and executes a cytotoxic response that culminates in the elimination of the targeted cells and the establishment of immunological memory (Galluzzi et al., 2020).

Natural stressors that lead to ICD are obligate intracellular pathogens, oncolytic viruses, and molecules with oncolytic potential. Besides, many types of chemotherapeutic agents can also induce ICD (Galluzzi et al., 2020). Also, ICD is involved in auto-immune disorders, caused when the immune system interprets a self-antigen as a pathogenic or oncogenic signal (Kroemer et al., 2022).

After infection, cells can sense microorganism-associated molecular patterns (MAMPs) by PRRs, which induces the cell to communicate to other cells of the organism about a potential treatment via the release of cytokines (Galluzzi et al., 2017b). When an infected cell dies, cellular components are detected by antigen-presenting cells (APCs), which causes the activation of T-cells and a cytotoxic response that induces ICD (Roche and Furuta, 2015).

Chemotherapeutic agents cause the exposure of DAMPs by cancer cells including calreticulin (CALR), protein disulfide isomerase family A member 3 (PDIA3), HSP70, and HSP90 (Obeid et al., 2007b, Panaretakis et al., 2008, Fucikova et al., 2011). These cells also release ATP, CXC-chemokine ligand 10 (CXCL10), high-mobility group box 1 (HMGB1), and annexin A1

(ANXA1) (Michaud et al., 2011, Sistigu et al., 2014, Apetoh et al., 2007, Vacchelli et al., 2015). These DAMPs are captured by APCs, which activate a cytotoxic response of αβ and γδ T cells.

ICD can also be induced by physical cues, including irradiation, photodynamic therapy, and hydrostatic pressure (Obeid et al., 2007a, Garg et al., 2012, Fucikova et al., 2014). Irradiation can induce ICD by the exposure of CALR or HSP70 and secretion of ATP, HMGB1, IFN, or IL-1β (Obeid et al., 2007a, Golden et al., 2014, Lim et al., 2014, Brusa et al., 2009, Chen et al., 2012). In the case of photodynamic therapy and hydrostatic pressure, ICD is triggered by exposure to CALR, HSP70, or HSP90 and the release of ATP and HMGB1 (Garg et al., 2012, Fucikova et al., 2011, Fucikova et al., 2014, Korbelik et al., 2011).

2.8.7 Entotic cell death

Entosis is a process in which a viable cell is engulfed by another cell. This engulfed cell can be killed by an RCD named entotic cell death (Krishna and Overholtzer, 2016). This type of cell cannibalism is seen in unicellular organisms in response to nutrient starvation, as in *Bacillus subtilis* and *Dictyostelium caveatum* (González-Pastor, 2011, Waddell and Duffy, 1986). This process is also seen in metazoan organisms and consists of the engulfment of viable cells by a diversity of mechanisms (Krishna and Overholtzer, 2016).

The mechanism of entosis depends on the adherens junction molecules E-cadherin and α-catenin (Overholtzer et al., 2007). The cell that is engulfed plays an active role in the process of entosis through the activity of RhoA-GTPase and Rho-kinase I and II (ROCK I/II), which drive the uptake of the adherens molecules (Overholtzer et al., 2007, Sun et al., 2014). Actin and myosin accumulate on the side of the engulfed cell as opposed to the contact with the engulfing cell. The actomyosin contraction is promoted and helps the process of engulfment (Purvanov et al., 2014,

Sun et al., 2014). Therefore, the entosis engulfment resembles a cell invasion due to the active involvement of the engulfed cell (Figure 2.12) (Krishna and Overholtzer, 2016).

Most of the cells engulfed by entosis die in a non-apoptotic process, without activation of CASP-3 (Overholtzer et al., 2007). Engulfed cells present upregulation of autophagy, as a reaction to nutrient starvation (Florey et al., 2011). At the side of the engulfing cell, autophagy is also activated, with LC3 into the vacuole that contains the engulfed cell. The lipidation of LC3 promotes the fusion of lysosomes with the entotic vacuole, resulting in the further degradation of the engulfed cell (Florey et al., 2011).

Entotic structures have been found in human cancers and seem to have contradictory effects on tumor growth (Huang et al., 2015, Schwegler et al., 2015). Entosis inhibits tumor growth of the engulfed cell in vitro (Overholtzer et al., 2007, Sun et al., 2014, Florey et al., 2011), but also induces aneuploidy in the engulfing cell, which has tumorigenic effects (Krajcovic et al., 2011).

Entosis and entotic cell death are also involved in embryo implantation, in which epithelial cells in the lumen of the uterus are engulfed by trophectoderm cells of the blastocyst (Li et al., 2015).

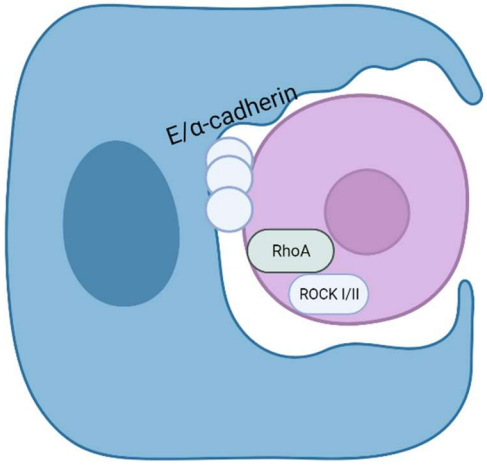

Figure 2.12 - Entotic cell death. The entotic cell death consists of the engulfment of one cell by another, which is mediated by the adherens junction molecules E/α-cadherin in the cell membrane and the activity of RhoA and ROCK I/II. Created with Biorender

2.8.8 NETosis

NETosis is an RCD pathway found in neutrophils. This RCD is a consequence of the formation of neutrophil extracellular traps (NETs), which are formed by chromatin released from the cell with inclusions of bactericidal proteins. The formation and release of NETs cause the death of the neutrophil (Vorobjeva and Chernyak, 2020). NETs have a protective role against microbial infection and are commonly formed in response to attacks on epithelial barriers in the eyes, skin, and mucosa (Vorobjeva and Chernyak, 2020). NETosis can also have pathological effects, being involved in thrombosis, pulmonary diseases, and autoimmune diseases (Martinod and Wagner, 2014, Moschonas and Tselepis, 2019, Ebrahimi et al., 2018, Vassallo et al., 2019, Uddin et al., 2019, Toussaint et al., 2017, Gupta and Kaplan, 2016).

The formation of NETs and NETosis depend on the release of ROS by NADPH oxygenase (Fuchs et al., 2007). NADPH oxygenase is activated by phosphorylation by protein kinase C (PKC) in conjunction with mitochondrial ROS (mtROS) (Dikalova et al., 2010). mtROS is released in response to the formation of mitochondrial permeability transition pores (mPTP), which are caused by Ca^{2+} overload in the mitochondria (Gupta and Kaplan, 2016).

The cascade of events that leads to cell death during NETosis starts with the release of enzymes from granules into the cytosol (Vorobjeva and Chernyak, 2020). These enzymes include serine proteases that break down cytoskeleton components and peptidyl-arginine deaminase 4 (PAD4), which translocate to the nucleus and cause chromatin decondensation, which, together with proteolytic degradation of the nuclear lamina, leads to the rupture of the nucleus envelope, releasing the chromatin in the cytosol (Vorobjeva and Chernyak, 2020). Finally, pores in the plasma membrane are formed by GSDMD and NETs are released to the extracellular space, along with the cell death (Vorobjeva and Chernyak, 2020)

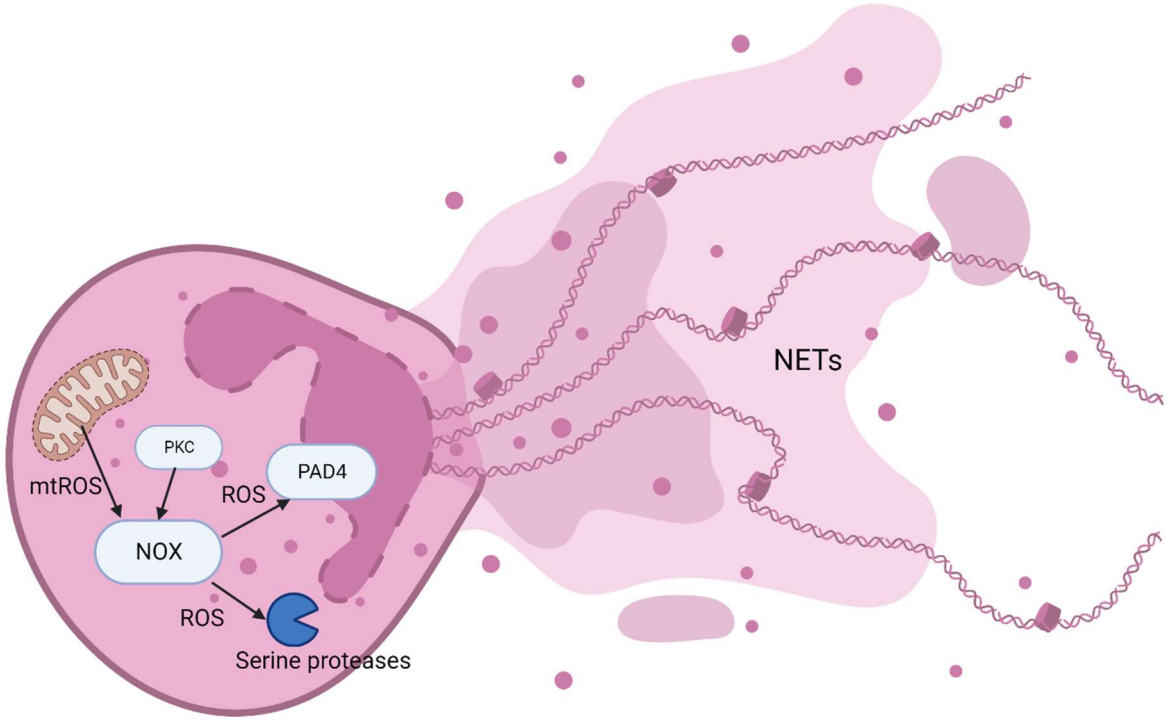

Figure 2.13 NETosis. Neutrophils release NETs as a defensive mechanism against microorganisms. This release causes the cell death. NETosis is initiated by the activation of NADPH oxidase by mtROS or PKC, which leads to the activation of PAD4, responsible for the formation of NETs, and serine proteases, which mediate the cell decomposition. Adapted from Biorender under permission.

2.8.9 Ferroptosis

Ferroptosis is an RCD pathway associated with oxidative stress. Oxidative stress occurs when ROS accumulates inside the cells, which causes damage to several cellular components, which include membranes, lipids, proteins, and DNA (Pizzino et al., 2017). One of these damages is lipid peroxidation, which destroys the cell membrane and can lead to cell death (Gaschler and Stockwell, 2017). Lipid peroxidation is caused by hydroxyl radicals (OH^-) that are generated due to the Fenton reaction, a reaction between ROS produced as a by-product of cellular respiration,

and iron (Tsuneda, 2020, Gaschler and Stockwell, 2017). This pathway is called ferroptosis because of the high levels of intracellular iron required for its induction (Dixon et al., 2012).

The level of lipid peroxidation that leads to ferroptosis depends on the balance between oxidative and anti-oxidative processes (Liang et al., 2022). On one side, superoxide is generated by the ETC in the mitochondria but is converted into H_2O_2 by superoxide dismutase (SOD), and H_2O_2 is converted into water by catalase (Sies, 1997). However, in the presence of iron, part of H_2O_2 is converted to OH^-, which can react with polyunsaturated fatty acids (PUFA) and generate lipid peroxides. Lipid peroxides are unstable and react with other PUFAs, generating more lipid peroxides, in a chain reaction that eventually destroys membranes (Gaschler and Stockwell, 2017). On the other side, the cell produces GSH, which is capable of neutralizing lipid peroxides, interrupting the chain reaction, and protecting cell membranes (Figure 13) (Forman et al., 2009).

Ferroptosis comprises interactions between the antioxidant system, iron, lipid, and glucose metabolism (Chen et al., 2021a). Therefore, regulation of this RCD may be executed in modulating any of these pathways. Some key elements are GPX4, which catalyzes the neutralization of lipid peroxides in the presence of GSH, and the system x^-_c, which is responsible for the uptake of cystine, a precursor of GSH (Chen et al., 2021a). Also, modulation of ROS generation, changes in lipid, iron metabolism or autophagy, and transcriptional or epigenetic modifications can regulate ferroptosis (Chen et al., 2021a).

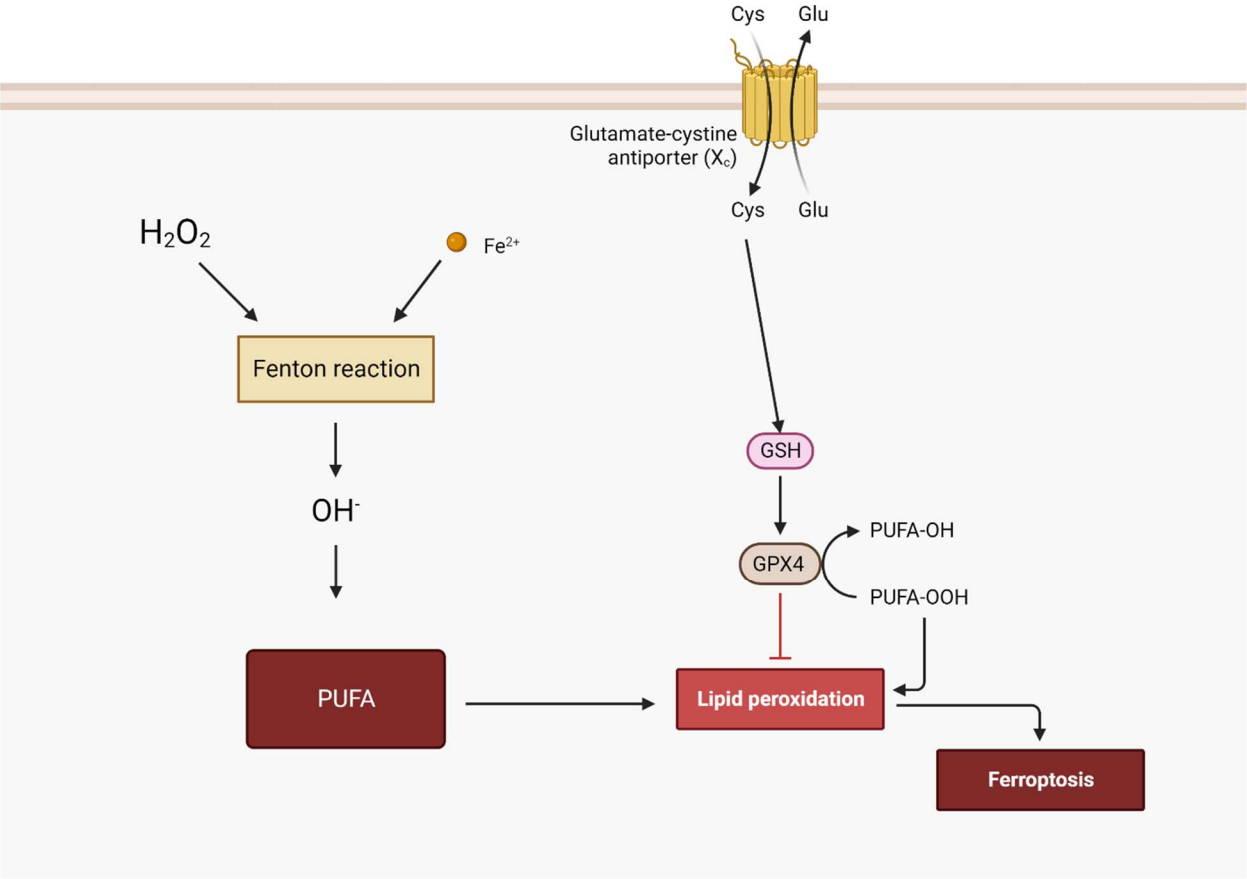

Figure 2.14 - Ferroptosis. An increase in intracellular ROS in the presence of Fe^{2+} results in the formation of OH^-, which can cause lipid peroxidation to PUFA, and cell death by ferroptosis as a consequence. Lipid peroxidation can be neutralized by GSH. Adapted from Biorender under permission.

2.8.10 MPT-driven necrosis

MPT-driven necrosis is an RCD pathway associated with the opening of mitochondrial permeability transition pores (MPTP). These pores transverse both mitochondrial membranes and are opened in response to perturbations in Ca^{2+} and redox homeostasis, and the opening of MPTP causes loss of mitochondrial transmembrane potential, which causes osmotic imbalance and breakdown of mitochondria, leading to cell death, often with necrotic morphology (Izzo et al., 2016, Bonora et al., 2015, Bernardi et al., 2015).

The structure and components of MPTP are not known. The only molecule that is certainly involved in the formation of these pores is peptidylprolyl isomerase F (PPIF, also named cyclophilin D, CYPD) (Baines et al., 2005). Possible components of MPTP are adenine nucleotide translocator (ANT), F_1F_0-ATPase, inorganic phosphate carrier (PHC/SLC25A3), SPG7, and voltage-dependent anion channel (VDAC) (Weaver et al., 2005, García et al., 2006, Leung et al., 2008, Shanmughapriya et al., 2015). The upstream regulation of MPTP is not well understood neither. Potential participants of this regulation are peripheral benzodiazepine receptor (PBR/TSPO), hexokinase (HXK) 1 and 2, protein kinase Cε (PRKCE), glycogen synthase kinase 3β, and proteins from the BCL-2 family, BCL2, BCL-X_L, BAX, BAK and BH3 interacting domain death agonist (BID), and tumor protein p53 (Decaudin et al., 2002, Smeele et al., 2011, Baines et al., 2003, Das et al., 2008, Shimizu et al., 1999, Arbel et al., 2012, Karch et al., 2013, Zamzami et al., 2000, Vaseva et al., 2012).

Triggers of MPT-driven necrosis include cytosolic and mitochondrial Ca^{2+} accumulation, alkalization, and accumulation of inorganic phosphate and long-chain fatty acids (Brenner and Grimm, 2006, Martens et al., 2022). The best-known inhibitor of MPT-driven is Cyclosporin A, which binds to CYPD, constraining the opening of MPTP (Galluzzi et al., 2018).

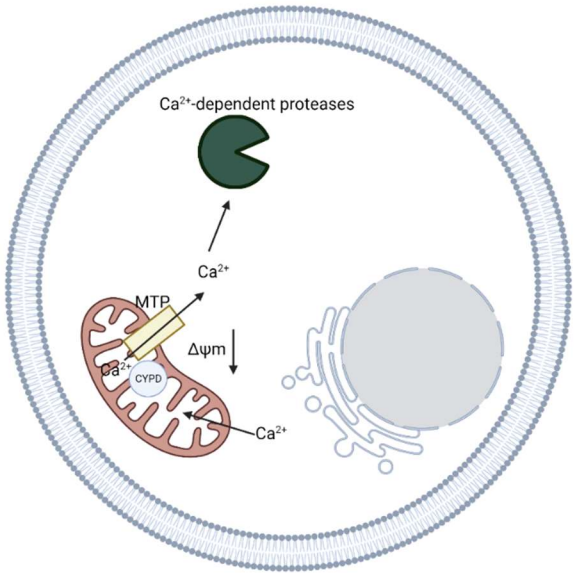

Figure 2.15 - MPT-driven necrosis. Excessive influx of Ca^{2+} into the mitochondria can promote the opening of mitochondrial transition pores, which are regulated by CYPD. Release of Ca^{2+} from mitochondria can reduce the mitochondria membrane potential and activate Ca^{2+}-dependent proteases. Created with Biorender.

2.8.11 Autophagy-dependent cell death (ADCD)

ADCD happens when the demise of the cell is mainly mediated by components of the autophagic machinery. Cell death induced by autophagy is highly context-specific, and the interaction between autophagy and some RCDs is common (Doherty and Baehrecke, 2018). Moreover, a classical classification of cell death based on cell morphology includes what is known as type II cell death, named autophagic cell death, in which cells present a large number of vesicles that resemble autophagosomes in their cytoplasm (Schweichel and Merker, 1973). Therefore, the determination of ADCD as an RCD is considerably controversial (Denton and Kumar, 2019).

A type of ADCD called autosis is mediated by the overactivation of Na^+ K^+-ATPase and can be triggered by starvation (Liu et al., 2013). ADCD can be seen in some transformed cells that present the oncogenic Ras (Byun et al., 2009). ADCD was also detected in A549 lung carcinoma cells after treatment with resveratrol (Dasari et al., 2017). Autophagy can contribute to cell death in *C. Elegans* germline due to genotoxic stress in the absence of apoptosis (Wang et al., 2013). The amoeba *Dictyostelium discoideum* is unequipped of apoptotic machinery and cell death in response to starvation and activation of differentiation-inducing factor (DIF-1) is mediated by autophagy (Cornillon et al., 1994). The most well-documented case of ADCD is the programmed cell death during larval-pupal transition in *Drosophila,* in which inhibition of autophagy reduces cell death (Denton et al., 2013).

In all cases where ADCD was demonstrated, inhibition of autophagy leads to cell death rescue without the activation of any other RCD pathways.

2.8.12 Ca^{2+} and cell death

Ca^{2+} is involved in many regulatory pathways in the cell, including mechanisms of RCD. Intracellular Ca^{2+} overload is a serious perturbation for many cellular functions and organelles, and it can be involved in cell death in different possible ways (Dhaouadi et al., 2023).

The ER is a major store of Ca^{2+}, and in response to dysfunction in the ER process, Ca^{2+} may be released in the cytosol. This release can activate CASP-12 which in turn activates effector caspases, causing apoptosis (Nakagawa et al., 2000).

Ca^{2+} is important for mitochondria function and the concentration of Ca^{2+} is higher in the mitochondria than in the cytosol. Rises in intracellular Ca^{2+} can lead to an overload in mitochondrial Ca^{2+} concentration. To keep this concentration in homeostatic conditions,

mitochondria open MPTP, which can lead to mitochondrial swelling and disruption (Zhivotovsky and Orrenius, 2011).

Multiple enzymes are activated by Ca^{2+}, including proteases, kinases, endonucleases, phosphatases, phospholipases, and NO synthases. Calpain is a Ca^{2+}-dependent protease implicated in different modalities of cell death (Zhivotovsky and Orrenius, 2011). Activated calpain in the intermembrane space of the mitochondria cleaves AIF, leading to parthanatos (Norberg et al., 2010). High levels of calpain activation in the cytosol can cause damage to the cytoskeleton with cytotoxic consequences (Zhivotovsky and Orrenius, 2011).

2.9 In vivo models of MS – characteristics and limitations

Animal models of MS have been very useful for unveiling mechanisms associated with the disease and testing potential therapies. However, these models focus on specific features of the disease and fail to represent the whole complexity of MS. Moreover, MS is a heterogeneous disease that cannot be captured by a single animal model (Procaccini et al., 2015). There are three main animal models of MS: Experimental autoimmune encephalomyelitis (EAE), toxic models of MS, and Theiler's murine encephalomyelitis virus (TMEV) (Procaccini et al., 2015).

The EAE is the most used model of MS because it mimics autoimmune injuries, the best well-characterized aspect of MS. EAE is induced by self-CNS antigens such as MBP, PLP, and MOG (Procaccini et al., 2015). The relapse-remitting course of the disease can be obtained by mice immunization with an epitope of PLP and a chronic phenotype can be induced by injection of the MOG_{35-55} peptide (Tuohy et al., 1989, Tompkins et al., 2002).

Toxic models of MS are characterized by the direct induction of demyelination of OLs and are useful for the study of the process of demyelination and remyelination (Blakemore and Franklin,

2008). Cuprizone, a copper chelator, is a common agent used in toxic models of MS. This agent induces demyelination due to mature OL apoptosis accompanied by activation of ASTs and microglia. Remyelination in this model is executed by the recruitment and differentiation of OPCs (Matsushima and Morell, 2001).

TMEV can induce demyelination in mice and is a neurotropic viral infection model of MS (Tsunoda and Fujinami, 2010). This model represents a chronic progressive course and presents inflammatory demyelination (Owens, 2006). In this model, axonal degeneration occurs before demyelination, representing an inside-out model, in which demyelination is not the initial aspect of the disease (Tsunoda et al., 2003).

Animal models of MS have several limitations. In the case of EAE, this model does not represent the progressive aspects of MS, which is currently the major challenge for treatments. In this model, lesions are randomly distributed in time and location, which complicates the study of remyelination. EAE mainly affects the spinal cord, while MS has a wider distribution throughout the CNS (Procaccini et al., 2015). In the case of toxic models, although they are good models for the study of demyelination and remyelination, they fail to consider external factors, especially the autoimmune influence in the disease and aspects related to its progression (Procaccini et al., 2015, Dedoni et al., 2023). In the case of the TMEV model, this virus only induces demyelination in mice, having no effects on human, which raise doubt about its translational potential. (Procaccini et al., 2015).

2.10 In vitro models of MS – characteristics and limitations

In vitro models are options for the study of cells or tissues in more detail, in a controlled environment. In the case of MS, these models include primary cell culture, immortalized cell lines, ex vivo models, and induced pluripotent stem cells (iPSC) (Dedoni et al., 2023).

2.10.1 Primary cell culture

The main cells of interest for the study of MS are OLs. Therefore, most of the *in vitro* studies in MS research use this type of cell for primary culture. These cells are mainly extracted from rodents, but human cells can also be used (Fedoroff and Richardson, 2008). Rat OPCs can be easily obtained from newborn animals, yielding a satisfactory number of cells for culture (Chen et al., 2007). These cells can be further differentiated into mature myelinating OLs (Chen et al., 2007). Thus, this model is useful for the study of cellular behavior as proliferation, differentiation, and myelination properties of OPCs and mature OLs, as well as their molecular mechanisms. hOLs can be obtained from surgical procedures or fetal tissues, which considerably limits their availability (Fedoroff and Richardson, 2008). However, the use of human cells is of paramount importance, due to the clear differences between them and those obtained from animals (Rao et al., 2017, Sax et al., 2022, Cui et al., 2010, De Paula et al., 2014). These cells can also be used in co-cultures with neurons or in plates containing nanofibers, allowing the study of their myelination process and properties (Pang et al., 2018, Lee et al., 2012a).

Interactions between ASTs and OLs are intense and disruptions in this relationship affect OLs functions and may cause them damage (Dedoni et al., 2023). ASTs can be obtained for primary culture or co-culture with OLs from rodents or human fetal materials, which can be cryopreserved (Dedoni et al., 2023, John, 2012). Co-culture with primary neuronal cultures is also possible, although difficult to prepare (Lopes et al., 2017, Pang et al., 2018).

2.10.2 Immortalized cell lines

Immortalized cell lines are the most practical and cost-efficient models for the study of cell behaviors and characteristics, although their resemblance with the cells they mimic is weak (Dedoni et al., 2023).

HCN, NT2, and SHSY5Y are neuronal-like cell lines and can be differentiated in cells that show neuronal features upon treatment with brain-derived neurotrophic factor (BDNF – for HCN and NT2) and retinoic acid (RA – for SHSY5Y) (Dedoni et al., 2023). CG4 is similar to oligodendrocyte-type 2 astrocyte precursors and can differentiate into OLs (Louis et al., 1992). Other OL-like cell lines include OLN93, Oli-Neu, O-2A/myc, N1, N20.1 obtained from immortalized rodent OPCs, and HOG, TC620, MO3.13, and KG-1C, which are tumoral-derived cell lines (Merrill and Matsushima, 1988, Kashima et al., 1993, Richter-Landsberg and Heinrich, 1996, Söhl et al., 2013, Barnett and Crouch, 1995, De Vries and Boullerne, 2010). C8-D1A and NHA are examples of astrocyte cell lines (Kumar et al., 2004, Sato et al., 2012).

2.10.3 Ex vivo

3D organotypic brain slides can be obtained from mice, humans, and rats and are good models for brain tissue architecture. This model enables manipulations difficult to perform in vivo and is useful for the analysis of axonal myelination in a system that keeps the actual interconnection between cells present in the brain (Sekizar and Williams, 2019, Mi et al., 2009, Doussau et al., 2017, Gianinazzi et al., 2005, Nogueira et al., 2022).

2.10.4 iPSC and organoids

iPSC lines represent a recently established *in vitro* approach for studying MS. Many cell lines have been derived from different individuals with varying ages, including some affected with

RRMS (Mutukula et al., 2021). iPSCs can be differentiated into neural progenitor cells (NPCs), OLs, ASTs, neurons, microglia, and vascular cells (Mutukula et al., 2021, Xie et al., 2016, Yamashita et al., 2017, Gunhanlar et al., 2018, Abud et al., 2017, Perriot et al., 2018, Shaltouki et al., 2013, Faal et al., 2019). Unfortunately, there are still limitations to the use of these cells. Each cell line requires constant DNA sequencing due to genetic modifications and residual epigenetic memory from cell sources can affect the characteristics of the iPSC-derived lines (Rebuzzini et al., 2016, Zhou et al., 2018).

iPSCs can also be differentiated into 3D organoids, allowing the study of the interaction between cells of a neural lineage (Wray, 2021). This system has been used to model genetic disorders and for preclinical drug screening (Madhavan et al., 2018). Cells that do not belong to the neural lineage, such as microglia, can be incorporated into the model to enhance its representativeness (Benito-Kwiecinski and Lancaster, 2020, Marton and Pașca, 2020).

CHAPTER 3: Age-related injury responses of human oligodendrocytes to metabolic insults: link to BCL-2 and autophagy pathways

Milton Guilherme Forestieri Fernandes[1], Julia Xiao Xuan Luo[1], Qiao-Ling Cui[1], Kelly Perlman[2], Florian Pernin[1], Moein Yaqubi[1], Jeffery A. Hall[3], Roy Dudley[4], Myriam Srour[5], Charles P. Couturier[3], Kevin Petrecca[3], Catherine Larochelle[6], Luke M. Healy[1], Jo Anne Stratton[1], Timothy E. Kennedy[7] & Jack P. Antel[1]

1 Neuroimmunology Unit, Montreal Neurological Institute and Department of Neurology and Neurosurgery, McGill University, 3801 University Street, Montreal, QC, H3A 2B4, Canada
2 Douglas Mental Health University Institute, 6875 Boulevard LaSalle, Verdun, QC, H4H 1R3, Canada
3 Department of Neurosurgery, McGill University Health Centre and Department of Neurology and Neurosurgery, McGill University, 3801 University Street, Montreal, QC, H3A 2B4, Canada
4 Department of Pediatric Neurosurgery, Montreal Children's Hospital, 1001 Décarie Boulevard, Montreal, QC, H4A 3J1, Canada
5 Division of Pediatric Neurology, Montreal Children's Hospital, 1001 Décarie Boulevard, Montreal, QC, H4A 3J1, Canada
6 Department of Neurology, University of Montreal, 1051 Saguinet Street, Montreal, QC, H2X 3E4, Canada
7 Department of Neurology and Neurosurgery; Department of Human Genetics and Bioengineering, McGill University, 3801 University Street, Montreal, QC, H3A 2B4, Canada

Corresponding author: Dr. Jack P. Antel, Neuroimmunology Unit, Montreal Neurological Institute and Department of Neurology and Neurosurgery, McGill University, 3801 University Street, Montreal, QC, H3A 2B4, Canada, e-mail: jack.antel@mcgill.ca

Published: 4 January 2021
Communications Biology, 4, Article number: 20 (2021)
DOI: https://doi.org/10.1038/s42003-020-01557-1

3.1 Abstract

Myelin destruction and OL death consequent to metabolic stress is a feature of CNS disorders across the age spectrum. Using cells derived from surgically resected tissue, we demonstrate that young (<age 5) pediatric-aged sample OLs are more resistant to in-vitro metabolic injury than fetal O4+ progenitor cells, but more susceptible to cell death and apoptosis than adult-derived OLs. Pediatric but not adult OLs show measurable levels of TUNEL+ cells, a feature of the fetal cell response. The ratio of anti- vs pro-apoptotic BCL-2 family genes is increased in adult vs pediatric (<age 5) mature OLs and in more mature OL lineage cells. Lysosomal gene expression was increased in adult and pediatric compared to fetal OL lineage cells. Cell death of OLs was increased by inhibiting pro-apoptotic BCL-2 gene and autophagy activity. These distinct age-related injury responses should be considered in designing therapies aimed at reducing myelin injury.

3.2 Introduction

Oligodendrocyte (OL) injury with subsequent cell death consequent to metabolic insults is a feature of several acquired disorders of the central nervous system (CNS) across the age spectrum. These include adult-onset multiple sclerosis (MS) and focal and diffuse injury in children. In the acute lesions in MS, there is limited loss of OLs (Kuhlmann et al., 2017, Lucchinetti et al., 2004) with inconsistent evidence of active cell death response mechanisms as measured by presence of OLs with morphologic features of apoptosis or cleaved caspase-3 (Prineas and Parratt, 2012, Barnett and Prineas, 2004). Surviving OLs show disruption of terminal cell processes consistent with a dying-back phenomenon (Ludwin and Johnson, 1981, RODRIGUEZ et al., 1993), which may reflect sub-lethal injury that is potentially reversible (Cui et al., 2017, Rone et al., 2016) and allow them to contribute to subsequent myelin repair (Yeung et al., 2019b, Duncan et al., 2018). In chronic lesions, there is universal loss of OLs (Kuhlmann et al., 2017). Although immune-mediated mechanisms are considered to underlie initial lesion formation, analysis of MS tissues provides evidence of local ischemia/hypoxia contributing to ongoing injury (Lassmann and van Horssen, 2016, Mahad et al., 2015, Aboul-Enein et al., 2003, Stadelmann et al., 2005, Trapp and Stys, 2009). These responses are attributed to disturbance of the micro-circulation due to focal edema or local production of toxic metabolites that interfere with energy metabolism (D'Haeseleer et al., 2015). Dutta and Trapp, using tissue micro-dissected from established MS lesions, found no evidence of activation of programmed cell death pathways to account for the OL loss (Dutta and Trapp, 2012). The variable myelin repair in MS is mainly attributed to OPCs present in lesions (Franklin and ffrench-Constant, 2017b). Our previous studies suggest that OPCs in MS lesions are even more susceptible to injury than mature OLs (Cui et al., 2013).

Across the pediatric age range, metabolic insults can result in permanent motor and cognitive deficits (Schneider and Miller, 2019). Underlying causes for such insults include systemic metabolic disorders and infection, trauma, and prolonged seizures (Volpe, 2012, Gunn and Thoresen, 2019, Glass, 2018, Plouin and Kaminska, 2013). Such insults in full term newborn infants are referred to as neonatal hypoxic/ischemic encephalopathy (reviewed in Volpe, 2012). The pathologic features include involvement of subcortical and central white matter similar to what is observed in periventricular leukomalacia that occurs in pre-term infants (Schneider and Miller, 2019). Pre-myelinating oligodendrocytes; phenotypically characterized as O4+/platelet derived growth factor-receptor α (PDGF-R+)/NG2+ progenitor cells, remain abundant after birth (Back et al., 2001, Chang et al., 2000, Leong et al., 2014) and are particularly vulnerable to this form of injury (Back et al., 2002, Giacci et al., 2018, Marin and Carmichael, 2019). Most injury was considered to be via necrosis although some degree of apoptosis could be observed (Edwards and Mehmet, 1996). We identified such a cell population in our previous single-cell RNA sequencing analysis of surgically derived pediatric age brain samples (Perlman et al., 2020). Cell death of OPCs was shown to occur by apoptosis in an in vivo neonatal rat model of hypoxic-ischemic injury (Segovia et al., 2008, Rao et al., 2017).

In our current study, we demonstrate the age-related differences in susceptibility of human OL lineage cells to metabolic injury and relate these to the underlying molecular mechanisms, specifically the interaction of BCL-2 family molecules that regulate the intrinsic apoptotic pathway (Balmer et al., 2013) (illustrated in Supplementary Fig. 3.1) and the autophagy pathway. The BCL-2 family is divided into three groups: the pro-apoptotic effector molecules BAX and BAK, the anti-apoptotic BCL-2, BCL-XL (encoded by *BCL2L1* gene), BCL-2A1, MCL-1, BCL-W (encoded by *BCL2L2* gene) and BCL-B (encoded by *BCL2L10* gene) and the sensor/activator

molecules from the BH3-only subfamily (BAD, BIM, BID, and others) (Kale et al., 2018, Happo et al., 2012, Guo et al., 2001). Under stress, BH3-only subfamily members are activated or upregulated. They can bind to the anti-apoptotic family members, preventing their interaction with BAX and BAK, or bind directly to BAX and BAK to result in their release from inhibition, triggering the apoptotic pathway. The BCL-2: BAX ratio has been used as a measure of the relative expression of anti- vs pro-apoptotic molecules (Kale et al., 2018). In vitro studies indicate that pro-apoptotic family members are constitutively expressed at a considerably higher level than anti-apoptotic family members in rat OPCs (Itoh et al., 2003, Khorchid et al., 2002). With differentiation, the expression of anti- vs pro-apoptotic members increases (Itoh et al., 2003, Khorchid et al., 2002, Yin et al., 1998), potentially increasing resistance to apoptosis. We provide evidence for the significance of the BCL-2 pathway in protecting human OLs.

Autophagy reflects a metabolic switch from anabolism to catabolism with degraded cellular components being used as a source of energy. This process initially supports the survival of the cell under nutrient starvation (Ashkenazi and Salvesen, 2014, Bankston et al., 2019). However, the formation of autophagosomes without a further fusion with lysosomes can be detrimental to the cell, ultimately leading to cell death (autophagic cell death); such cell death can occur either dependently or independently of apoptosis (Ashkenazi and Salvesen, 2014, Bankston et al., 2019, Button et al., 2017, Denton and Kumar, 2019, Galluzzi et al., 2017a, Galluzzi et al., 2016, Glick et al., 2010, Liu et al., 2013, Munson and Ganley, 2015, Nakamura and Yoshimori, 2017). In a neonatal mouse model of asphyxia, OL death was increased by preventing autophagy (Galluzzi et al., 2018, Yu et al., 2018). Neuman et al. found that fasting or treatment with metformin could reverse age-related decreases in metabolic function and protect against DNA damage in aged rat A2B5+ OPCs, resulting in enhanced myelination capacity (Neumann et al.,

2019b, Neumann et al., 2019a). In a previous study, we observed that metabolic stress conditions induced an enhanced autophagy response in adult human OLs as measured by increased expression of LC3 (Rone et al., 2016). We now address the role of autophagy in regulating OL cell death in response to metabolic insult.

For our study, we isolated OLs from surgical resections of pediatric and adult cases to (i) determine their relative susceptibility to metabolic insult (LG/NG) conditions in cell culture assays and (ii) identify molecular signatures related to cell death and potential protective pathways linked with the observed functional responses based on whole-cell single-cell RNA sequencing (scRNAseq). Comparisons are also made with OL lineage cells derived from second-trimester fetal brain samples. Our findings show that pediatric age OLs have acquired resistance to BCL-2 family apoptotic mediated injury compared to fetal OPCs but residual susceptibility persists relative to corresponding cells present in the adult CNS. We also now show that genes responsible for the formation of lysosomes are upregulated in pediatric and adult OLs ex vivo compared to fetal O4 + cells and use in vitro blocking assays to indicate the initial protective effect of the autophagy response induced by LG conditions.

3.3 Results

3.3.1 Functional studies demonstrate age-related differences in injury responses of human OLs to metabolic stress

To model conditions of metabolic stress in vitro and to investigate whether there is an age-related difference in the protective response to cell death, we utilized dissociated cultures of OLs derived from adult and pediatric surgical samples and O4+ cells derived from fetal samples. We

compared relative levels and underlying mechanisms of cell death between cells cultured in optimal conditions (DMEM/F12 + N1, hereafter referred to as N1) and cells cultured under sub-optimal conditions i.e. reduced overall nutrients (DMEM alone) plus low and no glucose (LG/NG) conditions. We documented that the cultures from the pediatric donors contain a high proportion (>90–95%) of O4+ cells (Supplementary Fig. 3.2 —control condition panel) as we have previously shown for adult donor derived cells (Esmonde-White et al., 2019). Previous flow cytometry studies indicated that the OLs express the late antigen MOG (Leong et al., 2014). We did not detect PDGFRα+ cells in these cultures at the time of functional injury studies.

As shown in Fig. 3.1a, for OLs derived from the human adult brain, there was no significant cell death (% propidium iodide (PI) positive cells) after 48 h of culture in LG or NG conditions. In contrast, at the same time point, significant cell death (% PI positive cells) was detected in OLs derived from pediatric donors under LG or NG conditions (Fig. 3.1b, illustrated in Supplementary Fig. 3.2 - LG and NG conditions panels). The mean % PI+ cells was significantly higher in the pediatric OLs compared to adults in NG conditions ($30.3 \pm 5.7\%$ vs $11.5 \pm 2.1\%$; $p < 0.05$) (Fig. 3.1a, b). Total cell numbers were also significantly reduced in the pediatric sample (Fig. 3.1i). A sub-analysis based on donor age suggested increased susceptibility in the younger donors (<age 5 vs >age 5, $23 \pm 5\%$ vs $8 \pm 1\%$; $p < 0.05$). The pediatric OLs were however more resistant to cell death (% PI+ cells) compared to O4+ cells isolated from fetal human brain samples under LG conditions at 2 days (Fig. 3.1c) ($16.9 \pm 4.0\%$ vs $32.1 \pm 6.0\%$; $p = 0.06$). For the pediatric samples, the proportion of TUNEL+ cells was also statistically higher in LG and NG conditions compared to N1 conditions (Fig. 3.1e); however, the percentage of TUNEL+ cells under NG conditions was significantly lower than the percentage of PI positive cells ($8.2 \pm 2.2\%$ vs $30.3 \pm 5.7\%$; $p < 0.05$) (Fig. 3.1b, e). For the fetal

cells, % TUNEL+ cell was comparable to the % PI+ cells (Fig. 3.1c, f) (37.5 ± 9.3% vs 43.8 ± 8.9%). As shown in Fig. 3.1g, h, prolonged (6 day) culture of the adult OLs under LG and NG conditions resulted in a higher % of PI+ cells that was not associated with any significant increase in % TUNEL+ cells. Cell numbers were also reduced under NG vs N1 conditions at day 6 in the adult cell cultures (Fig. 3.1j, k).

3.3.2 Identification of OL lineage subsets by whole-cell scRNA seq of immediately ex vivo cells

In order to identify sub-populations of OL lineage cells that may have distinct cell death responses, we applied unbiased cluster analysis to the pooled OL-lineage cells across a range of ages (Fig. 3.2a, b). Figure 3.2c presents violin plots showing relative expression levels across clusters of selected marker genes. In addition to the three subpopulations mature OLs (mOLs), late OPCs (lOPCs), and early OPCs (eOPCs) as identified in our previous report (Perlman et al., 2020), we identified an additional *PDGFRA- PTPRZ1+ MBP+* population, here labeled as committed pre-OLs (pOLs). A population expressing both immune and oligodendrocyte markers, akin to that described by Jäkel et al. (Jäkel et al., 2019), was also identified but not included in this analysis (Supplementary Fig. 3.3a).

As seen in Fig. 3.2 a, b, mature OLs comprised the large majority of OL lineage cells in both adult and pediatric samples although progenitors were apparently more abundant in the pediatric samples (quantified in Supplementary Fig. 3.3b). eOPCs were derived entirely from fetal samples.

3.3.3 Identification of OL lineage subsets by whole-cell scRNA seq of immediately ex vivo cells

To identify molecular signatures that would help understand the basis for the observed age-related differences in resistance to metabolic insult, we first considered the baseline expression of genes encoding pro- and anti-apoptotic BCL-2 family members in the OLs in our adult and pediatric samples.

Our initial analysis across age groups includes pooled total OL-lineage cells from all our donor samples as for some subsets there were insufficient numbers of cells to compare between individual samples. We divided the BCL-2 family genes into pro-apoptotic (*BAX, BAK1*) and anti-apoptotic (*BCL2A1, BCL2, BCL2L2*) categories, and further separated genes whose product activity depends on alternatively spliced products (*BCL2L1, MCL1*) (Senichkin et al., 2019, Rajan et al., 2009) (Fig. 3.3a-c). *BCL2L10* is not included as it was not captured due to dropout events in sequencing. Actual normalized expression values are presented in Supplementary Dataset 1. As presented in Fig. 3.3a, for the total OL cluster, the fetal derived OL cells expressed higher levels of pro-apoptotic gene *BAX* as compared to pediatric and adult donor cells. Comparison of OL sub-populations defined by differentiation stage indicates skewing to greater anti- vs pro-apoptotic gene expression with cell differentiation (Fig. 3.3b), particularly on comparison of mOLs and pOLs with lOPCs and eOPCs. As shown in Supplementary Fig. 3.4a, comparisons of different lineages within the pediatric age group indicate that there is skewing to greater anti- vs pro-apoptotic gene expression with cell differentiation. We are unable to draw a statistical conclusion from the adult cohort as the numbers of progenitor cells are too limited (Supplementary Fig. 3.4b).

Figure 3c presents the expression patterns for mature OLs from pediatric and adult samples, sub-dividing the pediatric group into <5 and >5-year subgroups, coinciding with our functional in

vitro studies. This analysis suggested an increase in anti- vs pro-apoptotic BCL-2 family gene expression pattern with age. Figure 3.3d presents ratios of expression of individual pro- and anti-apoptotic genes calculated from individual donors, as well as the pooled ratio of these genes. The pooled data indicates a significant increase in the anti- vs pro-apoptotic gene expression ratio in the adult compared to the overall pediatric samples. The main difference from the adult group is derived from the younger cohort.

We could not identify age and differentiation stage-related expression patterns in BCL-2 family genes whose product activity depends on alternatively spliced products. Additional data suggest that age-related differences in anti- vs pro-apoptotic BCL-2 family gene expression is also noted in lOPCs and pOLs though these did not reach significance (Supplementary Fig. 3.4c, d).

To address the hypothesis that the observed lack of apoptotic cell death of the adult donor cells may reflect the activation state of BH3-only molecules, we re-examined our previously described microarray of adult human OLs under LG conditions (Cui et al., 2013) for the expression of 25 previously characterized BH3-only subfamily members (Kønig et al., 2019). As shown in Fig. 4a, there are significant increases in the expression of *BCL2L11, BNIP3*, and *RAD9A* under LG condition for 48 h; at this time point, there was no significant change in expression of anti-apoptotic and pro-apoptotic genes (Supplementary Fig. 3.5) and no significant cell death (Fig. 3.1). These results suggest that the intrinsic apoptotic pathway was initiated by activation of some BH3-only molecules, but then inhibited by anti-apoptotic proteins.

To directly investigate the potential contribution of BCL-2 family anti-apoptotic molecules to cell survival in human adult OLs, we used ABT-737, an inhibitor of multiple BCL-2 family anti-apoptotic molecules (mainly BCL-XL, BCL-2, and BCL-W) and WEHI-539, a specific inhibitor of BCL-XL (Kline et al., 2007, Lessene et al., 2013). Addition of ABT-737 to adult donor OLs

significantly increased cell death in NG compared to control conditions, as measured by reduced number of surviving cells and increased % PI+ cells (Fig. 3.4b, c). Cell process extension was also reduced (Supplementary Fig. 3.6). There was also a significant increase in % TUNEL+ cells (Fig. 3.4d) indicating that the adult OLs have the capacity to activate the BCL-pro-apoptotic cascade if anti-apoptotic proteins are inhibited. The relative lack of effect of WEHI-539 suggests that inhibiting BCL-XL alone is not sufficient to inhibit apoptosis.

3.3.4 Contribution of autophagy pathway genes to age-related OL susceptibility to metabolic injury

To determine whether differences in the relative baseline expression of autophagy genes contributed to the observed age and differentiation linked injury responses, we examined the expression of a select number of genes contributing to the autophagy response in relation to these variables. As reviewed in (Glick et al., 2010, Nakamura and Yoshimori, 2017) autophagy can be divided into four stages: initiation, nucleation, elongation, and fusion. As shown in Fig. 5a, we detected a trend to decreased expression of lysosome-related genes in fetal total OL-lineage cells as compared to pediatric and adult OLs; in particular, *LAMP1* and *LAMP2* were significantly downregulated. Consistent age-related differences in expression of genes involved in autophagy initiation, nucleation, and elongation were not detected (Supplementary Fig. 3.7).

We did not detect differences in expression of autophagy genes involved in autophagy initiation in OLs under 48 h of glucose deprivation with the exception of *PIK3CG* which is downregulated (Fig. 3.5b). We did not detect a significant change in the expression levels of the elongation genes with glucose deprivation alone (Fig. 3.5c). Expression of genes encoding LC3 (*MAP1LC3B*) and p62 (*SQSTM1*) that were measured in the protein assays were suggestively

increased (Fig. 3.5c). Regarding the expression of genes involved in fusion of lysosomes and autophagosomes (Fig. 3.5d), only *VAMP8* is downregulated under low glucose. Among the genes that are involved in the lysosome formation (Fig. 3.5e), cathepsins C, H, and O are downregulated although there is no change in cathepsins B, D, and L.

To determine whether glucose deprivation conditions at a time prior to cell death were inducing a potential protective autophagy response, we treated cultures with chloroquine, which inhibits the fusion of autophagosomes with lysosomes (Mauthe et al., 2018) (Fig. 3.6a-c). We observed that chloroquine did not increase cell death in the human OLs under optimal culture conditions (N1) but significantly increased cell death (% PI+ cells) in glucose deprivation conditions (Fig. 3.6a-c). Cell process extension was also reduced (Supplementary Fig. 3.6). To further investigate the engagement of autophagy in the response of the OLs to LG/NG conditions and the effect of chloroquine, we analyzed the protein levels of the autophagosome components LC3 and p62 by western blot. We detected an increase in the levels of these markers in these conditions when combined with chloroquine (Fig. 3.6d-f). This was not seen when cells were cultured in optimal conditions. These results indicate that autophagy is activated in glucose deprivation conditions. Accumulation of autophagosomes in these cells indicates an impairment in the fusion with lysosomes induced by chloroquine. These combined functional and Western blot studies support the early protective effects of the autophagy response.

3.4 Discussion

Our data identify the BCL-2 family and autophagy pathways as contributors to age-linked responses of human OL lineage cells to metabolic injury. The viability of the cells isolated immediately from the surgical samples allowed us to perform both whole-cell scRNA seq, which

includes cytoplasmic RNA in contrast to single nucleus studies, and complementary in vitro functional assays. Samples were obtained from normal appearing tissue, within the corridor required to access the pathologic site. The status of the samples was confirmed by histopathologic analysis. The metabolic insult used was designed to model focal ischemic conditions found in MS lesions and in the penumbra of focal pediatric ischemic/hemorrhagic events.

The functional in vitro injury data indicate that under the stress conditions used (combining LG/NG with reduced nutrient supplements), human fetal OL lineage cells (O4+) were highly susceptible to cell death (within 24–48 h), with the majority of cells being TUNEL+. The OLs derived from the pediatric age samples were more resistant than the fetal cells but more susceptible to injury than the adult cells. The pediatric OLs showed measurable, although limited, apoptosis. Our data that active cell death pathways are prominent in early human OPCs in response to metabolic insults are supportive of findings from rat models of hypoxic cerebral hypoxia-ischemia. The latter showed that apoptotic mechanisms were several-fold more pronounced in immature than in juvenile and adult brains (Back et al., 2002, Zhu et al., 2005). For adult OLs, consistent with our previous report (Rone et al., 2016) the delayed cell death was not linked to induction of active cell death pathways.

The bioinformatics data provides insight into the molecular basis for the age-related functional injury responses that we detected. We selected representative members of the BCL-2 pathway that are well documented to be pro-or anti-apoptotic. Using the total OL population, we found that the highly injury susceptible fetal cells, containing the early OPC population, expressed the highest levels of pro-apoptotic genes. With OL differentiation, there is skewing to greater anti- vs pro-apoptotic gene expression. Our observation that pediatric donor mature OLs cells

still exhibit a relative increase in the expression of pro- vs anti-apoptotic genes compared to the adult derived cells, is consistent with our observed age-related susceptibility to injury. Our in vitro studies showing that blocking anti-apoptotic genes results in significant apoptotic cell death under the LG conditions indicate the functional relevance of the relative skewing to anti- vs pro-apoptotic gene expression in OLs. Our data suggest that anti-apoptotic genes are impeding the BH3-only family molecules, observed to be activated, from inducing the apoptosis pathway. BH3-only family members can be triggered by multiple pathologic conditions, including hypoxia (Happo et al., 2012, Guo et al., 2001, Lee and Paik, 2006).

The cell death induced by the metabolic insult used in this study is likely closely linked to energy failure. We previously documented immunocytochemically that the metabolic conditions used in the current study increased LC3 expression, an indicator of autophagy activation in adult human OLs (Rone et al., 2016). We now confirm by Western blotting for p62 and LC3-II that autophagy is activated in these cells and demonstrate that the response is initially protective, based on the increased cell death in the presence of chloroquine. The bioinformatics data derived from immediately ex vivo cells indicate that the fetal OL lineage cells that are highly susceptible to metabolic stress, have reduced expression of the lysosome forming genes, which are an integral part of the autophagy pathway. Our observations seem compatible with those of Neumann et al. that autophagy pathway gene expression is upregulated in A2B5 antibody selected progenitor cells in aged rats; these cells overall had reduced stem cell properties (Neumann et al., 2019a, Neumann et al., 2019b).

The microarray data from the adult human OLs cultured in LG for 2 days (the time when autophagy is activated) indicate that while expression of most genes involved in encoding the

autophagy pathway is unchanged, a limited number of genes were downregulated. These included *PIK3CG*, whose gene product inhibits autophagy initiation (Galluzzi et al., 2017a), and *VAMP8*, which encodes a SNARE protein that is necessary for the attachment of lysosomes to autophagosomes (Nakagawa et al., 2000). Among the genes involved in lysosome formation, cathepsins C, H, and O are downregulated although there is no change in cathepsins B, D, and L. This downregulation may reduce the digestion capacity of lysosomes, although it is possible that the overall concentration of cathepsins would be sufficient. p62 and LC3 are suggestively upregulated. We did not detect a significant change in the expression levels of elongation genes, including those encoding p62 and LC3. We consider that some downregulation of genes under our LG conditions can reflect overall reduction in metabolic activity of the cells as we have previously shown using the Seahorse bioanalyzer (Cui et al., 2017). Our overall results suggest that the observed autophagy activation most reflects post-translational changes.

Overall, our study provides molecular and functional data to document the susceptibility of human OL lineage cells to metabolic injury and elucidates the role of age and OL lineage cell maturity level in this process. Defining the mechanism of cell death can direct therapeutics aimed at protecting cells that may initially survive acute or chronic insults across the age spectrum, enhancing the possibility of their participation in subsequent myelin repair (Yeung et al., 2019b, Duncan et al., 2018).

3.5 Methods

3.5.1 Human cell samples

Brain tissue samples were obtained from surgical procedures. Anonymized adult samples were obtained via the Department of Neuropathology at the Montreal Neurological Institute and Hospital (MNI) and pediatric samples from the Montreal Children's Hospital with written consent from families. 2nd trimester (14–17 weeks) fetal samples were obtained from the University of Washington Birth Defects Research Laboratory (MP-37-2014-540; 13-244-PED; eReviews_3345). Demographics of the pediatric patients are given in Supplementary Table 1. Adult donors ranged in age from 30–65 years; all had non-tumor related focal epilepsy. Use of pediatric and adult tissues were approved by the MNI Neurosciences Research Ethics Board (Protocol ANTJ 1988/3) and the use of pediatric tissues approved by the Montreal Children's Hospital Research Ethics Board.

3.5.2 Cell isolation

Tissues from the surgical corridor from the adult and pediatric samples were collected into CUSA bags. Tissue derived from the CUSA bags was subjected to trypsin digestion followed by Percoll gradient centrifugation in order to obtain a myelin-depleted whole-cell fraction comprised mainly of OLs and microglia with few if any astrocytes or neurons. The scRNA seq data from the adult and pediatric surgical samples were derived from sequencing this total cell population. For in vitro studies of the adult and pediatric samples, we derived an enriched OL population by adhering the total cell population overnight to remove adherent microglia. Fetal cell isolation does not require a Percoll gradient step but in order to enrich for OL cells for our functional assays, we used immuno-magnetic beads coated with O4 antibody (IgM) to collect rare (1–5%) O4+ cells.

3.5.3 Cell culture

After selection, cells were plated in 96-wells or 24-wells plates coated with poly-lysine and extra-cellular matrix at a density of 3×10^4 cells (96-wells plate) or 1×10^6 cells (24-wells plate) per well. Cells were cultured in DMEM-F12 media supplemented with N1 (Sigma, Oakville, ON, Canada. For metabolic deprivation experiments, cells were cultured in DMEM containing 0.25 g/l of glucose (LG) or with no glucose added (NG).

3.5.4 Immunocytochemistry

Cells were live stained with propidium iodide (PI; Invitrogen) (1:200) for cell viability measurement and with O4 monoclonal antibody (R&D Systems, Minneapolis, MN) (1:200) for 15 min at 37 °C and then fixed with 4% paraformaldehyde for 10 min in room temperature. Goat anti-mouse IgM Cy3 (1:500) was used as secondary antibody to O4, 30 min at room temperature. Cells were stained with a commercial TUNEL kit (Promega, Madison, WI). Cell nuclei were stained with Hoechst 33258 (1:1000). Inhibitors used in these experiments were: Chloroquine (10 μM; Sigma, Oakville, ON, Canada), WEHI-539 (10 μM; Selleckchem, Houston, TX) and ABT-737 (10 μM; Selleckchem, Houston, TX).

3.5.5 Western blot

SDS-PAGE was run with 5–10 μg of protein in each sample in 15% acrylamide gels. Proteins were transferred to a PVDF membrane. The membranes were blocked with 5% milk and probed with the primary antibodies overnight at 4 °C. Bands were visualized with horseradish peroxidase-conjugated secondary antibody used in conjunction with an ECL Western blot detection kit (Cell Signaling, Danvers, MA). Primary antibodies used were LC3B (#2775 Cell

Signaling, Danvers, MA), SQSTM1/p62 (#5114 Cell Signaling, Danvers, MA) and β-actin (Sigma, Oakville, ON, Canada); the dilution used in all primary and secondary antibodies was 1:1000.

3.5.6 Single-cell RNA sequencing

Fetal, pediatric, and adult tissue samples were sent for sequencing at the McGill University and Génome Québec Centre. RNA sequencing libraries were prepared with 10X Chromium v2.0 and single cell RNA sequencing (scRNAseq) was performed on the Illumina HiSeq4000 PE75 sequencer. A droplet-based sequencing method by 10X Chromium was used to obtain single-cells. The 10XGenomics CellRanger pipeline was used to demultiplex cell and unique molecular identifier barcodes, and to align reads to the GRCh38 human reference genome. All subsequent analyses were primarily done using the Seurat (v3.1) R package (Butler et al., 2018, Stuart et al., 2019, van den Brink et al., 2017, Zhang et al., 2019b).

The standard Seurat pipeline for quality control, gene expression normalization, batch-effect correction, clustering, and differential expression analysis was used. For each sample, dead cells were filtered by removing cells with >5% mitochondrial gene content. Low quality cells and cell multiplets were removed by excluding cells with unique feature counts of less than 200 or over 2500 respectively. Expression counts were then natural log-normalized and scaled. A subset of the top 2000 highly variable features for each sample were identified to be prioritized during integration for batch correction, to adjust for sample-driven clustering. Integration was done using a method described by Stuart et al. (Stuart et al., 2019). Briefly, cell pairwise correspondences across datasets used to “anchor” the datasets were identified after canonical correlation analysis (CCA) reduction and L2-normalization to canonical correlation vectors.

Then, “correction” vectors for each cell were calculated and expression values were transformed to integrate datasets together for the purposes of clustering. All samples of pediatric and adult donors were integrated together into one dataset; all samples of fetal donors were integrated into a second dataset. Up to extracting OL-lineage cells, fetal samples were processed separately as their cell-type makeup was dramatically different from that of the pediatric and adult samples due to the earlier described differences in tissue processing. Running integration and batch correction in samples where cell types are extremely imbalanced can lead to incorrect alignment (Zhang et al., 2019b).

Principal component analysis (PCA) was used on each dataset to reduce the high-dimensional dataset to lower dimensions. For this analysis, genes highly associated with tissue dissociation were regressed to reduce the generation of artifacts in downstream analyses, such as creating a subpopulation that does not exist in vivo (van den Brink et al., 2017). A shared-nearest neighbor graph was constructed based on the PCA analysis of each large dataset and the Louvain clustering algorithm was used several times to identify clusters at multiple different resolutions. To visualize the clusters in two-dimensional space, uniform manifold approximation and projection (UMAP) was used for non-linear dimensional reduction. The clustree R package was used to construct a clustering tree (Zappia and Oshlack, 2018). The clustering tree visualizes the movement of cells between clustering branches and was used to determine the optimal resolution for the stable clustering. A high degree of movement between branches indicates over-clustering. A clustering resolution of 1.5 was chosen for the integrated fetal dataset and 0.5 was chosen for the integrated pediatric/adult dataset.

Clusters in each dataset were annotated as OL-lineage cells using relative expression of canonical markers such as SOX10 for OL-lineage cells*; PDGFRA, PTPRZ1* for oligodendrocyte

progenitor cells (OPCs); and *MBP, PLP1*, for mature OLs (mOLs). OL-lineage cells were extracted from each of the two integrated datasets and merged to create a final total OL-lineage dataset. Louvain clustering with clustering tree analysis was again applied on these total OL-lineage cells. A base resolution of 0.08 was chosen and one modification was made to this clustering solution. A higher resolution of 0.35 was used to separate a specific subpopulation as differing expression of canonical OL-lineage markers *PDGFRA, PTPRZ1, MBP* was apparent and those particular clusters remained very stable even at higher resolutions.

3.5.7 Statistics and reproducibility

In vitro studies

All statistics were measured by the mean and the standard error of the mean. The quantity of independent biological samples, statistical tests used and level of significance are indicated in the figure legends.

Single cell RNA seq differential expression analysis

Differential expression (DE) analysis based on the Wilcoxon rank sum test was done on the uncorrected expression values. Results were adjusted for familywise error rate (FWER) with Bonferroni correction. Genes were considered to be significantly up- or downregulated if they had an average log fold change (logFC) ≥ 0.25, adjusted p value < 0.05; lowly up- or downregulated if they had an average logFC ≥ 0.1, adjusted p value < 0.05. For comparisons between age groups, genes that were differentially expressed between samples of the same age group were removed from the DE list of that age group to account for human biological variability between samples.

3.6 Data availability

Source data for figures are provided in Supplementary Data 1. Uncropped scans of western blot are shown in Supplementary Figs. 3.8–3.10. Microarray and RNA-seq data were deposited at GEO under accession number GSE160813. Immunocytochemistry images will be provided upon request.

3.7 Acknowledgements

The study was supported by a grant (BRAVE in MS) from the International Progressive MS Alliance (J.P.A.).

3.8 Ethics declarations

Competing interests

The authors declare no competing interests.

3.9 Figures and figures legends

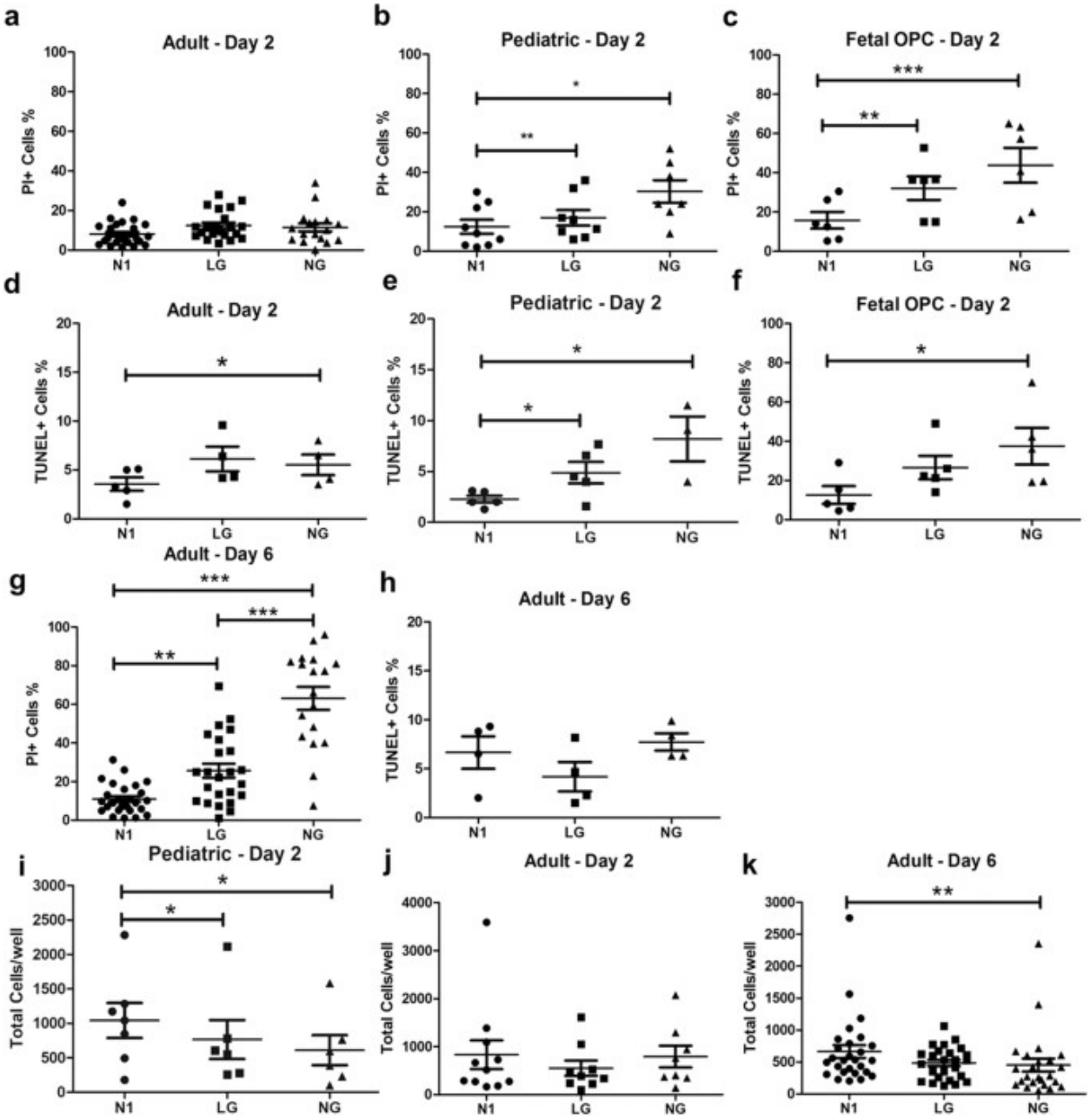

Figure 3.1- In vitro cell death response of adult, pediatric and fetal samples derived human OLs to glucose deprivation conditions. **a**–**c** % PI+ cells in 2-day cultures under N1, LG, and NG conditions. **a** Adult OLs show no significant increase in % PI+ cells under LG/NG conditions. **b** Pediatric OLs show significant increase in % PI+ cells under LG and more so under NG conditions. **c** Fetal O4+ cells show high levels of % PI+ cells under LG and more so

under NG conditions. **d**–**f** % TUNEL+ cells in 2-day cultures under N1, LG, and NG conditions. **d** Adult OLs show no significant increase in %TUNEL+ cells under LG/NG conditions. **e** Pediatric OLs show significant increase in %TUNEL+ cells under NG condition but lower than % PI+ cells. **f** Fetal O4+ cells show high levels of %TUNEL+ cells comparable to % PI+ cells under LG and NG conditions. **g**–**h** % PI+ and TUNEL+ adult OLs maintained in culture for 6 days. There are increased levels of % PI+ cells under LG and NG conditions (**g**), while there is no significant increase in %TUNEL+ cells (**h**). **i**–**k** Cell number/well in 2-day cultures under N1, LG, and NG conditions. Pediatric OLs at 2 days under LG and NG conditions and adult OLs at day 6 under NG conditions show significant decrease in cell numbers/well compared to N1 conditions. For some samples only LG or NG experimental conditions could be evaluated; all were compared to N1 control conditions. Each point in the graph corresponds to an independent biological sample. Mean ± SEM for each condition shown in the figure. Statistical significance was verified by Student's *t*-test: *(<0.05), **(<0.01), ***(<0.001).

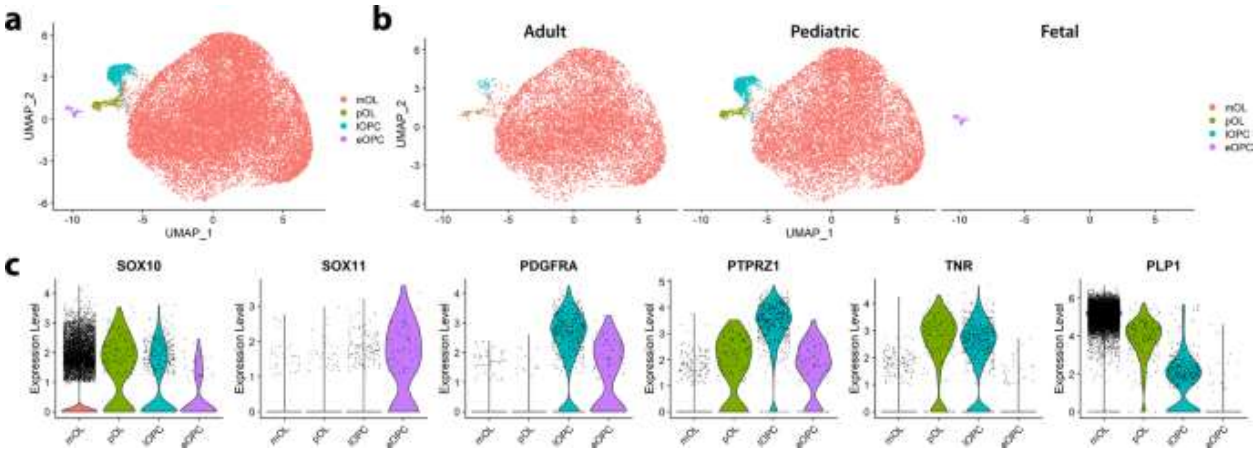

Figure 3.2: Sub-populations of human OL lineage cells as defined by whole scRNA sequencing. OL lineage cells derived from whole-cell sequencing of fetal, pediatric, and adult tissue samples cluster into distinct OL lineage subpopulations. **a** Uniform manifold approximation projection (UMAP) plots of pooled OL-lineage cells, visualizing 4 clusters: mOL, pOL, lOPC, and eOPC. Individual dots on UMAP plots represents single cells. **b** UMAP plots of OL-lineage cells split by age-group. **c** Violin plots showing relative expression level across clusters of selected marker genes, where expression levels are z-scored normalized average expression and gray dots indicate individual cells expressing the marker. Number of independent biological samples by age group: 4 adult, 7 pediatric and 4 fetal.

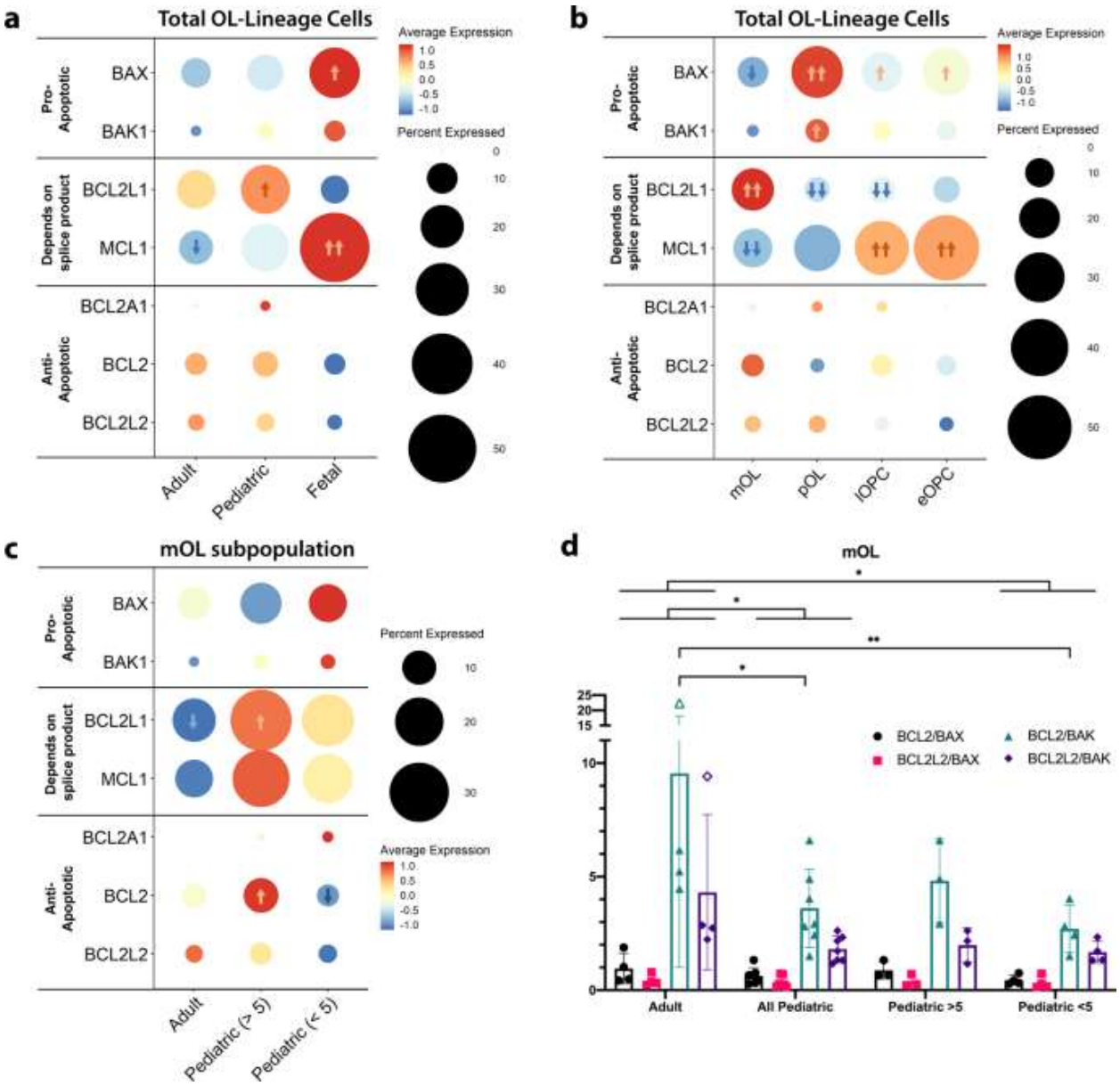

Figure 3.3 - Differential baseline BCL-2 family gene expression in adult, pediatric and fetal OL-lineage cells. **a**–**c** Relative expression of pro and anti-apoptotic BCL-2 family genes across OL lineage spectrum in relation to age and lineage. Scale is z-scores of averaged normalized gene expression across the cell types or age groups; percent expressed indicates the percentage of OL-lineage cells in the category on the *x*-axis expressing the gene. Arrows indicate up- (orange) or down- (blue) regulation (adj. $p < 0.05$) against all other groups, where one arrow $|\text{logFC}| > 0.1$, two arrows $|\text{logFC}| > 0.25$, by Wilcoxon rank sum differential expression testing with Bonferroni correction. **d** Data indicates the ratios of average expression of individual pro- and anti-apoptotic genes for mature OLs. Data under all pediatric are combined from pediatric >5 and pediatric <5.

Open circles indicate outliers by Grubbs' test. Comparison of summated and individual ratios between adult and all pediatric donors was done by two-way ANOVA with Sidak's correction for multiple comparisons both with and without the outliers, $*p < 0.05$. Age group comparisons of summated and individual ratios between adult, pediatric >5, and pediatric <5 was done by two-way ANOVA with Tukey's correction for multiple comparisons, both with and without the outliers, $*p < 0.05$, $**p < 0.01$. Number of independent biological samples by age group: 4 adult, 7 pediatric (3 pediatric >5, 4 pediatric <5) and 4 fetal.

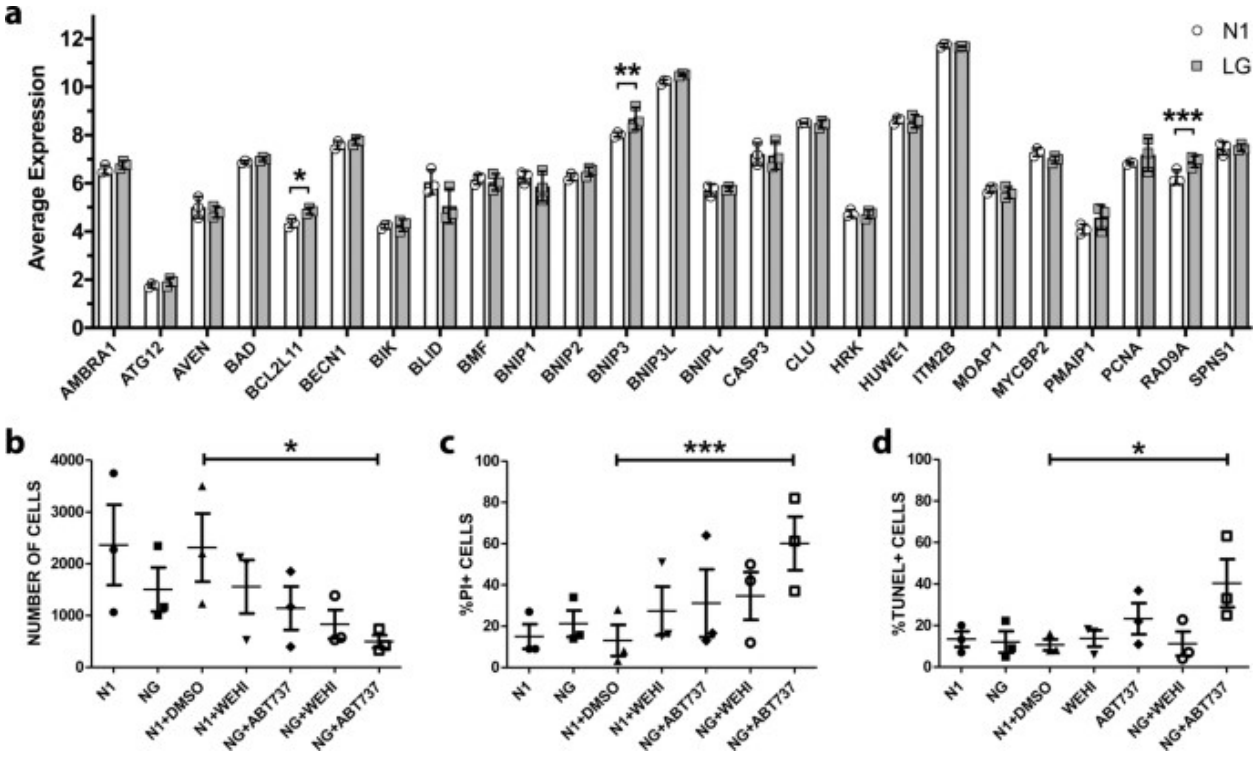

Figure 3.4 - Contribution of BCL-2 family genes to protecting human adult OLs from metabolic injury. **a** Changes in RNA expression of the BH3-only genes in human adult OLs due to glucose deprivation. Average RNA expression levels of members of the BH3-only family in media containing low concentration of glucose (LG) or in optimal culture media (N1) derived by microarray analysis of human adult OLs. $N = 3$ independent biological samples. **b**–**d** Effects of inhibition of the BCL-2 family on cell death of human adult OLs. Cells were cultured in optimal culture media (N1) and in media with no glucose (NG) and treated with the specific inhibitor of BCL-XL WEHI-539 and the non-specific inhibitor ABT737 in N1 and NG media for two days. Cells treated only with DMSO were used as the vehicle control. $N = 3$ independent biological samples. Data are presented as (**b**) number of cells present; **c** %PI+ cells and **d** %TUNEL+ cells. Mean ± SEM for each condition in the figure. Significant levels for the ANOVA/Dunnett's test for paired samples with DMSO as reference: *(<0.05), **(<0.01).

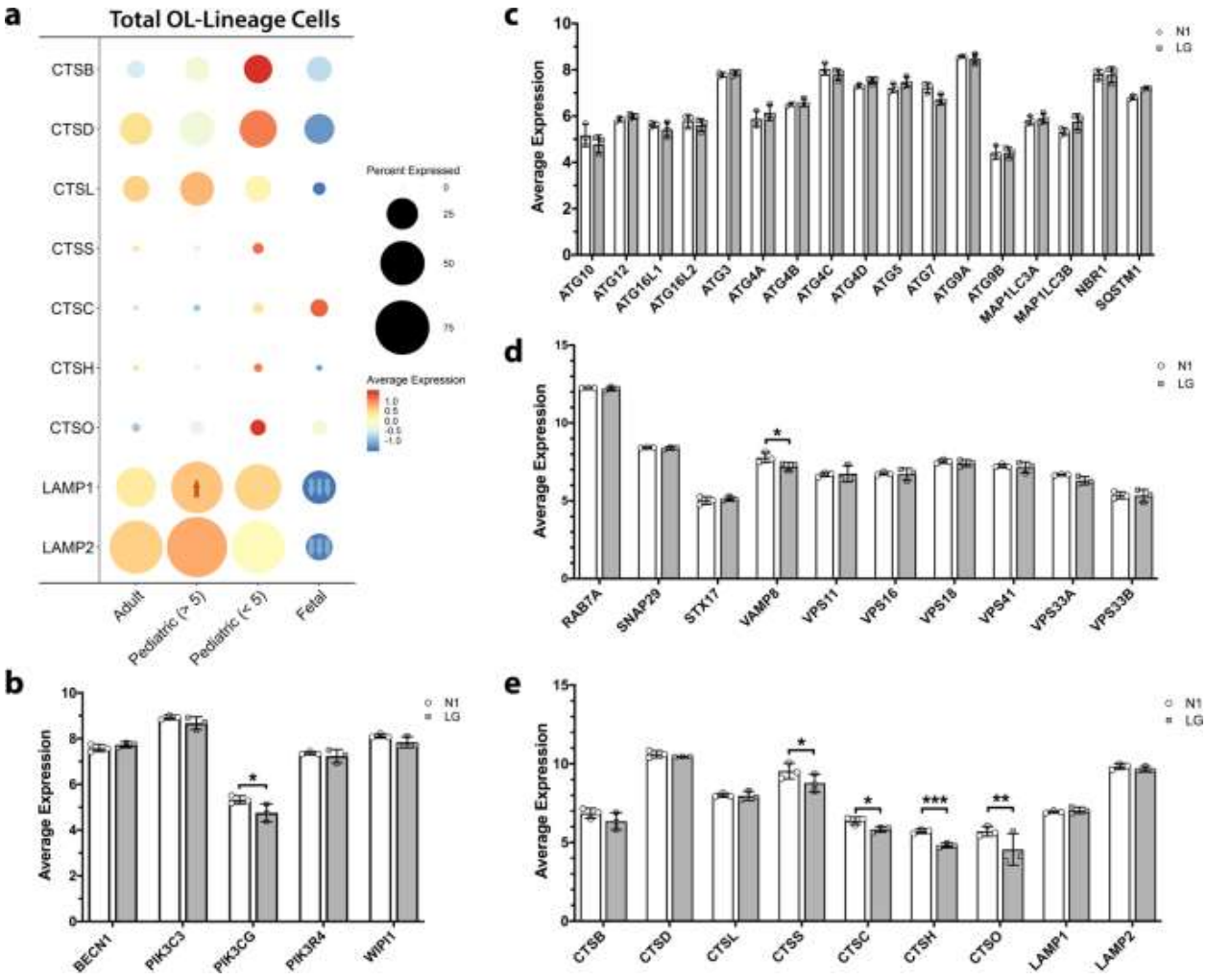

Figure 3.5 - Differential baseline expression of genes of the autophagy pathway in adult, pediatric, and fetal OL-lineage cells. **a** Relative expression of lysosome formation genes of the autophagy pathway in total OL lineage cells from adult, pediatric, and fetal samples. Scale is z-scores of averaged normalized gene expression across the age groups; percent expressed indicates the percentage of OL lineage cells in the age group expressing the gene. Arrows indicate up- (orange) or down- (blue) regulation (adj. $p < 0.05$) against all other groups where one arrow is $|\log FC| > 0.1$, two arrows $|\log FC| > 0.25$, three arrows $|\log FC| > 0.99$, by Wilcoxon rank sum differential expression testing with Bonferroni correction. Number of independent biological samples by age group: 4 adult, 7 pediatric and 4 fetal. **b**–**e** Relative expression of genes involved in nucleation of autophagosomes (**b**), elongation of autophagosomes (**c**), fusion of autophagosomes and lysosomes (**d**) and lysosome formation (**e**) in optimal conditions (N1) and low glucose (LG) in adult OLs. mRNA expression was measured by microarray analysis

with $N = 3$ independent biological samples from adult donors. Mean ± SEM for each condition in the figure. Statistical significance was verified by Student's *t*-test: *(<0.05), **(<0.01), ***(<0.001). *SQSTM1* encodes for p62 and *MAP1LC3B* encodes for LC3-II.

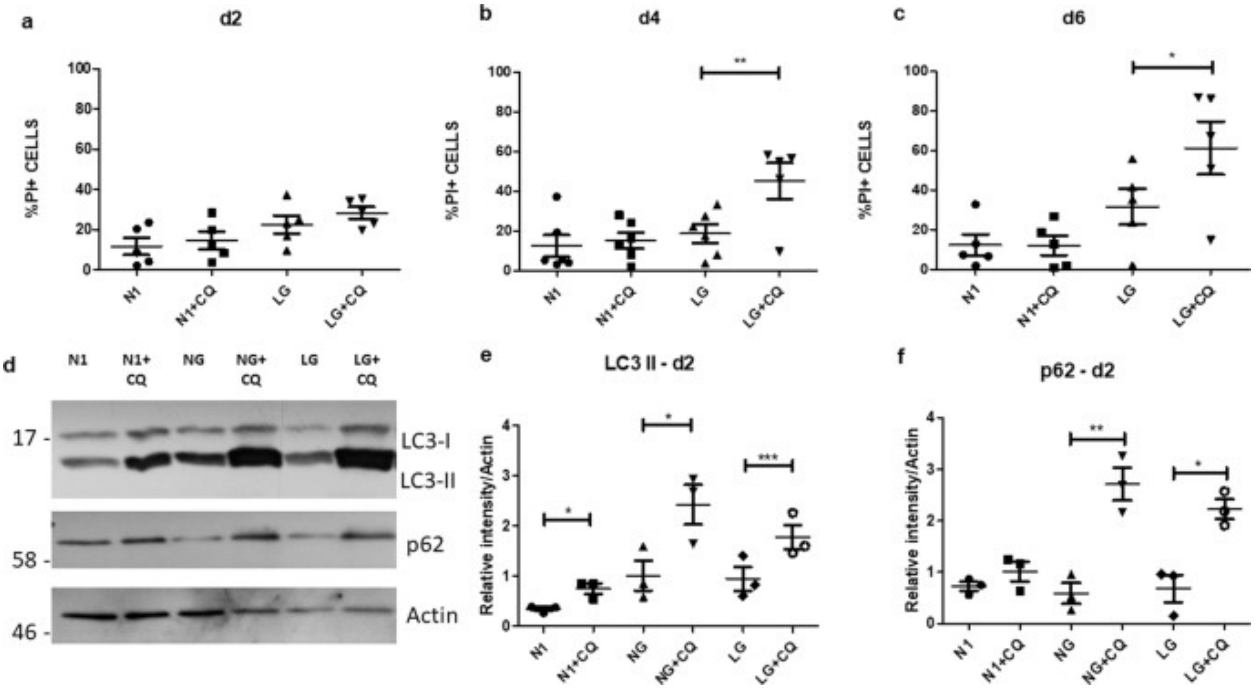

Figure 3.6 - Contribution of the autophagy pathway to protecting OLs from metabolic injury. **a**–**c** Protective effects of autophagy in human adult OLs. Cell death measured by % PI+ cells of human adult OLs cultured in optimal culture media (N1), in low glucose media (LG) and in combined treatment with chloroquine (N1 + CQ; LG + CQ) after two (**a**), four (**b**) and six days (**c**). Addition of CQ results in increase % PI+ cells at day 4 and 6. $N = 5$ independent biological samples. **d**–**f** Representative western blot for the combined treatment of N1, LG, and NG with and without chloroquine after two days ($N = 3$ independent biological samples) (**d**) and quantification of the relative expression compared to actin of LC3 II (**e**) and p62 (**f**). Mean ± SEM for each condition in the figure. Statistical significance was verified by ANOVA/Tukey test: *(<0.05), **(<0.01), ***(<0.001).

3.10 Supplementary Information

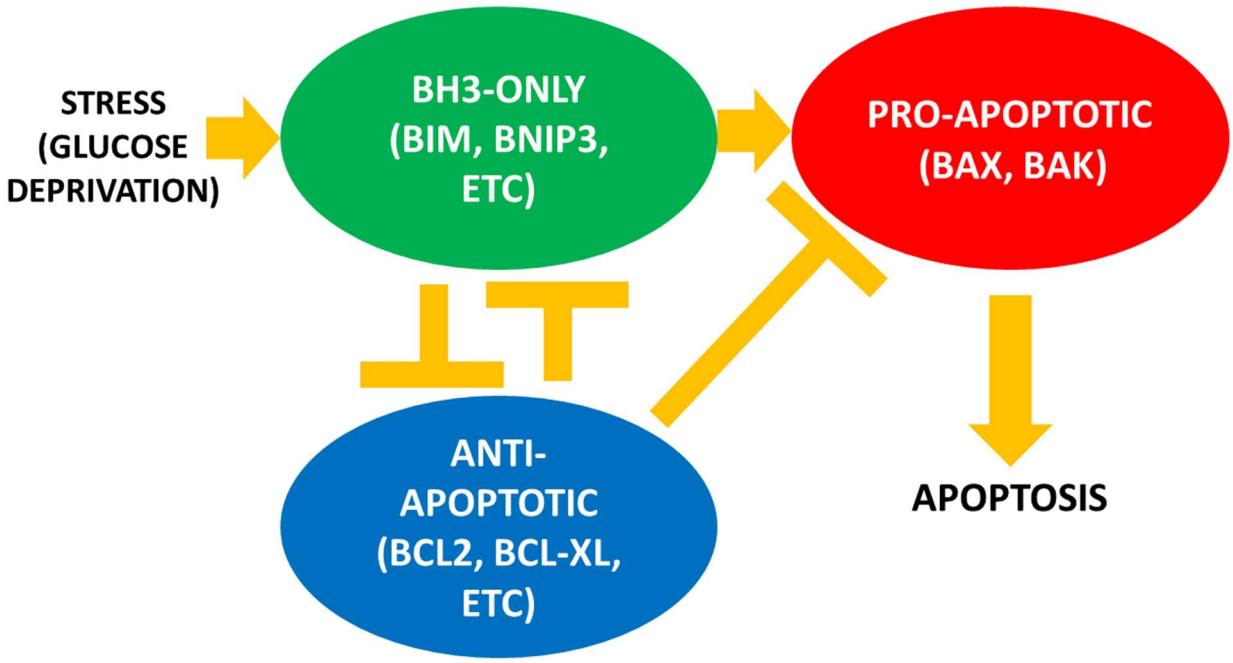

Supplementary Figure 3.1 – Role of BCL-2 sub-families interaction in the intrinsic apoptotic pathway. Illustration of how stress caused by glucose deprivation can activate the molecules of the BH3-only subfamily that in turn can directly activate the pro-apoptotic molecules or indirectly trigger apoptosis by inhibiting the anti-apoptotic subfamily. The anti-apoptotic molecules directly inhibit apoptosis by blocking the pro-apoptotic molecules or indirectly by blocking the action of BH3-only molecules on the pro-apoptotic molecules.

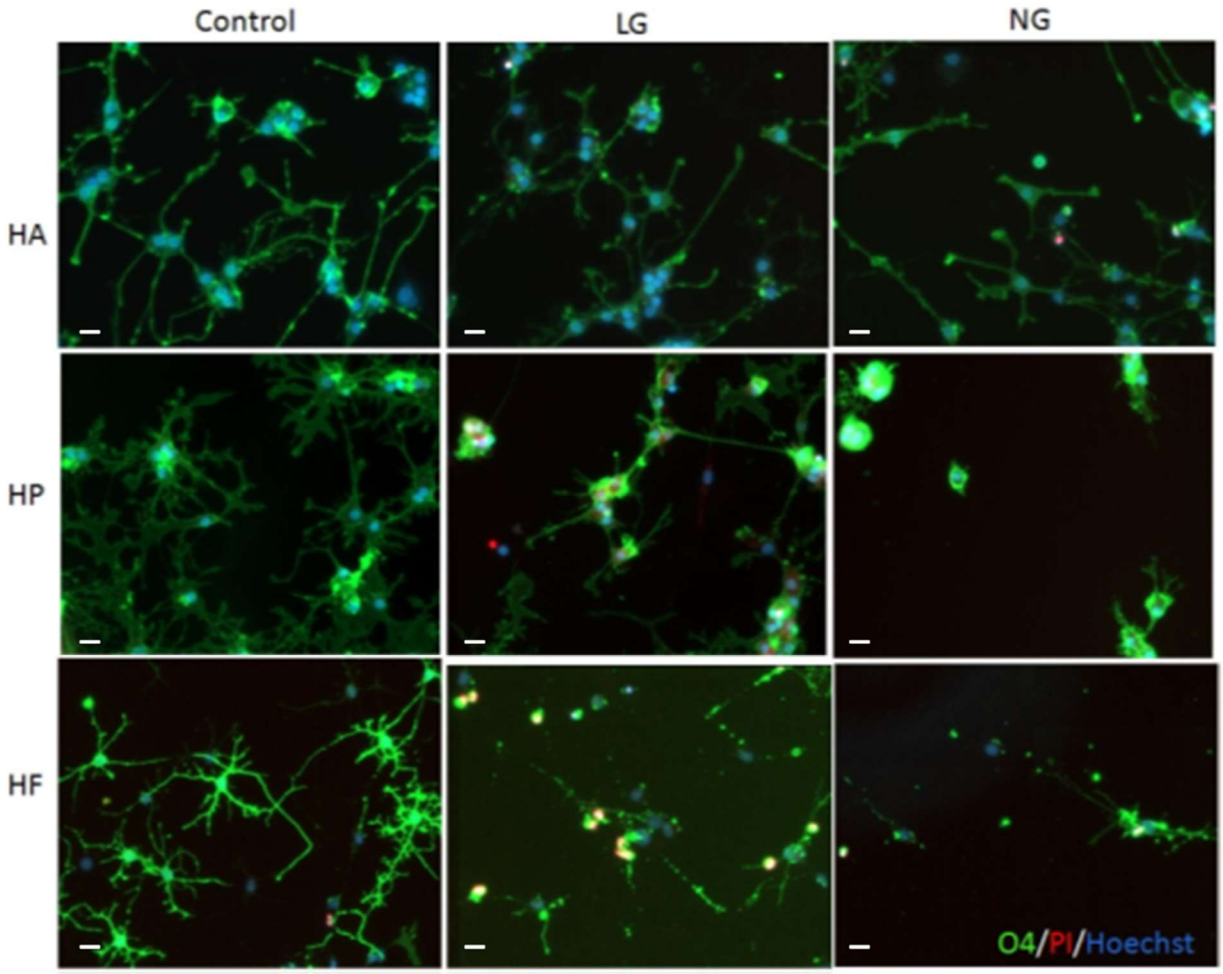

Supplementary Figure 3.2 - Expression of the oligodendrocyte marker O4 in adult, pediatric and fetal samples- dissociated culture of OLs derived from each of an adult (HA), pediatric (HP) and fetal (HF) sample under N1 control, LG and NG conditions for 2 days stained with anti-O4 antibody (green), propidium iodide (PI, red), and nuclear stain (Hoechst) blue, indicating presence of PI+ cells in pediatric and fetal O4+ cells in LG condition, and reduced cell numbers in NG condition. Scale bar = 20 µm is shown in the bottom right, all other figures are in the same scale.

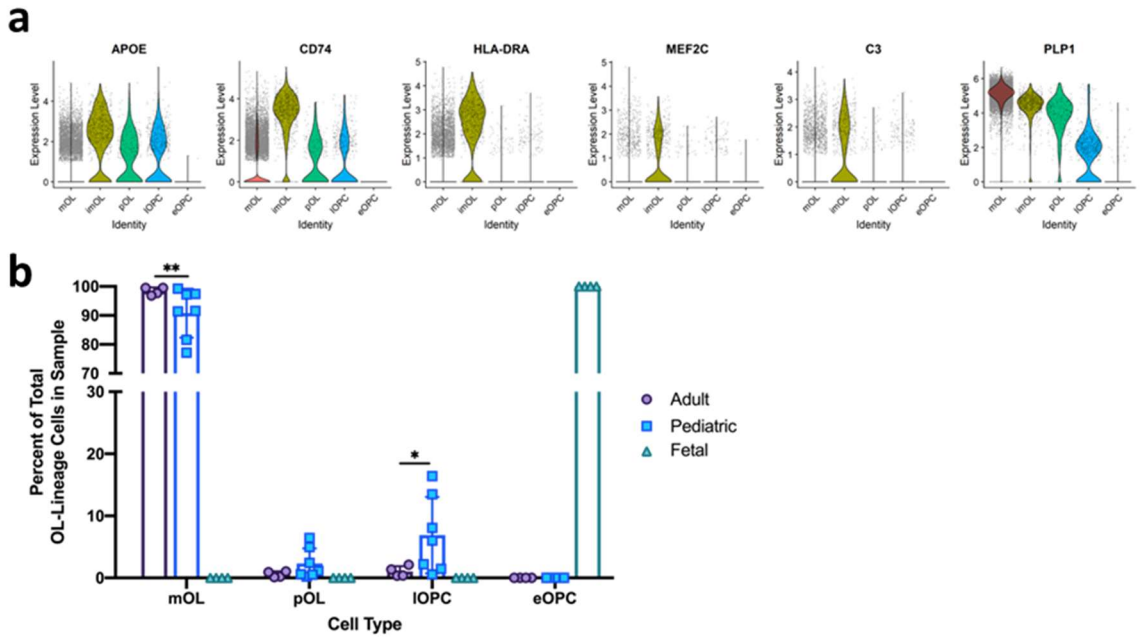

Supplementary Figure 3.3 – Expression of oligodendrocyte markers in the identified cell clusters. **a.** Expression of markers distinguishing immune-oligodendrocyte population identified by Jäkel et al. (2019). Expression levels are z-scored normalized average expression and grey dots indicate individual cells expressing the marker. **b.** OL lineage cell-type make-up differs in across age groups. Shown are percentage of cells in specific subpopulations out of total OL lineage cells for each sample by age-group. Two-way ANOVA with Tukey's correction for multiple comparisons was done, significance is adjusted $p<0.05$*, $p<0.01$**. Number of independent biological samples by age group: 4 adult, 7 pediatric and 4 fetal.

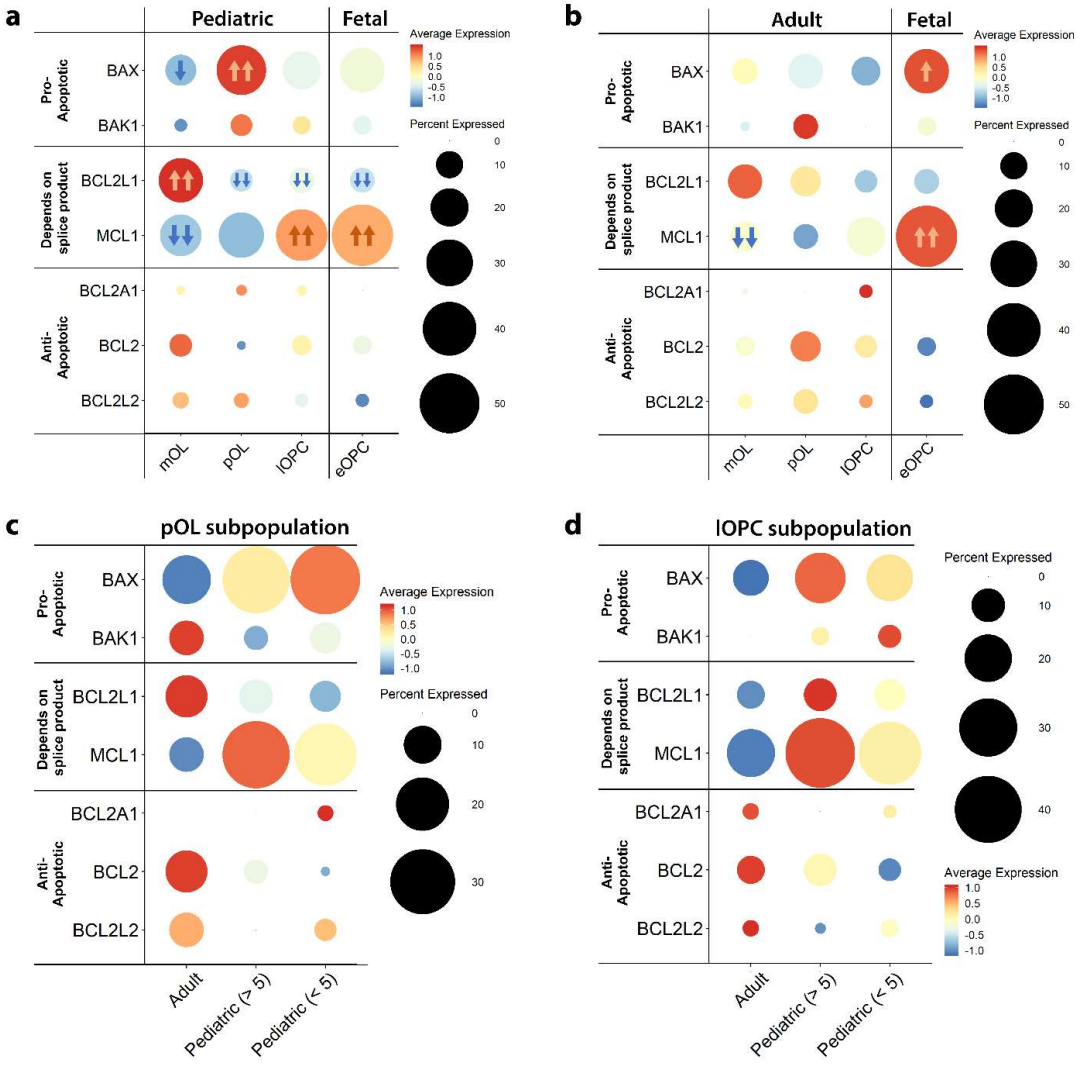

Supplementary Figure 3.4 – Relative expression of pro- and anti-apoptotic BCL-2 genes within age groups and OL-lineage cell types. Average expression in (a) OL-lineage cells within pediatric and fetal samples, (b) OL-lineage cells within adult and fetal samples, (c) pOLs across age groups, and (d) lOPCs across age groups. Scale is z-scores of averaged normalized gene expression across the cell types or age groups; percent expressed indicates the percentage of OL-lineage cells in the cell type or age group expressing the gene. Arrows indicate up- (orange) or down- (blue) regulation (adj. $p<0.05$) against all other groups on the x-axis, where one arrow $|logFC| > 0.1$, two arrows $|logFC| > 0.25$, by Wilcoxon rank sum differential expression testing with Bonferroni correction. Number of independent biological samples by age group: 4 adult, 7 pediatric (4 pediatric < 5; 3 pediatric >5), and 4 fetal.

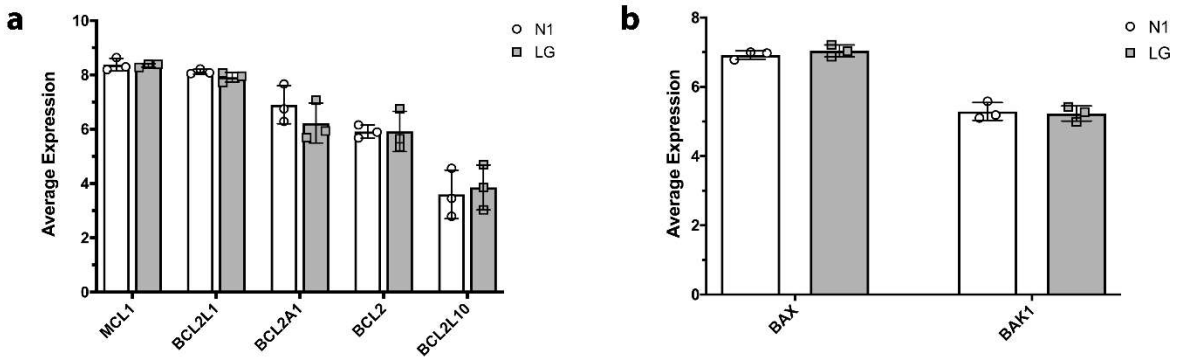

Supplementary Figure 3.5 - Changes of expression in the anti and pro-apoptotic molecules in human adult oligodendrocytes due to glucose deprivation. Average RNA level of the (**a**) anti-apoptotic and (**b**) pro-apoptotic molecules of the BCL-2 family in media containing low concentration of glucose (LG) or in optimal culture media (N1) derived by microarray analysis of adult human oligodendrocytes. N=3 independent biological samples. Mean SEM for each condition in the figure.

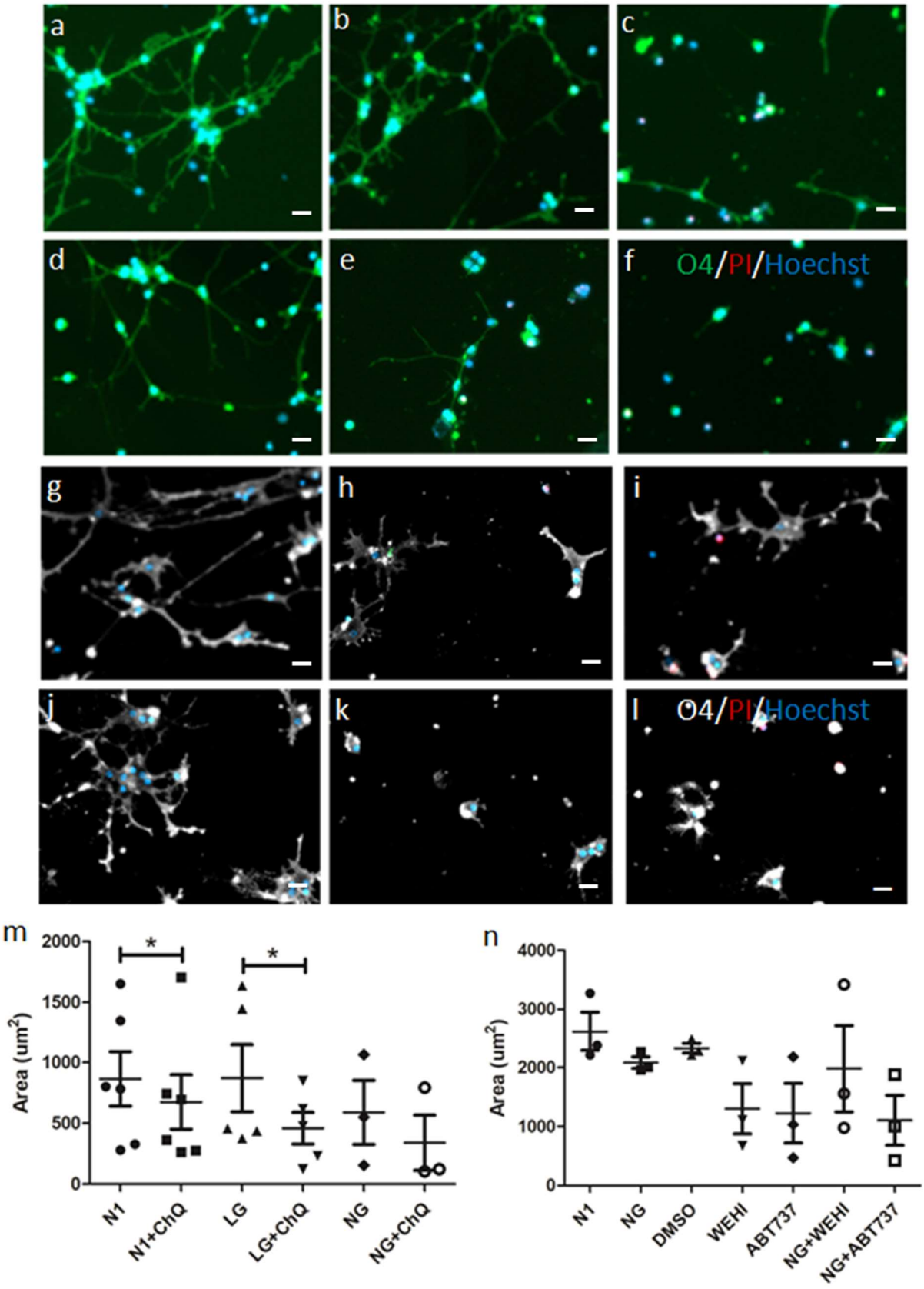
a
b
c
d
e
f
O4/PI/Hoechst
g
h
i
j
k
l
O4/PI/Hoechst
m
Area (um²)
2000
1500
1000
500
0
*
*
N1
N1+ChQ
LG
LG+ChQ
NG
NG+ChQ
n
Area (um²)
4000
3000
2000
1000
0
N1
NG
DMSO
WEHI
ABT737
NG+WEHI
NG+ABT737

Supplementary Figure 3.6 – Illustrations of changes in process extension by adult human OLs exposed to chloroquine or BCL-2 inhibitors under LG conditions for 2 days. a, g) N1 condition; b) LG condition; c, j) NG condition ;d) N1 condition + chloroquine; e) LG condition + chloroquine; f) NG condition + chloroquine; h) N1 condition + BCL-2 inhibitor WEHI; i) N1 + BCL-2 inhibitor ABT737; k) NG conditions + BCL-2 inhibitor WEHI, l) NG condition + BCL-2 inhibitor ABT737 ; m) summary the effects of chloroquine on cell area under N1, LG or NG conditions; n) summary the effects of BCL-2 inhibitors WEHI or ABT737 on cell area under N1 or NG conditions. Each dot corresponds to an independent biological samples. Mean SEM for each condition in the figure. Statistical significance was verified by ANOVA/Tukey test Compared to corresponding control conditions: * $p < 0.05$. Scale bar = 20 μm is shown in l), all other figures are in the same scale.

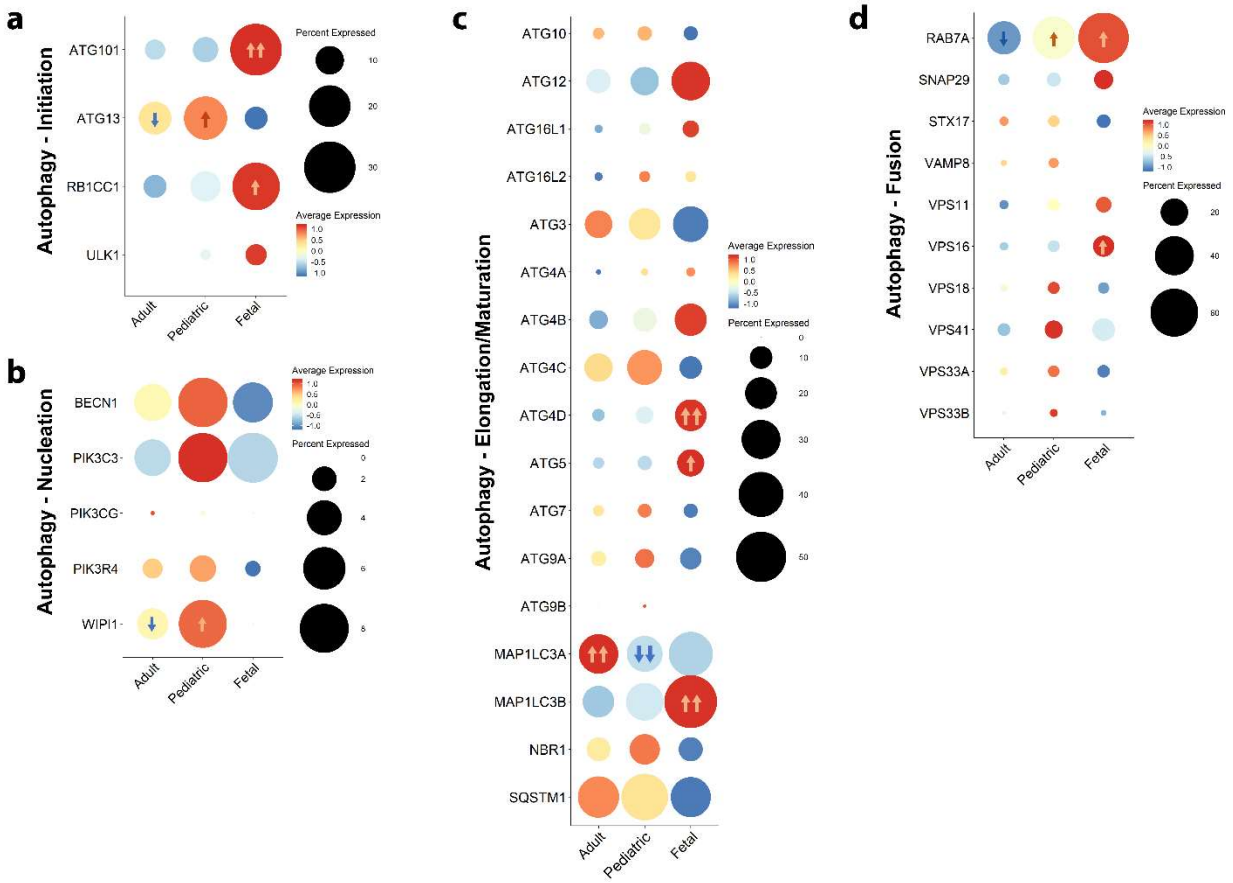

Supplementary Figure 3.7 – Relative expression of genes related to autophagy pathways. Expression level of genes related to autophagy (**a**) initiation, (**b**) nucleation, (**c**) elongation/maturation, and (**d**) fusion in total OL lineage cells of pooled adult, pediatric, and fetal samples. Scale is z-scores of averaged normalized gene expression across the age groups; percent expressed indicates the percentage of OL-lineage cells in the age group expressing the gene. Arrows indicate up- (orange) or down- (blue) regulation (adj. $p<0.05$) against all other groups, where one arrow $|\log FC| > 0.1$, two arrows $|\log FC| > 0.25$, by Wilcoxon rank sum differential expression testing with Bonferroni correction. Number of independent biological samples by age group: 4 adult, 7 pediatric and 4 fetal.

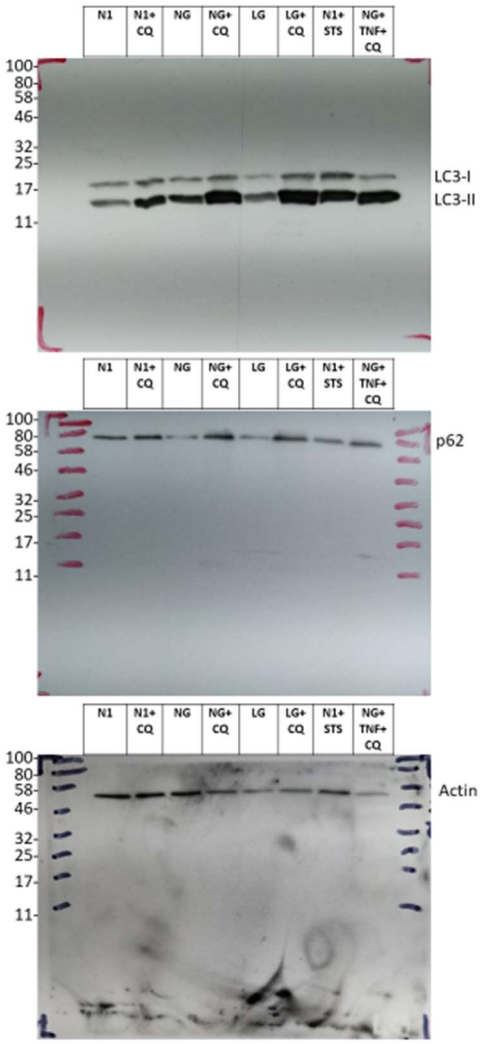

Supplementary Figure 3.8 – Uncropped blot images for LC3, p62 and Actin (loading control) measurement in the first human oligodendrocyte samples from Figure 6. Molecular weight is indicated at the left of each band and the corresponding protein on the right. Conditions of each lane is indicated at the top of each blot. The last two conditions on the right were not used for this study. All blots are derived from the same gel.

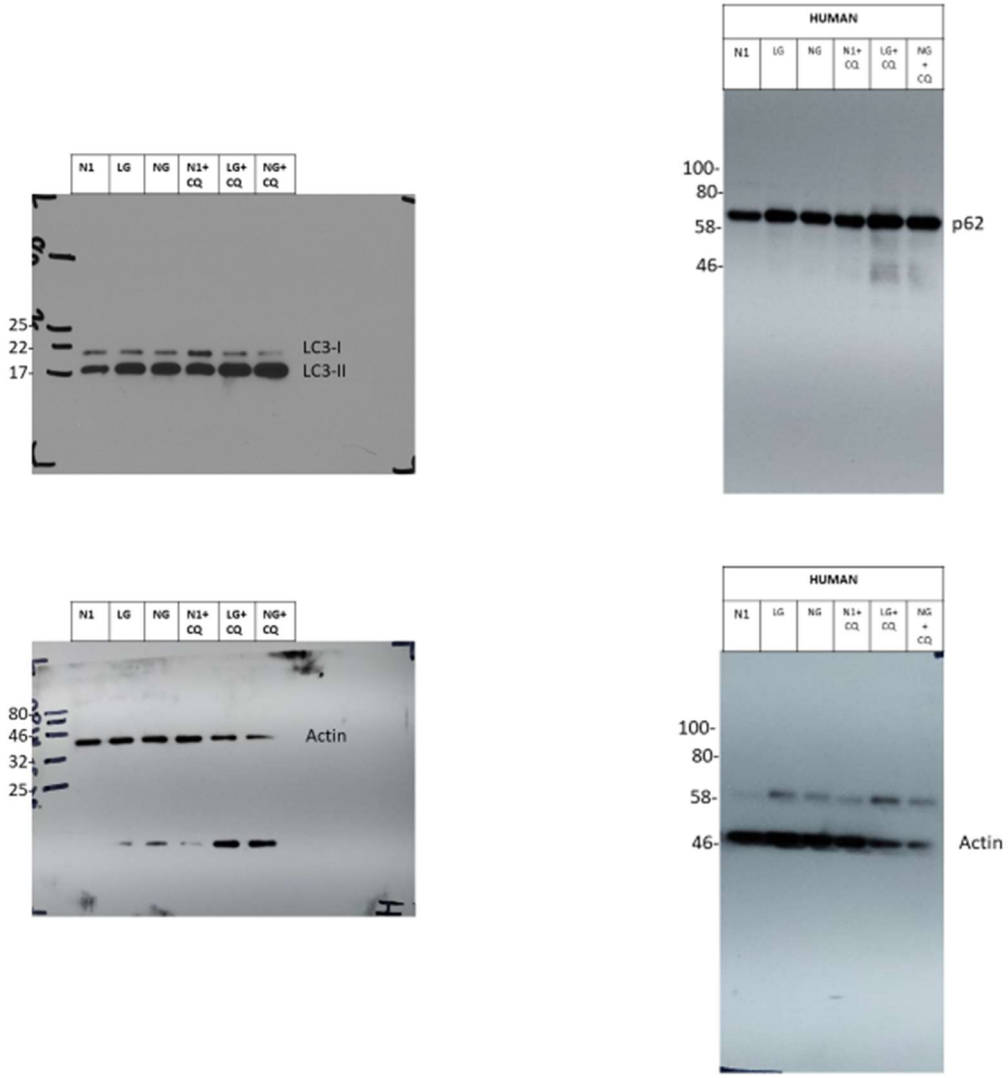

Supplementary Figure 3.9 – Uncropped blot images for LC3, p62 and Actin (loading control) measurement in the second human oligodendrocyte samples from Figure 6. Molecular weight is indicated at the left of each band and the corresponding protein on the right. Conditions of each lane is indicated at the top of each blot.

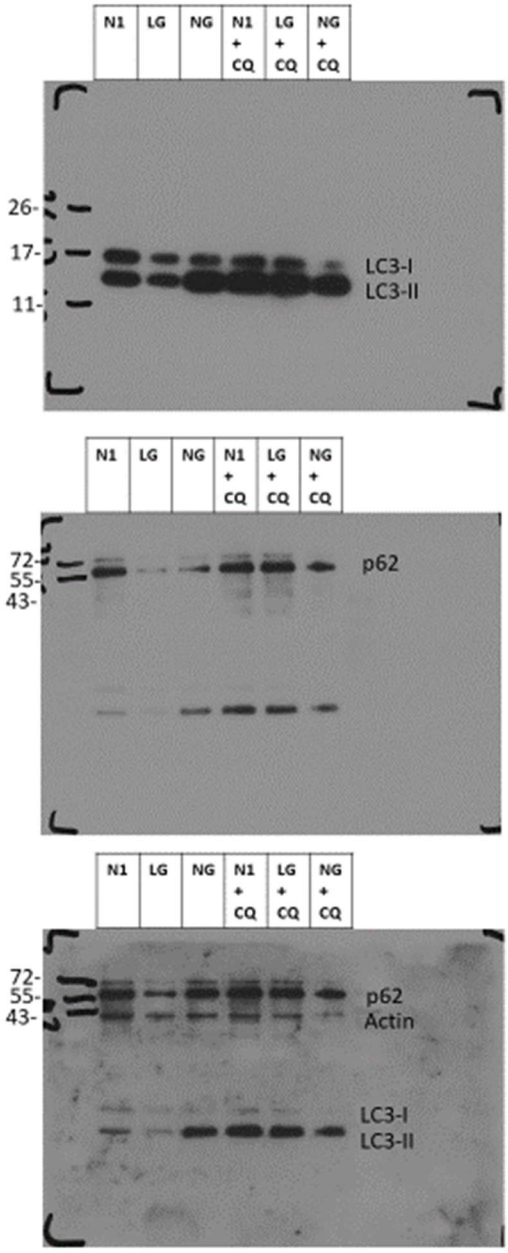

Supplementary Figure 3.10 – Uncropped blot images for LC3, p62 and Actin (loading control) measurement in the third human oligodendrocyte sample from Figure 6. Molecular weight is indicated at the left of each band and the corresponding protein on the right. Conditions of each lane is indicated at the top of each blot. All blots are derived from the same gel.

Supplementary Table 3.1 – Pediatric Patient Demographics

	Age	Sex	Diagnosis	scRNAseq	*in vitro* assays
< 5 years	1.5	M	focal cortical dysplasia	+	+
	2	F	focal cortical dysplasia		+
	2	F	megalencephaly	+	
	2	M	Rasmussen's encephalitis	+	+
	4	F	focal encephalomalacia		+
	4	M	focal cortical dysplasia	+	+
	5	M	focal cortical dysplasia		+
> 5 years	7	M	focal cortical dysplasia		+
	8	F	focal cortical dysplasia		+
	10	F	focal epilepsy	+	
	13	F	focal epilepsy	+	+
	14	F	congenital stroke	+	

3.11 References

Aboul-Enein, F. et al. Preferential loss of myelin-associated glycoprotein reflects hypoxia-like white matter damage in stroke and inflammatory brain diseases. *J. Neuropathol. Exp. Neurol.* 62, 25–33 (2003).

Ashkenazi, A. & Salvesen, G. Regulated cell death: signaling and mechanisms. *Annu Rev. Cell Dev. Biol.* 30, 337–356 (2014).

Back, S. A. et al. Late oligodendrocyte progenitors coincide with the developmental window of vulnerability for human perinatal white matter injury. *J. Neurosci.* 21, 1302–1312 (2001).

Back, S. A. et al. Selective vulnerability of late oligodendrocyte progenitors to hypoxia-ischemia. *J. Neurosci.* 22, 455–463 (2002).

Back, S. A. White matter injury in the preterm infant: pathology and mechanisms. *Acta Neuropathol.* 134, 331–349 (2017).

Balmer, D. et al. Autophagy defect is associated with low glucose-induced apoptosis in 661W photoreceptor cells. *PLoS ONE* 8, e74162 (2013).

Bankston, A. N. et al. Autophagy is essential for oligodendrocyte differentiation, survival, and proper myelination. *Glia* 67, 1745–1759 (2019).

Barnett, M. H. & Prineas, J. W. Relapsing and remitting multiple sclerosis: pathology of the newly forming lesion. *Ann. Neurol.* 55, 458–468 (2004).

Butler, A., Hoffman, P., Smibert, P., Papalexi, E. & Satija, R. Integrating single-cell transcriptomic data across different conditions, technologies, and species. *Nat. Biotechnol.* 36, 411–420 (2018).

Button, R. W., Roberts, S. L., Willis, T. L., Hanemann, C. O. & Luo, S. Accumulation of autophagosomes confers cytotoxicity. *J. Biol. Chem.* 292, 13599–13614 (2017).

Chang, A., Nishiyama, A., Peterson, J., Prineas, J. & Trapp, B. D. NG2-positive oligodendrocyte progenitor cells in adult human brain and multiple sclerosis lesions. *J. Neurosci.* 20, 6404–6412 (2000).

Cui, Q. L. et al. Oligodendrocyte progenitor cell susceptibility to injury in multiple sclerosis. *Am. J. Pathol.* 183, 516–525 (2013).

Cui, Q. L. et al. Sublethal oligodendrocyte injury: A reversible condition in multiple sclerosis? *Ann. Neurol.* 81, 811–824 (2017).

D'Haeseleer, M. et al. Cerebral hypoperfusion: a new pathophysiologic concept in multiple sclerosis? *J. Cereb. Blood Flow. Metab.* 35, 1406–1410 (2015).

Denton, D. & Kumar, S. Autophagy-dependent cell death. *Cell Death Differ.* 26, 605–616 (2019).

Duncan, I. D. et al. The adult oligodendrocyte can participate in remyelination. *Proc. Natl Acad. Sci. USA* 115, E11807–e11816 (2018).

Dutta, R. & Trapp, B. D. Gene expression profiling in multiple sclerosis brain. *Neurobiol. Dis.* 45, 108–114 (2012).

Edwards, A. D. & Mehmet, H. Apoptosis in perinatal hypoxic-ischaemic cerebral damage. *Neuropathol. Appl. Neurobiol.* 22, 494–498 (1996).

Esmonde-White, C. et al. Distinct function-related molecular profile of adult human A2B5-positive pre-oligodendrocytes versus mature oligodendrocytes. *J. Neuropathol. Exp. Neurol.* 78, 468–479 (2019).

Franklin, R. J. M., Ffrench-Constant, C. & Regenerating, C. N. S. myelin - from mechanisms to experimental medicines. *Nat. Rev. Neurosci.* 18, 753–769 (2017).

Galluzzi, L. et al. Molecular definitions of autophagy and related processes. *Embo J.* 36, 1811–1836 (2017).

Galluzzi, L. et al. Molecular mechanisms of cell death: recommendations of the Nomenclature Committee on Cell Death 2018. *Cell Death Differ.* 25, 486–541 (2018).

Galluzzi, L., Bravo-San Pedro, J. M., Blomgren, K. & Kroemer, G. Autophagy in acute brain injury. *Nat. Rev. Neurosci.* 17, 467–484 (2016).

Giacci, M. K. et al. Oligodendroglia are particularly vulnerable to oxidative damage after neurotrauma in vivo. *J. Neurosci.* 38, 6491–6504 (2018).

Glass, H. C. Hypoxic-ischemic encephalopathy and other neonatal encephalopathies. *Continuum (Minneap. Minn.)* 24, 57–71 (2018).

Glick, D., Barth, S. & Macleod, K. F. Autophagy: cellular and molecular mechanisms. *J. Pathol.* 221, 3–12 (2010).

Gunn, A. J. & Thoresen, M. Neonatal encephalopathy and hypoxic-ischemic encephalopathy. *Handb. Clin. Neurol.* 162, 217–237 (2019).

Guo, K. et al. Hypoxia induces the expression of the pro-apoptotic gene BNIP3. *Cell Death Differ.* 8, 367–376 (2001).

Happo, L., Strasser, A. & Cory, S. BH3-only proteins in apoptosis at a glance. *J. Cell Sci.* 125, 1081–1087 (2012).

Itoh, T., Itoh, A. & Pleasure, D. Bcl-2-related protein family gene expression during oligodendroglial differentiation. *J. Neurochem* 85, 1500–1512 (2003).

Jäkel, S. et al. Altered human oligodendrocyte heterogeneity in multiple sclerosis. *Nature* 566, 543–547 (2019).

Kale, J., Osterlund, E. J. & Andrews, D. W. BCL-2 family proteins: changing partners in the dance towards death. *Cell Death Differ.* 25, 65–80 (2018).

Khorchid, A., Fragoso, G., Shore, G. & Almazan, G. Catecholamine-induced oligodendrocyte cell death in culture is developmentally regulated and involves free radical generation and differential activation of caspase-3. *Glia* 40, 283–299 (2002).

Kline, M. P. et al. ABT-737, an inhibitor of Bcl-2 family proteins, is a potent inducer of apoptosis in multiple myeloma cells. *Leukemia* 21, 1549–1560 (2007).

Kønig, S. M., Rissler, V., Terkelsen, T., Lambrughi, M. & Papaleo, E. Alterations of the interactome of Bcl-2 proteins in breast cancer at the transcriptional, mutational and structural level. *PLoS Comput. Biol.* 15, e1007485 (2019).

Kuhlmann, T. et al. An updated histological classification system for multiple sclerosis lesions. *Acta Neuropathol.* 133, 13–24 (2017).

Lassmann, H. & van Horssen, J. Oxidative stress and its impact on neurons and glia in multiple sclerosis lesions. *Biochim. Biophys. Acta* 1862, 506–510 (2016).

Lee, H. & Paik, S. G. Regulation of BNIP3 in normal and cancer cells. *Mol. Cells* 21, 1–6 (2006).

Leong, S. Y. et al. Heterogeneity of oligodendrocyte progenitor cells in adult human brain. *Ann. Clin. Transl. Neurol.* 1, 272–283 (2014).

Lessene, G. et al. Structure-guided design of a selective BCL-X(L) inhibitor. *Nat. Chem. Biol.* 9, 390–397 (2013).

Liu, Y. et al. Autosis is a Na+,K+-ATPase-regulated form of cell death triggered by autophagy-inducing peptides, starvation, and hypoxia-ischemia. *Proc. Natl Acad. Sci. USA* 110, 20364–20371 (2013).

Lucchinetti, C. F., Bruck, W. & Lassmann, H. Evidence for pathogenic heterogeneity in multiple sclerosis. *Ann. Neurol.* 56, 308 (2004).

Ludwin, S. K. & Johnson, E. S. Evidence for a “dying-back” gliopathy in demyelinating disease. *Ann. Neurol.* 9, 301–305 (1981).

Mahad, D. H., Trapp, B. D. & Lassmann, H. Pathological mechanisms in progressive multiple sclerosis. *Lancet Neurol.* 14, 183–193 (2015).

Marin, M. A. & Carmichael, S. T. Mechanisms of demyelination and remyelination in the young and aged brain following white matter stroke. *Neurobiol. Dis.* 126, 5–12 (2019).

Mauthe, M. et al. Chloroquine inhibits autophagic flux by decreasing autophagosome-lysosome fusion. *Autophagy* 14, 1435–1455 (2018).

Munson, M. J. & Ganley, I. G. MTOR, PIK3C3, and autophagy: signaling the beginning from the end. *Autophagy* 11, 2375–2376 (2015).

Nakamura, S. & Yoshimori, T. New insights into autophagosome-lysosome fusion. *J. Cell Sci.* 130, 1209–1216 (2017).

Neumann, B. et al. Metformin restores CNS remyelination capacity by rejuvenating aged stem cells. *Cell Stem Cell* 25, 473–485.e478 (2019).

Neumann, B., Segel, M., Chalut, K. J. & Franklin, R. J. Remyelination and ageing: Reversing the ravages of time. *Mult. Scler.* 25, 1835–1841 (2019).

Perlman, K. et al. Developmental trajectory of oligodendrocyte progenitor cells in the human brain revealed by single cell RNA sequencing. *Glia* 68, 1291–1303 (2020).

Plouin, P. & Kaminska, A. Neonatal seizures. *Handb. Clin. Neurol.* 111, 467–476 (2013).

Prineas, J. W. & Parratt, J. D. Oligodendrocytes and the early multiple sclerosis lesion. *Ann. Neurol.* 72, 18–31 (2012).

Rajan, P., Elliott, D. J., Robson, C. N. & Leung, H. Y. Alternative splicing and biological heterogeneity in prostate cancer. *Nat. Rev. Urol.* 6, 454–460 (2009).

Rao, V. T. S. et al. Distinct age and differentiation-state dependent metabolic profiles of oligodendrocytes under optimal and stress conditions. *PLoS ONE* 12, e0182372 (2017).

Rodriguez, M., Scheithauer, B. W., Forbes, G. & Kelly, P. J. Oligodendrocyte injury is an early event in lesions of multiple sclerosis. *Mayo Clin. Proc.* 68, 627–636 (1993).

Rone, M. B. et al. Oligodendrogliopathy in multiple sclerosis: low glycolytic metabolic rate promotes oligodendrocyte survival. *J. Neurosci.* 36, 4698-4707 (2016).

Schneider, J. & Miller, S. P. Preterm brain Injury: White matter injury. *Handb. Clin. Neurol.* 162, 155–172 (2019).

Segovia, K. N. et al. Arrested oligodendrocyte lineage maturation in chronic perinatal white matter injury. *Ann. Neurol.* 63, 520–530 (2008).

Senichkin, V. V., Streletskaia, A. Y., Zhivotovsky, B. & Kopeina, G. S. Molecular Comprehension of Mcl-1: From Gene Structure to Cancer Therapy. *Trends Cell Biol.* 29, 549–562 (2019).

Stadelmann, C. et al. Tissue preconditioning may explain concentric lesions in Baló's type of multiple sclerosis. *Brain* 128, 979–987 (2005).

Stuart, T. et al. Comprehensive integration of single-cell data. *Cell* 177, 1888–1902.e1821 (2019).

Trapp, B. D. & Stys, P. K. Virtual hypoxia and chronic necrosis of demyelinated axons in multiple sclerosis. *Lancet Neurol.* 8, 280–291 (2009).

van den Brink, S. C. et al. Single-cell sequencing reveals dissociation-induced gene expression in tissue subpopulations. *Nat. Methods* 14, 935–936 (2017).

Volpe, J. J. Neonatal encephalopathy: an inadequate term for hypoxic-ischemic encephalopathy. *Ann. Neurol.* 72, 156–166 (2012).

Yeung, M. S. Y. et al. Dynamics of oligodendrocyte generation in multiple sclerosis. *Nature* 566, 538–542 (2019).

Yin, R. X. et al. Roles of bcl-2/bax expression and oligodendrocyte apoptosis in the pathogenesis of heroin-induced spongiform leukoencephalopathy. *Zhonghua Yi Xue Za Zhi* 88, 749–753 (2008).

Yu, L., Chen, Y. & Tooze, S. A. Autophagy pathway: cellular and molecular mechanisms. *Autophagy* 14, 207–215 (2018).

Zappia, L. & Oshlack, A. Clustering trees: a visualization for evaluating clusterings at multiple resolutions. *Gigascience* 7, giy083 (2018).

Zhang, F., Wu, Y. & Tian, W. A novel approach to remove the batch effect of single-cell data. *Cell Disco.* 5, 46 (2019).

Zhu, C. et al. The influence of age on apoptotic and other mechanisms of cell death after cerebral hypoxia-ischemia. *Cell Death Differ.* 12, 162–176 (2005).

Bridge between manuscripts

In Chapter 3, some of the research questions established in the aims were clarified. We could demonstrate that OLs are resistant to apoptosis and the mechanisms that underlie this resistance. We could also observe that this resistance is increased in mature OLs and OLs extracted from older individuals. Transcriptomics and functional assays indicated the important role in the expression of anti-apoptotic molecules of the BCL-2 family. This profile suggests that during development cells switch to a resistant phenotype, in which these mature cells are stably incorporated in the neural tissue, providing myelin for proper neural function. Loss of cells in these conditions would require a considerable cost for the organism for its substitution. In contrast, apoptosis is known to have a function in development. During development, OPCs proliferate and migrate, in search of positions in which they will differentiate and establish myelin sheaths around axons they eventually find. When OPCs are unable to find a position suitable for their differentiation, they undergo apoptosis to eliminate cells that are in excess (Hughes and Stockton, 2021a). Therefore, it is expected that mature cells resist not only apoptosis but also any kind of regulated cell death.

The comparison of OL lineage cells extracted from fetal, pediatric, and adult tissues, showed a profound difference between fetal and the other two age categories, as fetal cells are composed exclusively of early OPCs, which were not detected in the other categories. We also notice the presence of a considerable quantity of late OPCs in pediatric samples, which are less present in adults. This data suggests that OLs differentiate and acquire resistance early in life, and therefore are set to survive and execute their functions while the individual is alive.

The literature about the role of autophagy in cell death and survival is ambiguous. Some studies indicate that autophagy supports cell survival, while others indicate the existence of autophagy-mediated cell death (Lockshin and Zakeri, 2004, D'Arcy, 2019, Dikic and Elazar, 2018, Nakamoto et al., 2012, Rouschop et al., 2010). We observed that autophagy is activated in hOLs in response to metabolic stress and that the inhibition of autophagy accelerates cell death. Therefore, our data suggest that autophagy is not contributing to cell death. Moreover, the transcriptomics comparison between genes involved in the expression of components of the autophagy machinery indicates that older individuals have an improved autophagy apparatus. This improvement in combination with the increased resistance to apoptosis may indicate that the overall resistance to cell death of hOLs is increased during development and associated with the full differentiation of this type of cells.

After this study, many questions remained to be answered to fulfill the aims of this thesis. As apoptosis is not triggered by metabolic stress in hOLs, other RCD pathways need to be investigated. After examining the RCD described in the literature, we concluded that those that have a higher potential to occur in hOLs due to metabolic stress are ferroptosis and MPT-driven necrosis.

As autophagy was demonstrated to have a protective role, we hypothesized that autophagy would fail after long periods of metabolic stress, contributing to the demise of cells. Also, as autophagy is reported to contribute to energetic metabolism by supplying substrates to oxidative phosphorylation (White et al., 2015), we intended to verify if modulation of autophagy could affect cellular ATP levels and reduce cell death. We also aimed to investigate the occurrence of autophagy *in situ*, in samples of MS cases, which would indicate the presence of metabolic stress.

Finally, we aimed to verify the role of Ca^{2+} in the process of cell death, as it can contribute in many ways to cell death, as described in the literature review (Zhivotovsky and Orrenius, 2011).

CHAPTER 4: Mechanisms of metabolic stress induced cell death of human oligodendrocytes: relevance for progressive multiple sclerosis

Milton Guilherme Forestieri Fernandes[1], Abdulshakour Mohammadnia[1], Florian Pernin[1], Laura Eleonora Schmitz-Gielsdorf[2], Caroline Hodgins[1], Qiao-Ling Cui[1], Moein Yaqubi[1], Manon Blain[1], Jeffery Hall[3], Roy Dudley[4], Myriam Srour[5], Stephanie E. J. Zandee[6], Wendy Klement[6], Alexandre Prat[6], Jo Anne Stratton[1], Moses Rodriguez[8], Tanja Kuhlmann[2], Wayne Moore[1], Timothy E. Kennedy[7]& Jack P. Antel[1]

1. Neuroimmunology Unit, Montreal Neurological Institute, McGill University, 3801 Rue University, Montreal, QC, H3A 2B4, Canada
2. Institute of Neuropathology, University Hospital Münster, Albert-Schweitzer-Campus 1, 48149, Münster, Germany
3. Department of Neurosurgery, Department of Neurology and Neurosurgery, McGill University Health Centre, 3801 Rue University, Montreal, QC, H3A 2B4, Canada
4. Department of Pediatric Neurosurgery, Montreal Children's Hospital, 1001 Decarie Blvd, Montreal, QC, H4A 3J1, Canada
5. Division of Pediatric Neurology, Montreal Children's Hospital, 1001 Decarie Blvd, Montreal, QC, H4A 3J1, Canada
6. Department of Neuroscience, Faculty of Medicine, Université de Montréal, Pavillon Roger-Gaudry, 2900 Edouard Montpetit Blvd, Montreal, QC, H3T 1J4, Canada
7. Department of Neurology and Neurosurgery, McGill University, 3801 Rue University, Montreal, QC, H3A 2B4, Canada
8. Department of Neurology, Mayo Clinic Foundation, 1216 2nd St SW, Rochester, MN, 55902, USA

Corresponding author: Dr. Jack P. Antel, Neuroimmunology Unit, Montreal Neurological Institute and Department of Neurology and Neurosurgery, McGill University, 3801 University Street, Montreal, QC, H3A 2B4, Canada, e-mail: jack.antel@mcgill.ca

Published: 5 July, 2023
Acta Neuropathologica Communications, 11, Article number: 108 (2023)
DOI: https://doi.org/10.1186/s40478-023-01601-1

4.1 Abstract

OL injury and loss are central features of evolving lesions in multiple sclerosis. Potential causative mechanisms of OL loss include metabolic stress within the lesion microenvironment. Here we use the injury response of primary human OLs (hOLs) to metabolic stress (reduced glucose/nutrients) in vitro to help define the basis for the in situ features of OLs in cases of MS. Under metabolic stress in vitro, we detected reduction in ATP levels per cell that precede changes in survival. Autophagy was initially activated, although ATP levels were not altered by inhibitors (chloroquine) or activators (Torin-1). Prolonged stress resulted in autophagy failure, documented by non-fusion of autophagosomes and lysosomes. Consistent with our in vitro results, we detected higher expression of LC3, a marker of autophagosomes in OLs, in MS lesions compared to controls. Both *in vitro* and *in situ*, we observe a reduction in nuclear size of remaining OLs. Prolonged stress resulted in increased ROS and cleavage of spectrin, a target of Ca^{2+}-dependent proteases. Cell death was however not prevented by inhibitors of ferroptosis or MPT-driven necrosis, the regulated cell death (RCD) pathways most likely to be activated by metabolic stress. hOLs have decreased expression of VDAC1, VDAC2, and of genes regulating iron accumulation and cyclophilin. RNA sequencing analyses did not identify activation of these RCD pathways in vitro or in MS cases. We conclude that this distinct response of hOLs, including resistance to RCD, reflects the combined impact of autophagy failure, increased ROS, and calcium influx, resulting in metabolic collapse and degeneration of cellular structural integrity. Defining the basis of OL injury and death provides guidance for development of neuro-protective strategies.

4.2 Introduction

Demyelination within the CNS is the pathologic hallmark of multiple sclerosis (MS). Histologic analyses indicate that while the number of oligodendrocytes (OLs), the myelin producing cells, are relatively preserved in initial demyelinating white matter lesions ("relapsing phase"), there is detectible cell loss in active post-demyelinating lesions, with increasing loss in mixed active / inactive lesions (also named chronic active or smoldering lesions) (Heß et al., 2020, Kuhlmann et al., 2017). Actively demyelinating lesions are mostly found in patients with early relapsing remitting disease course, whereas the proportion of mixed lesions significantly increases in patients with progressive disease (Bitsch et al., 2001, Lassmann et al., 2012, Luchetti et al., 2018). Prineas et al. reported that surviving OLs at the lesion border in chronic active white matter lesions only rarely showed apoptotic nuclei and were not TUNEL positive (Prineas et al., 2001). Bonetti and Raine also concluded that the OLs associated with MS lesions in cases of chronic progressive MS do not undergo apoptosis (Bonetti and Raine, 1997).

Mechanisms of cell death have been considered under the broad categories of either accidental or regulated cell death (RCD) (Galluzzi et al., 2018). Accidental cell death is the end result of an instantaneous and catastrophic process that results in a state that is incompatible with cell survival; this is typically attributed to acute exposure of cells to severe external physical insults that result in rupture of the plasma membrane and release of cytoplasm into the extracellular space (Edinger and Thompson, 2004). In contrast, RCD implies a dedicated molecular machinery that can be modulated (Galluzzi et al., 2018). Multiple RCD pathways are now recognized that can also result from perturbations of the intra- or extracellular environments when adaptive responses cannot restore homeostasis (Galluzzi et al., 2018).

Conditions implicated in OL cell loss in progressive MS include infection/inflammation and metabolic stress (Galluzzi et al., 2018). In a previous study we showed that primary adult human OLs, a cell type that is heavily dependent on glycolysis as an energy source (Rone et al., 2016), when challenged with metabolic stress conditions, undergo delayed cell death without activation of apoptotic pathways when compared to young pediatric brain derived OLs and especially fetal brain derived progenitor cells (Cui et al., 2013, Fernandes et al., 2021). Exposure of adult human OLs to pro-inflammatory cytokines induced only sub-lethal injury (dying back of cell processes) (Cui et al., 2017, Pernin et al., 2022). Examining human MS lesions we detected increased expression of the integrated stress response (ISR) constituent phosphorylated EIF2α in situ, consistent with local metabolic stress. Further, RNA sequencing studies have revealed the upregulation of an array of metabolic stress related genes in OLs in MS lesions (Jäkel et al., 2019).

The central aim of the current study was to define the mechanistic basis of cell death of primary human OLs (hOLs) in vitro in response to metabolic stress (reduced glucose/nutrients) and relate this to the in situ features of OLs that evolve during the course of MS. Our in vitro studies using this model of metabolic stress demonstrate a significant reduction in ATP per hOL that precedes any change in cell survival. Both in the in vitro stress model and in situ MS lesions, we detect an increase in LC3 in OLs, a marker of autophagosomes, indicating that the initially activated autophagy pathway has stalled. We detected nuclear condensation and volume reduction (pyknosis) (Burgoyne, 1999) in hOLs in vitro under sustained stress conditions and in remaining OLs in “active/post-demyelinating” lesions. We show that prolonged stress in vitro results in increased ROS and cleavage of spectrin, a target of Ca^{2+}-dependent proteases in hOLs; however both in vitro and in situ, the hOLs resist triggering either ferroptosis or mitochondrial

permeability transition-driven necrosis (MPTN), RCD pathways commonly linked to metabolic stress and operative in MS related models including EAE and cuprizone toxicity (Galluzzi et al., 2018, Hu et al., 2019, Jhelum et al., 2020). We consider that the distinct cell death response of hOLs, a cell type resistant to activating RCD pathways, reflects the combined impact of autophagy failure, increased ROS and calcium influx, resulting in the collapse of cellular structural integrity. The prolonged time course of hOL cell death may provide an opportunity for therapeutic targeting.

4.3 Materials and methods

4.3.1 In situ immunohistochemical studies - MS and control tissue samples

For LC-3 immuno-fluorescence-based histochemistry, human rapid post-mortem brain tissue samples were obtained from the Neuroimmunology Research Laboratory, Centre de Recherche du Centre Hospitalier de l'Université de Montréal (CRCHUM) under ethical approval number BH07.001.31. Sections with areas of chronic active demyelination were selected based on Luxol Fast Blue-Hematoxylin and Eosin (LFB/H&E) staining and presence of macrophages, some of which contained LFB positive material. The immunohistochemistry procedure and confocal imaging were performed as previously described (Pernin et al., 2022). Sudan black was added to suppress autofluorescence. Primary antibodies used were LC3 (1:500, NB100-2220 Novus Biologicals) and Nogo-A (1:5000, University of Zurich). Secondary antibodies used were goat anti-rabbit Alexa Fluor 488 (1:500) and goat anti-mouse Alexa Fluor 555 (1:500). LC3 expression was quantified by pixel intensity in individual Nogo-A + cells. Data were derived by

blinded observers measuring 10–15 cells per region of interest. Results are expressed as mean pixel intensity of the cells counted in each region of interest.

For the tissue sections selected to assess OL nuclei in MS tissue sections, the immunohistochemical labeling procedures, and means of quantitating cell numbers are as detailed previously (Heß et al., 2020).

4.3.2 In vitro studies - human surgical samples

Anonymized surgically resected brain tissue samples were obtained from the Department of Neuropathology at the Montreal Neurological Institute and Hospital (MNI) and from the Montreal Children's Hospital. All had non-tumor related focal epilepsy. Data on individual samples are provided in the Supplementary table. Studies were approved by the MNI Neurosciences Research Ethics Board (Protocol ANTJ 1988/3) and the Montreal Children's Hospital Research Ethics Board.

4.3.3 Cell isolation

Normal appearing tissue was derived from "surgical corridors" resected to access sites of pathology. As previously described (Fernandes et al., 2021), tissue derived from CUSA bags was subjected to trypsin digestion followed by Percoll gradient centrifugation to obtain a myelin-depleted whole-cell fraction comprised mainly of OLs and microglia with few if any astrocytes or neurons. An enriched OL population was obtained by plating the total cell population overnight in culture flasks; the floating cell fraction was recovered, leaving behind adherent

microglia. The final culture contains an average of ~ 90% O4 positive cells (OLs), < 5% micorglia, and only rarely astrocytes.

4.3.4 Cell culture

After selection, primary human cells were plated in 96-well or 24-well plates coated with poly-lysine and extra-cellular matrix at a density of 3×10^4 cells (96-wells plate) or 1×10^6 cells (24-wells plate) per well. Cells were cultured in DMEM-F12 media supplemented with N1 (Sigma, Oakville, ON, Canada). For metabolic deprivation experiments, cells were cultured in DMEM containing 0.25 g/l of glucose (LG) or with no glucose added (NG). HeLa cells were cultured and treated in DMEM + 10% fetal calf serum.

4.3.5 Immunocytochemistry

Cells were live stained with propidium iodide (PI; Invitrogen) (1:200) for cell viability measurements and with O4 monoclonal antibody (R&D Systems, Minneapolis, MN) (1:200) for 15 min at 37 °C and then fixed with 4% paraformaldehyde for 10 min at rt. Goat anti-mouse IgM Cy3 (1:500) was used as secondary antibody, 30 min at rt. Staining of autophagosomes and lysosomes was done as previously described (Sharifi et al., 2015). Cells were washed and permabilized in 100% cold methanol for 10 min at -20 °C. Cells were incubated in blocking buffer for 30 min at rt. Labeling using primary antibodies against LAMP-1 (MA1-184, Invitrogen, mouse IgG1), LC3 (2775 S, Cell Signaling, rabbit) and alpha-II spectrin (PA5-35383, ThermoFisher, IgG rabbit) at 1:200 dilution was performed overnight at 4 °C. Cells were incubated in secondary antibodies coupled to Alexa 488 or Alexa 647 at 1:500 dilution for 2 h at

rt. Cell nuclei were stained with Hoechst 33258 (1:1000) for 1 h at rt. Coverslips were mounted with Prolong gold (Invitrogen) (Sharifi et al., 2015). Reagents used were: chloroquine (Sigma, Oakville, ON, Canada; 10 μM), erastin (Sigma-Aldridge, Saint Louis, MO, USA), H_2O_2 (Sigma, Oakville, ON, Canada), cyclosporine A (Sigma, Oakville, ON, Canada), ferrostatin-1 (Sigma-Aldridge, Saint Louis, MO, USA) and torin-1 (Selleckchem, Houston, TX, USA).

4.3.6 Confocal microscopy

Images of intracellular components were obtained using a Leica TCS SP8 with a 63x/1.4 n.a. oil immersion objective at rt. LAS X was used as acquisition software, ImageJ was used for quantification and R for data and statistical analysis.

4.3.7 Western blot analyses

Cellular homogenates, 5–20 μg of total protein in each sample, were resolved using 7.5% (high MW targets) or 15% (low MW targets) SDS-PAGE. Proteins were electroblotted to a nitrocellulose membrane. Membranes were blocked with 5% milk and probed with 1:5000 alpha-II spectrin polyclonal antibody (PA5-35383, ThermoFisher, IgG rabbit) and anti-Caspase 3 (31A1067 Novus Biological, IgG1 mouse). Anti-rabbit horseradish peroxidase- conjugated secondary antibody was applied and bands visualized using an ECL Western blot detection kit (Cell Signaling, Danvers, MA).

4.3.8 ATP and H_2O_2 assays

Levels of ATP and H_2O_2 were measured using Cell Titer-Glo 2.0 (Promega, G9242) and ROS-Glo H_2O_2 Assay (Promega G8820). Normalization to cell number was calculated using the ratio between the measures of ATP and H_2O_2 obtained in the assay and the number of cells counted after Hoechst 33258 staining (1:1000, 1 h at rt) using ImageJ.

4.3.9 Molecular studies

RNA was extracted from selected hOLs as previously described (Healy et al., 2016). Quality control of the bulk RNA samples, as well as the library preparation, RNA-sequencing, and alignment were performed as describe in Luo et al. (Luo et al., 2022). Raw read counts were normalized, variance-stabilized transformed and differential gene expression analysis were done using DESeq2 package in R (Love et al., 2014). Adjusted p-value < 0.05 and log2 fold change > 1 were used to identify DEGs. Single sample gene set enrichment analysis (ssGSEA) implanted in GenePattern (Reich et al., 2006) was used to run pathway level enrichment analysis on bulk RNA-seq data. To define reference for ssGSEA, we generated signatures for different cell death pathways derived from XDeathDB database (Fiore et al., 2022). We used Li et al., and Bauer et al., publications to define signatures of ferroptosis and MPT derived necrosis (Bauer and Murphy, 2020, Li et al., 2020). In addition to our local datasets, we used five datasets for HeLa cell lines with gene accession numbers GSE188567, GSE186370, GSE155493, GSE157717, and GSE174116 obtained from gene expression omnibus (GEO) database (Batie et al., 2022, Fiore et al., 2022, Haimovici et al., 2022). Normalized read counts were used for hierarchical clustering and results were visualized in heatmaps format using GenePattern (Reich et al., 2006). Single nuclear RNA-seq dataset from Jakel et al. (Jäkel et al., 2019) was downloaded and analyzed as previously described (Yaqubi et al., 2022).

4.3.10 Statistics and reproducibility

In vitro studies

All statistics are presented as the mean and standard error of the mean. The statistical test used and level of significance are indicated in the figure legends.

Transcriptome studies

Data were analyzed using GraphPad Prism version 8.3.0. Throughout the manuscript, *p-values* are indicated in the graphs and non-significant values are shown using “ns”.

4.4 Results

4.4.1 Metabolic stress rapidly reduces ATP in hOLs followed by autophagy failure

Reduction of ATP levels under metabolic stress in vitro - In a previous study, we showed that autophagic flux is increased in metabolically stressed hOLs and that inhibiting autophagic flux with chloroquine in metabolically stressed hOLs causes an accumulation of autophagosomes and increases cell death after 2 days (Fernandes et al., 2021); while cell death was not observed under stress conditions alone. We further verify activation of AMPK, a key regulator of autophagy, in hOL under NG conditions (Supplementary Fig. 4.1); To determine the impact of metabolic stress on cytoplasmic ATP, we assessed ATP levels per cell under such conditions. As shown in Fig. 1a, we detected a significant decrease in the amount of ATP in hOLs within 6 h in cell culture medium containing low glucose (LG) and no glucose (NG) compared to cells in optimal culture media (N1) (Fig. 4.1a). The decline in ATP levels continued during the following 2 and 4 days (Fig. 4.1b).

Autophagy modulation does not impact ATP levels - To assess the contribution of autophagy to the energy status of the cells under these stress conditions, we evaluated ATP levels in the presence of chloroquine, an autophagy inhibitor, and Torin-1, an inhibitor of mTOR, thus an activator of autophagy (Fig. 4.1a). Neither chloroquine nor Torin-1 had a measurable impact on ATP levels under basal or stress conditions.

Autophagy failure under metabolic stress– Autophagy provides cellular functions beyond energy production, including misfolded protein clearance and material recycling in the cell (Yan et al., 2019). Autophagy itself requires ATP for the transport and fusion of autophagosomes and lysosomes (Lőrincz and Juhász, 2020). Therefore, the ATP depletion detected during metabolic

stress could be the underlying cause of autophagy failure. To address the status of autophagy in hOLs when challenged with metabolic stress, we used confocal microscopy with LC3 as a marker of autophagosomes and LAMP1 as a lysosomal marker (Sharifi et al., 2015). After 2 days in culture, few LC3-positive vesicles (autophagosomes) were observed in N1 and NG conditions (Fig. 4.1c i-d i); the few LC3-positive vesicles detected were colocalized with LAMP1-positive vesicles (Fig. 4.1 c iii-d iii) indicating the formation of autolysosomes. After 4 days, a limited number of LC3-positive vesicles were detected in the N1 condition (Fig. 4.1e i) and most were colocalized with LAMP1-positive vesicles (Fig. 4.1e iii), indicating successful fusion with lysosomes. In NG conditions, we detected a considerable increase in the number of LC3-positive vesicles (Fig. 4.1f i), and most were not colocalized with LAMP1-positive vesicles (Fig. 4.1f iii), indicating autophagy failure. Quantification revealed a significant increase in the number of LC3-positive vesicles per cell induced by metabolic stress and in the number of LC3-positive vesicles not colocalized with LAMP1 in hOLs (Fig. 4.1g, h).

Increased presence of autophagosomes in OLs in situ *in MS* – To determine whether autophagosomes accumulate in situ in cases of MS, akin to their accumulation in hOLs in response to metabolic stress in vitro. we co-labeled tissue sections containing chronic active lesions with antibodies for NOGO A for OLs and LC3 as a marker of autophagosomes. Examples of the range of LC3 expression are provided in Fig. 4.2a. Expression of LC3 in OLs was significantly increased in the MS cases, both in the chronic active lesions and in normal appearing white matter (NAWM), compared to control tissue samples from non-MS cases (Fig. 4.2b).

Autophagy inhibition causes cell process loss and shedding of membrane fragments - We have previously observed hOL process retraction at day 6 when challenged by metabolic stress alone

(Pernin et al., 2022). Comparing N1 conditions alone (Fig. 4.3a-b), NG conditions alone (Fig. 4.3c-d), or N1 conditions containing the autophagy inhibitor chloroquine (Fig. 4.3e-f), hOLs treated with chloroquine under NG conditions exhibited a marked reduction of cellular process thickness and length by 2 and 4 days (Fig. 4.3g-h). NG conditions or N1 conditions combined with chloroquine, resulted in a limited number of small O4-positive membranous fragments outside the cells (Fig. 4.3c-f). These were not observed in N1 conditions alone (Fig. 4.3a-b). Inhibition of autophagy with chloroquine in NG conditions resulted in a larger number of extracellular O4-positive fragments (Fig. 4.3g-h).

4.4.2 hOL loss and shrinkage of nuclear size in MS lesions and under metabolic stress in vitro

In a previous study, we evaluated OL cell numbers in MS lesions characterized as active/demyelinating, active post-demyelinating, and mixed active/inactive lesions (Heß et al., 2020). For active demyelinating lesions, characterized by the presence of macrophages/microglia throughout the whole lesion area and a significant subset of these phagocytes containing myelin degradation products (Kuhlmann et al., 2017), we observed OL numbers comparable to normal appearing white matter (NAWM) (Heß et al., 2020). In contrast, mixed active/inactive lesions, which have a hypocellular lesion center and a rim of macrophages/microglia at the lesion border (subsequently named mixed lesions) as well as inactive lesions, which are almost completely devoid of phagocytes, show an almost complete loss of oligodendrocytes (Heß et al., 2020). In active post-demyelinating lesions, which represent a transition stage from active/demyelinating lesions to either mixed lesions or inactive lesions, macrophages/microglia are present throughout the lesion areas, but there are no myelin degradation products within the phagocytes. OL numbers are variably reduced in this lesion type, as are the mean numbers of CD68 positive

macrophages/microglia compared to active/demyelinating lesions (Heß et al., 2020). For the current study, we selected 9 "active/post-demyelinating" lesions from autopsies from 4 patients. All lesions were in the white matter of the brain ($n = 8$) or the cerebellum ($n = 1$). An example of such a lesion is provided in Supplementary Fig. 4.2. We confirmed our previous findings (Hess et al. (Heß et al., 2020) of reduced numbers of OLs (178 +/- 79 cells/mm^2 vs. 1081 +/- 27 cells/mm^2) and macrophages/microglia (715 +/- 111 /mm^2 vs. 2491 +/- 112 mm^2) in active/post-demyelinating lesions versus active/demyelinating lesions. We observed a high variability in the number of macrophages/microglia and oligodendrocytes between the individual lesions (between 2 and 618 OLs/mm^2 and between 283 and 1333 macrophages/microglia/mm^2). In lesions with a relative preservation of OLs, we found a graded loss of OLs from the lesion border to the lesion center (Supplementary Fig. 4.2d).

Nuclear condensation and volume reduction (pyknosis) are hallmarks of cell death. Pyknosis can occur in two forms: nucleolytic and anucleolytic. Metabolic stress causes anucleolytic pyknosis (Burgoyne, 1999). We observed a significant decrease in nuclear area size of surviving OLs within the lesions compared to OLs in NAWM (Fig. 4.4a-b). Under in vitro stress conditions, mean nuclear size was reduced in OLs at day 4 (Fig. 4.4c-d), a time when significant cell death was initially detected (Cui et al., 2017).

4.4.3 Limited contribution of ROS to hOL injury under metabolic stress

We compared the susceptibility of primary hOLs to exogenous oxidative stress to HeLa cells, a cell type used in previous studies of this mechanism of injury (Gryzik et al., 2021). Addition of H_2O_2 as an exogenous source of ROS is toxic to hOLs only at concentrations greater than required for HeLa cells, i.e., the proportion of PI-positive cells following treatment with 400 µM

of H_2O_2 is higher in HeLa cells than hOLs (Fig. 4.5a-b). As glutathione protects against ROS, we exposed hOLs and HeLa cells to Erastin, which inhibits glutathione synthesis. Erastin alone applied for 24 h, as previously shown (Gryzik et al., 2021), results in significant HeLa cell death (Fig. 4.5c). In contrast, primary hOLs under N1 conditions were resistant to Erastin induced cell death (Fig. 4.5d). Under NG conditions, Erastin increased hOL cell death (Fig. 4.5d), and was associated with increased ROS within 1 day (Fig. 4.5e). These data indicate that anti-oxidative mechanisms are limiting the injury effects of the increased ROS produced in the hOLs by metabolic stress conditions.

To identify a mechanistic basis for hOL resistance, we compared expression of ROS and iron regulating genes between hOLs and HeLa cells cultured under basal conditions. Examining ROS related pathways, we found that VDAC1 and VDAC2, which control the exchange of small metabolites between the mitochondria and the cytosol (Li et al., 2020), are relatively downregulated in the hOLs, potentially contributing to reduction of ROS formation (Fig. 4.5f). Examining gene products that contribute to the regulation of iron levels, we detected increased expression of HMOX1, which degrades the heme molecular complex, along with its regulators NRF2 and KEAP1 (Li et al., 2020). Genes related to iron uptake, SLC39A14, SLC39A8, SLC11A2, TRFC and a transcription factor that regulates their expression, HSPB (with the exception of SLC11A2 (Li et al., 2020) were downregulated in hOLs as a result of metabolic stress. In contrast, the iron export-related gene SLC40A1 (Li et al., 2020) was upregulated. Three genes involved in glutathione precursors uptake, SLC1A5, SLC38A1 and SLC7A11, are downregulated, while CDKN1A, a gene responsible for reduction in sensitivity to ferroptosis, is upregulated (Li et al., 2020). Amongst four key gene products related to lipid metabolism in the regulation of ferroptosis (Li et al., 2020), only SAT was differentially regulated. These

transcriptional profiles suggest that hOLs are more resistant to iron accumulation than HeLa cells.

Lack of evidence of Ferroptosis - endogenous oxidative stress is shown to react with iron to cause lipid peroxidation. This can trigger the RCD referred to as ferroptosis. To determine if these treatments triggered mechanisms associated with ferroptosis mediated cell death, we applied ferrostatin-1. No protection from cell death was detected (Fig. 4.5g). We have also used buthionine sulfoximine (BSO) to evaluate ferroptosis inhibition; this agent also had no effect on hOL cell death induced by metabolic stress (data not shown).

Using an enrichment score of pathways mediating a wider range of RCD pathways, we did not observe any differences in the ferroptosis related transcriptome of primary hOLs cultured under optimal versus metabolic stress conditions (Fig. 4.5h). Using nuclear RNA sequencing databases from MS tissues (Batie et al., 2022, Fiore et al., 2022, Haimovici et al., 2022), this RCD pathway was not activated in OLs in the MS cases compared to control tissues (Fig. 4.5i).

4.4.4 Calcium-dependent mechanisms degrade hOL cytoskeleton components under metabolic stress

We hypothesized that decreased intracellular ATP, due to metabolic stress, could lead to an increase in cytosolic Ca^{2+} concentration $[Ca^{2+}]_i$ and that this could contribute to hOL degeneration via activation of calcium-dependent proteases that target the cytoskeleton (Lynch and Baudry, 1987). We therefore evaluated cleavage of spectrin, a substrate of the calcium-dependent protease calpain. Cleavage of spectrin was detected after 2 and 4 days in low glucose and no glucose conditions (Fig. 4.6a). As spectrin is also a substrate of caspase-3, we performed western blots using an anti-caspase-3 antibody capable of detecting both procaspase-3 and its

activated cleaved form. Cleaveage of caspase-3 was not identified after 2 days of treatment, either in low or no glucose conditions, in contrast to Hela cells treated with staurosporine (Fig. 4.6b). Using the same sample as in Fig. 4.6a, we also did not detect cleavage of caspase-3 after day 4 when cultured in low and no glucose conditions (Fig. 4.6c).

To further test the hypothesis that activation of calcium-dependent proteases is critical to the hOL cell death induced by metabolic stress, the cells were treated with the calcium chelator EGTA in combination with the no glucose condition. At day 4, we determined that spectrin is preserved in hOLs in EGTA treated no glucose cultures, in contrast with the no glucose alone condition, in which spectrin had been almost completely degraded (Fig. 4.6d).

These findings support the hypothesis that the activation of a calcium-dependent protease contributes to the metabolic stress induced degradation of the hOL cytoskeleton.

Lack of evidence of MPT mediated necrosis - This RCD pathway triggers cell death by opening the mitochondrial permeability transition pore complex due to overloaded cytosolic calcium (Galluzzi et al., 2018). We determined if the increased cytoplasmic calcium described above might be linked to MPT-driven necrosis. To test this, primary hOLs were treated with cyclosporin A, which inhibits cyclophilin, a calcium activated protein that regulates the transition pore complex (Bauer and Murphy, 2020). No changes were detected in cell number or cell death compared to untreated cells in N1 or NG conditions (Fig. 4.7a-b).

Examining the expression of MPT related genes, PPIF, the gene encoding cyclophilin, is expressed at a lower level in hOLs compared to HeLa cells (Fig. 4.7c). No consistent differences in gene expression were detected between hOLs and HeLa cells for gene products related to calcium influx (Fig. 4.7c). Among MPT pore related genes, we identified five that are expressed at a significantly lower level in hOLs than HeLa cells (Fig. 4.7c). Overall, the transcriptomic

analysis of genes encoding proteins that regulate MPT pore function suggest that hOLs are more resistant to MPT pore formation than HeLa cells. As with our ferroptosis enrichment score analyses, we did not observe any differences in the transcriptomes of primary hOLs cultured under optimal versus metabolic stressed conditions (Fig. 4.7d) or any significant upregulation of this pathway in OLs from MS lesions (Fig. 4.7e).

Our findings provide evidence that metabolic stress results in elevated intracellular calcium concentration $[Ca^{2+}]_i$ in hOLs, yet without activation of MPT driven necrosis.

4.5 Discussion

Here we investigate the mechanisms underlying the distinct injury response of human mature OLs to metabolic stress.

4.5.1 Metabolic stress reduces cellular ATP and compromises autophagic flux in hOLs

ATP depletion - Our time-course studies showed that the delayed cell death of hOLs was preceded by a significant and progressive reduction in ATP per cell. We previously used a Seahorse bio-analyzer to show that hOLs when challenged with metabolic stress exhibit a strong dependence on glycolysis and a comparatively low rate of ATP production (Rone et al., 2016). When internal levels of ATP are low, AMP-activated protein kinase (AMPK) is activated. This kinase inhibits the activity of the mammalian target of rapamycin (mTOR), causing a reduction in protein synthesis and activation of autophagy (García-Prat et al., 2016, Glick et al., 2010, Gross and Graef, 2020, Mizushima, 2007). Autophagy provides substrates for the tricarboxylic acid (TCA) cycle (Gross and Graef, 2020). However, as mentioned, hOLs exhibit a reduced

reliance on oxidative phosphorylation and are more dependent on glycolysis for energy production (Rone et al., 2016). We did not observe any significant effect of inhibition or activation of autophagy with chloroquine or Torin-1 on ATP levels under either basal or stress conditions, suggesting that in hOLs autophagy is not a major mechanism contributing to the modulation of energy production.

Autophagy failure – we used LC3, a marker of autophagosomes to assess autophagy status in vitro (in combination with LAMP1) and in MS cases. Our data indicate that autophagy failure occurs under sustained metabolic stress. As sustained activation of autophagy depends on ATP (Yang et al., 2019), this may be a consequence of ATP depletion. Autophagosomes are transported by dyneins while lysosomes are transported by kinesins. Both of these families of motor molecules depend on ATP for motility (Zhao et al., 2021). The fusion between autophagosomes and lysosomes depends on RAB7, a small GTPase, also dependent on ATP availability. Thus, a lack of ATP would impair the transport and fusion of autophagosomes and lysosomes and cause the autophagy failure observed in hOL under metabolic stress (Zhao et al., 2021). We confirmed our previous observation that inhibiting autophagy progression exaggerates cell death (Fernandes et al., 2021).

Assessing autophagosome formation and fusion with lysosomes in vitro, after 2 days of metabolic stress when ATP levels were already reduced, we found limited buildup of unfused autophagosomes, indicating a functioning if not heightened autophagy pathway activation. Autophagy, however, was not able to sustain ATP levels and we did not detect a burst of ATP production at the earliest time points tested under stress conditions. With prolonged stress, accumulation of unfused autophagosomes was present, indicating autophagy failure. Such failure can lead to a disruption in the regulation of cytoskeleton remodeling as identified by He el al.

(He et al., 2016) or an impairment of myelination as shown by Karim et al. (Karim et al., 2007), We detected many O4-positive fragments outside the cells indicating that cellular material is being lost to the environment.

Our *in situ* studies of MS cases parallel our in vitro findings. We detected significant reduction of OL numbers in both our in vitro model and active post demyelinating and chronic active lesions (Heß et al., 2020). We now document reduced size of nuclei (pyknosis) (Burgoyne, 1999) in hOLs in vitro and in MS lesions, suggesting substantial cellular distress and potentially ongoing cell death. Immunohistochemical analyses of MS cases revealed a build-up of autophagosomes (increased expression of LC3) in OLs serving as an indicator of metabolic stress. We note that Satoh et al. did not detect LC3 expression in OLs in MS cases, in comparison to the high expression noted in cases of Nasu-Hakola disease (Satoh et al., 2014). The increase of LC3 in NAWM indicates that stress is not restricted to the lesion area, potentially preceding the formation of new lesions.

4.5.2 Basis of metabolic stress induced cell injury

Limited contribution of ROS to hOL injury - The stress conditions we applied to hOLs in vitro increased the production of ROS, which promotes lipid peroxidation. Further, combining Erastin with glucose deprivation increased cell death, indicating a protective role for antioxidants. Our functional data however suggest that ROS makes a relatively minor contribution to hOL injury induced by these metabolic stress conditions, possibly because hOLs have a lower rate of oxidative phosphorylation compared to rat OLs and OPCs (Rone et al., 2016).

Our transcriptomic analyses provide insight into the mechanism underlying the relative resistance of hOLs to exogenous H_2O_2 compared to HeLa cells. Our findings revealed

downregulation of VDAC1 and VDAC2, which control the exchange of small metabolites between the mitochondria and the cytosol (Li et al., 2020), as well as resistance to iron accumulation in hOLs compared to HeLa cells. These differences in transcriptional profile could compensate for the observed reduction of glutathione synthesis related genes. We then addressed if the production of ROS under stress conditions triggered ferroptosis (Galluzzi et al., 2018, Jhelum et al., 2020, McKenzie et al., 2020, McKenzie et al., 2018). Blocking ferroptosis with ferrostatin did not protect the cells from death under the stress conditions applied here, supporting the conclusion that ferroptosis is not the primary underlying mechanism of cell death. Analyses of publicly available molecular databases did not identify changes in expression of the ferroptosis RCD pathway in OLs in active MS lesions (Jäkel et al., 2019).

Increase in $[Ca^{2+}]_i$ and activation of Ca^{2+}-dependent proteases - Our findings support the hypothesis that metabolic stress triggers hOL cell death via a mechanism that depends on an increase in $[Ca^{2+}]_i$ that then leads to the proteolytic degradation of the cytoskeleton. Myelin produced by hOLs is a plastic structure that constantly adjusts its morphology to adapt to neural activity. Local changes in myelin sheets are dependent on Ca^{2+} signaling that is regulated by voltage-gated and ligant-gated channels, modulating conformation changes in the cytoskeleton via Ca^{2+} influx (Paez and Lyons, 2020). Considerable energy is required to maintain the calcium gradient across the plasma membrane, engaging the plasma membrane calcium ATPase transporter (PMCA) (Frandsen et al., 2020). Calcium is also extruded by the Na^+/Ca^{2+}-exchanger (NCX) and $Na^+/Ca^{2+}/K^+$-exchanger (NCKX) (Frandsen et al., 2020). Low levels of ATP in the cell compromize the capacity of the cell to maintain the steep ionic gradients across the plasma membrane, which can ultimately lead to metabolic collapse and cell death.

As a readout of abnormally high cytoplasmic calcium, we documented metabolic stress induced cleavage of spectrin, a major cytoskeletal component that is a target of the Ca^{2+}-dependent protease calpain (Rajgopal and Vemuri, 2002). This cleavage was not caspase-3 dependent but was inhibited by chelating extracellular Ca^{2+} with EGTA. Possible contributing sources of the increased intracellular Ca^{2+} include transmembrane flux from the extracellular space, or release from intracellular stores including endoplasmic reticulum and mitochondria (Bauer and Murphy, 2020, Zhang et al., 2022). Notably, release of calcium from intracellular stores can activate the MPT-driven necrosis RCD pathway (Galluzzi et al., 2018), however, addition of cyclosporine A to inhibit cyclophilin, a central participant in mitochondrial pore opening (Zhang et al., 2019a), did not protect hOLs in the conditions tested, providing evidence that MPT-driven necrosis does not contribute to hOL death in these conditions.

4.6 Conclusion

Here we demonstrate that the response of hOLs to metabolic stress is distinct from RCD mechanisms that are readily triggered in other cell types (Fig. 4.8). Although the cause of OL cell death in MS cases has not yet been identified, our studies of hOLs in vitro indicate that metabolic failure is the most consistent cause of death (Cui et al., 2017, Fernandes et al., 2021, Pernin et al., 2022, Rone et al., 2016). Other mediators of cellular stress, particularly cytokines, resulted in only sublethal injury without significant cell death (Pernin et al., 2022). We consider that the hOL cell death described here results primarily from energy depletion, followed by autophagy failure. Our studies link the distinct response of these cells to metabolic insults to their low basal metabolic state and dependence on glycolytic metabolism (Rao et al., 2017, Rone et al., 2016), together with a genetic program of resistance to RCD activation. Notably, our

detection in vitro of cell and nuclear shrinkage, autophagosome accumulation, and lack of RCD activation is paralleled by in situ observations of MS lesions. We postulate that the observed release of cellular contents would engage interactions with surrounding glia, engaging an ongoing injury response. Defining the distinct bases of OL injury and death provides guidance for the development of neuro-protective interventions.

4.7 Data availability

The dataset used and/or analysed during the current study are available from the corresponding author on reasonable request.

4.8 Abbreviations

OL: Oligodendrocyte

hOL: Human oligodendrocyte

RCD: Regulated cell death

MS: Multiple sclerosis

ISR: Integrated stress response

MPTN: Mitochondrial permeability transition-driven necrosis

CRCHUM: Centre Hospitalier de l'Université de Montréal

LFB: Luxol Fast Blye

H&E: Hematoxylin and Eosin

MNI: Montreal Neurological Institute

LG: Low glucose

NG: No glucose

PI: Propidium iodide

ssGSEA: Single samples gene set enrichment analysis

GEO: Gene expression omnibus

N1: Optimal media

CQ: Chloroquine

NAWM: Normal appearing white matter

DIV: Days in vitro

BSO: Buthionine sulfoximine

AMPK: AMP-activated protein kinase

mTOR: Mammalian target of rapamycin

TCA: Tricarboxylic acid

PMCA: Plasma membrane calcium ATPase transporter

NCX: Na^+/Ca^{2+}-exchanger

NCKX: $Na^+/Ca^{2+}/K^+$-exchanger

4.9 Funding

The study was supported by a grant (BRAVE in MS) from the International Progressive MS Alliance (J.P.A.) and Le Grand Portage.

4.10 Ethics declarations

Ethics approval

Human rapid post-mortem brain tissue samples were obtained from the Neuroimmunology Research Laboratory, Centre de Recherche du Centre Hospitalier de l'Université de Montréal (CRCHUM) under ethical approval number BH07.001.31. Human cell studies were approved by the MNI Neurosciences Research Ethics Board (Protocol ANTJ 1988/3) and the Montreal Children's Hospital Research Ethics Board.

Consent for publication

Not applicable.

Competing interests

The authors declare that they have no competing interests.

Acknowledgments

Not applicable.

4.11 Figures and legends

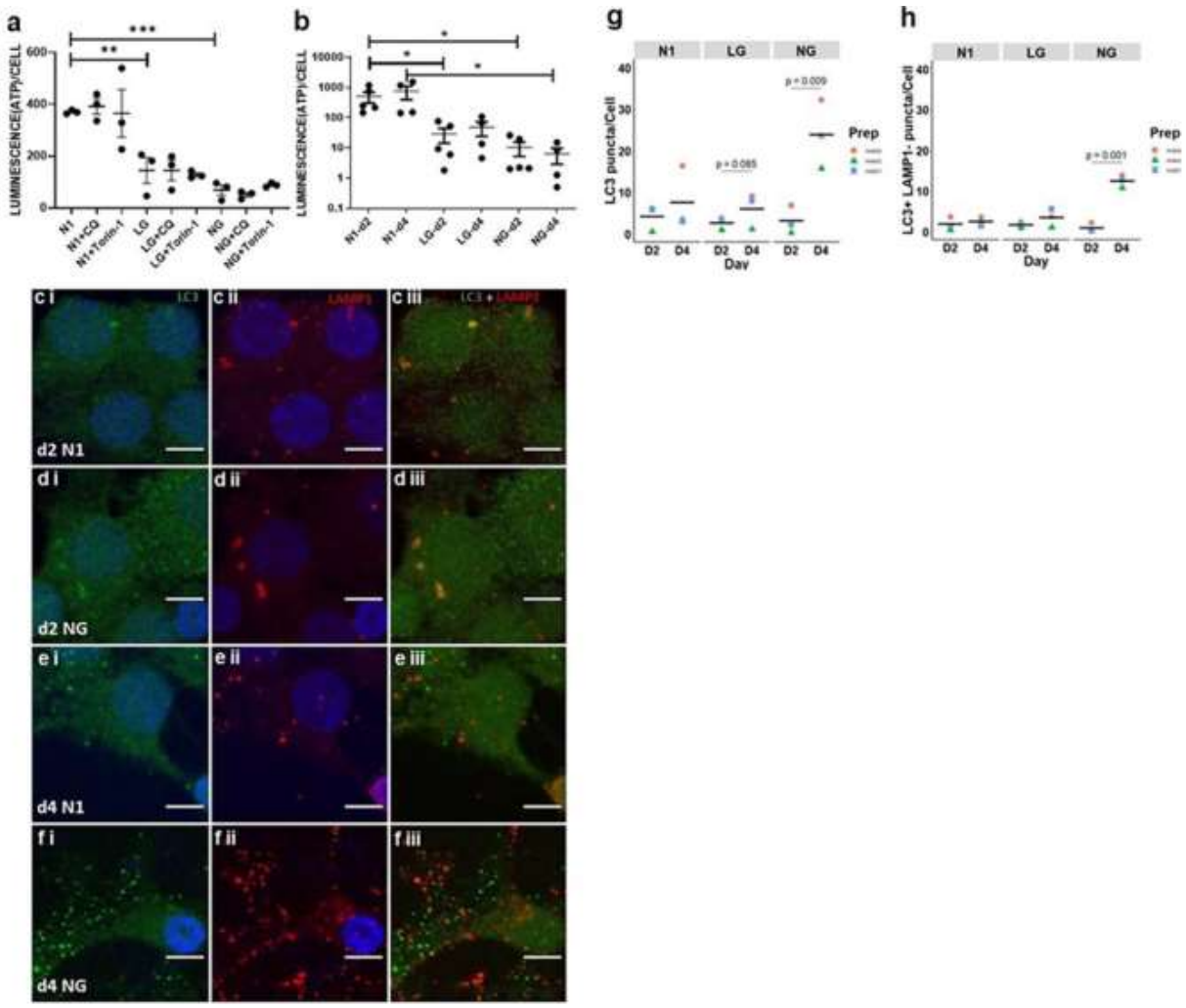

Figure 4.1 - Metabolic stress reduces ATP resulting in failure of autophagic flux in hOLs. **a** ATP levels in hOLs cultured in optimal (N1), low glucose (LG), and no glucose (NG) conditions combined with chloroquine (CQ) or Torin-1. 6 h of treatment resulted in a significant decline in ATP under LG and NG conditions without an additive effect of CQ or Torin-1. Statistical significance was verified by ANOVA/Dunnett's test: **(< 0.01), ***(< 0.001) **b** ATP levels in hOL cultured in N1, LG, and NG conditions. After 2 and 4 days of treatment, ATP levels continue to decline in LG and NG conditions. Mean ± SEM for each condition shown in the figure. Statistical significance was verified by ANOVA/Dunnett's test: *(< 0.05). **c-f** Confocal images of autophagosomes (LC3 - green) and lysosomes (LAMP1 – red) in hOLs under control (N1) or no glucose (NG) conditions. After 2 days of treatment under N1 **c** and NG **d** conditions,

few autophagosomes (LC3 puncta) were detected (**c i**, **d i)**. The majority of these autophagosomes were fused with lysosomes (LAMP1 puncta) **(c iii**, **d iii)**. **e** After 4 days of treatment under N1 conditions, few autophagosomes (LC3 puncta) were detected (**e i**). The majority of these autophagosomes were fused with lysosomes (LAMP1 puncta) (**e iii**). **f** After 4 days of treatment under NG conditions, many autophagosomes (LC3 puncta) were detected (**f i**); most were not fused with lysosomes (LAMP1 puncta) (**f iii**). **g** Quantification of autophagosomes (LC3 puncta) per cell in N1, LG and LG conditions after 2 and 4 days of treatment. After 2 days, in all conditions, the number of autophagosomes per cell was low. After 4 days, this number was slightly increased in LG conditions and strongly increased in NG conditions. Statistical significance was verified by Student's t-test. **h** Quantification of autophagosomes not fused with lysosomes (LC3 + ve LAMP1 -ve puncta) per cell in N1, LG and NG conditions after 2 and 4 days of treatment. After 2 days, in all conditions, the number of autophagosomes not fused with lysosomes per cell was low. After 4 days, this number increased in NG conditions. Each dot-color corresponds to an independent biological sample. Bar indicates the mean. hOLs were marked with DAPI (blue), indicating the cell nucleus. Statistical significance was verified by Student's t-test.

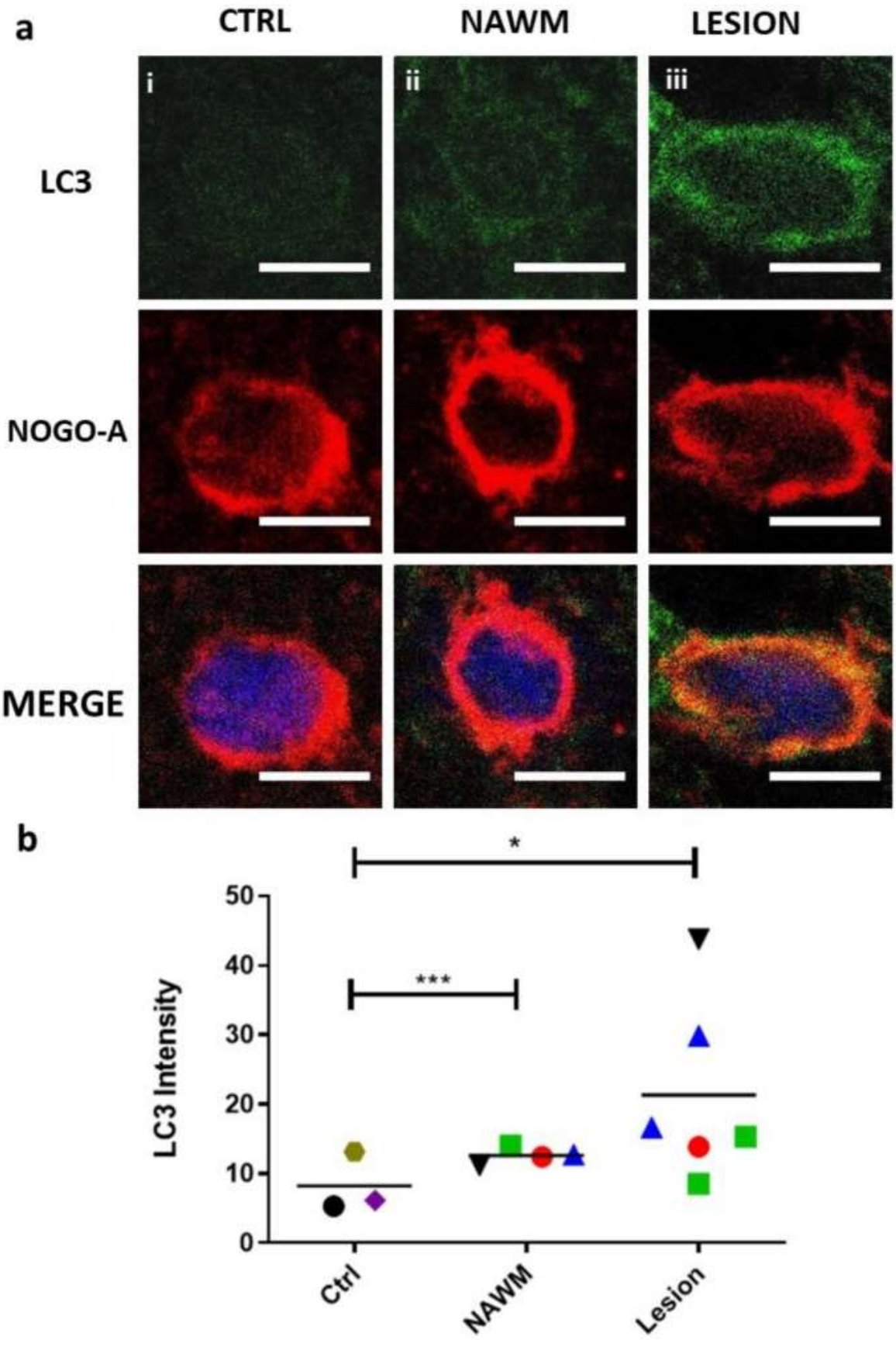
a
CTRL
NAWM
LESION
i
ii
iii
LC3
NOGO-A
MERGE
b
*
***
LC3 Intensity
50
40
30
20
10
0
Ctrl
NAWM
Lesion

Figure 4.2 - Increased expression of the autophagy marker LC3 in MS lesions and NAWM compared to controls. **a** Sample images showing relative expression of LC3 in a non-MS CTRL case, in NAWM from an MS case, and in a chronic active lesion of an MS case. Scale bars correspond to 5 μm. **b** Quantification of LC3 expression as measured by average immunofluorescence intensity of LC3 in OLs in healthy controls, NAWM, and chronic active MS lesions. Individual regions of interest are indicated by color and shape corresponding to 3 non-MS controls, 4 NAWM regions, and 6 lesions from 4 individuals with MS. Statistical significance was assessed using Student's t-test: * (< 0.05), *** (< 0.001)

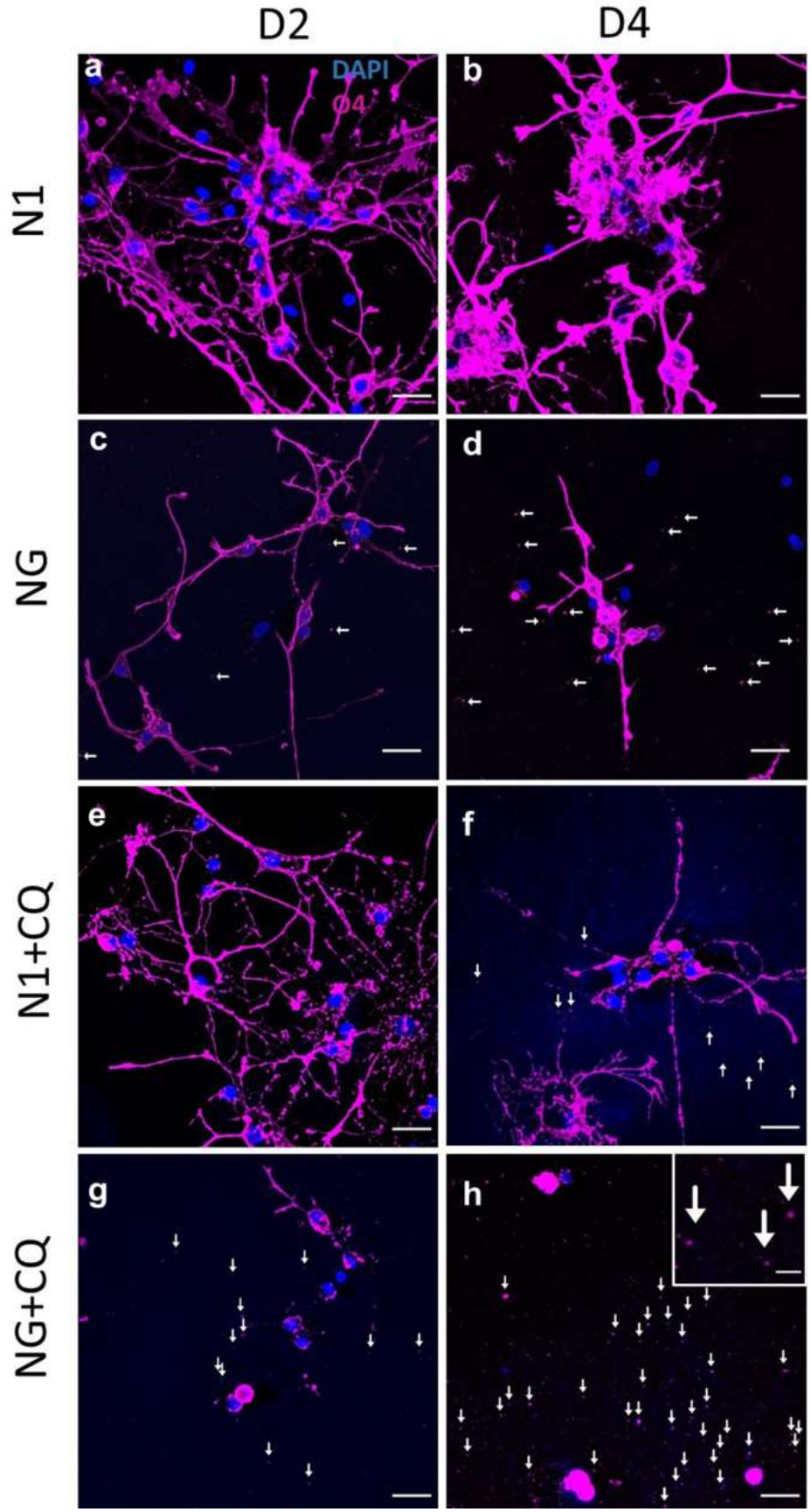
D2
D4
N1
NG
N1+CQ
NG+CQ
a
DAPI
Φ4
b
c
d
e
f
g
h

Figure 4.3 - No glucose conditions and treatment with chloroquine cause cell process loss and shedding of membrane fragments. **a, b** hOLs project long processes in N1 conditions at 2 and 4 days in vitro (DIV). **c, d** With NG, processes show signs of contraction. O4 positive fragments are visible in the media (indicated by arrows). **e** In N1 conditions combined with chloroquine, the morphology of hOLs was similar to N1 conditions without chloroquine after 2 DIV. **f** After 4 days of treatment in N1 combined with chloroquine, some process retraction and some O4 + fragments can be observed outside the cell (fragments indicated by arrows). **g, h** Combined treatment of NG and chloroquine after 2 and 4 DIV resulted in greater retraction of processes and the presence of many fragments outside the cell. Cell size was decreased. The inset picture in **h** illustrates a magnified view of the O4 positive fragments. Scale bars correspond to 20 μm in the large figures and 2.5 μm in the inset in panel **h**

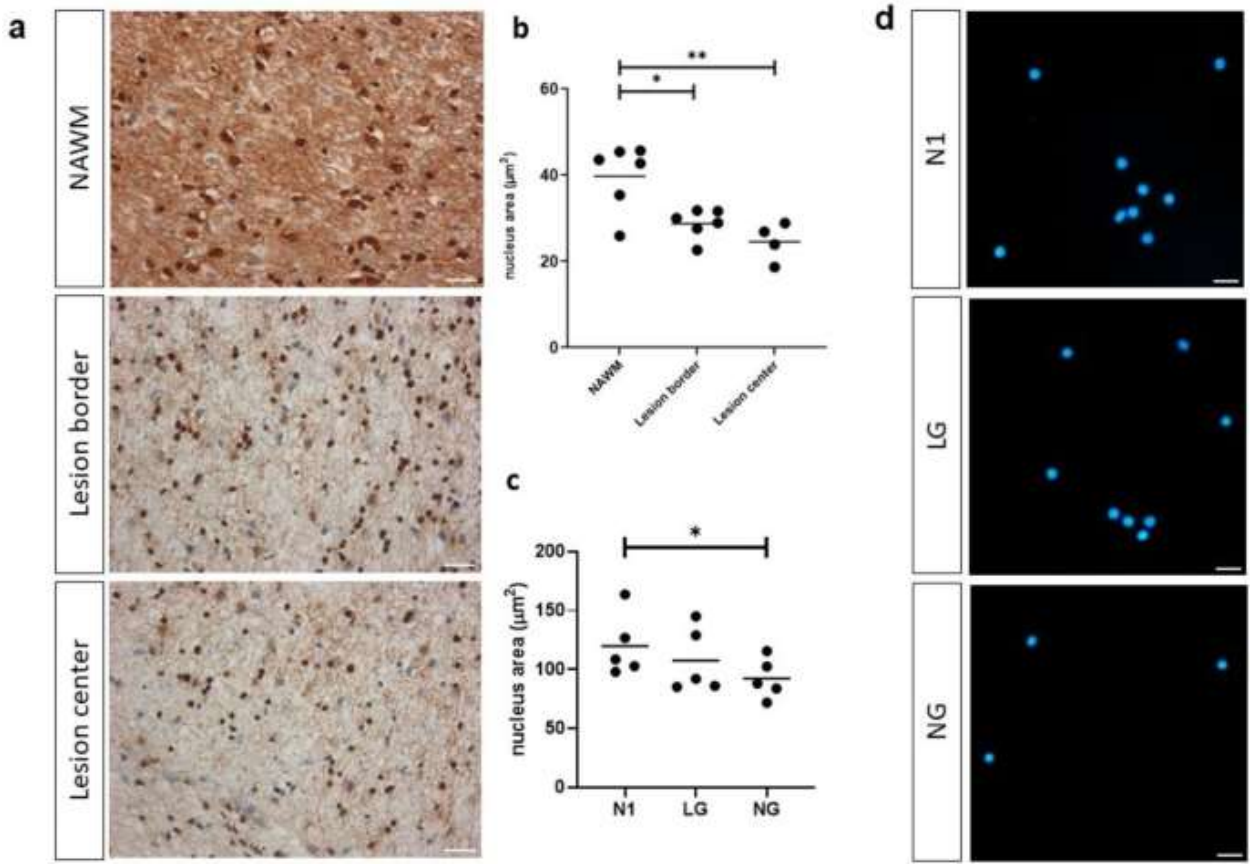

Figure 4.4 - Shrinkage of hOL nuclear size in MS lesions and under metabolic stress in vitro. **a** Sample images of an MS case showing nucleus size in NAWM, lesion edge, and lesion center. Scale bars correspond to 10 µm. **b** Quantification of nuclear size (surface area) in NAWM, lesion edge, and lesion center, showing nuclear size reduced in the lesion center and edge compared to NAWM. Statistical significance was assessed using ANOVA/Dunnett's test: *(< 0.05), **(< 0.01). **c** Quantification of nuclear size in optimal (N1), low glucose (LG) and no glucose (NG) conditions at 4 days, showing nuclear size reduced under metabolic stress. Statistical significance was assessed using ANOVA/Dunnett's test: *(< 0.05). **d** Sample images illustrating nucleus size (DAPI staining) in vitro under N1, LG and NG conditions. Scale bars correspond to 20 µm.

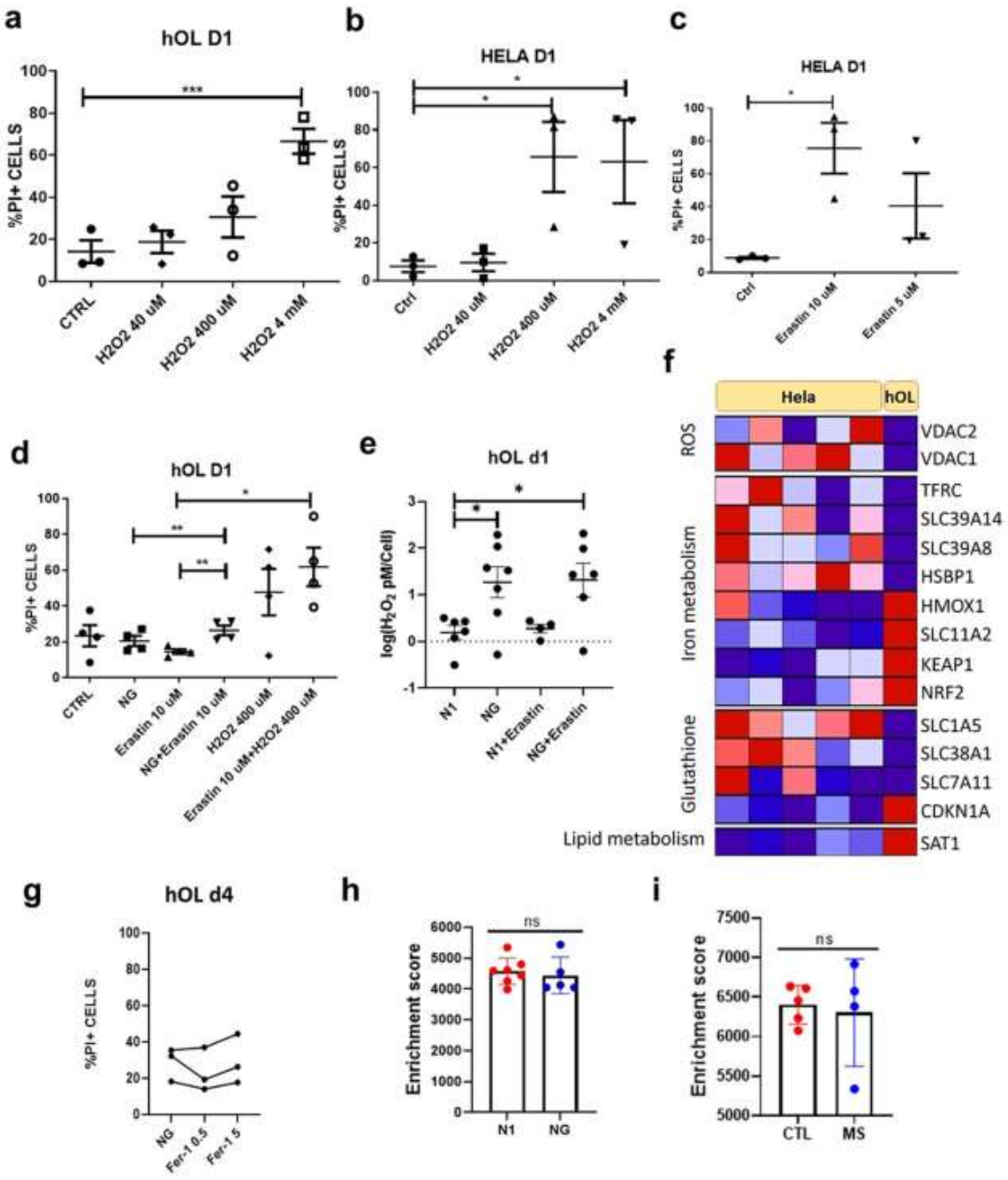

Figure 4.5 - ROS mediates limited damage in hOL following metabolic stress. **a-b** hOLs and HeLa cells were treated with hydrogen peroxide for 1 day at different concentrations and rate of cell death was measured by PI assay. **a** hOL cell death was increased only by 4 mM H_2O_2. **b** HeLa cell death was substantially increased by 400 µm of H_2O_2. Statistical significance was assessed using an ANOVA/Tukey test: *(< 0.05), ***(< 0.001). **c** HeLa cells were treated with Erastin at different concentrations for 1 day. Cell death was significantly increased by

treatment with 10 µM of erastin. Statistical significance was assessed using a Student's t-test: *(< 0.05). **d** hOLs were treated with Erastin, NG, H_2O_2 or combination of these treatments for 1 day. Cell death was only significantly increased with the combined treatment of Erastin with NG and not with NG or Erastin alone. Statistical significance was assessed using a Student's t-test: *(< 0.05), **(< 0.01). **e** H_2O_2 levels measured in hOLs treated with Erastin in optimal and NG conditions. H_2O_2 levels were increased under NG conditions alone. No additional effect of Erastin was detected. Statistical significance was assessed using an ANOVA/Dunnett's test: *(< 0.05). **f** Genes presenting significant difference in their transcriptional expression in hOLs compared to HeLa cells were categorised according to the pathway involved in ferroptosis. Genes upregulated are shown in red and downregulated in blue. HeLa cell data were obtained from publicly available databases (Batie et al., 2022, Fiore et al., 2022, Haimovici et al., 2022). hOLs data was obtained from a bulk RNA sequencing database that we have previously published (Luo et al., 2022). **g** Rate of hOL cell death under NG conditions following treatment with Ferrostatin-1 for 4 days, measured by PI assay. No significant differences were observed between treatment conditions. Each dot/line in the graphs corresponds to an independent biological sample. Statistical significance was assessed using an ANOVA/Dunnett's test. **h** Comparison of the enrichment score of genes related to ferroptosis in N1 and NG conditions in vitro. Mean ± SEM for each condition shown in the figure. Statistical significance was assessed using a Student's t-test: *(< 0.05). **i** Enrichment score of genes related to ferroptosis in MS cases compared to "control" individuals. Mean ± SEM for each condition shown in the figure. Statistical significance was assessed using a Student's t-test: *(< 0.05)

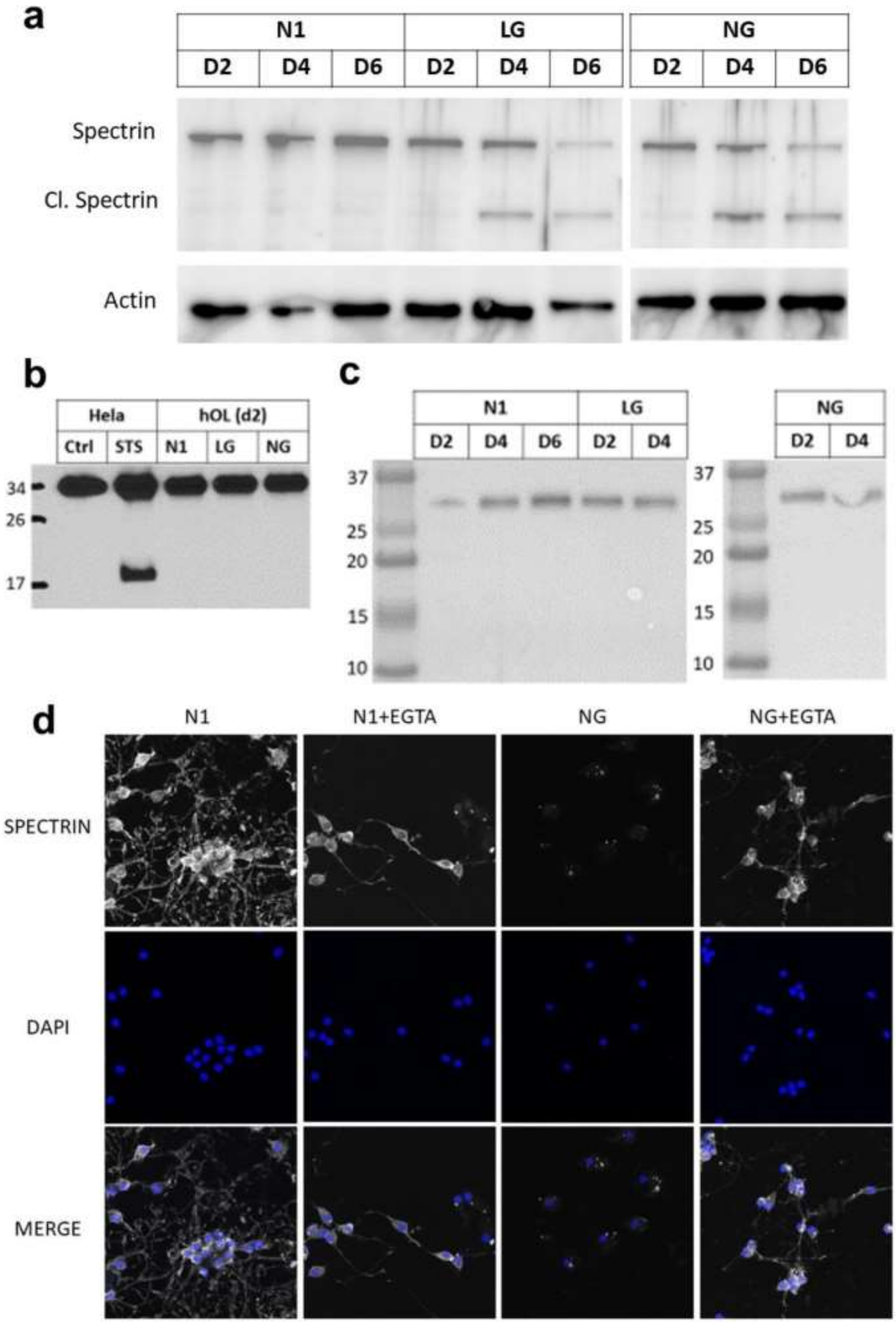
a
N1
LG
NG
D2
D4
D6
D2
D4
D6
D2
D4
D6
Spectrin
Cl. Spectrin
Actin
b
Hela
hOL (d2)
Ctrl
STS
N1
LG
NG
34
26
17
c
N1
LG
NG
D2
D4
D6
D2
D4
D2
D4
37
25
20
15
10
37
25
20
15
10
d
N1
N1+EGTA
NG
NG+EGTA
SPECTRIN
DAPI
MERGE

Figure 4.6 - hOL cytoskeleton is degraded by a mechanism dependent on calcium activation. **a** hOLs were cultured in N1, LG and NG conditions for 2, 4 and 6 days. Spectrin cleavage was assessed by Western Blot. **b** Hela cells were treated with the apoptosis activator staurosporine and hOL were cultured in N1, LG and NG conditions for 2 days. Procaspase-3 is detected at 32 kDa, while cleaved caspase-3 at 17 kDa. **c** In the same sample used in a), cleavage of caspase-3 was not detected after 4 days in low and no glucose conditions. **d** hOLs were treated under N1 and NG conditions in combination with EGTA for 4 days and immunocytochemistry for Spectrin and O4 (hOL marker) was performed, followed by confocal imaging.

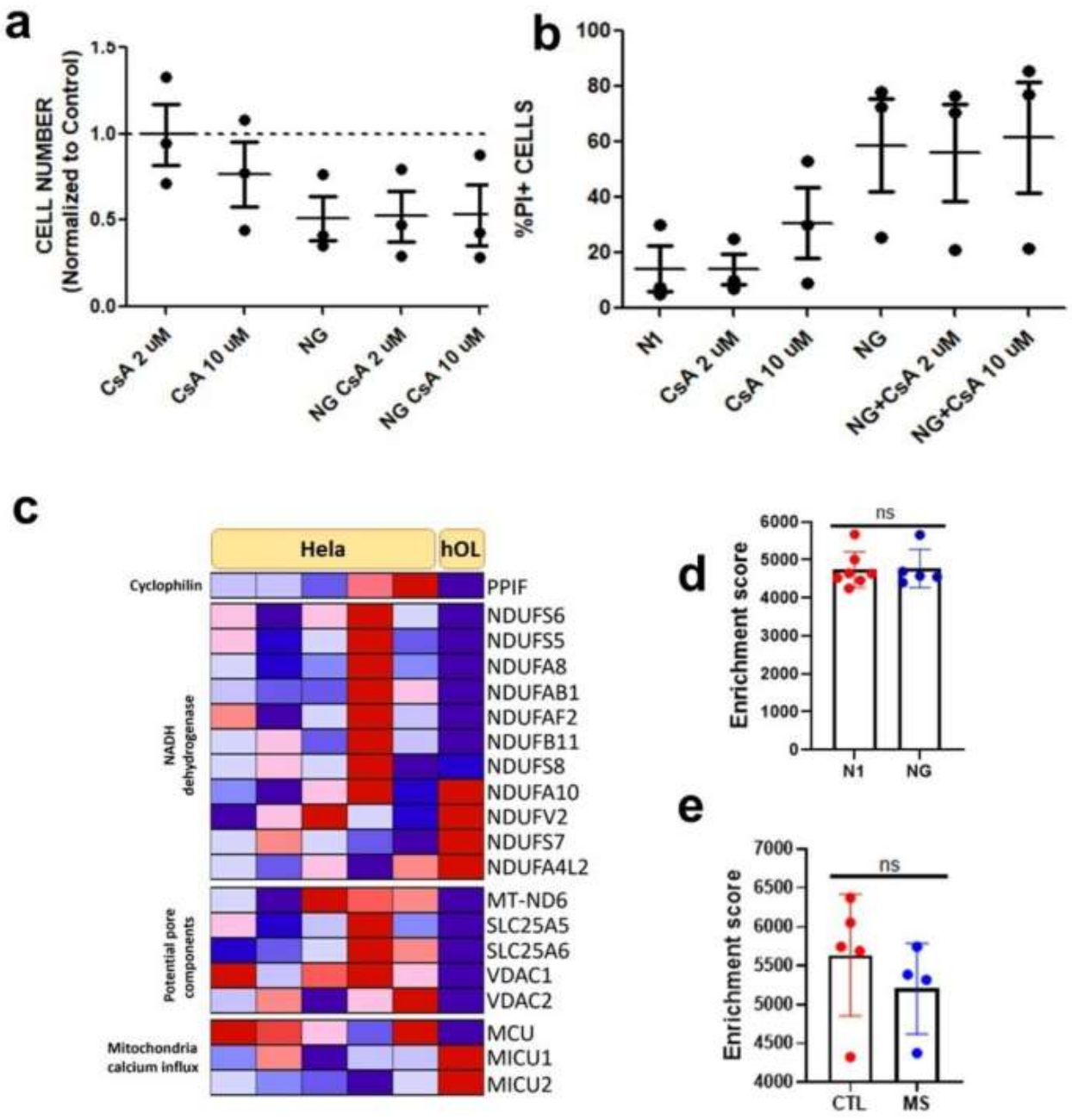

Figure 4.7 Metabolic stress triggers spectrin cleavage without activation of MPT-driven necrosis. **a-b** hOLs treated with CsA at 2 µM and 10 µM in combination with N1 and NG conditions did not cause a reduction in cell number or increase in PI-positive cells after 4 days of treatment. Each dot in the graphs corresponds to an independent biological sample. Mean ± SEM for each condition is shown in the figure. Statistical significance was assessed using a ANOVA/Dunnett's test. **c** Genes presenting significant differences in their transcriptional expression in hOLs compared to HeLa cells were categorised according to pathways involved in

MPT-driven necrosis. Genes upregulated are shown in red and downregulated in blue. HeLa cell data was obtained from publicly available databases (Batie et al., 2022, Fiore et al., 2022, Haimovici et al., 2022). hOLs data was obtained from a bulk RNA sequencing database that we have previously published (Luo et al., 2022). **d** Comparison of the enrichment score of genes related to MPT-driven necrosis in N1 and NG conditions in vitro. Mean ± SEM for each condition shown in the figure. Statistical significance was assessed using a Student's t-test: *(< 0.05). **e** Enrichment score of genes related to MPT-driven necrosis in MS cases compared to "control" individuals. Mean ± SEM for each condition shown in the figure. Statistical significance was assessed using a Student's t-test: *(< 0.05)

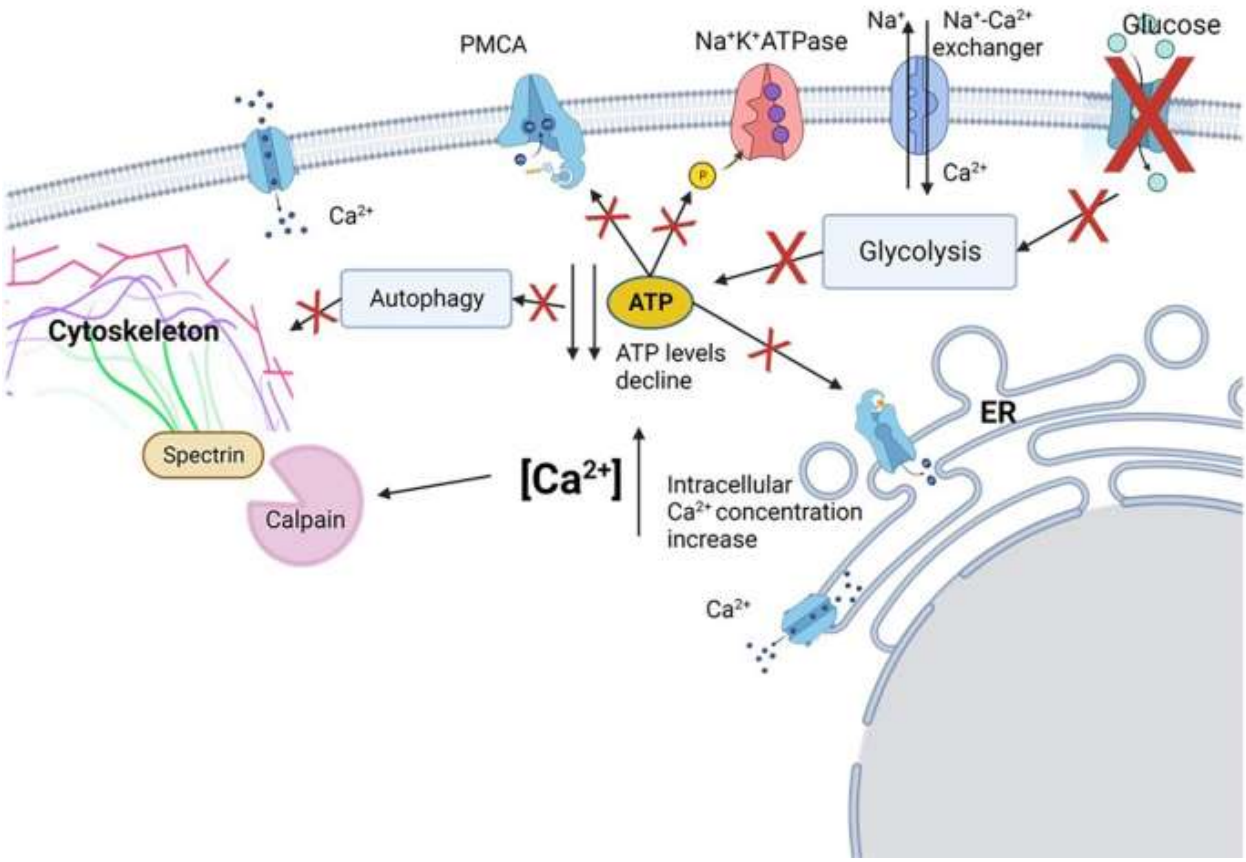

Figure 4.8 Mechanisms of human OL lethal injury. In the absence of glucose uptake, glycolysis, the main source of ATP in hOL, is reduced. As ATP is necessary for the transport and fusion of autophagosomes and lysosomes, autophagy is impaired. Autophagy blockage results in process disruption in OLs, indicating that this mechanism is important for the structural integrity of the cell. Reduction in ATP levels also causes a decrease in the activity of ATP-dependent Ca^{2+} pumps, like plasma membrane calcium ATPase (PMCA), and the $Na^{+}K^{+}$ATPase, leading to an increase in cytosolic Ca^{2+} and Na^{+}. The raise in intracellular Na^{+} increases the activity of Na^{+}-Ca^{2+} exchangers, what causes an additional influx of Ca^{2+}. High levels of Ca^{2+} activate Ca^{2+}-dependent proteases as calpain, which cleave spectrin, an essential component for the integrity of the cytoskeleton. These mechanisms initially contribute to loss of hOL processes (sub-lethal injury) and subsequently to cell death. Figure created using Biorender.

4.12 Supplementary information

Supplementary Table 1. Clinical details of samples used for functional and biochemical assays

Prep	Age	Sex	ATP 6h	ATP 2/4 d	Autophagy	Nucleus	H2O2/PI	Erastin/PI	H2O2	Fer-1	WB	CsA	IHC
HA820	12	F				+							
HA831	16	F				+							
HA832	11	M				+							
HA833	11	M				+							
HA834	23	F				+							
HA836	42	M		+									
HA837	28	F		+									
HA838	13	F		+									
HA841	24	M		+									
HA842	68	M		+	+								
HA843	8	F		+	+								
HA849	54	M		+			+						
HA850	64	F		+			+	+					
HA851	18	F		+	+		+	+					
HA853	6	N						+					
HA854	39	F						+					
HA855	48	F										+	
HA857	13	M										+	
HA858	12	F							+			+	
HA859	44	F							+		+		
HA861	14	F							+				
HA862	26	M	+										
HA863	32	F	+										
HA865	56	M	+										
HA867	12	F											
HA868	75	M											
HA869	10	M											
AB103	48	M											
AB129	33	F											+
AB187	26	M											+
AB203	44	F											+
AB159	67	M											+
P18	59												+
P24	56												+
P30	61												+

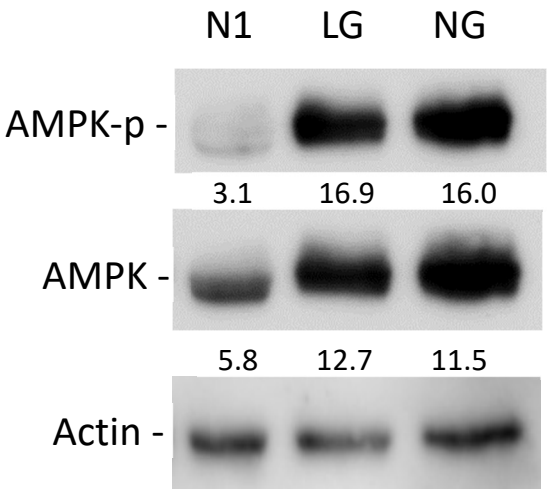

Supplementary Figure 4.1 – Metabolic stress induces activation of AMPK in hOL. hOL were treated for 2 days in optimal culture conditions (N1), low glucose (LG) and no glucose conditions (NG). Actin was used as loading control. Numbers correspond to the level of AMPK related to actin.

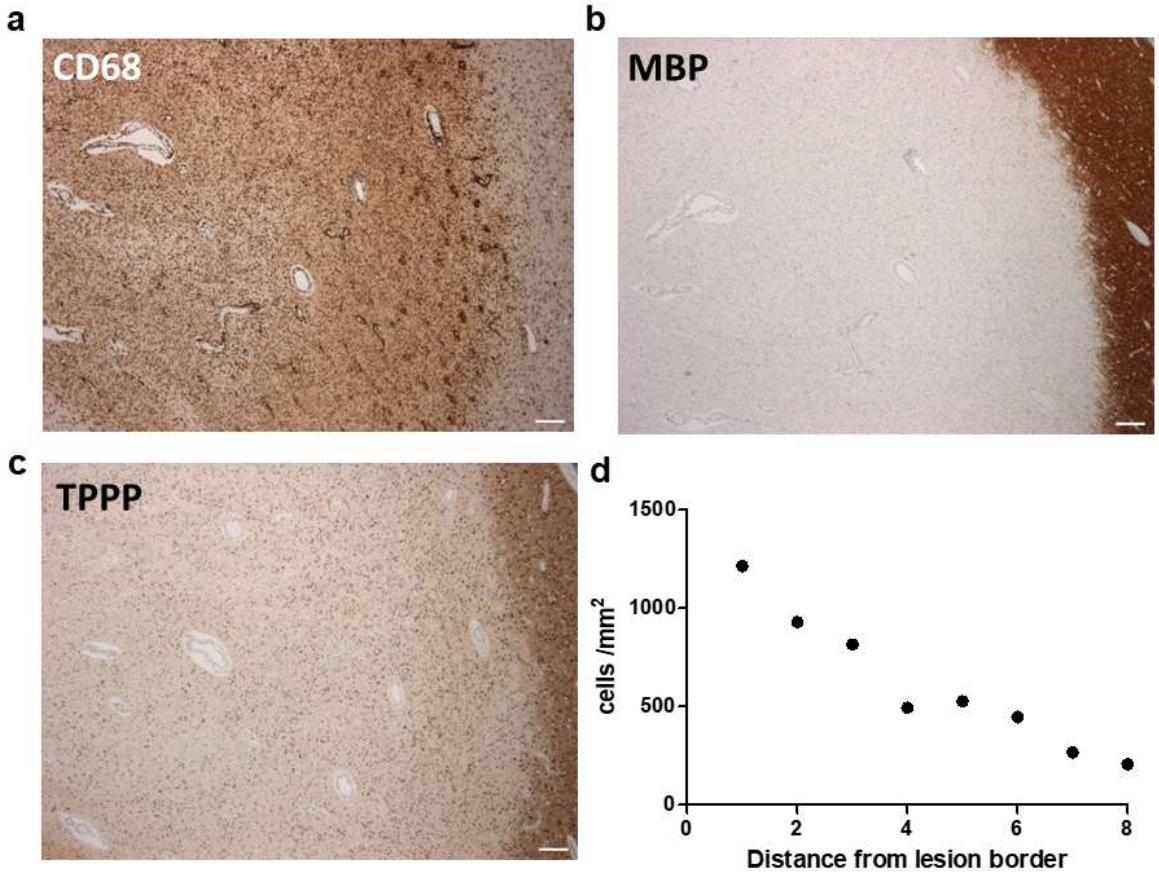

Supplementary Figure 4.2 - Loss of hOL is intensified in the center of MS lesions. **a-c** Sample images of an MS case showing adjacent normal appearing white matter (NAWM), lesion edge, and lesion center, immunolabeled with anti-CD68 (microglia/macrophages) (A), anti-MBP (myelin) (B), and anti TPP (OLs) antibodies (C). Scale bar correspond to 200 µm. **d** Number of hOLs from the border (0-2mm^2) to the center (6-8mm^2) of MS lesions.

4.13 References

Batie M, Frost J, Shakir D, Rocha S (2022) Regulation of chromatin accessibility by hypoxia and HIF. Biochem J 479:767–786. https://doi.org/10.1042/BCJ20220008

Bauer TM, Murphy E (2020) Role of mitochondrial calcium and the permeability transition pore in regulating cell death. Circ Res 126:280–293. https://doi.org/10.1161/circresaha.119.316306

Bitsch A, Kuhlmann T, Stadelmann C, Lassmann H, Lucchinetti C, Brück W (2001) A longitudinal MRI study of histopathologically defined hypointense multiple sclerosis lesions. Ann Neurol 49:793–796. https://doi.org/10.1002/ana.1053

Bonetti B, Raine CS (1997) Multiple sclerosis: oligodendrocytes display cell death-related molecules in situ but do not undergo apoptosis. Ann Neurol 42:74–84. https://doi.org/10.1002/ana.410420113

Burgoyne LA (1999) The mechanisms of pyknosis: hypercondensation and death. Exp Cell Res 248:214–222. https://doi.org/10.1006/excr.1999.4406

Cui QL, Khan D, Rone M, Johnson VTSR, Lin RM, Bilodeau YH, Hall PA, Rodriguez JA, Kennedy M TE et al (2017) Sublethal oligodendrocyte injury: a reversible condition in multiple sclerosis? Ann Neurol 81:811–824. https://doi.org/10.1002/ana.24944

Cui QL, Kuhlmann T, Miron VE, Leong SY, Fang J, Gris P, Kennedy TE, Almazan G, Antel J (2013) Oligodendrocyte progenitor cell susceptibility to injury in multiple sclerosis. Am J Pathol 183:516–525. https://doi.org/10.1016/j.ajpath.2013.04.016

Edinger AL, Thompson CB (2004) Death by design: apoptosis, necrosis and autophagy. Curr Opin Cell Biol 16:663–669. https://doi.org/10.1016/j.ceb.2004.09.011

Fernandes MGF, Luo JXX, Cui Q-L, Perlman K, Pernin F, Yaqubi M, Hall JA, Dudley R, Srour M, Couturier CP et al (2021) Age-related injury responses of human oligodendrocytes to metabolic insults: link to BCL-2 and autophagy pathways. Commun Biology 4:20. https://doi.org/10.1038/s42003-020-01557-1

Fiore A, Zeitler L, Russier M, Groß A, Hiller M-K, Parker JL, Stier L, Köcher T, Newstead S, Murray PJJMC (2022) Kynurenine importation by SLC7A11 propagates anti-ferroptotic signaling. 82:920–932 e927

Frandsen S, Vissing M, Gehl J (2020) A Comprehensive Review of Calcium Electroporation—A Novel Cancer Treatment Modality. Cancers 12:290. https://doi.org/10.3390/cancers12020290

Galluzzi L, Vitale I, Aaronson SA, Abrams JM, Adam D, Agostinis P, Alnemri ES, Altucci L, Amelio I, Andrews DW et al (2018) Molecular mechanisms of cell death:

recommendations of the Nomenclature Committee on Cell Death 2018. Cell Death & Differentiation 25: 486–541 https://doi.org/10.1038/s41418-017-0012-4

García-Prat L, Martínez-Vicente M, Perdiguero E, Ortet L, Rodríguez-Ubreva J, Rebollo E, Ruiz-Bonilla V, Gutarra S, Ballestar E, Serrano ALet al (2016) Autophagy maintains stemness by preventing senescence. Nature 529:37–42. https://doi.org/10.1038/nature16187

Glick D, Barth S, Macleod KF (2010) Autophagy: cellular and molecular mechanisms. J Pathol 221:3–12. https://doi.org/10.1002/path.2697

Gross AS, Graef M (2020) Mechanisms of Autophagy in metabolic stress response. J Mol Biol 432:28–52. https://doi.org/10.1016/j.jmb.2019.09.005

Gryzik M, Asperti M, Denardo A, Arosio P, Poli M (2021) NCOA4-mediated ferritinophagy promotes ferroptosis induced by erastin, but not by RSL3 in HeLa cells. Biochim Biophys Acta Mol Cell Res 1868:118913. https://doi.org/10.1016/j.bbamcr.2020.118913

Haimovici A, Höfer C, Badr MT, Bavafaye Haghighi E, Amer T, Boerries M, Bronsert P, Glavynskyi I, Fanfone D, Ichim Get al et al (2022) Spontaneous activity of the mitochondrial apoptosis pathway drives chromosomal defects, the appearance of micronuclei and cancer metastasis through the caspase-activated DNAse. Cell Death Dis 13:315. https://doi.org/10.1038/s41419-022-04768-y

He M, Ding Y, Chu C, Tang J, Xiao Q, Luo ZG (2016) Autophagy induction stabilizes microtubules and promotes axon regeneration after spinal cord injury. Proc Natl Acad Sci USA 113:11324–11329. https://doi.org/10.1073/pnas.1611282113

Healy LM, Perron G, Won S-Y, Michell-Robinson MA, Rezk A, Ludwin SK, Moore CS, Hall JA, Bar-Or A, Antel JP (2016) MerTK is a Functional Regulator of myelin phagocytosis by human myeloid cells. J Immunol 196:3375–3384. https://doi.org/10.4049/jimmunol.1502562

Heß K, Starost L, Kieran NW, Thomas C, Vincenten MCJ, Antel J, Martino G, Huitinga I, Healy L, Kuhlmann T (2020) Lesion stage-dependent causes for impaired remyelination in MS. Acta Neuropathol 140:359–375. https://doi.org/10.1007/s00401-020-02189-9

Hu CL, Nydes M, Shanley KL, Morales Pantoja IE, Howard TA, Bizzozero OA (2019) Reduced expression of the ferroptosis inhibitor glutathione peroxidase-4 in multiple sclerosis and experimental autoimmune encephalomyelitis. J Neurochem 148:426–439. https://doi.org/10.1111/jnc.14604

Jäkel S, Agirre E, Mendanha Falcão A, van Bruggen D, Lee KW, Knuesel I, Malhotra D, ffrench-Constant C, Williams A, Castelo-Branco G (2019) Altered human oligodendrocyte heterogeneity in multiple sclerosis. Nature 566:543–547.

Jhelum P, Santos-Nogueira E, Teo W, Haumont A, Lenoël I, Stys PK, David S (2020) Ferroptosis mediates Cuprizone-Induced loss of oligodendrocytes and demyelination. J Neurosci 40:9327–9341. https://doi.org/10.1523/jneurosci.1749-20.2020

Karim SA, Barrie JA, McCulloch MC, Montague P, Edgar JM, Kirkham D, Anderson TJ, Nave KA, Griffiths IR, McLaughlin M (2007) PLP overexpression perturbs myelin protein composition and myelination in a mouse model of Pelizaeus-Merzbacher disease. Glia 55:341–351. https://doi.org/10.1002/glia.20465

Kuhlmann T, Ludwin S, Prat A, Antel J, Brück W, Lassmann H (2017) An updated histological classification system for multiple sclerosis lesions. Acta Neuropathol 133:13–24. https://doi.org/10.1007/s00401-016-1653-y

Lassmann H, van Horssen J, Mahad D (2012) Progressive multiple sclerosis: pathology and pathogenesis. Nat Reviews Neurol 8:647–656. https://doi.org/10.1038/nrneurol.2012.168

Li J, Cao F, Yin H-l, Huang Z-j, Lin Z-t, Mao N, Sun B, Wang G (2020) Ferroptosis: past, present and future. Cell Death Dis 11:88. https://doi.org/10.1038/s41419-020-2298-2

Lőrincz P, Juhász G (2020) Autophagosome-Lysosome Fusion. J Mol Biol 432:2462–2482. https://doi.org/10.1016/j.jmb.2019.10.028

Love MI, Huber W, Anders S (2014) Moderated estimation of fold change and dispersion for RNA-seq data with DESeq2. Genome Biol 15:550. https://doi.org/10.1186/s13059-014-0550-8

Luchetti S, Fransen NL, van Eden CG, Ramaglia V, Mason M, Huitinga I (2018) Progressive multiple sclerosis patients show substantial lesion activity that correlates with clinical disease severity and sex: a retrospective autopsy cohort analysis. Acta Neuropathol 135:511–528. https://doi.org/10.1007/s00401-018-1818-y

Luo JXX, Cui QL, Yaqubi M, Hall JA, Dudley R, Srour M, Addour N, Jamann H, Larochelle C Blain M (2022) human oligodendrocyte myelination potential; relation to age and differentiation. Ann Neurol 91: 178–191 https://doi.org/10.1002/ana.26288

Lynch G, Baudry M (1987) Brain spectrin, calpain and long-term changes in synaptic efficacy. Brain Res Bull 18:809–815. https://doi.org/10.1016/0361-9230(87)90220-6

McKenzie BA, Dixit VM, Power C (2020) Fiery cell death: pyroptosis in the Central Nervous System. Trends Neurosci 43:55–73. https://doi.org/10.1016/j.tins.2019.11.005

McKenzie BA, Mamik MK, Saito LB, Boghozian R, Monaco MC, Major EO, Lu JQ, Branton WG, Power C (2018) Caspase-1 inhibition prevents glial inflammasome activation and pyroptosis in models of multiple sclerosis. Proc Natl Acad Sci USA 115:E6065–e6074. https://doi.org/10.1073/pnas.1722041115

Mizushima N (2007) Autophagy: process and function. Genes Dev 21:2861–2873

Paez PM, Lyons DA (2020) Calcium Signaling in the Oligodendrocyte lineage: regulators and consequences. Annu Rev Neurosci 43:163–186. https://doi.org/10.1146/annurev-neuro-100719-093305

Pernin F, Luo J, Cui QL, Blain M, Fernandes MGF, Yaqubi M, Srour M, Hall J, Dudley R Jamann H (2022) diverse injury responses of human oligodendrocyte to mediators implicated in multiple sclerosis. Brain : https://doi.org/10.1093/brain/awac075

Prineas JW, Kwon EE, Cho E-S, Sharer LR, Barnett MH, Oleszak EL, Hoffman B, Morgan BP (2001) Immunopathology of secondary-progressive multiple sclerosis. Ann Neurol 50:646–657. https://doi.org/10.1002/ana.1255

Rajgopal Y, Vemuri MC (2002) Calpain activation and alpha-spectrin cleavage in rat brain by ethanol. Neurosci Lett 321:187–191. https://doi.org/10.1016/s0304-3940(02)00063 – 0

Rao VTS, Khan D, Cui QL, Fuh SC, Hossain S, Almazan G, Multhaup G, Healy LM, Kennedy TE, Antel JP (2017) Distinct age and differentiation-state dependent metabolic profiles of oligodendrocytes under optimal and stress conditions. PLoS ONE 12:e0182372. https://doi.org/10.1371/journal.pone.0182372

Reich M, Liefeld T, Gould J, Lerner J, Tamayo P, Mesirov JP (2006) GenePattern 2.0. Nat Genet 38:500–501. https://doi.org/10.1038/ng0506-500

Rone MB, Cui QL, Fang J, Wang LC, Zhang J, Khan D, Bedard M, Almazan G, Ludwin SK, Jones Ret al et al (2016) Oligodendrogliopathy in multiple sclerosis: low glycolytic metabolic rate promotes oligodendrocyte survival. J Neurosci 36:4698–4707. https://doi.org/10.1523/jneurosci.4077-15.2016

Satoh J, Motohashi N, Kino Y, Ishida T, Yagishita S, Jinnai K, Arai N, Nakamagoe K, Tamaoka A, Saito Y al (2014) LC3, an autophagosome marker, is expressed on oligodendrocytes in Nasu-Hakola disease brains. Orphanet J Rare Dis 9:68. https://doi.org/10.1186/1750-1172-9-68

Sharifi MN, Mowers EE, Drake LE, Macleod KF (2015) Measuring autophagy in stressed cells. In: Oslowski CM (ed) Stress responses: methods and protocols. Springer New York, City, pp 129–150

Yan X, Zhou R, Ma Z (2019) Autophagy-cell survival and death. Adv Exp Med Biol 1206:667–696. https://doi.org/10.1007/978-981-15-0602-4_29

Yang J, Zhou R, Ma Z (2019) Autophagy and energy metabolism. Adv Exp Med Biol 1206:329–357. https://doi.org/10.1007/978-981-15-0602-4_16

Yaqubi M, Luo JXX, Baig S, Cui QL, Petrecca K, Desu H, Larochelle C, Afanasiev E, Hall JA, Dudley Ret al et al (2022) Regional and age-related diversity of human mature oligodendrocytes. Glia 70:1938–1949. https://doi.org/10.1002/glia.24230

Zhang C-x, Cheng Y, Liu D-z, Liu M, Cui H, Zhang B-l, Mei Q-b, Zhou S-y (2019) Mitochondria-targeted cyclosporin A delivery system to treat myocardial ischemia reperfusion injury of rats. J Nanobiotechnol 17:18. https://doi.org/10.1186/s12951-019-0451-9

Zhang ZV (2022) The integrated stress response in ischemic diseases. Cell Death & Differentiation 29:750–757. https://doi.org/10.1038/s41418-021-00889-7

Zhao YG, Codogno P, Zhang H (2021) Machinery, regulation and pathophysiological implications of autophagosome maturation. Nat Rev Mol Cell Biol 22:733–750. https://doi.org/10.1038/s41580-021-00392-4

CHAPTER 5: Discussion

5.1 Resistance to apoptosis

In this study, we investigated the possible molecular mechanisms that potentially cause hOL death in response to metabolic stress based on the current literature on RCD pathways. We first confirmed that hOLs are resistant to apoptosis and this resistance increases with age and differentiation. Metabolic stress can potentially induce apoptosis through the intrinsic pathway, by the activation of the pro-apoptotic molecules BAX and BAK (Balmer et al., 2013). We showed that activation of BAX and BAK are inhibited by anti-apoptotic molecules of the BCL-2 family.

The role of these anti-apoptotic molecules is essential for the inhibition of apoptosis in metabolic stress conditions, considering that some BH3-only molecules are activated. As extensively analysed by Kønig et al., there are potentially 282 BH3-only molecules and 26 of these were characterized to some extent in the literature (Kønig et al., 2019). As these molecules are the stress sensors of the intrinsic apoptotic pathway, and considering that they can be activated by a plethora of different stresses, it is fair to suppose that the upregulation of the anti-apoptotic molecules gives OLs an overall resistance to apoptosis. However, interactions between BH3-only and the other members of the BCL-2 family vary according to potential stresses and environments (Kale et al., 2018), implying that apoptosis can be potentially triggered in OLs under different circumstances than metabolic stress.

A relevant example is the activation of apoptosis mediated by $CD4^+$ Th17 cells (Jamann et al., 2022). Th17 cells are identified in active MS lesions and their presence is increased in the

circulation of MS patients during relapses (Fujii et al., 2016, Matusevicius et al., 1999, Tzartos et al., 2008). Contact between hOLs and $CD4^{+}$Th17 cells induces cell death in association with the release of Granzyme-B by the T-cells (Jamann et al., 2022). Granzyme-B is known to initiate the intrinsic apoptotic pathway by cleaving BH3 interacting-domain death agonist (BID), as its name implies, a member of the BH3-only family (Sutton et al., 2000). There are situations when the elimination of cells by apoptosis is desired, in the case of neoplasia, for example. However, this pathway is also susceptible to dysregulation at the organism and intracellular level, which justifies further investigation of possible pathological implications of apoptosis in human OLs in potentially neurodegenerative conditions.

5.2 Ferroptosis

In addition to apoptosis, we have analysed two other RCD pathways: ferroptosis and MPT-driven necrosis. These pathways were selected as we reasoned that they have the most potential to be triggered by metabolic stress in hOLs. There was no clear evidence that these pathways are activated.

Ferroptosis is a consequence of severe lipid peroxidation of the cell membrane, which is caused by ROS intracellular accumulation, in particular hydroxyl radicals (Chen et al., 2021a). Hydroxyl radicals are produced by the Fenton reaction, which consists of the oxidation of iron by hydrogen peroxide (Tsuneda, 2020). Therefore, the presence of iron is an important factor in the induction of ferroptosis. We have detected an increase in intracellular H_2O_2 that could potentially cause lipid peroxidation and ferroptosis to hOLs. However, as cell death was not attenuated by ferrostatin-1, which is a potent inhibitor of lipid peroxidation, there is no evidence that the H_2O_2 generated as a consequence of metabolic stress causes cell death in hOL.

Glutathione is the most important antioxidant of the cell and is capable of neutralizing H_2O_2 (Forman et al., 2009). Erastin inhibits glutathione synthesis by reducing cellular uptake of its precursor cystine (Dixon et al., 2012). We did not observe an induction of ferroptosis in hOLs when treated with Erastin, in contrast with an increase in cell death in HeLa cells. Therefore, the level of glutathione is not a decisive factor for the protection of hOLs from ferroptosis. Potential factors for this protection are low levels of intracellular iron and levels of ROS that do not surpass a lethal threshold.

As in the case of apoptosis, it is relevant to consider that, although metabolic stress in isolation does not induce ferroptosis, a combination of other factors can cause this RCD. As shown in Chapter 4, high levels of external H_2O_2 are lethal to hOLs. Besides, an increase in intracellular iron could also lead to fatal consequences. In addition, glutamate, an excitotoxin associated with neurodegeneration can reduce the antioxidant resistance by impairing the uptake of cystine (Chen et al., 2021a). Therefore, it is reasonable to accept that ferroptosis could occur in conditions presenting high levels of ROS, internally and externally produced, high levels of intracellular iron and glutamate toxicity.

5.3 MPT-driven necrosis

MPT-driven necrosis is an RCD pathway in which mitochondria are saturated with Ca^{2+} and permeability transition pores are opened, returning this ion to the cytosol and increasing its cytosolic concentration (Baines et al., 2005). Although we have evidence of the role of Ca^{2+} and the activation of Ca^{2+}-dependent proteases in hOL in response to metabolic stress, the origin of Ca^{2+} does not appear to be the mitochondria, as treatment with cyclosporin A, an inhibitor of the

opening of permeability transition pores, did not reduce levels of cell death in hOLs under metabolic stress.

A possible explanation for the resistance of hOLs to MPT-driven necrosis is the downregulation of cyclophilin D, which is the main regulator of the opening of the mitochondrial permeability transition pore, and potential components of these pores, including VDAC1, which also participates in the transport of Ca^{2+} between the mitochondria and the cytosol (Shoshan-Barmatz et al., 2018).

5.4 PANoptosis

Pyroptosis, intrinsic apoptosis, and necroptosis are currently perceived as a complex response to infection and tissue damage that leads to cell death. These three RCD pathways have clear molecular mechanisms. While apoptosis is mainly executed by caspases, which are intracellular proteases, pyroptosis, and necroptosis are mediated by GSDMD and MLKL respectively. Apoptosis is immunologically silent, in contrast with the other two pathways that trigger immunological reactions (Malireddi et al., 2019). It is hypothesized that pyroptosis and necroptosis were evolutionary adaptations of organisms that developed defenses against pathogens capable of inhibiting apoptosis in infected cells (Tummers and Green, 2022).

The main triggers of these pathways are TNF and activation of TLRs by PAMPs and DAMPs (Bertheloot et al., 2021). As this study is restricted to cell death directly caused by metabolic stress, pyroptosis, and necroptosis were not included in our investigations. However, it is plausible to consider that these pathways could occur as a secondary cause of cell death in cases in which metabolic stress is the primary cause. In these cases, after death, cells would release DAMPs that could trigger either pyroptosis or necroptosis in neighboring cells.

Evidence of pyroptosis was observed in MS patients, in which clear detection of cells expressing GSDMD and IL-1β was present. Exposure of hOL *in vitro* to TNFα also induced GSDMD activation (McKenzie et al., 2018). Therefore, pyroptosis and necroptosis cannot be discarded as possible mediators of cell death in MS and other conditions in which the presence of DAMPs or TNFα is suspected.

5.5 Other RCD pathways

Another RCD pathway that was not analysed in this study is parthanatos. The main reason is that one of the main hallmarks of this pathway is DNA fragmentation and this feature could be detected by the TUNEL assay (David et al., 2009). The proportion of TUNEL-positive cells detected in our *in vitro* experiments in hOLs subjected to metabolic stress is consistently low, indicating that parthanatos is not being activated.

We also reasoned that lysosome-dependent cell death is unlikely to occur. This RCD pathway is dependent on LMP formation, which can be caused by a series of stresses, including ROS (Aits and Jäättelä, 2013). However, we verified that the level of ROS produced in hOLs as a consequence of metabolic stress is not sufficient to cause cell death. Nevertheless, it would be relevant to evaluate this mode of RCD in models where hOLs are exposed to a combination of external ROS, metabolic stress, and glutamate.

Some studies reported evidence of entosis, in which OLs can be engulfed by ASTs (Ghatak, 1992, Shintaku and Yutani, 2004). This mode of RCD must be taken into consideration in future studies with co-cultures of OLs and ASTs or other models that investigate the interaction between these two types of cells.

5.6 ATP levels (Glycolysis vs. OXPHOS)

A clear aspect of the response of hOLs to metabolic stress is the drastic decrease in ATP levels. This decrease is considerably fast, as it is detected hours after initiation of treatment. As it is reasonable to expect that ATP production decreases as a consequence of glucose deprivation, which implies less glycolysis and eventually less OXPHOS, it is more difficult to understand how these cells can survive for 4 to 6 days without ATP as a source of energy. One possible explanation is that energy may be stored in other molecules as GTP and other phosphorylated proteins.

Under metabolic stress, low levels of ATP and increased levels of AMP activate AMPK, which promotes a metabolic switch in the cell. AMPK phosphorylates and inhibits mTOR, which is a pro-anabolic and anti-catabolic factor. As a consequence, protein synthesis is reduced and catabolic mechanisms such as autophagy are activated (Lipton and Sahin, 2014, Zoncu et al., 2011). Although in previous studies a sharp decline in ATP production was observed (Rone et al., 2016), a possible outcome of glucose deprivation would be that the cell enters an economic mode, which would slow down the decline in ATP consumption and keep sufficient ATP levels to support cell functions for an extended period.

Another possible outcome of glucose deprivation is the production of ATP using stored material as an energy source. Glycogen or lipid droplets could be degraded into glucose and acyl-CoA and used in glycolysis and OXPHOS for the production of ATP (Roach et al., 2012, Olzmann and Carvalho, 2019). Our results suggest that this degradation of intracellular energy sources is not sufficient to compensate for the decrease in energy production. According to the literature, glycogen is mainly stored in ASTs in the brain (Alberini et al., 2018) and it is not clear how

much glycogen is kept in OLs. Therefore, in the CNS parenchyma, shortages of energetic metabolites are compensated by the mobilization of glycogen storage in ASTs, transferring energetic metabolites to neurons and OLs (Brown and Ransom, 2015). In this way, an exclusive culture of OLs cannot capture this mechanism. Future studies with co-cultures of ASTs and OLs, *in vivo* or *ex vivo* models that preserve the interactive structures between ASTs and OLs could provide valuable information on this energetic support in metabolic stress conditions.

As reported in previous studies, mature hOLs rely less on OXPHOS than glycolysis for ATP production. Under glucose deprivation conditions, the production of ATP by OXPHOS is even lower (Rone et al., 2016). A possible explanation for this low cellular respiration in hOLs is the low expression of VDAC1 and VDAC2, which are the mitochondrial channels responsible for the transport of energetic metabolites, mainly pyruvate. Moreover, as myelin requires lipid biosynthesis for its maintenance, a large proportion of acetyl-CoA is directed to the production of lipids instead of energy (Bauernfeind et al., 2014). A reduction in OXPHOS also contributes to reduced levels of ROS, as discussed in the section about ferroptosis.

5.7 Autophagy

This study indicates that autophagy is necessary for the survival of hOLs and its activity is increased when cells are deprived of glucose. The inhibition of autophagy in these deprived conditions leads to an acceleration of cell death. Therefore, we hypothesized that autophagy could contribute to cell survival by providing substrates for energy production. Protein and lipids degraded in the autophagic process could be transformed into amino acids and acetyl-CoA and used in glycolysis and OXPHOS for the production of ATP (Meijer and Codogno, 2006). We then expected that the inhibition of autophagy would cause a decrease in ATP levels. In contrast,

autophagy activation would contribute to an increase in ATP levels. However, the use of chloroquine, an autophagy inhibitor, and Torin-1, an autophagy activator, did not cause changes in the intracellular ATP levels in hOLs, especially under glucose deprivation conditions, when autophagy is activated and cells need energy. A possible explanation for this lack of autophagy influence in ATP production is that hOLs rely preferentially on glycolysis for energy production than OXPHOS, as discussed in the last section. Autophagy may capture and degrade intracellular material in the cytosol, but this material is directed to other ends, possibly for recycling and remodeling the internal cell structure in response to an environment scarce in energy sources.

5.8 ATP and autophagy

Our results indicate that not only autophagy does not contribute to ATP production in the cell, but ATP depletion may be causing failure in the autophagic flux. As discussed in Chapter 4, autophagy needs dyneins and kinesins for the transport of autophagosomes and lysosomes, and these molecules use ATP to propel their movements. The fusion between autophagosomes also indirectly requires ATP, as this process is mediated by GTPases (Zhao et al., 2021). This ATP dependence may be the underlying cause of the autophagosome accumulation in hOLs after 4 days of glucose deprivation presented in Chapter 4.

Autophagy inhibition, in addition to accelerating cell death, was also associated with the reduction of hOLs processes length and the release of debris in the culture media. A possible explanation for this injury is that materials that should be used for recycling cellular components are captured in autophagosomes.

Some studies support that failure of autophagy can disrupt cytoskeleton integrity. He el al. found that autophagy has a role in the regulation of microtubules in axons. This regulation is mediated

by superior cervical ganglia protein 10 (SCG10), which is a microtubule disassembly protein expressed in neurons. In this same study, the induction of autophagy contributed to axon regeneration after nerve injury (He et al., 2016).

In studies using a mouse model of Pelizaeus-Merzbacher disease (PMD), overexpression of PLP was associated with hypomyelination (Karim et al., 2010, Karim et al., 2007). OLs in this model presented an accumulation of autolysosomes, and colocalization of PLP and LAMP1, indicating that PLP was captured in these autolysosomes. This accumulation caused a dysregulation of myelin protein expression, in particular MBP (Karim et al., 2007). Treatments with rapamycin, an autophagy activator, increased the accumulation of PLP in autophagosomes (Karim et al., 2010).

These examples demonstrate that autophagy can be implicated in different cellular functions, and its impairment can cause an imbalance in the availability of cellular components with deleterious consequences to the cell.

5.9 The role of Ca^{2+} in hOL death in response to metabolic stress

As discussed in Chapter 4, our findings suggest that Ca^{2+} has an important role in the hOLs death process in response to sustained metabolic stress, as it activates Ca^{2+}-dependant proteases, which target cytoskeleton components (Rajgopal and Vemuri, 2002). We hypothesized that this regulation is linked to ATP availability, which is necessary for the maintenance of intracellular Ca^{2+} gradients (Frandsen et al., 2020).

As our data indicates that MPT-driven necrosis is not activated, these results suggest that hOL death caused by metabolic stress is a passive process, not actively regulated by the cell.

Considering the long-lived nature of hOLs (Yeung et al., 2019a), this resistance to metabolic stress may integrate the set of mechanisms that support the survival capacity of these cells.

5.10 Perspectives

Given the findings obtained in this study, we can point to opportunities for further investigation of the potential causes of cell death in hOLs in MS and other disorders, and the development of protective therapies.

5.10.1 Improving the in vitro model

The *in vitro* model used in this study consists of a purified culture containing on average 90% O4+ OLs. The optimal culture condition (N1) used as control has a considerably high level of glucose of 25 mM. Normal levels of glucose in the blood of rats vary in the range of 3 to 8 mM, and healthy human blood glucose levels between 4 and 6.5 mM are considered normal (Levin et al., 2011) (Hindmarsh and Geertsma, 2017). In the extracellular space of rat brains, glucose concentration ranges between 0.4 and 2.5 mM (Levin et al., 2011). Furthermore, glucose is not the only substrate used by OLs as energy, as these cells are also capable of uptake and metabolizing lactate and ketone bodies (Tepavčević, 2021). More realistic models should have a considerably lower concentration of glucose in the media, and should also contain other energetic metabolites. Experiments that explore the influence of different levels of these metabolites could give better insights into the energetic metabolism and responses to treatment in hOLs.

Energetic metabolites in the blood must traverse the BBB to reach OLs, which involves the participation of endothelial cells and ASTs. It is possible to develop an *in vitro* model that better represents the BBB using transwell systems (Stone et al., 2019). In this model, a layer of

endothelial cells is formed at the bottom of a transwell insert. A layer of pericytes and ASTs is formed under the layer of endothelial cells, simulating a BBB. Neurons or microglia are cultured in the underlying well, so this system can test how treatments are affected by the BBB (Stone et al., 2019). This system could be used to culture OLs or co-cultures of OLs and neurons and test treatments and responses to the availability of energetic metabolites to OLs and other types of cells in the system. A possible improvement of this system could be the addition of a microfluid system that models capillaries as described by Sivandzade & Cucullo (Sivandzade and Cucullo, 2018).

5.10.2 Therapeutic potential of metabolism regulation

The findings presented in this thesis have translational and clinical potential. The impact of metabolic stress and the described hOL cell death pathway provide new insight into the mechanisms that underlie MS and demyelinating diseases pathology. Each of these features have potential as targets for the development of therapeutic interventions.

As we found that hOL death in response to metabolic stress is directly associated with ATP depletion, a therapeutic strategy to avoid this depletion could be to increase the efficacy of cellular respiration. This efficacy could be improved by modulating molecular mechanisms that regulate OXPHOS. PDK is an inhibitor of PDH, which converts pyruvate into acyl-CoA (Patel et al., 2014). Pharmaceutical inhibition of PDK could induce hOLs to metabolize more acetyl-CoA that could be used to produce ATP (Mayers et al., 2003). Another potential target is lactate dehydrogenase (LDH) which mutually converts pyruvate into lactate. This enzyme has two forms, LDHA, which preferably converts pyruvate to lactate, and LDHB, which preferably catalyzes the inverse reaction (Kolappan et al., 2015). Inhibition of LDHA could increase the availability of pyruvate which could be directed to increase OXPHOS. The activation of the transcription factor

proliferator-activated receptor γ (PPARγ) could also stimulate OXPHOS by promoting Ca^{2+} oscillations, which improves the function of mitochondrial dehydrogenases (Bernardo et al., 2013).

5.10.3 Cerebral hypoperfusion

Another strategy to avoid hOL death in response to metabolic stress could target the metabolic stress itself. Therefore, treatments that improve cerebral perfusion could reduce hOL injury. As described in Chapter 2, ET-1 is a potent vasoconstrictor and is released by endothelial cells and ASTs. Pharmaceutical inhibition of ET-1 could help increase cerebral perfusion and availability of nutrients to hOLs, avoiding metabolic stress (Michinaga et al., 2020)

5.10.4 Astrocytes

As ASTs have an important role in the BBB and the metabolic support of hOLs and neurons (Bélanger et al., 2011), these cells may have a significant role in the survival of hOLs. ASTs can transmit energetic metabolites by gap junctions and MCT channels (John, 2012). How the flux of these metabolites is controlled is not very well characterized. Also, it is unclear how changes in AST phenotypes could influence this flux. Further studies on this process could contribute to the understanding of the dynamics of metabolic stress on hOLs and represent another target for treatments.

5.11 Conclusion

The main objective of this work was to understand the mechanisms by which metabolic stress causes hOLs death. Based on the results obtained, we can conclude that hOLs do not trigger any known RCD pathway in response to metabolic stress, and cell death occurs in a slow process of cellular integrity disruption caused by ATP depletion. Due to this ATP shortage, autophagy, a process that supports hOL survival, fails, leading to processes retraction and loss of myelin.

Evidence of autophagy failure was identified in lesions and NAWM of MS patients, indicating that this mechanism occurs in this disease and may be a consequence of metabolic stress. ATP depletion also entails an increase in Ca^{2+} concentration, activation of Ca^{2+}-dependent proteases, and cleavage of cytoskeleton components. Adult hOLs are resistant to apoptosis. This resistance is supported by an increased expression of anti-apoptotic molecules of the BCL-2 family and a decrease in the expression of pro-apoptotic molecules of this same family.

hOLs death and injury are hallmarks of MS and other demyelinating diseases (Baumann and Pham-Dinh, 2001, RODRIGUEZ et al., 1993) and the findings in this study contribute to the understanding of this pathological process by uncovering the molecular mechanism involved in response to metabolic stress, which may be caused by cerebral hypoperfusion, a feature consistently identified in MS patients (D'Haeseleer et al., 2015). This understanding can contribute to therapeutic approaches to attenuate the progressive pattern of MS.

This study demonstrated that hOLs are resilient cells that are not prone to succumb to cell death. Our results focused on the resistance of these cells to injuries caused by metabolic stress. Some insights were given on their resistance to oxidative stress. Further studies could investigate hOLs response to combined stresses including metabolic and oxidative stress, glutamate excitotoxicity, the influence of cytokines and interactions with cells of the immune system. The development of models that can better represent how impairments in the supply of energetic metabolites affect OLs could also contribute to identifying potentially harmful mechanisms and targets for treatment.

Our findings indicate opportunities for therapeutic strategies that could increase hOLs capacity to survive in a metabolic challenged environment and possible alternatives to attenuate metabolic stress, potentially contributing to treatments for MS and other demyelinating diseases.

References

ABBOTT, N. J., RÖNNBÄCK, L. & HANSSON, E. 2006. Astrocyte-endothelial interactions at the blood-brain barrier. *Nat Rev Neurosci,* 7**,** 41-53.

ABOUL-ENEIN, F., KRSSÁK, M., HÖFTBERGER, R., PRAYER, D. & KRISTOFERITSCH, W. 2010. Reduced NAA-levels in the NAWM of patients with MS is a feature of progression. A study with quantitative magnetic resonance spectroscopy at 3 Tesla. *PLoS One,* 5**,** e11625.

ABOUL-ENEIN, F. & LASSMANN, H. 2005. Mitochondrial damage and histotoxic hypoxia: a pathway of tissue injury in inflammatory brain disease? *Acta Neuropathol,* 109**,** 49-55.

ABOUL-ENEIN, F., RAUSCHKA, H., KORNEK, B., STADELMANN, C., STEFFERL, A., BRÜCK, W., LUCCHINETTI, C., SCHMIDBAUER, M., JELLINGER, K. & LASSMANN, H. 2003. Preferential loss of myelin-associated glycoprotein reflects hypoxia-like white matter damage in stroke and inflammatory brain diseases. *J Neuropathol Exp Neurol,* 62**,** 25-33.

ABRAMS, C. K. & SCHERER, S. S. 2012. Gap junctions in inherited human disorders of the central nervous system. *Biochim Biophys Acta,* 1818**,** 2030-47.

ABUD, E. M., RAMIREZ, R. N., MARTINEZ, E. S., HEALY, L. M., NGUYEN, C. H., NEWMAN, S. A., YEROMIN, A. V., SCARFONE, V. M., MARSH, S. E. & FIMBRES, C. 2017. iPSC-derived human microglia-like cells to study neurological diseases. *Neuron,* 94**,** 278-293. e9.

ADAMS, L., FRANCO, M. C. & ESTEVEZ, A. G. 2015. Reactive nitrogen species in cellular signaling. *Exp Biol Med (Maywood),* 240**,** 711-7.

ADHYA, S., JOHNSON, G., HERBERT, J., JAGGI, H., BABB, J. S., GROSSMAN, R. I. & INGLESE, M. 2006. Pattern of hemodynamic impairment in multiple sclerosis: dynamic susceptibility contrast perfusion MR imaging at 3.0 T. *Neuroimage,* 33**,** 1029-35.

AGRAWAL, A. & MABALIRAJAN, U. 2016. Rejuvenating cellular respiration for optimizing respiratory function: targeting mitochondria. *American Journal of Physiology-Lung Cellular and Molecular Physiology,* 310**,** L103-L113.

AITS, S. & JÄÄTTELÄ, M. 2013. Lysosomal cell death at a glance. *Journal of Cell Science,* 126**,** 1905-1912.

AKERFELT, M., MORIMOTO, R. I. & SISTONEN, L. 2010. Heat shock factors: integrators of cell stress, development and lifespan. *Nat Rev Mol Cell Biol,* 11**,** 545-55.

ÅKERFELT, M., MORIMOTO, R. I. & SISTONEN, L. 2010. Heat shock factors: integrators of cell stress, development and lifespan. *Nature reviews Molecular cell biology,* 11**,** 545-555.

AL REFAII, A. & ALIX, J. H. 2009. Ribosome biogenesis is temperature-dependent and delayed in Escherichia coli lacking the chaperones DnaK or DnaJ. *Mol Microbiol,* 71**,** 748-62.

ALBERINI, C. M., CRUZ, E., DESCALZI, G., BESSIÈRES, B. & GAO, V. 2018. Astrocyte glycogen and lactate: New insights into learning and memory mechanisms. *Glia,* 66**,** 1244-1262.

ANDRABI, S. A., DAWSON, T. M. & DAWSON, V. L. 2008. Mitochondrial and nuclear cross talk in cell death: parthanatos. *Ann N Y Acad Sci,* 1147**,** 233-41.

ANDRABI, S. A., KIM, N. S., YU, S. W., WANG, H., KOH, D. W., SASAKI, M., KLAUS, J. A., OTSUKA, T., ZHANG, Z., KOEHLER, R. C., HURN, P. D., POIRIER, G. G., DAWSON, V. L. & DAWSON, T. M. 2006. Poly(ADP-ribose) (PAR) polymer is a death signal. *Proc Natl Acad Sci U S A,* 103**,** 18308-13.

ANTEL, J. P., LIN, Y. H., CUI, Q. L., PERNIN, F., KENNEDY, T. E., LUDWIN, S. K. & HEALY, L. M. 2019. Immunology of oligodendrocyte precursor cells in vivo and in vitro. *J Neuroimmunol,* 331**,** 28-35.

APÁTIGA-PÉREZ, R., SOTO-ROJAS, L. O., CAMPA-CÓRDOBA, B. B., LUNA-VIRAMONTES, N. I., CUEVAS, E., VILLANUEVA-FIERRO, I., ONTIVEROS-TORRES, M. A., BRAVO-MUÑOZ, M., FLORES-RODRÍGUEZ, P., GARCÉS-RAMIREZ, L., DE LA CRUZ, F., MONTIEL-SOSA, J. F., PACHECO-HERRERO, M. & LUNA-

MUÑOZ, J. 2022. Neurovascular dysfunction and vascular amyloid accumulation as early events in Alzheimer's disease. *Metab Brain Dis,* 37**,** 39-50.

APETOH, L., GHIRINGHELLI, F., TESNIERE, A., OBEID, M., ORTIZ, C., CRIOLLO, A., MIGNOT, G., MAIURI, M. C., ULLRICH, E., SAULNIER, P., YANG, H., AMIGORENA, S., RYFFEL, B., BARRAT, F. J., SAFTIG, P., LEVI, F., LIDEREAU, R., NOGUES, C., MIRA, J. P., CHOMPRET, A., JOULIN, V., CLAVEL-CHAPELON, F., BOURHIS, J., ANDRÉ, F., DELALOGE, S., TURSZ, T., KROEMER, G. & ZITVOGEL, L. 2007. Toll-like receptor 4-dependent contribution of the immune system to anticancer chemotherapy and radiotherapy. *Nat Med,* 13**,** 1050-9.

ARAGONÉS, J., SCHNEIDER, M., VAN GEYTE, K., FRAISL, P., DRESSELAERS, T., MAZZONE, M., DIRKX, R., ZACCHIGNA, S., LEMIEUX, H., JEOUNG, N. H., LAMBRECHTS, D., BISHOP, T., LAFUSTE, P., DIEZ-JUAN, A., HARTEN, S. K., VAN NOTEN, P., DE BOCK, K., WILLAM, C., TJWA, M., GROSFELD, A., NAVET, R., MOONS, L., VANDENDRIESSCHE, T., DEROOSE, C., WIJEYEKOON, B., NUYTS, J., JORDAN, B., SILASI-MANSAT, R., LUPU, F., DEWERCHIN, M., PUGH, C., SALMON, P., MORTELMANS, L., GALLEZ, B., GORUS, F., BUYSE, J., SLUSE, F., HARRIS, R. A., GNAIGER, E., HESPEL, P., VAN HECKE, P., SCHUIT, F., VAN VELDHOVEN, P., RATCLIFFE, P., BAES, M., MAXWELL, P. & CARMELIET, P. 2008. Deficiency or inhibition of oxygen sensor Phd1 induces hypoxia tolerance by reprogramming basal metabolism. *Nat Genet,* 40**,** 170-80.

ARBEL, N., BEN-HAIL, D. & SHOSHAN-BARMATZ, V. 2012. Mediation of the antiapoptotic activity of Bcl-xL protein upon interaction with VDAC1 protein. *Journal of Biological Chemistry,* 287**,** 23152-23161.

ARMSTRONG, R., DORN, H., KUFTA, C., FRIEDMAN, E. & DUBOIS-DALCQ, M. 1992. Pre-oligodendrocytes from adult human CNS. *Journal of Neuroscience,* 12**,** 1538-1547.

ARMULIK, A., GENOVÉ, G. & BETSHOLTZ, C. 2011. Pericytes: developmental, physiological, and pathological perspectives, problems, and promises. *Dev Cell,* 21**,** 193-215.

ASCHERIO, A., MUNGER, K. L., WHITE, R., KÖCHERT, K., SIMON, K. C., POLMAN, C. H., FREEDMAN, M. S., HARTUNG, H. P., MILLER, D. H., MONTALBÁN, X., EDAN, G., BARKHOF, F., PLEIMES, D., RADÜ, E. W., SANDBRINK, R., KAPPOS, L. & POHL, C. 2014. Vitamin D as an early predictor of multiple sclerosis activity and progression. *JAMA Neurol,* 71**,** 306-14.

ASHKENAZI, A. & SALVESEN, G. 2014. Regulated cell death: signaling and mechanisms. *Annu Rev Cell Dev Biol,* 30**,** 337-56.

BACK, S. A., HAN, B. H., LUO, N. L., CHRICTON, C. A., XANTHOUDAKIS, S., TAM, J., ARVIN, K. L. & HOLTZMAN, D. M. 2002. Selective vulnerability of late oligodendrocyte progenitors to hypoxia-ischemia. *J Neurosci,* 22**,** 455-63.

BACK, S. A., LUO, N. L., BORENSTEIN, N. S., LEVINE, J. M., VOLPE, J. J. & KINNEY, H. C. 2001. Late oligodendrocyte progenitors coincide with the developmental window of vulnerability for human perinatal white matter injury. *J Neurosci,* 21**,** 1302-12.

BAINES, C. P., KAISER, R. A., PURCELL, N. H., BLAIR, N. S., OSINSKA, H., HAMBLETON, M. A., BRUNSKILL, E. W., SAYEN, M. R., GOTTLIEB, R. A., DORN, G. W., ROBBINS, J. & MOLKENTIN, J. D. 2005. Loss of cyclophilin D reveals a critical role for mitochondrial permeability transition in cell death. *Nature,* 434**,** 658-62.

BAINES, C. P., SONG, C.-X., ZHENG, Y.-T., WANG, G.-W., ZHANG, J., WANG, O.-L., GUO, Y., BOLLI, R., CARDWELL, E. M. & PING, P. 2003. Protein kinase Cε interacts with and inhibits the permeability transition pore in cardiac mitochondria. *Circulation research,* 92**,** 873-880.

BAKER, P. J., DE NARDO, D., MOGHADDAS, F., TRAN, L. S., BACHEM, A., NGUYEN, T., HAYMAN, T., TYE, H., VINCE, J. E., BEDOUI, S., FERRERO, R. L. & MASTERS, S. L. 2017. Posttranslational Modification as a Critical Determinant of Cytoplasmic Innate Immune Recognition. *Physiol Rev,* 97**,** 1165-1209.

BALMER, D., EMERY, M., ANDREUX, P., AUWERX, J., GINET, V., PUYAL, J., SCHORDERET, D. F. & RODUIT, R. 2013. Autophagy defect is associated with low glucose-induced apoptosis in 661W photoreceptor cells. *PLoS One,* 8**,** e74162.

BANKSTON, A. N., FORSTON, M. D., HOWARD, R. M., ANDRES, K. R., SMITH, A. E., OHRI, S. S., BATES, M. L., BUNGE, M. B. & WHITTEMORE, S. R. 2019. Autophagy is essential for oligodendrocyte differentiation, survival, and proper myelination. *Glia,* 67**,** 1745-1759.

BARNETT, M. H. & PRINEAS, J. W. 2004. Relapsing and remitting multiple sclerosis: pathology of the newly forming lesion. *Ann Neurol,* 55**,** 458-68.

BARNETT, S. C. & CROUCH, D. H. 1995. The effect of oncogenes on the growth and differentiation of oligodendrocyte type 2 astrocyte progenitor cells. *Cell Growth and Differentiation-Publication American Association for Cancer Research,* 6**,** 69-80.

BARRERA, G. 2012. Oxidative stress and lipid peroxidation products in cancer progression and therapy. *International Scholarly Research Notices,* 2012.

BASTIAN, C., QUINN, J., DOHERTY, C., FRANKE, C., FARIS, A., BRUNET, S. & BALTAN, S. 2019. Role of Brain Glycogen During Ischemia, Aging and Cell-to-Cell Interactions. *Adv Neurobiol,* 23**,** 347-361.

BATIE, M., FROST, J., SHAKIR, D. & ROCHA, S. 2022. Regulation of chromatin accessibility by hypoxia and HIF. *Biochem J,* 479**,** 767-786.

BAUER, T. M. & MURPHY, E. 2020. Role of Mitochondrial Calcium and the Permeability Transition Pore in Regulating Cell Death. *Circ Res,* 126**,** 280-293.

BAUERNFEIND, A. L., BARKS, S. K., DUKA, T., GROSSMAN, L. I., HOF, P. R. & SHERWOOD, C. C. 2014. Aerobic glycolysis in the primate brain: reconsidering the implications for growth and maintenance. *Brain Struct Funct,* 219**,** 1149-67.

BAUMANN, N. & PHAM-DINH, D. 2001. Biology of oligodendrocyte and myelin in the mammalian central nervous system. *Physiol Rev,* 81**,** 871-927.

BÉLANGER, M., ALLAMAN, I. & MAGISTRETTI, P. J. 2011. Brain energy metabolism: focus on astrocyte-neuron metabolic cooperation. *Cell Metab,* 14**,** 724-38.

BELL, R. D., WINKLER, E. A., SAGARE, A. P., SINGH, I., LARUE, B., DEANE, R. & ZLOKOVIC, B. V. 2010. Pericytes control key neurovascular functions and neuronal phenotype in the adult brain and during brain aging. *Neuron,* 68**,** 409-27.

BENARROCH, E. E. 2005. Neuron-astrocyte interactions: partnership for normal function and disease in the central nervous system. *Mayo Clin Proc,* 80**,** 1326-38.

BENARROCH, E. E. 2009. Hypoxia-induced mediators and neurologic disease. *Neurology,* 73**,** 560-5.

BENITO-KWIECINSKI, S. & LANCASTER, M. A. 2020. Brain organoids: human neurodevelopment in a dish. *Cold Spring Harbor perspectives in biology,* 12**,** a035709.

BERGSLAND, N., HORAKOVA, D., DWYER, M. G., UHER, T., VANECKOVA, M., TYBLOVA, M., SEIDL, Z., KRASENSKY, J., HAVRDOVA, E. & ZIVADINOV, R. 2018. Gray matter atrophy patterns in multiple sclerosis: a 10-year source-based morphometry study. *NeuroImage: Clinical,* 17**,** 444-451.

BERNARDI, P., RASOLA, A., FORTE, M. & LIPPE, G. 2015. The mitochondrial permeability transition pore: channel formation by F-ATP synthase, integration in signal transduction, and role in pathophysiology. *Physiological reviews,* 95**,** 1111-1155.

BERNARDO, A., DE SIMONE, R., DE NUCCIO, C., VISENTIN, S. & MINGHETTI, L. 2013. The nuclear receptor peroxisome proliferator-activated receptor-γ promotes oligodendrocyte differentiation through mechanisms involving mitochondria and oscillatory Ca2+ waves. *Biol Chem,* 394**,** 1607-14.

BERTHELOOT, D., LATZ, E. & FRANKLIN, B. S. 2021. Necroptosis, pyroptosis and apoptosis: an intricate game of cell death. *Cell Mol Immunol,* 18**,** 1106-1121.

BEVAN, R. J., EVANS, R., GRIFFITHS, L., WATKINS, L. M., REES, M. I., MAGLIOZZI, R., ALLEN, I., MCDONNELL, G., KEE, R. & NAUGHTON, M. 2018. Meningeal inflammation and cortical demyelination in acute multiple sclerosis. *Annals of neurology,* 84**,** 829-842.

BHAT, A. H., DAR, K. B., ANEES, S., ZARGAR, M. A., MASOOD, A., SOFI, M. A. & GANIE, S. A. 2015. Oxidative stress, mitochondrial dysfunction and neurodegenerative diseases; a mechanistic insight. *Biomedicine & Pharmacotherapy,* 74**,** 101-110.

BITSCH, A., KUHLMANN, T., STADELMANN, C., LASSMANN, H., LUCCHINETTI, C. & BRÜCK, W. 2001. A longitudinal MRI study of histopathologically defined hypointense multiple sclerosis lesions. *Ann Neurol,* 49**,** 793-6.

BLAKEMORE, W. F. & FRANKLIN, R. J. 2008. Remyelination in experimental models of toxin-induced demyelination. *Curr Top Microbiol Immunol,* 318**,** 193-212.

BOISON, D., BÜSSOW, H., D'URSO, D., MÜLLER, H. W. & STOFFEL, W. 1995. Adhesive properties of proteolipid protein are responsible for the compaction of CNS myelin sheaths. *J Neurosci,* 15**,** 5502-13.

BOLTON, S., GREENWOOD, K., HAMILTON, N. & BUTT, A. M. 2006. Regulation of the astrocyte resting membrane potential by cyclic AMP and protein kinase A. *Glia,* 54**,** 316-28.

BONETTI, B. & RAINE, C. S. 1997. Multiple sclerosis: oligodendrocytes display cell death-related molecules in situ but do not undergo apoptosis. *Ann Neurol,* 42**,** 74-84.

BONORA, M., WIECKOWSKI, M. R., CHINOPOULOS, C., KEPP, O., KROEMER, G., GALLUZZI, L. & PINTON, P. 2015. Molecular mechanisms of cell death: central implication of ATP synthase in mitochondrial permeability transition. *Oncogene,* 34**,** 1475-1486.

BONVENTO, G. & BOLAÑOS, J. P. 2021. Astrocyte-neuron metabolic cooperation shapes brain activity. *Cell Metab,* 33**,** 1546-1564.

BOYA, P. 2012. Lysosomal function and dysfunction: mechanism and disease. *Antioxid Redox Signal,* 17**,** 766-74.

BOYA, P. & KROEMER, G. 2008. Lysosomal membrane permeabilization in cell death. *Oncogene,* 27**,** 6434-51.

BRENNER, C. & GRIMM, S. 2006. The permeability transition pore complex in cancer cell death. *Oncogene,* 25**,** 4744-4756.

BROOKS, D. J., LEENDERS, K. L., HEAD, G., MARSHALL, J., LEGG, N. J. & JONES, T. 1984. Studies on regional cerebral oxygen utilisation and cognitive function in multiple sclerosis. *J Neurol Neurosurg Psychiatry,* 47**,** 1182-91.

BROWN, A. M. & RANSOM, B. R. 2015. Astrocyte glycogen as an emergency fuel under conditions of glucose deprivation or intense neural activity. *Metab Brain Dis,* 30**,** 233-9.

BROWN, R. A., NARAYANAN, S. & ARNOLD, D. L. 2013. Segmentation of magnetization transfer ratio lesions for longitudinal analysis of demyelination and remyelination in multiple sclerosis. *Neuroimage,* 66**,** 103-9.

BRUSA, D., MIGLIORE, E., GARETTO, S., SIMONE, M. & MATERA, L. 2009. Immunogenicity of 56 degrees C and UVC-treated prostate cancer is associated with release of HSP70 and HMGB1 from necrotic cells. *Prostate,* 69**,** 1343-52.

BURGOYNE, L. A. 1999. The mechanisms of pyknosis: hypercondensation and death. *Exp Cell Res,* 248**,** 214-22.

BUTLER, A., HOFFMAN, P., SMIBERT, P., PAPALEXI, E. & SATIJA, R. 2018. Integrating single-cell transcriptomic data across different conditions, technologies, and species. *Nat Biotechnol,* 36**,** 411-420.

BUTT, A. M. & KALSI, A. 2006. Inwardly rectifying potassium channels (Kir) in central nervous system glia: a special role for Kir4.1 in glial functions. *J Cell Mol Med,* 10**,** 33-44.

BUTTON, R. W., ROBERTS, S. L., WILLIS, T. L., HANEMANN, C. O. & LUO, S. 2017. Accumulation of autophagosomes confers cytotoxicity. *J Biol Chem,* 292**,** 13599-13614.

BYUN, J. Y., YOON, C. H., AN, S., PARK, I. C., KANG, C. M., KIM, M. J. & LEE, S. J. 2009. The Rac1/MKK7/JNK pathway signals upregulation of Atg5 and subsequent autophagic cell death in response to oncogenic Ras. *Carcinogenesis,* 30**,** 1880-8.

CAI, W., ZHANG, K., LI, P., ZHU, L., XU, J., YANG, B., HU, X., LU, Z. & CHEN, J. 2017. Dysfunction of the neurovascular unit in ischemic stroke and neurodegenerative diseases: An aging effect. *Ageing Res Rev,* 34**,** 77-87.

CAI, Z., JITKAEW, S., ZHAO, J., CHIANG, H. C., CHOKSI, S., LIU, J., WARD, Y., WU, L. G. & LIU, Z. G. 2014. Plasma membrane translocation of trimerized MLKL protein is required for TNF-induced necroptosis. *Nat Cell Biol,* 16**,** 55-65.

CALDECOTT, K. W. 2008. Single-strand break repair and genetic disease. *Nature Reviews Genetics,* 9**,** 619-631.

CAMBRON, M., D'HAESELEER, M., LAUREYS, G., CLINCKERS, R., DEBRUYNE, J. & DE KEYSER, J. 2012. White-matter astrocytes, axonal energy metabolism, and axonal degeneration in multiple sclerosis. *J Cereb Blood Flow Metab,* 32**,** 413-24.

CASTELLAZZI, M., LAMBERTI, G., RESI, M. V., BALDI, E., CANIATTI, L. M., GALANTE, G., PERRI, P. & PUGLIATTI, M. 2019. Increased Levels of Endothelin-1 in Cerebrospinal Fluid Are a Marker of Poor Visual Recovery after Optic Neuritis in Multiple Sclerosis Patients. *Dis Markers,* 2019**,** 9320791.

CHABRIAT, H., JOUTEL, A., DICHGANS, M., TOURNIER-LASSERVE, E. & BOUSSER, M. G. 2009. Cadasil. *Lancet Neurol,* 8**,** 643-53.

CHAI, J., DU, C., WU, J. W., KYIN, S., WANG, X. & SHI, Y. 2000. Structural and biochemical basis of apoptotic activation by Smac/DIABLO. *Nature,* 406**,** 855-62.

CHANG, A., NISHIYAMA, A., PETERSON, J., PRINEAS, J. & TRAPP, B. D. 2000. NG2-positive oligodendrocyte progenitor cells in adult human brain and multiple sclerosis lesions. *J Neurosci,* 20**,** 6404-12.

CHANG, H. C. & GUARENTE, L. 2014. SIRT1 and other sirtuins in metabolism. *Trends Endocrinol Metab,* 25**,** 138-45.

CHANG, K. J., ZOLLINGER, D. R., SUSUKI, K., SHERMAN, D. L., MAKARA, M. A., BROPHY, P. J., COOPER, E. C., BENNETT, V., MOHLER, P. J. & RASBAND, M. N. 2014. Glial ankyrins facilitate paranodal axoglial junction assembly. *Nat Neurosci,* 17**,** 1673-81.

CHARD, D. T. & MILLER, D. H. 2016. What lies beneath grey matter atrophy in multiple sclerosis? *Brain,* 139**,** 7-10.

CHEN, L. C., WANG, L. J., TSANG, N. M., OJCIUS, D. M., CHEN, C. C., OUYANG, C. N., HSUEH, C., LIANG, Y., CHANG, K. P., CHEN, C. C. & CHANG, Y. S. 2012. Tumour inflammasome-derived IL-1β recruits neutrophils and improves local recurrence-free survival in EBV-induced nasopharyngeal carcinoma. *EMBO Mol Med,* 4**,** 1276-93.

CHEN, X., LI, J., KANG, R., KLIONSKY, D. J. & TANG, D. 2021a. Ferroptosis: machinery and regulation. *Autophagy,* 17**,** 2054-2081.

CHEN, X., YAO, N., LIN, Z. & WANG, Y. 2021b. Inhibition of the Immunoproteasome Subunit LMP7 Ameliorates Cerebral White Matter Demyelination Possibly via TGFβ/Smad Signaling. *Evid Based Complement Alternat Med,* 2021**,** 6426225.

CHEN, Y., BALASUBRAMANIYAN, V., PENG, J., HURLOCK, E. C., TALLQUIST, M., LI, J. & LU, Q. R. 2007. Isolation and culture of rat and mouse oligodendrocyte precursor cells. *Nature Protocols,* 2**,** 1044-1051.

CHENG, J., KORTE, N., NORTLEY, R., SETHI, H., TANG, Y. & ATTWELL, D. 2018. Targeting pericytes for therapeutic approaches to neurological disorders. *Acta Neuropathol,* 136**,** 507-523.

CHOI, H., PARK, H.-H., KOH, S.-H., CHOI, N.-Y., YU, H.-J., PARK, J., LEE, Y. J. & LEE, K.-Y. 2012. Coenzyme Q10 protects against amyloid beta-induced neuronal cell death by inhibiting oxidative stress and activating the P13K pathway. *Neurotoxicology,* 33**,** 85-90.

CONFAVREUX, C. & VUKUSIC, S. 2006. Age at disability milestones in multiple sclerosis. *Brain,* 129**,** 595-605.

CORNILLON, S., FOA, C., DAVOUST, J., BUONAVISTA, N., GROSS, J. D. & GOLSTEIN, P. 1994. Programmed cell death in Dictyostelium. *J Cell Sci,* 107 (Pt 10)**,** 2691-704.

CORREALE, J., GAITÁN, M. I., YSRRAELIT, M. C. & FIOL, M. P. 2016. Progressive multiple sclerosis: from pathogenic mechanisms to treatment. *Brain,* 140**,** 527-546.

CORREALE, J., GAITÁN, M. I., YSRRAELIT, M. C. & FIOL, M. P. 2017. Progressive multiple sclerosis: from pathogenic mechanisms to treatment. *Brain,* 140**,** 527-546.

CORREIA, S. C. & MOREIRA, P. I. 2010. Hypoxia-inducible factor 1: a new hope to counteract neurodegeneration? *J Neurochem,* 112**,** 1-12.

CORTES-CANTELI, M. & IADECOLA, C. 2020. Alzheimer's Disease and Vascular Aging: JACC Focus Seminar. *J Am Coll Cardiol,* 75**,** 942-951.

CRAELIUS, W., MIGDAL, M. W., LUESSENHOP, C. P., SUGAR, A. & MIHALAKIS, I. 1982. Iron deposits surrounding multiple sclerosis plaques. *Arch Pathol Lab Med,* 106**,** 397-9.

CREE, B. A. C., ARNOLD, D. L., CHATAWAY, J., CHITNIS, T., FOX, R. J., POZO RAMAJO, A., MURPHY, N. & LASSMANN, H. 2021. Secondary Progressive Multiple Sclerosis: New Insights. *Neurology,* 97**,** 378-388.

CUI, Q.-L., KUHLMANN, T., MIRON, V. E., LEONG, S. Y., FANG, J., GRIS, P., KENNEDY, T. E., ALMAZAN, G. & ANTEL, J. 2013. Oligodendrocyte Progenitor Cell Susceptibility to Injury in Multiple Sclerosis. *The American Journal of Pathology,* 183**,** 516-525.

CUI, Q. L., FRAGOSO, G., MIRON, V. E., DARLINGTON, P. J., MUSHYNSKI, W. E., ANTEL, J. & ALMAZAN, G. 2010. Response of Human Oligodendrocyte Progenitors to Growth Factors and Axon Signals. *Journal of Neuropathology & Experimental Neurology,* 69**,** 930-944.

CUI, Q. L., KHAN, D., RONE, M., V, T. S. R., JOHNSON, R. M., LIN, Y. H., BILODEAU, P. A., HALL, J. A., RODRIGUEZ, M., KENNEDY, T. E., LUDWIN, S. K. & ANTEL, J. P. 2017. Sublethal oligodendrocyte injury: A reversible condition in multiple sclerosis? *Ann Neurol,* 81**,** 811-824.

CUNNIFFE, N. & COLES, A. 2021. Promoting remyelination in multiple sclerosis. *J Neurol,* 268**,** 30-44.

D'HAESELEER, M., BEELEN, R., FIERENS, Y., CAMBRON, M., VANBINST, A. M., VERBORGH, C., DEMEY, J. & DE KEYSER, J. 2013. Cerebral hypoperfusion in multiple sclerosis is reversible and mediated by endothelin-1. *Proc Natl Acad Sci U S A,* 110**,** 5654-8.

D'HAESELEER, M., CAMBRON, M., VANOPDENBOSCH, L. & DE KEYSER, J. 2011. Vascular aspects of multiple sclerosis. *Lancet Neurol,* 10**,** 657-66.

D'HAESELEER, M., HOSTENBACH, S., PEETERS, I., SANKARI, S. E., NAGELS, G., DE KEYSER, J. & D'HOOGHE M, B. 2015. Cerebral hypoperfusion: a new pathophysiologic concept in multiple sclerosis? *J Cereb Blood Flow Metab,* 35**,** 1406-10.

D'ARCY, M. S. 2019. Cell death: a review of the major forms of apoptosis, necrosis and autophagy. *Cell Biology International,* 43**,** 582-592.

DANSEN, T. B. 2011. Forkhead Box O transcription factors: key players in redox signaling. Mary Ann Liebert, Inc. 140 Huguenot Street, 3rd Floor New Rochelle, NY 10801 USA.

DAS, S., WONG, R., RAJAPAKSE, N., MURPHY, E. & STEENBERGEN, C. 2008. Glycogen synthase kinase 3 inhibition slows mitochondrial adenine nucleotide transport and regulates voltage-dependent anion channel phosphorylation. *Circulation research,* 103**,** 983-991.

DASARI, S. K., BIALIK, S., LEVIN-ZAIDMAN, S., LEVIN-SALOMON, V., MERRILL, A. H., JR., FUTERMAN, A. H. & KIMCHI, A. 2017. Signalome-wide RNAi screen identifies GBA1 as a positive mediator of autophagic cell death. *Cell Death Differ,* 24**,** 1288-1302.

DAVID, K. K., ANDRABI, S. A., DAWSON, T. M. & DAWSON, V. L. 2009. Parthanatos, a messenger of death. *Front Biosci (Landmark Ed),* 14**,** 1116-28.

DAVIES, A. L., DESAI, R. A., BLOOMFIELD, P. S., MCINTOSH, P. R., CHAPPLE, K. J., LININGTON, C., FAIRLESS, R., DIEM, R., KASTI, M., MURPHY, M. P. & SMITH, K. J. 2013. Neurological deficits caused by tissue hypoxia in neuroinflammatory disease. *Ann Neurol,* 74**,** 815-25.

DAVSON, H. & OLDENDORF, W. H. 1967. Symposium on membrane transport. Transport in the central nervous system. *Proc R Soc Med,* 60**,** 326-9.

DE KEYSER, J., STEEN, C., MOSTERT, J. P. & KOCH, M. W. 2008. Hypoperfusion of the cerebral white matter in multiple sclerosis: possible mechanisms and pathophysiological significance. *J Cereb Blood Flow Metab,* 28**,** 1645-51.

DE KEYSER, J., WILCZAK, N., LETA, R. & STREETLAND, C. 1999. Astrocytes in multiple sclerosis lack beta-2 adrenergic receptors. *Neurology,* 53**,** 1628-33.

DE KEYSER, J., ZEINSTRA, E., MOSTERT, J. & WILCZAK, N. 2004. Beta 2-adrenoceptor involvement in inflammatory demyelination and axonal degeneration in multiple sclerosis. *Trends Pharmacol Sci,* 25**,** 67-71.

DE PAULA, M. L., CUI, Q. L., HOSSAIN, S., ANTEL, J. & ALMAZAN, G. 2014. The PTEN inhibitor bisperoxovanadium enhances myelination by amplifying IGF-1 signaling in rat and human oligodendrocyte progenitors. *Glia,* 62**,** 64-77.

DE VRIES, G. H. & BOULLERNE, A. I. 2010. Glial cell lines: an overview. *Neurochemical research,* 35**,** 1978-2000.

DECAUDIN, D., CASTEDO, M., NEMATI, F., BEURDELEY-THOMAS, A., DE PINIEUX, G., CARON, A., POUILLART, P., WIJDENES, J., ROUILLARD, D. & KROEMER, G. 2002. Peripheral benzodiazepine receptor ligands reverse apoptosis resistance of cancer cells in vitro and in vivo. *Cancer research,* 62**,** 1388-1393.

DEDONI, S., SCHERMA, M., CAMOGLIO, C., SIDDI, C., DAZZI, L., PULIGA, R., FRAU, J., COCCO, E. & FADDA, P. 2023. An overall view of the most common experimental models for multiple sclerosis. *Neurobiology of Disease,* 184**,** 106230.

DEHOUCK, M. P., MÉRESSE, S., DELORME, P., FRUCHART, J. C. & CECCHELLI, R. 1990. An easier, reproducible, and mass-production method to study the blood-brain barrier in vitro. *J Neurochem,* 54**,** 1798-801.

DENTON, D., AUNG-HTUT, M. T. & KUMAR, S. 2013. Developmentally programmed cell death in Drosophila. *Biochim Biophys Acta,* 1833**,** 3499-3506.

DENTON, D. & KUMAR, S. 2019. Autophagy-dependent cell death. *Cell Death Differ,* 26**,** 605-616.

DESAI, R. A., DAVIES, A. L., DEL ROSSI, N., TACHROUNT, M., DYSON, A., GUSTAVSON, B., KAYNEZHAD, P., MACKENZIE, L., VAN DER PUTTEN, M. A., MCELROY, D., SCHIZA, D., LININGTON, C., SINGER, M., HARVEY, A. R., TACHTSIDIS, I., GOLAY, X. & SMITH, K. J. 2020. Nimodipine Reduces Dysfunction and Demyelination in Models of Multiple Sclerosis. *Ann Neurol,* 88**,** 123-136.

DEY, S., BAIRD, T. D., ZHOU, D., PALAM, L. R., SPANDAU, D. F. & WEK, R. C. 2010. Both transcriptional regulation and translational control of ATF4 are central to the integrated stress response. *J Biol Chem,* 285**,** 33165-33174.

DHAOUADI, N., VITTO, V. A. M., PINTON, P., GALLUZZI, L. & MARCHI, S. 2023. Ca2+ signaling and cell death. *Cell Calcium,* 113**,** 102759.

DIENEL, G. A. 2019. Brain Glucose Metabolism: Integration of Energetics with Function. *Physiol Rev,* 99**,** 949-1045.

DIKALOVA, A. E., BIKINEYEVA, A. T., BUDZYN, K., NAZAREWICZ, R. R., MCCANN, L., LEWIS, W., HARRISON, D. G. & DIKALOV, S. I. 2010. Therapeutic targeting of mitochondrial superoxide in hypertension. *Circ Res,* 107**,** 106-16.

DIKIC, I. & ELAZAR, Z. 2018. Mechanism and medical implications of mammalian autophagy. *Nat Rev Mol Cell Biol,* 19**,** 349-364.
DIXON, S. J., LEMBERG, K. M., LAMPRECHT, M. R., SKOUTA, R., ZAITSEV, E. M., GLEASON, C. E., PATEL, D. N., BAUER, A. J., CANTLEY, A. M., YANG, W. S., MORRISON, B., 3RD & STOCKWELL, B. R. 2012. Ferroptosis: an iron-dependent form of nonapoptotic cell death. *Cell,* 149**,** 1060-72.
DOHERTY, J. & BAEHRECKE, E. H. 2018. Life, death and autophagy. *Nat Cell Biol,* 20**,** 1110-1117.
DONNELLY, N., GORMAN, A. M., GUPTA, S. & SAMALI, A. 2013. The eIF2α kinases: their structures and functions. *Cell Mol Life Sci,* 70**,** 3493-511.
DOSHI, A. & CHATAWAY, J. 2016. Multiple sclerosis, a treatable disease. *Clin Med (Lond),* 16**,** s53-s59.
DOUSSAU, F., DUPONT, J.-L., NEEL, D., SCHNEIDER, A., POULAIN, B. & BOSSU, J. L. 2017. Organotypic cultures of cerebellar slices as a model to investigate demyelinating disorders. *Expert Opinion on Drug Discovery,* 12**,** 1011-1022.
DUNCAN, I. D., RADCLIFF, A. B., HEIDARI, M., KIDD, G., AUGUST, B. K. & WIERENGA, L. A. 2018. The adult oligodendrocyte can participate in remyelination. *Proc Natl Acad Sci U S A,* 115**,** E11807-e11816.
DUTTA, R. & TRAPP, B. D. 2012. Gene expression profiling in multiple sclerosis brain. *Neurobiol Dis,* 45**,** 108-14.
EBRAHIMI, F., GIAGLIS, S., HAHN, S., BLUM, C. A., BAUMGARTNER, C., KUTZ, A., VAN BREDA, S. V., MUELLER, B., SCHUETZ, P., CHRIST-CRAIN, M. & HASLER, P. 2018. Markers of neutrophil extracellular traps predict adverse outcome in community-acquired pneumonia: secondary analysis of a randomised controlled trial. *Eur Respir J,* 51.
EDINGER, A. L. & THOMPSON, C. B. 2004. Death by design: apoptosis, necrosis and autophagy. *Curr Opin Cell Biol,* 16**,** 663-9.
EDWARDS, A. D. & MEHMET, H. 1996. Apoptosis in perinatal hypoxic-ischaemic cerebral damage. *Neuropathol Appl Neurobiol,* 22**,** 494-8.
EGAN, D. F., SHACKELFORD, D. B., MIHAYLOVA, M. M., GELINO, S., KOHNZ, R. A., MAIR, W., VASQUEZ, D. S., JOSHI, A., GWINN, D. M. & TAYLOR, R. 2011. Phosphorylation of ULK1 (hATG1) by AMP-activated protein kinase connects energy sensing to mitophagy. *Science,* 331**,** 456-461.
ELBAZ, B. & POPKO, B. 2019. Molecular Control of Oligodendrocyte Development. *Trends Neurosci,* 42**,** 263-277.
ELLIS, R. J., VAN DER VIES, S. M. & HEMMINGSEN, S. M. 1989. The molecular chaperone concept. *Biochem Soc Symp,* 55**,** 145-53.
ELMORE, S. 2007. Apoptosis: a review of programmed cell death. *Toxicol Pathol,* 35**,** 495-516.
ESMONDE-WHITE, C., YAQUBI, M., BILODEAU, P. A., CUI, Q. L., PERNIN, F., LAROCHELLE, C., GHADIRI, M., XU, Y. K. T., KENNEDY, T. E., HALL, J., HEALY, L. M. & ANTEL, J. P. 2019. Distinct Function-Related Molecular Profile of Adult Human A2B5-Positive Pre-Oligodendrocytes Versus Mature Oligodendrocytes. *J Neuropathol Exp Neurol,* 78**,** 468-479.
FAAL, T., PHAN, D. T., DAVTYAN, H., SCARFONE, V. M., VARADY, E., BLURTON-JONES, M., HUGHES, C. C. & INLAY, M. A. 2019. Induction of mesoderm and neural crest-derived pericytes from human pluripotent stem cells to study blood-brain barrier interactions. *Stem cell reports,* 12**,** 451-460.
FALKOWSKA, A., GUTOWSKA, I., GOSCHORSKA, M., NOWACKI, P., CHLUBEK, D. & BARANOWSKA-BOSIACKA, I. 2015. Energy Metabolism of the Brain, Including the Cooperation between Astrocytes and Neurons, Especially in the Context of Glycogen Metabolism. *Int J Mol Sci,* 16**,** 25959-81.
FATOKUN, A. A., DAWSON, V. L. & DAWSON, T. M. 2014. Parthanatos: mitochondrial-linked mechanisms and therapeutic opportunities. *Br J Pharmacol,* 171**,** 2000-16.
FEDOROFF, S. & RICHARDSON, A. 2008. *Protocols for neural cell culture*, Springer Science & Business Media.

FERNANDES, M. G. F., LUO, J. X. X., CUI, Q. L., PERLMAN, K., PERNIN, F., YAQUBI, M., HALL, J. A., DUDLEY, R., SROUR, M., COUTURIER, C. P., PETRECCA, K., LAROCHELLE, C., HEALY, L. M., STRATTON, J. A., KENNEDY, T. E. & ANTEL, J. P. 2021. Age-related injury responses of human oligodendrocytes to metabolic insults: link to BCL-2 and autophagy pathways. *Commun Biol,* 4**,** 20.

FINK, S. L. & COOKSON, B. T. 2005. Apoptosis, pyroptosis, and necrosis: mechanistic description of dead and dying eukaryotic cells. *Infect Immun,* 73**,** 1907-16.

FIORE, A., ZEITLER, L., RUSSIER, M., GROß, A., HILLER, M. K., PARKER, J. L., STIER, L., KÖCHER, T., NEWSTEAD, S. & MURRAY, P. J. 2022. Kynurenine importation by SLC7A11 propagates anti-ferroptotic signaling. *Mol Cell,* 82**,** 920-932.e7.

FISCHER, M. T., SHARMA, R., LIM, J. L., HAIDER, L., FRISCHER, J. M., DREXHAGE, J., MAHAD, D., BRADL, M., VAN HORSSEN, J. & LASSMANN, H. 2012. NADPH oxidase expression in active multiple sclerosis lesions in relation to oxidative tissue damage and mitochondrial injury. *Brain,* 135**,** 886-899.

FLOREY, O., KIM, S. E., SANDOVAL, C. P., HAYNES, C. M. & OVERHOLTZER, M. 2011. Autophagy machinery mediates macroendocytic processing and entotic cell death by targeting single membranes. *Nat Cell Biol,* 13**,** 1335-43.

FORMAN, H. J., ZHANG, H. & RINNA, A. 2009. Glutathione: overview of its protective roles, measurement, and biosynthesis. *Mol Aspects Med,* 30**,** 1-12.

FOUDA, A. Y., FAGAN, S. C. & ERGUL, A. 2019. Brain Vasculature and Cognition. *Arterioscler Thromb Vasc Biol,* 39**,** 593-602.

FRANDSEN, S. K., VISSING, M. & GEHL, J. 2020. A Comprehensive Review of Calcium Electroporation -A Novel Cancer Treatment Modality. *Cancers (Basel),* 12.

FRANKLIN, R. J., FFRENCH-CONSTANT, C., EDGAR, J. M. & SMITH, K. J. 2012. Neuroprotection and repair in multiple sclerosis. *Nat Rev Neurol,* 8**,** 624-34.

FRANKLIN, R. J. M. & FFRENCH-CONSTANT, C. 2017a. Regenerating CNS myelin - from mechanisms to experimental medicines. *Nat Rev Neurosci,* 18**,** 753-769.

FRANKLIN, R. J. M. & FFRENCH-CONSTANT, C. 2017b. Regenerating CNS myelin — from mechanisms to experimental medicines. *Nature Reviews Neuroscience,* 18**,** 753-769.

FREDMAN, P., MAGNANI, J. L., NIRENBERG, M. & GINSBURG, V. 1984. Monoclonal antibody A2B5 reacts with many gangliosides in neuronal tissue. *Arch Biochem Biophys,* 233**,** 661-6.

FRISCHER, J. M., WEIGAND, S. D., GUO, Y., KALE, N., PARISI, J. E., PIRKO, I., MANDREKAR, J., BRAMOW, S., METZ, I., BRÜCK, W., LASSMANN, H. & LUCCHINETTI, C. F. 2015. Clinical and pathological insights into the dynamic nature of the white matter multiple sclerosis plaque. *Ann Neurol,* 78**,** 710-21.

FUCHS, T. A., ABED, U., GOOSMANN, C., HURWITZ, R., SCHULZE, I., WAHN, V., WEINRAUCH, Y., BRINKMANN, V. & ZYCHLINSKY, A. 2007. Novel cell death program leads to neutrophil extracellular traps. *J Cell Biol,* 176**,** 231-41.

FUCIKOVA, J., KRALIKOVA, P., FIALOVA, A., BRTNICKY, T., ROB, L., BARTUNKOVA, J. & SPÍSEK, R. 2011. Human tumor cells killed by anthracyclines induce a tumor-specific immune response. *Cancer Res,* 71**,** 4821-33.

FUCIKOVA, J., MOSEROVA, I., TRUXOVA, I., HERMANOVA, I., VANCUROVA, I., PARTLOVA, S., FIALOVA, A., SOJKA, L., CARTRON, P. F., HOUSKA, M., ROB, L., BARTUNKOVA, J. & SPISEK, R. 2014. High hydrostatic pressure induces immunogenic cell death in human tumor cells. *Int J Cancer,* 135**,** 1165-77.

FUJII, C., KONDO, T., OCHI, H., OKADA, Y., HASHI, Y., ADACHI, T., SHIN-YA, M., MATSUMOTO, S., TAKAHASHI, R., NAKAGAWA, M. & MIZUNO, T. 2016. Altered T cell phenotypes associated with clinical relapse of multiple sclerosis patients receiving fingolimod therapy. *Sci Rep,* 6**,** 35314.

FÜNFSCHILLING, U., SUPPLIE, L. M., MAHAD, D., BORETIUS, S., SAAB, A. S., EDGAR, J., BRINKMANN, B. G., KASSMANN, C. M., TZVETANOVA, I. D., MÖBIUS, W., DIAZ, F., MEIJER, D., SUTER, U.,

HAMPRECHT, B., SEREDA, M. W., MORAES, C. T., FRAHM, J., GOEBBELS, S. & NAVE, K. A. 2012. Glycolytic oligodendrocytes maintain myelin and long-term axonal integrity. *Nature,* 485**,** 517-21.

GALLUZZI, L., BAEHRECKE, E. H., BALLABIO, A., BOYA, P., BRAVO-SAN PEDRO, J. M., CECCONI, F., CHOI, A. M., CHU, C. T., CODOGNO, P., COLOMBO, M. I., CUERVO, A. M., DEBNATH, J., DERETIC, V., DIKIC, I., ESKELINEN, E. L., FIMIA, G. M., FULDA, S., GEWIRTZ, D. A., GREEN, D. R., HANSEN, M., HARPER, J. W., JÄÄTTELÄ, M., JOHANSEN, T., JUHASZ, G., KIMMELMAN, A. C., KRAFT, C., KTISTAKIS, N. T., KUMAR, S., LEVINE, B., LOPEZ-OTIN, C., MADEO, F., MARTENS, S., MARTINEZ, J., MELENDEZ, A., MIZUSHIMA, N., MÜNZ, C., MURPHY, L. O., PENNINGER, J. M., PIACENTINI, M., REGGIORI, F., RUBINSZTEIN, D. C., RYAN, K. M., SANTAMBROGIO, L., SCORRANO, L., SIMON, A. K., SIMON, H. U., SIMONSEN, A., TAVERNARAKIS, N., TOOZE, S. A., YOSHIMORI, T., YUAN, J., YUE, Z., ZHONG, Q. & KROEMER, G. 2017a. Molecular definitions of autophagy and related processes. *Embo j,* 36**,** 1811-1836.

GALLUZZI, L., BRAVO-SAN PEDRO, J. M., BLOMGREN, K. & KROEMER, G. 2016. Autophagy in acute brain injury. *Nat Rev Neurosci,* 17**,** 467-84.

GALLUZZI, L., BUQUÉ, A., KEPP, O., ZITVOGEL, L. & KROEMER, G. 2017b. Immunogenic cell death in cancer and infectious disease. *Nature Reviews Immunology,* 17**,** 97-111.

GALLUZZI, L., VITALE, I., AARONSON, S. A., ABRAMS, J. M., ADAM, D., AGOSTINIS, P., ALNEMRI, E. S., ALTUCCI, L., AMELIO, I., ANDREWS, D. W., ANNICCHIARICO-PETRUZZELLI, M., ANTONOV, A. V., ARAMA, E., BAEHRECKE, E. H., BARLEV, N. A., BAZAN, N. G., BERNASSOLA, F., BERTRAND, M. J. M., BIANCHI, K., BLAGOSKLONNY, M. V., BLOMGREN, K., BORNER, C., BOYA, P., BRENNER, C., CAMPANELLA, M., CANDI, E., CARMONA-GUTIERREZ, D., CECCONI, F., CHAN, F. K. M., CHANDEL, N. S., CHENG, E. H., CHIPUK, J. E., CIDLOWSKI, J. A., CIECHANOVER, A., COHEN, G. M., CONRAD, M., CUBILLOS-RUIZ, J. R., CZABOTAR, P. E., D'ANGIOLELLA, V., DAWSON, T. M., DAWSON, V. L., DE LAURENZI, V., DE MARIA, R., DEBATIN, K.-M., DEBERARDINIS, R. J., DESHMUKH, M., DI DANIELE, N., DI VIRGILIO, F., DIXIT, V. M., DIXON, S. J., DUCKETT, C. S., DYNLACHT, B. D., EL-DEIRY, W. S., ELROD, J. W., FIMIA, G. M., FULDA, S., GARCÍA-SÁEZ, A. J., GARG, A. D., GARRIDO, C., GAVATHIOTIS, E., GOLSTEIN, P., GOTTLIEB, E., GREEN, D. R., GREENE, L. A., GRONEMEYER, H., GROSS, A., HAJNOCZKY, G., HARDWICK, J. M., HARRIS, I. S., HENGARTNER, M. O., HETZ, C., ICHIJO, H., JÄÄTTELÄ, M., JOSEPH, B., JOST, P. J., JUIN, P. P., KAISER, W. J., KARIN, M., KAUFMANN, T., KEPP, O., KIMCHI, A., KITSIS, R. N., KLIONSKY, D. J., KNIGHT, R. A., KUMAR, S., LEE, S. W., LEMASTERS, J. J., LEVINE, B., LINKERMANN, A., LIPTON, S. A., LOCKSHIN, R. A., LÓPEZ-OTÍN, C., LOWE, S. W., LUEDDE, T., LUGLI, E., MACFARLANE, M., MADEO, F., MALEWICZ, M., MALORNI, W., MANIC, G., et al. 2018. Molecular mechanisms of cell death: recommendations of the Nomenclature Committee on Cell Death 2018. *Cell Death & Differentiation,* 25**,** 486-541.

GALLUZZI, L., VITALE, I., WARREN, S., ADJEMIAN, S., AGOSTINIS, P., MARTINEZ, A. B., CHAN, T. A., COUKOS, G., DEMARIA, S., DEUTSCH, E., DRAGANOV, D., EDELSON, R. L., FORMENTI, S. C., FUCIKOVA, J., GABRIELE, L., GAIPL, U. S., GAMEIRO, S. R., GARG, A. D., GOLDEN, E., HAN, J., HARRINGTON, K. J., HEMMINKI, A., HODGE, J. W., HOSSAIN, D. M. S., ILLIDGE, T., KARIN, M., KAUFMAN, H. L., KEPP, O., KROEMER, G., LASARTE, J. J., LOI, S., LOTZE, M. T., MANIC, G., MERGHOUB, T., MELCHER, A. A., MOSSMAN, K. L., PROSPER, F., REKDAL, Ø., RESCIGNO, M., RIGANTI, C., SISTIGU, A., SMYTH, M. J., SPISEK, R., STAGG, J., STRAUSS, B. E., TANG, D., TATSUNO, K., VAN GOOL, S. W., VANDENABEELE, P., YAMAZAKI, T., ZAMARIN, D., ZITVOGEL, L., CESANO, A. & MARINCOLA, F. M. 2020. Consensus guidelines for the definition, detection and interpretation of immunogenic cell death. *J Immunother Cancer,* 8.

GARCÍA-PRAT, L., MARTÍNEZ-VICENTE, M., PERDIGUERO, E., ORTET, L., RODRÍGUEZ-UBREVA, J., REBOLLO, E., RUIZ-BONILLA, V., GUTARRA, S., BALLESTAR, E., SERRANO, A. L., SANDRI, M. &

MUÑOZ-CÁNOVES, P. 2016. Autophagy maintains stemness by preventing senescence. *Nature,* 529**,** 37-42.
GARCÍA, J. J., MORALES-RÍOS, E., CORTÉS-HERNÁNDEZ, P. & RODRÍGUEZ-ZAVALA, J. S. 2006. The inhibitor protein (IF1) promotes dimerization of the mitochondrial F1F0-ATP synthase. *Biochemistry,* 45**,** 12695-12703.
GARG, A. D., KRYSKO, D. V., VANDENABEELE, P. & AGOSTINIS, P. 2012. Hypericin-based photodynamic therapy induces surface exposure of damage-associated molecular patterns like HSP70 and calreticulin. *Cancer Immunol Immunother,* 61**,** 215-221.
GASCHLER, M. M. & STOCKWELL, B. R. 2017. Lipid peroxidation in cell death. *Biochem Biophys Res Commun,* 482**,** 419-425.
GE, Y., LAW, M., JOHNSON, G., HERBERT, J., BABB, J. S., MANNON, L. J. & GROSSMAN, R. I. 2005. Dynamic susceptibility contrast perfusion MR imaging of multiple sclerosis lesions: characterizing hemodynamic impairment and inflammatory activity. *AJNR Am J Neuroradiol,* 26**,** 1539-47.
GHATAK, N. R. 1992. Occurrence of oligodendrocytes within astrocytes in demyelinating lesions. *J Neuropathol Exp Neurol,* 51**,** 40-6.
GIACCI, M. K., BARTLETT, C. A., SMITH, N. M., IYER, K. S., TOOMEY, L. M., JIANG, H., GUAGLIARDO, P., KILBURN, M. R. & FITZGERALD, M. 2018. Oligodendroglia Are Particularly Vulnerable to Oxidative Damage after Neurotrauma In Vivo. *J Neurosci,* 38**,** 6491-6504.
GIANINAZZI, C., SCHILD, M., MÜLLER, N., LEIB, S., SIMON, F., NUNEZ, S., JOSS, P. & GOTTSTEIN, B. 2005. Organotypic slice cultures from rat brain tissue: a new approach for Naegleria fowleri CNS infection in vitro. *Parasitology,* 132**,** 797-804.
GLASS, H. C. 2018. Hypoxic-Ischemic Encephalopathy and Other Neonatal Encephalopathies. *Continuum (Minneap Minn),* 24**,** 57-71.
GLICK, D., BARTH, S. & MACLEOD, K. F. 2010. Autophagy: cellular and molecular mechanisms. *J Pathol,* 221**,** 3-12.
GLORIEUX, C. & CALDERON, P. B. 2017. Catalase, a remarkable enzyme: targeting the oldest antioxidant enzyme to find a new cancer treatment approach. *Biol Chem,* 398**,** 1095-1108.
GOLDEN, E. B., FRANCES, D., PELLICCIOTTA, I., DEMARIA, S., HELEN BARCELLOS-HOFF, M. & FORMENTI, S. C. 2014. Radiation fosters dose-dependent and chemotherapy-induced immunogenic cell death. *Oncoimmunology,* 3**,** e28518.
GOLDSCHMIDT, T., ANTEL, J., KÖNIG, F. B., BRÜCK, W. & KUHLMANN, T. 2009. Remyelination capacity of the MS brain decreases with disease chronicity. *Neurology,* 72**,** 1914-21.
GONZÁLEZ-PASTOR, J. E. 2011. Cannibalism: a social behavior in sporulating Bacillus subtilis. *FEMS Microbiol Rev,* 35**,** 415-24.
GORDAN, J. D., THOMPSON, C. B. & SIMON, M. C. 2007. HIF and c-Myc: sibling rivals for control of cancer cell metabolism and proliferation. *Cancer Cell,* 12**,** 108-13.
GORELICK, P. B., COUNTS, S. E. & NYENHUIS, D. 2016. Vascular cognitive impairment and dementia. *Biochim Biophys Acta,* 1862**,** 860-8.
GOW, A., SOUTHWOOD, C. M., LI, J. S., PARIALI, M., RIORDAN, G. P., BRODIE, S. E., DANIAS, J., BRONSTEIN, J. M., KACHAR, B. & LAZZARINI, R. A. 1999. CNS myelin and sertoli cell tight junction strands are absent in Osp/claudin-11 null mice. *Cell,* 99**,** 649-59.
GRAUMANN, U., REYNOLDS, R., STECK, A. J. & SCHAEREN-WIEMERS, N. 2003. Molecular changes in normal appearing white matter in multiple sclerosis are characteristic of neuroprotective mechanisms against hypoxic insult. *Brain Pathol,* 13**,** 554-73.
GREEN, D. R. & LLAMBI, F. 2015. Cell Death Signaling. *Cold Spring Harb Perspect Biol,* 7.

GRIFFITHS, I., KLUGMANN, M., ANDERSON, T., YOOL, D., THOMSON, C., SCHWAB, M. H., SCHNEIDER, A., ZIMMERMANN, F., MCCULLOCH, M., NADON, N. & NAVE, K. A. 1998. Axonal swellings and degeneration in mice lacking the major proteolipid of myelin. *Science,* 280**,** 1610-3.

GROSS, A. S. & GRAEF, M. 2020. Mechanisms of Autophagy in Metabolic Stress Response. *J Mol Biol,* 432**,** 28-52.

GRYZIK, M., ASPERTI, M., DENARDO, A., AROSIO, P. & POLI, M. 2021. NCOA4-mediated ferritinophagy promotes ferroptosis induced by erastin, but not by RSL3 in HeLa cells. *Biochim Biophys Acta Mol Cell Res,* 1868**,** 118913.

GUAN, B. J., KROKOWSKI, D., MAJUMDER, M., SCHMOTZER, C. L., KIMBALL, S. R., MERRICK, W. C., KOROMILAS, A. E. & HATZOGLOU, M. 2014. Translational control during endoplasmic reticulum stress beyond phosphorylation of the translation initiation factor eIF2α. *J Biol Chem,* 289**,** 12593-611.

GUNHANLAR, N., SHPAK, G., VAN DER KROEG, M., GOUTY-COLOMER, L., MUNSHI, S., LENDEMEIJER, B., GHAZVINI, M., DUPONT, C., HOOGENDIJK, W. & GRIBNAU, J. 2018. A simplified protocol for differentiation of electrophysiologically mature neuronal networks from human induced pluripotent stem cells. *Molecular psychiatry,* 23**,** 1336-1344.

GUNN, A. J. & THORESEN, M. 2019. Neonatal encephalopathy and hypoxic-ischemic encephalopathy. *Handb Clin Neurol,* 162**,** 217-237.

GUO, K., SEARFOSS, G., KROLIKOWSKI, D., PAGNONI, M., FRANKS, C., CLARK, K., YU, K. T., JAYE, M. & IVASHCHENKO, Y. 2001. Hypoxia induces the expression of the pro-apoptotic gene BNIP3. *Cell Death Differ,* 8**,** 367-76.

GUPTA, S. & KAPLAN, M. J. 2016. The role of neutrophils and NETosis in autoimmune and renal diseases. *Nat Rev Nephrol,* 12**,** 402-13.

HAIMOVICI, A., HÖFER, C., BADR, M. T., BAVAFAYE HAGHIGHI, E., AMER, T., BOERRIES, M., BRONSERT, P., GLAVYNSKYI, I., FANFONE, D., ICHIM, G., THILMANY, N., WEBER, A., BRUMMER, T., SPOHR, C., ÖLLINGER, R., JANSSEN, K.-P., RAD, R. & HÄCKER, G. 2022. Spontaneous activity of the mitochondrial apoptosis pathway drives chromosomal defects, the appearance of micronuclei and cancer metastasis through the Caspase-Activated DNAse. *Cell Death & Disease,* 13**,** 315.

HALL, C. N., REYNELL, C., GESSLEIN, B., HAMILTON, N. B., MISHRA, A., SUTHERLAND, B. A., O'FARRELL, F. M., BUCHAN, A. M., LAURITZEN, M. & ATTWELL, D. 2014. Capillary pericytes regulate cerebral blood flow in health and disease. *Nature,* 508**,** 55-60.

HALLIWELL, B. 2006. Oxidative stress and neurodegeneration: where are we now? *J Neurochem,* 97**,** 1634-58.

HAPPO, L., STRASSER, A. & CORY, S. 2012. BH3-only proteins in apoptosis at a glance. *J Cell Sci,* 125**,** 1081-7.

HARRIS, J. J. & ATTWELL, D. 2012. The energetics of CNS white matter. *J Neurosci,* 32**,** 356-71.

HARTUNG, H. P., GONSETTE, R., KÖNIG, N., KWIECINSKI, H., GUSEO, A., MORRISSEY, S. P., KRAPF, H. & ZWINGERS, T. 2002. Mitoxantrone in progressive multiple sclerosis: a placebo-controlled, double-blind, randomised, multicentre trial. *Lancet,* 360**,** 2018-25.

HASELOFF, R. F., BLASIG, I. E., BAUER, H. C. & BAUER, H. 2005. In search of the astrocytic factor(s) modulating blood-brain barrier functions in brain capillary endothelial cells in vitro. *Cell Mol Neurobiol,* 25**,** 25-39.

HAUFSCHILD, T., SHAW, S. G., KESSELRING, J. & FLAMMER, J. 2001. Increased endothelin-1 plasma levels in patients with multiple sclerosis. *J Neuroophthalmol,* 21**,** 37-8.

HAYASHI, Y., NOMURA, M., YAMAGISHI, S., HARADA, S., YAMASHITA, J. & YAMAMOTO, H. 1997. Induction of various blood-brain barrier properties in non-neural endothelial cells by close apposition to co-cultured astrocytes. *Glia,* 19**,** 13-26.

HAYES, G., PINTO, J., SPARKS, S. N., WANG, C., SURI, S. & BULTE, D. P. 2022. Vascular smooth muscle cell dysfunction in neurodegeneration. *Frontiers in Neuroscience,* 16**,** 1010164.

HAZE, K., YOSHIDA, H., YANAGI, H., YURA, T. & MORI, K. 1999. Mammalian transcription factor ATF6 is synthesized as a transmembrane protein and activated by proteolysis in response to endoplasmic reticulum stress. *Mol Biol Cell,* 10**,** 3787-99.

HE, M., DING, Y., CHU, C., TANG, J., XIAO, Q. & LUO, Z. G. 2016. Autophagy induction stabilizes microtubules and promotes axon regeneration after spinal cord injury. *Proc Natl Acad Sci U S A,* 113**,** 11324-11329.

HE, S., LIANG, Y., SHAO, F. & WANG, X. 2011. Toll-like receptors activate programmed necrosis in macrophages through a receptor-interacting kinase-3-mediated pathway. *Proc Natl Acad Sci U S A,* 108**,** 20054-9.

HEALY, L. M., PERRON, G., WON, S. Y., MICHELL-ROBINSON, M. A., REZK, A., LUDWIN, S. K., MOORE, C. S., HALL, J. A., BAR-OR, A. & ANTEL, J. P. 2016. MerTK Is a Functional Regulator of Myelin Phagocytosis by Human Myeloid Cells. *J Immunol,* 196**,** 3375-84.

HEILIG, R., DICK, M. S., SBORGI, L., MEUNIER, E., HILLER, S. & BROZ, P. 2018. The Gasdermin-D pore acts as a conduit for IL-1β secretion in mice. *Eur J Immunol,* 48**,** 584-592.

HELLEDAY, T., ESHTAD, S. & NIK-ZAINAL, S. 2014. Mechanisms underlying mutational signatures in human cancers. *Nature reviews genetics,* 15**,** 585-598.

HEß, K., STAROST, L., KIERAN, N. W., THOMAS, C., VINCENTEN, M. C. J., ANTEL, J., MARTINO, G., HUITINGA, I., HEALY, L. & KUHLMANN, T. 2020. Lesion stage-dependent causes for impaired remyelination in MS. *Acta Neuropathol,* 140**,** 359-375.

HETZ, C., ZHANG, K. & KAUFMAN, R. J. 2020. Mechanisms, regulation and functions of the unfolded protein response. *Nat Rev Mol Cell Biol,* 21**,** 421-438.

HIETAKANGAS, V., AHLSKOG, J. K., JAKOBSSON, A. M., HELLESUO, M., SAHLBERG, N. M., HOLMBERG, C. I., MIKHAILOV, A., PALVIMO, J. J., PIRKKALA, L. & SISTONEN, L. 2003. Phosphorylation of serine 303 is a prerequisite for the stress-inducible SUMO modification of heat shock factor 1. *Mol Cell Biol,* 23**,** 2953-68.

HILDEBRAND, C., REMAHL, S., PERSSON, H. & BJARTMAR, C. 1993. Myelinated nerve fibres in the CNS. *Prog Neurobiol,* 40**,** 319-84.

HINDMARSH, P. C. & GEERTSMA, K. 2017. Chapter 19 - Glucose and Cortisol. *In:* HINDMARSH, P. C. & GEERTSMA, K. (eds.) *Congenital Adrenal Hyperplasia.* Academic Press.

HITOSHI, Y., LORENS, J., KITADA, S. I., FISHER, J., LABARGE, M., RING, H. Z., FRANCKE, U., REED, J. C., KINOSHITA, S. & NOLAN, G. P. 1998. Toso, a cell surface, specific regulator of Fas-induced apoptosis in T cells. *Immunity,* 8**,** 461-71.

HOLLER, N., ZARU, R., MICHEAU, O., THOME, M., ATTINGER, A., VALITUTTI, S., BODMER, J. L., SCHNEIDER, P., SEED, B. & TSCHOPP, J. 2000. Fas triggers an alternative, caspase-8-independent cell death pathway using the kinase RIP as effector molecule. *Nat Immunol,* 1**,** 489-95.

HOLLIEN, J., LIN, J. H., LI, H., STEVENS, N., WALTER, P. & WEISSMAN, J. S. 2009. Regulated Ire1-dependent decay of messenger RNAs in mammalian cells. *J Cell Biol,* 186**,** 323-31.

HSU, H., XIONG, J. & GOEDDEL, D. V. 1995. The TNF receptor 1-associated protein TRADD signals cell death and NF-kappa B activation. *Cell,* 81**,** 495-504.

HU, C. J., WANG, L. Y., CHODOSH, L. A., KEITH, B. & SIMON, M. C. 2003. Differential roles of hypoxia-inducible factor 1alpha (HIF-1alpha) and HIF-2alpha in hypoxic gene regulation. *Mol Cell Biol,* 23**,** 9361-74.

HU, C. L., NYDES, M., SHANLEY, K. L., MORALES PANTOJA, I. E., HOWARD, T. A. & BIZZOZERO, O. A. 2019. Reduced expression of the ferroptosis inhibitor glutathione peroxidase-4 in multiple sclerosis and experimental autoimmune encephalomyelitis. *J Neurochem,* 148**,** 426-439.

HUANG, B., WU, P., BOWKER-KINLEY, M. M. & HARRIS, R. A. 2002. Regulation of pyruvate dehydrogenase kinase expression by peroxisome proliferator-activated receptor-alpha ligands, glucocorticoids, and insulin. *Diabetes,* 51**,** 276-83.

HUANG, H., CHEN, A., WANG, T., WANG, M., NING, X., HE, M., HU, Y., YUAN, L., LI, S., WANG, Q., LIU, H., CHEN, Z., REN, J. & SUN, Q. 2015. Detecting cell-in-cell structures in human tumor samples by E-cadherin/CD68/CD45 triple staining. *Oncotarget,* 6**,** 20278-87.

HUANG, P., CHEN, G., JIN, W., MAO, K., WAN, H. & HE, Y. 2022. Molecular Mechanisms of Parthanatos and Its Role in Diverse Diseases. *Int J Mol Sci,* 23.

HUGHES, E. G. & STOCKTON, M. E. 2021a. Premyelinating Oligodendrocytes: Mechanisms Underlying Cell Survival and Integration. *Front Cell Dev Biol,* 9**,** 714169.

HUGHES, E. G. & STOCKTON, M. E. 2021b. Premyelinating oligodendrocytes: Mechanisms underlying cell survival and integration. *Frontiers in Cell and Developmental Biology,* 9**,** 714169.

HUSEBY, E. S., LIGGITT, D., BRABB, T., SCHNABEL, B., OHLÉN, C. & GOVERMAN, J. 2001. A pathogenic role for myelin-specific CD8(+) T cells in a model for multiple sclerosis. *J Exp Med,* 194**,** 669-76.

IADECOLA, C. 2017. The Neurovascular Unit Coming of Age: A Journey through Neurovascular Coupling in Health and Disease. *Neuron,* 96**,** 17-42.

IADECOLA, C., DUERING, M., HACHINSKI, V., JOUTEL, A., PENDLEBURY, S. T., SCHNEIDER, J. A. & DICHGANS, M. 2019. Vascular Cognitive Impairment and Dementia: JACC Scientific Expert Panel. *J Am Coll Cardiol,* 73**,** 3326-3344.

INOKI, K., ZHU, T. & GUAN, K.-L. 2003. TSC2 mediates cellular energy response to control cell growth and survival. *Cell,* 115**,** 577-590.

ITOH, T., ITOH, A. & PLEASURE, D. 2003. Bcl-2-related protein family gene expression during oligodendroglial differentiation. *J Neurochem,* 85**,** 1500-12.

IZZO, V., BRAVO-SAN PEDRO, J. M., SICA, V., KROEMER, G. & GALLUZZI, L. 2016. Mitochondrial Permeability Transition: New Findings and Persisting Uncertainties. *Trends in Cell Biology,* 26**,** 655-667.

JACKSON, R. J., MELTZER, J. C., NGUYEN, H., COMMINS, C., BENNETT, R. E., HUDRY, E. & HYMAN, B. T. 2022. APOE4 derived from astrocytes leads to blood-brain barrier impairment. *Brain,* 145**,** 3582-3593.

JÄKEL, S., AGIRRE, E., MENDANHA FALCÃO, A., VAN BRUGGEN, D., LEE, K. W., KNUESEL, I., MALHOTRA, D., FFRENCH-CONSTANT, C., WILLIAMS, A. & CASTELO-BRANCO, G. 2019. Altered human oligodendrocyte heterogeneity in multiple sclerosis. *Nature,* 566**,** 543-547.

JAKIMOVSKI, D., GIBNEY, B. L., MARR, K., RAMASAMY, D. P., DWYER, M. G., BERGSLAND, N., WEINSTOCK-GUTTMAN, B., RAMANATHAN, M. & ZIVADINOV, R. 2022. Lower cerebral arterial blood flow is associated with greater serum neurofilament light chain levels in multiple sclerosis patients. *Eur J Neurol,* 29**,** 2299-2308.

JAMANN, H., CUI, Q. L., DESU, H. L., PERNIN, F., TASTET, O., HALAWEH, A., FARZAM-KIA, N., MAMANE, V. H., OUÉDRAOGO, O., CLERET-BUHOT, A., DAIGNEAULT, A., BALTHAZARD, R., KLEMENT, W., LEMAÎTRE, F., ARBOUR, N., ANTEL, J., STRATTON, J. A. & LAROCHELLE, C. 2022. Contact-Dependent Granzyme B-Mediated Cytotoxicity of Th17-Polarized Cells Toward Human Oligodendrocytes. *Front Immunol,* 13**,** 850616.

JANTSCHITSCH, C. & TRAUTINGER, F. 2003. Heat shock and UV-B-induced DNA damage and mutagenesis in skin. *Photochemical & Photobiological Sciences,* 2**,** 899-903.

JEON, S. M. 2016. Regulation and function of AMPK in physiology and diseases. *Exp Mol Med,* 48**,** e245.

JHELUM, P., SANTOS-NOGUEIRA, E., TEO, W., HAUMONT, A., LENOËL, I., STYS, P. K. & DAVID, S. 2020. Ferroptosis Mediates Cuprizone-Induced Loss of Oligodendrocytes and Demyelination. *J Neurosci,* 40**,** 9327-9341.

JOHN, G. R. 2012. Investigation of astrocyte - oligodendrocyte interactions in human cultures. *Methods Mol Biol,* 814**,** 401-14.
KAELIN, W. G., JR. 2005. ROS: really involved in oxygen sensing. *Cell Metab,* 1**,** 357-8.
KAELIN, W. G., JR. & RATCLIFFE, P. J. 2008. Oxygen sensing by metazoans: the central role of the HIF hydroxylase pathway. *Mol Cell,* 30**,** 393-402.
KALE, J., OSTERLUND, E. J. & ANDREWS, D. W. 2018. BCL-2 family proteins: changing partners in the dance towards death. *Cell Death Differ,* 25**,** 65-80.
KAPLAN, L., CHOW, B. W. & GU, C. 2020. Neuronal regulation of the blood-brain barrier and neurovascular coupling. *Nat Rev Neurosci,* 21**,** 416-432.
KAPPOS, L., BAR-OR, A., CREE, B. A. C., FOX, R. J., GIOVANNONI, G., GOLD, R., VERMERSCH, P., ARNOLD, D. L., ARNOULD, S., SCHERZ, T., WOLF, C., WALLSTRÖM, E. & DAHLKE, F. 2018. Siponimod versus placebo in secondary progressive multiple sclerosis (EXPAND): a double-blind, randomised, phase 3 study. *Lancet,* 391**,** 1263-1273.
KARCH, J., KWONG, J. Q., BURR, A. R., SARGENT, M. A., ELROD, J. W., PEIXOTO, P. M., MARTINEZ-CABALLERO, S., OSINSKA, H., CHENG, E. H. & ROBBINS, J. 2013. Bax and Bak function as the outer membrane component of the mitochondrial permeability pore in regulating necrotic cell death in mice. *elife,* 2**,** e00772.
KARIM, S. A., BARRIE, J. A., MCCULLOCH, M. C., MONTAGUE, P., EDGAR, J. M., IDEN, D. L., ANDERSON, T. J., NAVE, K. A., GRIFFITHS, I. R. & MCLAUGHLIN, M. 2010. PLP/DM20 expression and turnover in a transgenic mouse model of Pelizaeus-Merzbacher disease. *Glia,* 58**,** 1727-38.
KARIM, S. A., BARRIE, J. A., MCCULLOCH, M. C., MONTAGUE, P., EDGAR, J. M., KIRKHAM, D., ANDERSON, T. J., NAVE, K. A., GRIFFITHS, I. R. & MCLAUGHLIN, M. 2007. PLP overexpression perturbs myelin protein composition and myelination in a mouse model of Pelizaeus-Merzbacher disease. *Glia,* 55**,** 341-351.
KARIN, M. 2006. Nuclear factor-κB in cancer development and progression. *Nature,* 441**,** 431-436.
KARMAKAR, A., DAS, A. K., GHOSH, N. & SIL, P. C. 2022. Chapter2.7 - Superoxide dismutase. *In:* NABAVI, S. M. & SILVA, A. S. (eds.) *Antioxidants Effects in Health.* Elsevier.
KASHIMA, T., TIU, S. N., MERRILL, J. E., VINTERS, H. V., DAWSON, G. & CAMPAGNONI, A. T. 1993. Expression of oligodendrocyte-associated genes in cell lines derived from human gliomas and neuroblastomas. *Cancer Research,* 53**,** 170-175.
KAUFMAN, R. J. 2002. Orchestrating the unfolded protein response in health and disease. *The Journal of Clinical Investigation,* 110**,** 1389-1398.
KELLY, B. D., HACKETT, S. F., HIROTA, K., OSHIMA, Y., CAI, Z., BERG-DIXON, S., ROWAN, A., YAN, Z., CAMPOCHIARO, P. A. & SEMENZA, G. L. 2003. Cell type-specific regulation of angiogenic growth factor gene expression and induction of angiogenesis in nonischemic tissue by a constitutively active form of hypoxia-inducible factor 1. *Circ Res,* 93**,** 1074-81.
KERMODE, A. G., THOMPSON, A. J., TOFTS, P., MACMANUS, D. G., KENDALL, B. E., KINGSLEY, D. P., MOSELEY, I. F., RUDGE, P. & MCDONALD, W. I. 1990. Breakdown of the blood-brain barrier precedes symptoms and other MRI signs of new lesions in multiple sclerosis. Pathogenetic and clinical implications. *Brain,* 113 (Pt 5)**,** 1477-89.
KHORCHID, A., FRAGOSO, G., SHORE, G. & ALMAZAN, G. 2002. Catecholamine-induced oligodendrocyte cell death in culture is developmentally regulated and involves free radical generation and differential activation of caspase-3. *Glia,* 40**,** 283-99.
KI, Y.-W., PARK, J. H., LEE, J. E., SHIN, I. C. & KOH, H. C. 2013. JNK and p38 MAPK regulate oxidative stress and the inflammatory response in chlorpyrifos-induced apoptosis. *Toxicology letters,* 218**,** 235-245.
KIST, M. & VUCIC, D. 2021. Cell death pathways: intricate connections and disease implications. *Embo j,* 40**,** e106700.

KITADA, M. & ROWITCH, D. H. 2006. Transcription factor co-expression patterns indicate heterogeneity of oligodendroglial subpopulations in adult spinal cord. *Glia,* 54**,** 35-46.
KLEIN, J. A. & ACKERMAN, S. L. 2003. Oxidative stress, cell cycle, and neurodegeneration. *The Journal of clinical investigation,* 111**,** 785-793.
KLIMOVA, T. & CHANDEL, N. S. 2008. Mitochondrial complex III regulates hypoxic activation of HIF. *Cell Death & Differentiation,* 15**,** 660-666.
KLINE, M. P., RAJKUMAR, S. V., TIMM, M. M., KIMLINGER, T. K., HAUG, J. L., LUST, J. A., GREIPP, P. R. & KUMAR, S. 2007. ABT-737, an inhibitor of Bcl-2 family proteins, is a potent inducer of apoptosis in multiple myeloma cells. *Leukemia,* 21**,** 1549-60.
KNOT, H. J. & NELSON, M. T. 1998. Regulation of arterial diameter and wall [Ca2+] in cerebral arteries of rat by membrane potential and intravascular pressure. *J Physiol,* 508 (Pt 1)**,** 199-209.
KOINZER, S., REINECKE, K., HERDEGEN, T., ROIDER, J. & KLETTNER, A. 2015. Oxidative stress induces biphasic ERK1/2 activation in the RPE with distinct effects on cell survival at early and late activation. *Current eye research,* 40**,** 853-857.
KOLAPPAN, S., SHEN, D. L., MOSI, R., SUN, J., MCEACHERN, E. J., VOCADLO, D. J. & CRAIG, L. 2015. Structures of lactate dehydrogenase A (LDHA) in apo, ternary and inhibitor-bound forms. *Acta Crystallogr D Biol Crystallogr,* 71**,** 185-95.
KØNIG, S. M., RISSLER, V., TERKELSEN, T., LAMBRUGHI, M. & PAPALEO, E. 2019. Alterations of the interactome of Bcl-2 proteins in breast cancer at the transcriptional, mutational and structural level. *PLoS Comput Biol,* 15**,** e1007485.
KOPP, C. W., SIEGEL, J. B., HANCOCK, W. W., ANRATHER, J., WINKLER, H., GECZY, C. L., KACZMAREK, E., BACH, F. H. & ROBSON, S. C. 1997. Effect of porcine endothelial tissue factor pathway inhibitor on human coagulation factors. *Transplantation,* 63**,** 749-58.
KORBELIK, M., ZHANG, W. & MERCHANT, S. 2011. Involvement of damage-associated molecular patterns in tumor response to photodynamic therapy: surface expression of calreticulin and high-mobility group box-1 release. *Cancer Immunol Immunother,* 60**,** 1431-7.
KOTTER, M. R., LI, W. W., ZHAO, C. & FRANKLIN, R. J. 2006. Myelin impairs CNS remyelination by inhibiting oligodendrocyte precursor cell differentiation. *J Neurosci,* 26**,** 328-32.
KRAJCOVIC, M., JOHNSON, N. B., SUN, Q., NORMAND, G., HOOVER, N., YAO, E., RICHARDSON, A. L., KING, R. W., CIBAS, E. S., SCHNITT, S. J., BRUGGE, J. S. & OVERHOLTZER, M. 2011. A non-genetic route to aneuploidy in human cancers. *Nat Cell Biol,* 13**,** 324-30.
KRISHNA, S. & OVERHOLTZER, M. 2016. Mechanisms and consequences of entosis. *Cell Mol Life Sci,* 73**,** 2379-86.
KROEMER, G., GALASSI, C., ZITVOGEL, L. & GALLUZZI, L. 2022. Immunogenic cell stress and death. *Nat Immunol,* 23**,** 487-500.
KROEMER, G., GALLUZZI, L., KEPP, O. & ZITVOGEL, L. 2013. Immunogenic cell death in cancer therapy. *Annu Rev Immunol,* 31**,** 51-72.
KUGLER, E. C., GREENWOOD, J. & MACDONALD, R. B. 2021. The "Neuro-Glial-Vascular" Unit: The Role of Glia in Neurovascular Unit Formation and Dysfunction. *Front Cell Dev Biol,* 9**,** 732820.
KUHLE, J., HARDMEIER, M., DISANTO, G., GUGLETA, K., ECSEDI, M., LIENERT, C., AMATO, M. P., BAUM, K., BUTTMANN, M., BAYAS, A., BRASSAT, D., BROCHET, B., CONFAVREUX, C., EDAN, G., FÄRKKILÄ, M., FREDRIKSON, S., FRONTONI, M., D'HOOGHE, M., HUTCHINSON, M., DE KEYSER, J., KIESEIER, B. C., KÜMPFEL, T., RIO, J., POLMAN, C., ROULLET, E., STOLZ, C., VASS, K., WANDINGER, K. P. & KAPPOS, L. 2016. A 10-year follow-up of the European multicenter trial of interferon β-1b in secondary-progressive multiple sclerosis. *Mult Scler,* 22**,** 533-43.
KUHLMANN, T., LUDWIN, S., PRAT, A., ANTEL, J., BRÜCK, W. & LASSMANN, H. 2017. An updated histological classification system for multiple sclerosis lesions. *Acta Neuropathol,* 133**,** 13-24.

KUHLMANN, T., MIRON, V., CUI, Q., WEGNER, C., ANTEL, J. & BRÜCK, W. 2008. Differentiation block of oligodendroglial progenitor cells as a cause for remyelination failure in chronic multiple sclerosis. *Brain,* 131**,** 1749-58.

KUMAR, A. M., REDDI, H. V., KUNG, A. Y., DAL CANTO, M. & LIPTON, H. L. 2004. Virus persistence in an animal model of multiple sclerosis requires virion attachment to sialic acid coreceptors. *Journal of virology,* 78**,** 8860-8867.

KWON, E. E. & PRINEAS, J. W. 1994. Blood-brain barrier abnormalities in longstanding multiple sclerosis lesions. An immunohistochemical study. *J Neuropathol Exp Neurol,* 53**,** 625-36.

LAMB, Y. N. 2022. Ocrelizumab: A Review in Multiple Sclerosis. *Drugs,* 82**,** 323-334.

LASSMANN, H. 2003. Hypoxia-like tissue injury as a component of multiple sclerosis lesions. *J Neurol Sci,* 206**,** 187-91.

LASSMANN, H. 2018. Pathogenic Mechanisms Associated With Different Clinical Courses of Multiple Sclerosis. *Front Immunol,* 9**,** 3116.

LASSMANN, H. & VAN HORSSEN, J. 2011. The molecular basis of neurodegeneration in multiple sclerosis. *FEBS letters,* 585**,** 3715-3723.

LASSMANN, H. & VAN HORSSEN, J. 2016. Oxidative stress and its impact on neurons and glia in multiple sclerosis lesions. *Biochim Biophys Acta,* 1862**,** 506-10.

LASSMANN, H., VAN HORSSEN, J. & MAHAD, D. 2012. Progressive multiple sclerosis: pathology and pathogenesis. *Nat Rev Neurol,* 8**,** 647-56.

LASTER, S. M., WOOD, J. G. & GOODING, L. R. 1988. Tumor necrosis factor can induce both apoptic and necrotic forms of cell lysis. *J Immunol,* 141**,** 2629-34.

LAW, M., SAINDANE, A. M., GE, Y., BABB, J. S., JOHNSON, G., MANNON, L. J., HERBERT, J. & GROSSMAN, R. I. 2004a. Microvascular abnormality in relapsing-remitting multiple sclerosis: perfusion MR imaging findings in normal-appearing white matter. *Radiology,* 231**,** 645-52.

LAW, M., SAINDANE, A. M., GE, Y., BABB, J. S., JOHNSON, G., MANNON, L. J., HERBERT, J. & GROSSMAN, R. I. 2004b. Microvascular abnormality in relapsing-remitting multiple sclerosis: perfusion MR imaging findings in normal-appearing white matter. *Radiology,* 231**,** 645-652.

LEE, H. & PAIK, S. G. 2006. Regulation of BNIP3 in normal and cancer cells. *Mol Cells,* 21**,** 1-6.

LEE, I. H. 2019. Mechanisms and disease implications of sirtuin-mediated autophagic regulation. *Exp Mol Med,* 51**,** 1-11.

LEE, S., LEACH, M. K., REDMOND, S. A., CHONG, S. Y., MELLON, S. H., TUCK, S. J., FENG, Z. Q., COREY, J. M. & CHAN, J. R. 2012a. A culture system to study oligodendrocyte myelination processes using engineered nanofibers. *Nat Methods,* 9**,** 917-22.

LEE, Y., MORRISON, B. M., LI, Y., LENGACHER, S., FARAH, M. H., HOFFMAN, P. N., LIU, Y., TSINGALIA, A., JIN, L., ZHANG, P. W., PELLERIN, L., MAGISTRETTI, P. J. & ROTHSTEIN, J. D. 2012b. Oligodendroglia metabolically support axons and contribute to neurodegeneration. *Nature,* 487**,** 443-8.

LEONG, S. Y., RAO, V. T., BIN, J. M., GRIS, P., SANGARALINGAM, M., KENNEDY, T. E. & ANTEL, J. P. 2014. Heterogeneity of oligodendrocyte progenitor cells in adult human brain. *Ann Clin Transl Neurol,* 1**,** 272-83.

LESSENE, G., CZABOTAR, P. E., SLEEBS, B. E., ZOBEL, K., LOWES, K. N., ADAMS, J. M., BAELL, J. B., COLMAN, P. M., DESHAYES, K., FAIRBROTHER, W. J., FLYGARE, J. A., GIBBONS, P., KERSTEN, W. J., KULASEGARAM, S., MOSS, R. M., PARISOT, J. P., SMITH, B. J., STREET, I. P., YANG, H., HUANG, D. C. & WATSON, K. G. 2013. Structure-guided design of a selective BCL-X(L) inhibitor. *Nat Chem Biol,* 9**,** 390-7.

LEUNG, A. W., VARANYUWATANA, P. & HALESTRAP, A. P. 2008. The mitochondrial phosphate carrier interacts with cyclophilin D and may play a key role in the permeability transition. *Journal of Biological Chemistry,* 283**,** 26312-26323.

LEVIN, B. E., MAGNAN, C., DUNN-MEYNELL, A. & LE FOLL, C. 2011. Metabolic sensing and the brain: who, what, where, and how? *Endocrinology,* 152**,** 2552-7.
LI, J., CAO, F., YIN, H.-L., HUANG, Z.-J., LIN, Z.-T., MAO, N., SUN, B. & WANG, G. 2020. Ferroptosis: past, present and future. *Cell Death & Disease,* 11**,** 88.
LI, S. & SHENG, Z. H. 2022. Energy matters: presynaptic metabolism and the maintenance of synaptic transmission. *Nat Rev Neurosci,* 23**,** 4-22.
LI, Y., SUN, X. & DEY, S. K. 2015. Entosis allows timely elimination of the luminal epithelial barrier for embryo implantation. *Cell Rep,* 11**,** 358-65.
LIANG, D., MINIKES, A. M. & JIANG, X. 2022. Ferroptosis at the intersection of lipid metabolism and cellular signaling. *Mol Cell,* 82**,** 2215-2227.
LILLIG, C. H. & HOLMGREN, A. 2007. Thioredoxin and related molecules–from biology to health and disease. *Antioxidants & redox signaling,* 9**,** 25-47.
LIM, J. Y., GERBER, S. A., MURPHY, S. P. & LORD, E. M. 2014. Type I interferons induced by radiation therapy mediate recruitment and effector function of CD8(+) T cells. *Cancer Immunol Immunother,* 63**,** 259-71.
LIN, M. T. & BEAL, M. F. 2006. Mitochondrial dysfunction and oxidative stress in neurodegenerative diseases. *Nature,* 443**,** 787-795.
LIPTON, J. O. & SAHIN, M. 2014. The neurology of mTOR. *Neuron,* 84**,** 275-91.
LIPTON, S. A. 1998. Neuronal injury associated with HIV-1: approaches to treatment. *Annu Rev Pharmacol Toxicol,* 38**,** 159-77.
LIU, D. & XU, Y. 2011. p53, oxidative stress, and aging. *Antioxidants & redox signaling,* 15**,** 1669-1678.
LIU, S. & LIN, Z. 2022. Vascular Smooth Muscle Cells Mechanosensitive Regulators and Vascular Remodeling. *J Vasc Res,* 59**,** 90-113.
LIU, Y., SHOJI-KAWATA, S., SUMPTER, R. M., JR., WEI, Y., GINET, V., ZHANG, L., POSNER, B., TRAN, K. A., GREEN, D. R., XAVIER, R. J., SHAW, S. Y., CLARKE, P. G., PUYAL, J. & LEVINE, B. 2013. Autosis is a Na+,K+-ATPase-regulated form of cell death triggered by autophagy-inducing peptides, starvation, and hypoxia-ischemia. *Proc Natl Acad Sci U S A,* 110**,** 20364-71.
LOBO, V., PATIL, A., PHATAK, A. & CHANDRA, N. 2010. Free radicals, antioxidants and functional foods: Impact on human health. *Pharmacogn Rev,* 4**,** 118-26.
LOCKSHIN, R. A. & ZAKERI, Z. 2004. Apoptosis, autophagy, and more. *Int J Biochem Cell Biol,* 36**,** 2405-19.
LOCKSLEY, R. M., KILLEEN, N. & LENARDO, M. J. 2001. The TNF and TNF receptor superfamilies: integrating mammalian biology. *Cell,* 104**,** 487-501.
LOEFFLER, M., DAUGAS, E., SUSIN, S. A., ZAMZAMI, N., METIVIER, D., NIEMINEN, A. L., BROTHERS, G., PENNINGER, J. M. & KROEMER, G. 2001. Dominant cell death induction by extramitochondrially targeted apoptosis-inducing factor. *Faseb j,* 15**,** 758-67.
LOPES, F. M., BRISTOT, I. J., DA MOTTA, L. L., PARSONS, R. B. & KLAMT, F. 2017. Mimicking Parkinson's disease in a dish: merits and pitfalls of the most commonly used dopaminergic in vitro models. *NeuroMolecular Medicine,* 19**,** 241-255.
LŐRINCZ, P. & JUHÁSZ, G. 2020. Autophagosome-Lysosome Fusion. *J Mol Biol,* 432**,** 2462-2482.
LOUIS, J., MAGAL, E., MUIR, D., MANTHORPE, M. & VARON, S. 1992. CG-4, a new bipotential glial cell line from rat brain, is capable of differentiating in vitro into either mature oligodendrocytes or type-2 astrocytes. *Journal of neuroscience research,* 31**,** 193-204.
LOVE, M. I., HUBER, W. & ANDERS, S. 2014. Moderated estimation of fold change and dispersion for RNA-seq data with DESeq2. *Genome Biology,* 15**,** 550.
LOVE, S. 2006. Demyelinating diseases. *J Clin Pathol,* 59**,** 1151-9.
LUCCHINETTI, C. F., BRUCK, W. & LASSMANN, H. 2004. Evidence for pathogenic heterogeneity in multiple sclerosis. *Ann Neurol,* 56**,** 308.

LUCHETTI, S., FRANSEN, N. L., VAN EDEN, C. G., RAMAGLIA, V., MASON, M. & HUITINGA, I. 2018. Progressive multiple sclerosis patients show substantial lesion activity that correlates with clinical disease severity and sex: a retrospective autopsy cohort analysis. *Acta Neuropathol,* 135**,** 511-528.

LUDWIN, S. K. & JOHNSON, E. S. 1981. Evidence for a "dying-back" gliopathy in demyelinating disease. *Ann Neurol,* 9**,** 301-5.

LUNN, K. F., BAAS, P. W. & DUNCAN, I. D. 1997. Microtubule organization and stability in the oligodendrocyte. *J Neurosci,* 17**,** 4921-32.

LUO, J. X. X., CUI, Q. L., YAQUBI, M., HALL, J. A., DUDLEY, R., SROUR, M., ADDOUR, N., JAMANN, H., LAROCHELLE, C., BLAIN, M., HEALY, L. M., STRATTON, J. A., SONNEN, J. A., KENNEDY, T. E. & ANTEL, J. P. 2022. Human Oligodendrocyte Myelination Potential; Relation to Age and Differentiation. *Ann Neurol,* 91**,** 178-191.

LYCKE, J., WIKKELSÖ, C., BERGH, A. C., JACOBSSON, L. & ANDERSEN, O. 1993. Regional cerebral blood flow in multiple sclerosis measured by single photon emission tomography with technetium-99m hexamethylpropyleneamine oxime. *Eur Neurol,* 33**,** 163-7.

LYNCH, G. & BAUDRY, M. 1987. Brain spectrin, calpain and long-term changes in synaptic efficacy. *Brain Res Bull,* 18**,** 809-15.

MADHAVAN, M., NEVIN, Z. S., SHICK, H. E., GARRISON, E., CLARKSON-PAREDES, C., KARL, M., CLAYTON, B. L., FACTOR, D. C., ALLAN, K. C. & BARBAR, L. 2018. Induction of myelinating oligodendrocytes in human cortical spheroids. *Nature methods,* 15**,** 700-706.

MAHAD, D. H., TRAPP, B. D. & LASSMANN, H. 2015. Pathological mechanisms in progressive multiple sclerosis. *Lancet Neurol,* 14**,** 183-93.

MAHON, P. C., HIROTA, K. & SEMENZA, G. L. 2001. FIH-1: a novel protein that interacts with HIF-1alpha and VHL to mediate repression of HIF-1 transcriptional activity. *Genes Dev,* 15**,** 2675-86.

MAHONEY, D. J., CHEUNG, H. H., MRAD, R. L., PLENCHETTE, S., SIMARD, C., ENWERE, E., ARORA, V., MAK, T. W., LACASSE, E. C., WARING, J. & KORNELUK, R. G. 2008. Both cIAP1 and cIAP2 regulate TNFalpha-mediated NF-kappaB activation. *Proc Natl Acad Sci U S A,* 105**,** 11778-83.

MAJMUNDAR, A. J., WONG, W. J. & SIMON, M. C. 2010. Hypoxia-inducible factors and the response to hypoxic stress. *Mol Cell,* 40**,** 294-309.

MALIREDDI, R. K. S., KESAVARDHANA, S. & KANNEGANTI, T. D. 2019. ZBP1 and TAK1: Master Regulators of NLRP3 Inflammasome/Pyroptosis, Apoptosis, and Necroptosis (PAN-optosis). *Front Cell Infect Microbiol,* 9**,** 406.

MALMENDAL, A., OVERGAARD, J., BUNDY, J. G., SØRENSEN, J. G., NIELSEN, N. C., LOESCHCKE, V. & HOLMSTRUP, M. 2006. Metabolomic profiling of heat stress: hardening and recovery of homeostasis in Drosophila. *Am J Physiol Regul Integr Comp Physiol,* 291**,** R205-12.

MANALO, D. J., ROWAN, A., LAVOIE, T., NATARAJAN, L., KELLY, B. D., YE, S. Q., GARCIA, J. G. & SEMENZA, G. L. 2005. Transcriptional regulation of vascular endothelial cell responses to hypoxia by HIF-1. *Blood,* 105**,** 659-69.

MARCUS, R. 2022. What Is Multiple Sclerosis? *Jama,* 328**,** 2078.

MARIN, M. A. & CARMICHAEL, S. T. 2019. Mechanisms of demyelination and remyelination in the young and aged brain following white matter stroke. *Neurobiol Dis,* 126**,** 5-12.

MARSHALL, O., LU, H., BRISSET, J. C., XU, F., LIU, P., HERBERT, J., GROSSMAN, R. I. & GE, Y. 2014. Impaired cerebrovascular reactivity in multiple sclerosis. *JAMA Neurol,* 71**,** 1275-81.

MARTENS, M. D., KARCH, J. & GORDON, J. W. 2022. The molecular mosaic of regulated cell death in the cardiovascular system. *Biochimica et Biophysica Acta (BBA) - Molecular Basis of Disease,* 1868**,** 166297.

MARTINEZ SOSA, S. & SMITH, K. J. 2017. Understanding a role for hypoxia in lesion formation and location in the deep and periventricular white matter in small vessel disease and multiple sclerosis. *Clin Sci (Lond),* 131**,** 2503-2524.
MARTINOD, K. & WAGNER, D. D. 2014. Thrombosis: tangled up in NETs. *Blood,* 123**,** 2768-76.
MARTON, R. M. & PAȘCA, S. P. 2020. Organoid and assembloid technologies for investigating cellular crosstalk in human brain development and disease. *Trends in Cell Biology,* 30**,** 133-143.
MASCALI, D., VILLANI, A., CHIARELLI, A. M., BIONDETTI, E., LIPP, I., DIGIOVANNI, A., POZZILLI, V., CAPORALE, A. S., RISPOLI, M. G., AJDINAJ, P., D'APOLITO, M., GRASSO, E., SENSI, S. L., MURPHY, K., TOMASSINI, V. & WISE, R. G. 2023. Pathophysiology of multiple sclerosis damage and repair: Linking cerebral hypoperfusion to the development of irreversible tissue loss in multiple sclerosis using magnetic resonance imaging. *Eur J Neurol*.
MATSUSHIMA, G. K. & MORELL, P. 2001. The neurotoxicant, cuprizone, as a model to study demyelination and remyelination in the central nervous system. *Brain Pathol,* 11**,** 107-16.
MATTHEWS, P. M. 2019. Chronic inflammation in multiple sclerosis—seeing what was always there. *Nature Reviews Neurology,* 15**,** 582-593.
MATUSEVICIUS, D., KIVISÄKK, P., HE, B., KOSTULAS, N., OZENCI, V., FREDRIKSON, S. & LINK, H. 1999. Interleukin-17 mRNA expression in blood and CSF mononuclear cells is augmented in multiple sclerosis. *Mult Scler,* 5**,** 101-4.
MAUTHE, M., ORHON, I., ROCCHI, C., ZHOU, X., LUHR, M., HIJLKEMA, K. J., COPPES, R. P., ENGEDAL, N., MARI, M. & REGGIORI, F. 2018. Chloroquine inhibits autophagic flux by decreasing autophagosome-lysosome fusion. *Autophagy,* 14**,** 1435-1455.
MAYERS, R. M., BUTLIN, R. J., KILGOUR, E., LEIGHTON, B., MARTIN, D., MYATT, J., ORME, J. P. & HOLLOWAY, B. R. 2003. AZD7545, a novel inhibitor of pyruvate dehydrogenase kinase 2 (PDHK2), activates pyruvate dehydrogenase in vivo and improves blood glucose control in obese (fa/fa) Zucker rats. *Biochem Soc Trans,* 31**,** 1165-7.
MCALLISTER, M. S., KRIZANAC-BENGEZ, L., MACCHIA, F., NAFTALIN, R. J., PEDLEY, K. C., MAYBERG, M. R., MARRONI, M., LEAMAN, S., STANNESS, K. A. & JANIGRO, D. 2001. Mechanisms of glucose transport at the blood-brain barrier: an in vitro study. *Brain Res,* 904**,** 20-30.
MCKENZIE, B. A., DIXIT, V. M. & POWER, C. 2020. Fiery Cell Death: Pyroptosis in the Central Nervous System. *Trends Neurosci,* 43**,** 55-73.
MCKENZIE, B. A., MAMIK, M. K., SAITO, L. B., BOGHOZIAN, R., MONACO, M. C., MAJOR, E. O., LU, J. Q., BRANTON, W. G. & POWER, C. 2018. Caspase-1 inhibition prevents glial inflammasome activation and pyroptosis in models of multiple sclerosis. *Proc Natl Acad Sci U S A,* 115**,** E6065-e6074.
MEIJER, A. J. & CODOGNO, P. 2006. Signalling and autophagy regulation in health, aging and disease. *Molecular Aspects of Medicine,* 27**,** 411-425.
MERGENTHALER, P., LINDAUER, U., DIENEL, G. A. & MEISEL, A. 2013. Sugar for the brain: the role of glucose in physiological and pathological brain function. *Trends Neurosci,* 36**,** 587-97.
MERRILL, J. & MATSUSHIMA, K. 1988. Production of and response to interleukin 1 by cloned human oligodendroglioma cell lines. *Journal of Biological Regulators and Homeostatic Agents,* 2**,** 77-86.
MI, S., MILLER, R. H., TANG, W., LEE, X., HU, B., WU, W., ZHANG, Y., SHIELDS, C. B., ZHANG, Y. & MIKLASZ, S. 2009. Promotion of central nervous system remyelination by induced differentiation of oligodendrocyte precursor cells. *Annals of Neurology: Official Journal of the American Neurological Association and the Child Neurology Society,* 65**,** 304-315.
MICHAUD, M., MARTINS, I., SUKKURWALA, A. Q., ADJEMIAN, S., MA, Y., PELLEGATTI, P., SHEN, S., KEPP, O., SCOAZEC, M., MIGNOT, G., RELLO-VARONA, S., TAILLER, M., MENGER, L., VACCHELLI, E., GALLUZZI, L., GHIRINGHELLI, F., DI VIRGILIO, F., ZITVOGEL, L. & KROEMER, G. 2011. Autophagy-

dependent anticancer immune responses induced by chemotherapeutic agents in mice. *Science,* 334**,** 1573-7.
MICHEAU, O., THOME, M., SCHNEIDER, P., HOLLER, N., TSCHOPP, J., NICHOLSON, D. W., BRIAND, C. & GRÜTTER, M. G. 2002. The long form of FLIP is an activator of caspase-8 at the Fas death-inducing signaling complex. *J Biol Chem,* 277**,** 45162-71.
MICHINAGA, S., INOUE, A., YAMAMOTO, H., RYU, R., INOUE, A., MIZUGUCHI, H. & KOYAMA, Y. 2020. Endothelin receptor antagonists alleviate blood-brain barrier disruption and cerebral edema in a mouse model of traumatic brain injury: A comparison between bosentan and ambrisentan. *Neuropharmacology,* 175**,** 108182.
MIRON, V. E., BOYD, A., ZHAO, J. W., YUEN, T. J., RUCKH, J. M., SHADRACH, J. L., VAN WIJNGAARDEN, P., WAGERS, A. J., WILLIAMS, A., FRANKLIN, R. J. M. & FFRENCH-CONSTANT, C. 2013. M2 microglia and macrophages drive oligodendrocyte differentiation during CNS remyelination. *Nat Neurosci,* 16**,** 1211-1218.
MIZUSHIMA, N. 2007. Autophagy: process and function. *Genes Dev,* 21**,** 2861-73.
MONTI, D. A., ZABRECKY, G., LEIST, T. P., WINTERING, N., BAZZAN, A. J., ZHAN, T. & NEWBERG, A. B. 2020. N-acetyl Cysteine Administration Is Associated With Increased Cerebral Glucose Metabolism in Patients With Multiple Sclerosis: An Exploratory Study. *Front Neurol,* 11**,** 88.
MOSCHONAS, I. C. & TSELEPIS, A. D. 2019. The pathway of neutrophil extracellular traps towards atherosclerosis and thrombosis. *Atherosclerosis,* 288**,** 9-16.
MOSEVOLL, K. A., JOHANSEN, S., WENDELBO, Ø., NEPSTAD, I., BRUSERUD, Ø. & REIKVAM, H. 2018. Cytokines, Adhesion Molecules, and Matrix Metalloproteases as Predisposing, Diagnostic, and Prognostic Factors in Venous Thrombosis. *Front Med (Lausanne),* 5**,** 147.
MOT, A. I., DEPP, C. & NAVE, K. A. 2018. An emerging role of dysfunctional axon-oligodendrocyte coupling in neurodegenerative diseases. *Dialogues Clin Neurosci,* 20**,** 283-292.
MOUJALLED, D., STRASSER, A. & LIDDELL, J. R. 2021. Molecular mechanisms of cell death in neurological diseases. *Cell Death Differ,* 28**,** 2029-2044.
MUNSON, M. J. & GANLEY, I. G. 2015. MTOR, PIK3C3, and autophagy: Signaling the beginning from the end. *Autophagy,* 11**,** 2375-6.
MUOIO, V., PERSSON, P. B. & SENDESKI, M. M. 2014. The neurovascular unit - concept review. *Acta Physiol (Oxf),* 210**,** 790-8.
MUTUKULA, N., MAN, Z., TAKAHASHI, Y., MARTINEZ, F. I., MORALES, M., CARREON-GUARNIZO, E., CLARES, R. H., GARCIA-BERNAL, D., MARTINEZ, L. M. & LAJARA, J. 2021. Generation of RRMS and PPMS specific iPSCs as a platform for modeling Multiple Sclerosis. *Stem cell research,* 53**,** 102319.
NA, S., COLLIN, O., CHOWDHURY, F., TAY, B., OUYANG, M., WANG, Y. & WANG, N. 2008. Rapid signal transduction in living cells is a unique feature of mechanotransduction. *Proc Natl Acad Sci U S A,* 105**,** 6626-31.
NAKAGAWA, T., ZHU, H., MORISHIMA, N., LI, E., XU, J., YANKNER, B. A. & YUAN, J. 2000. Caspase-12 mediates endoplasmic-reticulum-specific apoptosis and cytotoxicity by amyloid-β. *Nature,* 403**,** 98-103.
NAKAMOTO, M., MOY, R. H., XU, J., BAMBINA, S., YASUNAGA, A., SHELLY, S. S., GOLD, B. & CHERRY, S. 2012. Virus recognition by Toll-7 activates antiviral autophagy in Drosophila. *Immunity,* 36**,** 658-667.
NAKAMURA, S. & YOSHIMORI, T. 2017. New insights into autophagosome-lysosome fusion. *J Cell Sci,* 130**,** 1209-1216.
NARAYANA, P. A., ZHOU, Y., HASAN, K. M., DATTA, S., SUN, X. & WOLINSKY, J. S. 2014. Hypoperfusion and T1-hypointense lesions in white matter in multiple sclerosis. *Mult Scler,* 20**,** 365-73.
NAVE, K.-A. 2010. Myelination and support of axonal integrity by glia. *Nature,* 468**,** 244-252.

NEUMANN, B., BAROR, R., ZHAO, C., SEGEL, M., DIETMANN, S., RAWJI, K. S., FOERSTER, S., MCCLAIN, C. R., CHALUT, K., VAN WIJNGAARDEN, P. & FRANKLIN, R. J. M. 2019a. Metformin Restores CNS Remyelination Capacity by Rejuvenating Aged Stem Cells. *Cell Stem Cell,* 25**,** 473-485.e8.

NEUMANN, B., SEGEL, M., CHALUT, K. J. & FRANKLIN, R. J. 2019b. Remyelination and ageing: Reversing the ravages of time. *Mult Scler,* 25**,** 1835-1841.

NIE, X. J. & OLSSON, Y. 1996. Endothelin peptides in brain diseases. *Rev Neurosci,* 7**,** 177-86.

NOGUEIRA, G. O., GARCEZ, P. P., BARDY, C., CUNNINGHAM, M. O. & SEBOLLELA, A. 2022. Modeling the human brain with ex vivo slices and in vitro organoids for translational neuroscience. *Frontiers in Neuroscience,* 16**,** 838594.

NORBERG, E., GOGVADZE, V., VAKIFAHMETOGLU, H., ORRENIUS, S. & ZHIVOTOVSKY, B. 2010. Oxidative modification sensitizes mitochondrial apoptosis-inducing factor to calpain-mediated processing. *Free Radical Biology and Medicine,* 48**,** 791-797.

NORTLEY, R., KORTE, N., IZQUIERDO, P., HIRUNPATTARASILP, C., MISHRA, A., JAUNMUKTANE, Z., KYRARGYRI, V., PFEIFFER, T., KHENNOUF, L., MADRY, C., GONG, H., RICHARD-LOENDT, A., HUANG, W., SAITO, T., SAIDO, T. C., BRANDNER, S., SETHI, H. & ATTWELL, D. 2019. Amyloid β oligomers constrict human capillaries in Alzheimer's disease via signaling to pericytes. *Science,* 365.

NOSSAL, G. J. 1994. Negative selection of lymphocytes. *Cell,* 76**,** 229-39.

NOVOA, I., ZENG, H., HARDING, H. P. & RON, D. 2001. Feedback inhibition of the unfolded protein response by GADD34-mediated dephosphorylation of eIF2alpha. *J Cell Biol,* 153**,** 1011-22.

OBEID, M., PANARETAKIS, T., JOZA, N., TUFI, R., TESNIERE, A., VAN ENDERT, P., ZITVOGEL, L. & KROEMER, G. 2007a. Calreticulin exposure is required for the immunogenicity of gamma-irradiation and UVC light-induced apoptosis. *Cell Death Differ,* 14**,** 1848-50.

OBEID, M., TESNIERE, A., GHIRINGHELLI, F., FIMIA, G. M., APETOH, L., PERFETTINI, J. L., CASTEDO, M., MIGNOT, G., PANARETAKIS, T., CASARES, N., MÉTIVIER, D., LAROCHETTE, N., VAN ENDERT, P., CICCOSANTI, F., PIACENTINI, M., ZITVOGEL, L. & KROEMER, G. 2007b. Calreticulin exposure dictates the immunogenicity of cancer cell death. *Nat Med,* 13**,** 54-61.

OBENG, E. 2021. Apoptosis (programmed cell death) and its signals - A review. *Braz J Biol,* 81**,** 1133-1143.

OGAWA, Y., SCHAFER, D. P., HORRESH, I., BAR, V., HALES, K., YANG, Y., SUSUKI, K., PELES, E., STANKEWICH, M. C. & RASBAND, M. N. 2006. Spectrins and ankyrinB constitute a specialized paranodal cytoskeleton. *J Neurosci,* 26**,** 5230-9.

OHOKA, N., YOSHII, S., HATTORI, T., ONOZAKI, K. & HAYASHI, H. 2005. TRB3, a novel ER stress-inducible gene, is induced via ATF4-CHOP pathway and is involved in cell death. *Embo j,* 24**,** 1243-55.

OLIVER, F. J., MENISSIER-DE MURCIA, J. & DE MURCIA, G. 1999. Poly(ADP-ribose) polymerase in the cellular response to DNA damage, apoptosis, and disease. *Am J Hum Genet,* 64**,** 1282-8.

OLZMANN, J. A. & CARVALHO, P. 2019. Dynamics and functions of lipid droplets. *Nat Rev Mol Cell Biol,* 20**,** 137-155.

OPPENHEIM, R. W., FLAVELL, R. A., VINSANT, S., PREVETTE, D., KUAN, C. Y. & RAKIC, P. 2001. Programmed cell death of developing mammalian neurons after genetic deletion of caspases. *J Neurosci,* 21**,** 4752-60.

OSTROW, L. W., LANGAN, T. J. & SACHS, F. 2000. Stretch-induced endothelin-1 production by astrocytes. *J Cardiovasc Pharmacol,* 36**,** S274-7.

OVERHOLTZER, M., MAILLEUX, A. A., MOUNEIMNE, G., NORMAND, G., SCHNITT, S. J., KING, R. W., CIBAS, E. S. & BRUGGE, J. S. 2007. A nonapoptotic cell death process, entosis, that occurs by cell-in-cell invasion. *Cell,* 131**,** 966-79.

OWENS, T. 2006. Animal models for multiple sclerosis. *Adv Neurol,* 98**,** 77-89.

PAEZ, P. M. & LYONS, D. A. 2020. Calcium Signaling in the Oligodendrocyte Lineage: Regulators and Consequences. *Annu Rev Neurosci,* 43**,** 163-186.

PAKOS-ZEBRUCKA, K., KORYGA, I., MNICH, K., LJUJIC, M., SAMALI, A. & GORMAN, A. M. 2016. The integrated stress response. *EMBO reports,* 17**,** 1374-1395.

PANARETAKIS, T., JOZA, N., MODJTAHEDI, N., TESNIERE, A., VITALE, I., DURCHSCHLAG, M., FIMIA, G. M., KEPP, O., PIACENTINI, M., FROEHLICH, K. U., VAN ENDERT, P., ZITVOGEL, L., MADEO, F. & KROEMER, G. 2008. The co-translocation of ERp57 and calreticulin determines the immunogenicity of cell death. *Cell Death Differ,* 15**,** 1499-509.

PANG, Y., SIMPSON, K., MIGUEL-HIDALGO, J. J. & SAVICH, R. 2018. Neuron/Oligodendrocyte Myelination Coculture. *Methods Mol Biol,* 1791**,** 131-144.

PAPADAKI, E. Z., MASTORODEMOS, V. C., AMANAKIS, E. Z., TSEKOURAS, K. C., PAPADAKIS, A. E., TSAVALAS, N. D., SIMOS, P. G., KARANTANAS, A. H., PLAITAKIS, A. & MARIS, T. G. 2012. White matter and deep gray matter hemodynamic changes in multiple sclerosis patients with clinically isolated syndrome. *Magn Reson Med,* 68**,** 1932-42.

PATEL, M. S., NEMERIA, N. S., FUREY, W. & JORDAN, F. 2014. The pyruvate dehydrogenase complexes: structure-based function and regulation. *J Biol Chem,* 289**,** 16615-23.

PATRIKIOS, P., STADELMANN, C., KUTZELNIGG, A., RAUSCHKA, H., SCHMIDBAUER, M., LAURSEN, H., SORENSEN, P. S., BRÜCK, W., LUCCHINETTI, C. & LASSMANN, H. 2006. Remyelination is extensive in a subset of multiple sclerosis patients. *Brain,* 129**,** 3165-72.

PAUL, G. & ELABI, O. F. 2022. Microvascular Changes in Parkinson's Disease- Focus on the Neurovascular Unit. *Front Aging Neurosci,* 14**,** 853372.

PERLMAN, K., COUTURIER, C. P., YAQUBI, M., TANTI, A., CUI, Q. L., PERNIN, F., STRATTON, J. A., RAGOUSSIS, J., HEALY, L., PETRECCA, K., DUDLEY, R., SROUR, M., HALL, J. A., KENNEDY, T. E., MECHAWAR, N. & ANTEL, J. P. 2020. Developmental trajectory of oligodendrocyte progenitor cells in the human brain revealed by single cell RNA sequencing. *Glia,* 68**,** 1291-1303.

PERNIN, F., LUO, J. X. X., CUI, Q. L., BLAIN, M., FERNANDES, M. G. F., YAQUBI, M., SROUR, M., HALL, J., DUDLEY, R., JAMANN, H., LAROCHELLE, C., ZANDEE, S. E. J., PRAT, A., STRATTON, J. A., KENNEDY, T. E. & ANTEL, J. P. 2022. Diverse injury responses of human oligodendrocyte to mediators implicated in multiple sclerosis. *Brain,* 145**,** 4320-4333.

PERRIOT, S., MATHIAS, A., PERRIARD, G., CANALES, M., JONKMANS, N., MERIENNE, N., MEUNIER, C., EL KASSAR, L., PERRIER, A. L. & LAPLAUD, D.-A. 2018. Human induced pluripotent stem cell-derived astrocytes are differentially activated by multiple sclerosis-associated cytokines. *Stem cell reports,* 11**,** 1199-1210.

PETERS, A. 1991. The fine structure of the nervous system. *Neurons and their supporting cells***,** 211-218.

PEYSSONNAUX, C., CEJUDO-MARTIN, P., DOEDENS, A., ZINKERNAGEL, A. S., JOHNSON, R. S. & NIZET, V. 2007. Cutting edge: Essential role of hypoxia inducible factor-1alpha in development of lipopolysaccharide-induced sepsis. *J Immunol,* 178**,** 7516-9.

PFEIFFER, S. E., WARRINGTON, A. E. & BANSAL, R. 1993. The oligodendrocyte and its many cellular processes. *Trends Cell Biol,* 3**,** 191-7.

PHILIPS, T. & ROTHSTEIN, J. D. 2017. Oligodendroglia: metabolic supporters of neurons. *J Clin Invest,* 127**,** 3271-3280.

PIECHOTA, A., POLAŃCZYK, A. & GORACA, A. 2010. Role of endothelin-1 receptor blockers on hemodynamic parameters and oxidative stress. *Pharmacol Rep,* 62**,** 28-34.

PIETROCOLA, F., IZZO, V., NISO-SANTANO, M., VACCHELLI, E., GALLUZZI, L., MAIURI, M. C. & KROEMER, G. 2013. Regulation of autophagy by stress-responsive transcription factors. *Seminars in Cancer Biology,* 23**,** 310-322.

PIZZINO, G., IRRERA, N., CUCINOTTA, M., PALLIO, G., MANNINO, F., ARCORACI, V., SQUADRITO, F., ALTAVILLA, D. & BITTO, A. 2017. Oxidative Stress: Harms and Benefits for Human Health. *Oxid Med Cell Longev,* 2017**,** 8416763.

PLEMEL, J. R., MANESH, S. B., SPARLING, J. S. & TETZLAFF, W. 2013. Myelin inhibits oligodendroglial maturation and regulates oligodendrocytic transcription factor expression. *Glia,* 61**,** 1471-87.

PLOUIN, P. & KAMINSKA, A. 2013. Neonatal seizures. *Handb Clin Neurol,* 111**,** 467-76.

POON, I. K., LUCAS, C. D., ROSSI, A. G. & RAVICHANDRAN, K. S. 2014. Apoptotic cell clearance: basic biology and therapeutic potential. *Nat Rev Immunol,* 14**,** 166-80.

PRAHLAD, V. & MORIMOTO, R. I. 2009. Integrating the stress response: lessons for neurodegenerative diseases from C. elegans. *Trends Cell Biol,* 19**,** 52-61.

PRINEAS, J. W., KWON, E. E., CHO, E.-S., SHARER, L. R., BARNETT, M. H., OLESZAK, E. L., HOFFMAN, B. & MORGAN, B. P. 2001. Immunopathology of secondary-progressive multiple sclerosis. *Annals of Neurology,* 50**,** 646-657.

PRINEAS, J. W. & PARRATT, J. D. 2012. Oligodendrocytes and the early multiple sclerosis lesion. *Ann Neurol,* 72**,** 18-31.

PROCACCINI, C., DE ROSA, V., PUCINO, V., FORMISANO, L. & MATARESE, G. 2015. Animal models of Multiple Sclerosis. *Eur J Pharmacol,* 759**,** 182-91.

PSACHOULIA, K., JAMEN, F., YOUNG, K. M. & RICHARDSON, W. D. 2009. Cell cycle dynamics of NG2 cells in the postnatal and ageing brain. *Neuron Glia Biol,* 5**,** 57-67.

PURVANOV, V., HOLST, M., KHAN, J., BAARLINK, C. & GROSSE, R. 2014. G-protein-coupled receptor signaling and polarized actin dynamics drive cell-in-cell invasion. *Elife,* 3.

RAICHLE, M. E. & GUSNARD, D. A. 2002. Appraising the brain's energy budget. *Proc Natl Acad Sci U S A,* 99**,** 10237-9.

RAJAN, P., ELLIOTT, D. J., ROBSON, C. N. & LEUNG, H. Y. 2009. Alternative splicing and biological heterogeneity in prostate cancer. *Nat Rev Urol,* 6**,** 454-60.

RAJGOPAL, Y. & VEMURI, M. C. 2002. Calpain activation and alpha-spectrin cleavage in rat brain by ethanol. *Neurosci Lett,* 321**,** 187-91.

RANKIN, E. B., RHA, J., SELAK, M. A., UNGER, T. L., KEITH, B., LIU, Q. & HAASE, V. H. 2009. Hypoxia-inducible factor 2 regulates hepatic lipid metabolism. *Mol Cell Biol,* 29**,** 4527-38.

RANSOHOFF, R. M. 2023. Multiple sclerosis: role of meningeal lymphoid aggregates in progression independent of relapse activity. *Trends in Immunology*.

RAO, V. T. S., KHAN, D., CUI, Q. L., FUH, S. C., HOSSAIN, S., ALMAZAN, G., MULTHAUP, G., HEALY, L. M., KENNEDY, T. E. & ANTEL, J. P. 2017. Distinct age and differentiation-state dependent metabolic profiles of oligodendrocytes under optimal and stress conditions. *PLoS One,* 12**,** e0182372.

RASBAND, M. N., PARK, E. W., VANDERAH, T. W., LAI, J., PORRECA, F. & TRIMMER, J. S. 2001. Distinct potassium channels on pain-sensing neurons. *Proc Natl Acad Sci U S A,* 98**,** 13373-8.

RASMUSSEN, S. B., HORAN, K. A., HOLM, C. K., STRANKS, A. J., METTENLEITER, T. C., SIMON, A. K., JENSEN, S. B., RIXON, F. J., HE, B. & PALUDAN, S. R. 2011. Activation of autophagy by α-herpesviruses in myeloid cells is mediated by cytoplasmic viral DNA through a mechanism dependent on stimulator of IFN genes. *The journal of immunology,* 187**,** 5268-5276.

RATHINAM, V. A. & FITZGERALD, K. A. 2016. Inflammasome Complexes: Emerging Mechanisms and Effector Functions. *Cell,* 165**,** 792-800.

RAWJI, K. S. & YONG, V. W. 2013. The benefits and detriments of macrophages/microglia in models of multiple sclerosis. *Clin Dev Immunol,* 2013**,** 948976.

READHEAD, C., POPKO, B., TAKAHASHI, N., SHINE, H. D., SAAVEDRA, R. A., SIDMAN, R. L. & HOOD, L. 1987. Expression of a myelin basic protein gene in transgenic shiverer mice: correction of the dysmyelinating phenotype. *Cell,* 48**,** 703-12.

REBUZZINI, P., ZUCCOTTI, M., REDI, C. A. & GARAGNA, S. 2016. Chromosomal abnormalities in embryonic and somatic stem cells. *Cytogenetic and Genome Research,* 147**,** 1-9.
REICH, M., LIEFELD, T., GOULD, J., LERNER, J., TAMAYO, P. & MESIROV, J. P. 2006. GenePattern 2.0. *Nat Genet,* 38**,** 500-1.
RICHTER-LANDSBERG, C. & HEINRICH, M. 1996. OLN-93: A new permanent oligodendroglia cell line derived from primary rat brain glial cultures. *Journal of neuroscience research,* 45**,** 161-173.
RICHTER, K., HASLBECK, M. & BUCHNER, J. 2010. The heat shock response: life on the verge of death. *Molecular cell,* 40**,** 253-266.
RINHOLM, J. E., HAMILTON, N. B., KESSARIS, N., RICHARDSON, W. D., BERGERSEN, L. H. & ATTWELL, D. 2011. Regulation of oligodendrocyte development and myelination by glucose and lactate. *J Neurosci,* 31**,** 538-48.
RISSANEN, E., TUISKU, J., ROKKA, J., PAAVILAINEN, T., PARKKOLA, R., RINNE, J. O. & AIRAS, L. 2014. In vivo detection of diffuse inflammation in secondary progressive multiple sclerosis using PET imaging and the radioligand 11C-PK11195. *Journal of Nuclear Medicine,* 55**,** 939-944.
ROACH, A., BOYLAN, K., HORVATH, S., PRUSINER, S. B. & HOOD, L. E. 1983. Characterization of cloned cDNA representing rat myelin basic protein: absence of expression in brain of shiverer mutant mice. *Cell,* 34**,** 799-806.
ROACH, A., TAKAHASHI, N., PRAVTCHEVA, D., RUDDLE, F. & HOOD, L. 1985. Chromosomal mapping of mouse myelin basic protein gene and structure and transcription of the partially deleted gene in shiverer mutant mice. *Cell,* 42**,** 149-55.
ROACH, P. J., DEPAOLI-ROACH, A. A., HURLEY, T. D. & TAGLIABRACCI, V. S. 2012. Glycogen and its metabolism: some new developments and old themes. *Biochem J,* 441**,** 763-87.
ROBINSON, S. & MILLER, R. H. 1999. Contact with central nervous system myelin inhibits oligodendrocyte progenitor maturation. *Dev Biol,* 216**,** 359-68.
ROCHE, P. A. & FURUTA, K. 2015. The ins and outs of MHC class II-mediated antigen processing and presentation. *Nat Rev Immunol,* 15**,** 203-16.
RODRIGUEZ, M., SCHEITHAUER, B. W., FORBES, G. & KELLY, P. J. Oligodendrocyte injury is an early event in lesions of multiple sclerosis. Mayo Clinic proceedings, 1993. Elsevier, 627-636.
RON, D. & WALTER, P. 2007. Signal integration in the endoplasmic reticulum unfolded protein response. *Nature Reviews Molecular Cell Biology,* 8**,** 519-529.
RONE, M. B., CUI, Q. L., FANG, J., WANG, L. C., ZHANG, J., KHAN, D., BEDARD, M., ALMAZAN, G., LUDWIN, S. K., JONES, R., KENNEDY, T. E. & ANTEL, J. P. 2016. Oligodendrogliopathy in Multiple Sclerosis: Low Glycolytic Metabolic Rate Promotes Oligodendrocyte Survival. *J Neurosci,* 36**,** 4698-707.
ROSENBLUTH, J. 2009. Multiple functions of the paranodal junction of myelinated nerve fibers. *J Neurosci Res,* 87**,** 3250-8.
ROUSCHOP, K. M., VAN DEN BEUCKEN, T., DUBOIS, L., NIESSEN, H., BUSSINK, J., SAVELKOULS, K., KEULERS, T., MUJCIC, H., LANDUYT, W. & VONCKEN, J. W. 2010. The unfolded protein response protects human tumor cells during hypoxia through regulation of the autophagy genes MAP1LC3B and ATG5. *The Journal of clinical investigation,* 120**,** 127-141.
RUBIN, L. L., HALL, D. E., PORTER, S., BARBU, K., CANNON, C., HORNER, H. C., JANATPOUR, M., LIAW, C. W., MANNING, K., MORALES, J. & ET AL. 1991. A cell culture model of the blood-brain barrier. *J Cell Biol,* 115**,** 1725-35.
RÜHL, S., SHKARINA, K., DEMARCO, B., HEILIG, R., SANTOS, J. C. & BROZ, P. 2018. ESCRT-dependent membrane repair negatively regulates pyroptosis downstream of GSDMD activation. *Science,* 362**,** 956-960.

RUTKOWSKI, D. T., ARNOLD, S. M., MILLER, C. N., WU, J., LI, J., GUNNISON, K. M., MORI, K., SADIGHI AKHA, A. A., RADEN, D. & KAUFMAN, R. J. 2006. Adaptation to ER stress is mediated by differential stabilities of pro-survival and pro-apoptotic mRNAs and proteins. *PLoS Biol,* 4**,** e374.

SAAB, A. S., TZVETANOVA, I. D. & NAVE, K. A. 2013. The role of myelin and oligodendrocytes in axonal energy metabolism. *Curr Opin Neurobiol,* 23**,** 1065-72.

SÁNCHEZ-ABARCA, L. I., TABERNERO, A. & MEDINA, J. M. 2001. Oligodendrocytes use lactate as a source of energy and as a precursor of lipids. *Glia,* 36**,** 321-9.

SATO, W., TOMITA, A., ICHIKAWA, D., LIN, Y., KISHIDA, H., MIYAKE, S., OGAWA, M., OKAMOTO, T., MURATA, M., KUROIWA, Y., ARANAMI, T. & YAMAMURA, T. 2012. CCR2+CCR5+ T Cells Produce Matrix Metalloproteinase-9 and Osteopontin in the Pathogenesis of Multiple Sclerosis. *The Journal of Immunology,* 189**,** 5057-5065.

SATOH, J.-I., MOTOHASHI, N., KINO, Y., ISHIDA, T., YAGISHITA, S., JINNAI, K., ARAI, N., NAKAMAGOE, K., TAMAOKA, A., SAITO, Y. & ARIMA, K. 2014. LC3, an autophagosome marker, is expressed on oligodendrocytes in Nasu-Hakola disease brains. *Orphanet Journal of Rare Diseases,* 9**,** 68.

SAX, J. L., HERSHMAN, S. N., HUBLER, Z., ALLIMUTHU, D., ELITT, M. S., BEDERMAN, I. & ADAMS, D. J. 2022. Enhancers of Human and Rodent Oligodendrocyte Formation Predominantly Induce Cholesterol Precursor Accumulation. *ACS Chemical Biology,* 17**,** 2188-2200.

SCHAEFFER, S. & IADECOLA, C. 2021. Revisiting the neurovascular unit. *Nat Neurosci,* 24**,** 1198-1209.

SCHINKEL, A. H. 1999. P-Glycoprotein, a gatekeeper in the blood-brain barrier. *Adv Drug Deliv Rev,* 36**,** 179-194.

SCHNAAR, R. L. & LOPEZ, P. H. 2009. Myelin-associated glycoprotein and its axonal receptors. *J Neurosci Res,* 87**,** 3267-76.

SCHNEIDER, J. & MILLER, S. P. 2019. Preterm brain Injury: White matter injury. *Handb Clin Neurol,* 162**,** 155-172.

SCHWEGLER, M., WIRSING, A. M., SCHENKER, H. M., OTT, L., RIES, J. M., BÜTTNER-HEROLD, M., FIETKAU, R., PUTZ, F. & DISTEL, L. V. 2015. Prognostic Value of Homotypic Cell Internalization by Nonprofessional Phagocytic Cancer Cells. *Biomed Res Int,* 2015**,** 359392.

SCHWEICHEL, J. U. & MERKER, H. J. 1973. The morphology of various types of cell death in prenatal tissues. *Teratology,* 7**,** 253-66.

SEGOVIA, K. N., MCCLURE, M., MORAVEC, M., LUO, N. L., WAN, Y., GONG, X., RIDDLE, A., CRAIG, A., STRUVE, J., SHERMAN, L. S. & BACK, S. A. 2008. Arrested oligodendrocyte lineage maturation in chronic perinatal white matter injury. *Ann Neurol,* 63**,** 520-30.

SEKIZAR, S. & WILLIAMS, A. 2019. Ex vivo slice cultures to study myelination, demyelination, and remyelination in mouse brain and spinal cord. *Oligodendrocytes: Methods and Protocols***,** 169-183.

SEMENZA, G. L. 2007. Hypoxia-inducible factor 1 (HIF-1) pathway. *Science's STKE,* 2007**,** cm8-cm8.

SENICHKIN, V. V., STRELETSKAIA, A. Y., ZHIVOTOVSKY, B. & KOPEINA, G. S. 2019. Molecular Comprehension of Mcl-1: From Gene Structure to Cancer Therapy. *Trends Cell Biol,* 29**,** 549-562.

SETTEMBRE, C., DI MALTA, C., POLITO, V. A., GARCIA ARENCIBIA, M., VETRINI, F., ERDIN, S., ERDIN, S. U., HUYNH, T., MEDINA, D., COLELLA, P., SARDIELLO, M., RUBINSZTEIN, D. C. & BALLABIO, A. 2011. TFEB links autophagy to lysosomal biogenesis. *Science,* 332**,** 1429-33.

SHALTOUKI, A., PENG, J., LIU, Q., RAO, M. S. & ZENG, X. 2013. Efficient generation of astrocytes from human pluripotent stem cells in defined conditions. *Stem cells,* 31**,** 941-952.

SHANMUGHAPRIYA, S., RAJAN, S., HOFFMAN, N. E., HIGGINS, A. M., TOMAR, D., NEMANI, N., HINES, K. J., SMITH, D. J., EGUCHI, A. & VALLEM, S. 2015. SPG7 is an essential and conserved component of the mitochondrial permeability transition pore. *Molecular cell,* 60**,** 47-62.

SHARIFI, M. N., MOWERS, E. E., DRAKE, L. E. & MACLEOD, K. F. 2015. Measuring autophagy in stressed cells. *Methods Mol Biol,* 1292**,** 129-50.

SHI, H., KORONYO, Y., RENTSENDORJ, A., REGIS, G. C., SHEYN, J., FUCHS, D. T., KRAMEROV, A. A., LJUBIMOV, A. V., DUMITRASCU, O. M., RODRIGUEZ, A. R., BARRON, E., HINTON, D. R., BLACK, K. L., MILLER, C. A., MIRZAEI, N. & KORONYO-HAMAOUI, M. 2020. Identification of early pericyte loss and vascular amyloidosis in Alzheimer's disease retina. *Acta Neuropathol,* 139**,** 813-836.

SHIELDS, S. A., GILSON, J. M., BLAKEMORE, W. F. & FRANKLIN, R. J. 1999. Remyelination occurs as extensively but more slowly in old rats compared to young rats following gliotoxin-induced CNS demyelination. *Glia,* 28**,** 77-83.

SHIMIZU, S., NARITA, M., TSUJIMOTO, Y. & TSUJIMOTO, Y. 1999. Bcl-2 family proteins regulate the release of apoptogenic cytochrome c by the mitochondrial channel VDAC. *Nature,* 399**,** 483-487.

SHINTAKU, M. & YUTANI, C. 2004. Oligodendrocytes within astrocytes ("emperipolesis") in the white matter in Creutzfeldt-Jakob disease. *Acta Neuropathol,* 108**,** 201-6.

SHOSHAN-BARMATZ, V., KRELIN, Y. & SHTEINFER-KUZMINE, A. 2018. VDAC1 functions in Ca(2+) homeostasis and cell life and death in health and disease. *Cell Calcium,* 69**,** 81-100.

SIES, H. 1997. Oxidative stress: oxidants and antioxidants. *Exp Physiol,* 82**,** 291-5.

SIM, F. J., ZHAO, C., PENDERIS, J. & FRANKLIN, R. J. 2002. The age-related decrease in CNS remyelination efficiency is attributable to an impairment of both oligodendrocyte progenitor recruitment and differentiation. *J Neurosci,* 22**,** 2451-9.

SISTIGU, A., YAMAZAKI, T., VACCHELLI, E., CHABA, K., ENOT, D. P., ADAM, J., VITALE, I., GOUBAR, A., BARACCO, E. E., REMÉDIOS, C., FEND, L., HANNANI, D., AYMERIC, L., MA, Y., NISO-SANTANO, M., KEPP, O., SCHULTZE, J. L., TÜTING, T., BELARDELLI, F., BRACCI, L., LA SORSA, V., ZICCHEDDU, G., SESTILI, P., URBANI, F., DELORENZI, M., LACROIX-TRIKI, M., QUIDVILLE, V., CONFORTI, R., SPANO, J. P., PUSZTAI, L., POIRIER-COLAME, V., DELALOGE, S., PENAULT-LLORCA, F., LADOIRE, S., ARNOULD, L., CYRTA, J., DESSOLIERS, M. C., EGGERMONT, A., BIANCHI, M. E., PITTET, M., ENGBLOM, C., PFIRSCHKE, C., PRÉVILLE, X., UZÈ, G., SCHREIBER, R. D., CHOW, M. T., SMYTH, M. J., PROIETTI, E., ANDRÉ, F., KROEMER, G. & ZITVOGEL, L. 2014. Cancer cell-autonomous contribution of type I interferon signaling to the efficacy of chemotherapy. *Nat Med,* 20**,** 1301-9.

SIVANDZADE, F. & CUCULLO, L. 2018. In-vitro blood-brain barrier modeling: A review of modern and fast-advancing technologies. *J Cereb Blood Flow Metab,* 38**,** 1667-1681.

SKOFF, R. P. & BENJAMINS, J. A. 2014. Oligodendrocytes. *In:* AMINOFF, M. J. & DAROFF, R. B. (eds.) *Encyclopedia of the Neurological Sciences (Second Edition).* Oxford: Academic Press.

SMEELE, K. M., SOUTHWORTH, R., WU, R., XIE, C., NEDERLOF, R., WARLEY, A., NELSON, J. K., VAN HORSSEN, P., VAN DEN WIJNGAARD, J. P. & HEIKKINEN, S. 2011. Disruption of hexokinase II–mitochondrial binding blocks ischemic preconditioning and causes rapid cardiac necrosis. *Circulation research,* 108**,** 1165-1169.

SNAIDERO, N. & SIMONS, M. 2017. The logistics of myelin biogenesis in the central nervous system. *Glia,* 65**,** 1021-1031.

SOBUE, K., YAMAMOTO, N., YONEDA, K., HODGSON, M. E., YAMASHIRO, K., TSURUOKA, N., TSUDA, T., KATSUYA, H., MIURA, Y., ASAI, K. & KATO, T. 1999. Induction of blood-brain barrier properties in immortalized bovine brain endothelial cells by astrocytic factors. *Neurosci Res,* 35**,** 155-64.

SÖHL, G., HOMBACH, S., DEGEN, J. & ODERMATT, B. 2013. The oligodendroglial precursor cell line Oli-neu represents a cell culture system to examine functional expression of the mouse gap junction gene connexin29 (Cx29). *Frontiers in pharmacology,* 4**,** 83.

SONG, H., LIU, B., HUAI, W., YU, Z., WANG, W., ZHAO, J., HAN, L., JIANG, G., ZHANG, L., GAO, C. & ZHAO, W. 2016. The E3 ubiquitin ligase TRIM31 attenuates NLRP3 inflammasome activation by promoting proteasomal degradation of NLRP3. *Nat Commun,* 7**,** 13727.

SORENSEN, P. S., FOX, R. J. & COMI, G. 2020. The window of opportunity for treatment of progressive multiple sclerosis. *Curr Opin Neurol,* 33**,** 262-270.

SPAIN, R., POWERS, K., MURCHISON, C., HERIZA, E., WINGES, K., YADAV, V., CAMERON, M., KIM, E., HORAK, F., SIMON, J. & BOURDETTE, D. 2017. Lipoic acid in secondary progressive MS: A randomized controlled pilot trial. *Neurol Neuroimmunol Neuroinflamm,* 4**,** e374.
SPECIALE, L., SARASELLA, M., RUZZANTE, S., CAPUTO, D., MANCUSO, R., CALVO, M. G., GUERINI, F. R. & FERRANTE, P. 2000. Endothelin and nitric oxide levels in cerebrospinal fluid of patients with multiple sclerosis. *J Neurovirol,* 6 Suppl 2**,** S62-6.
STADELMANN, C., LUDWIN, S., TABIRA, T., GUSEO, A., LUCCHINETTI, C. F., LEEL-OSSY, L., ORDINARIO, A. T., BRÜCK, W. & LASSMANN, H. 2005. Tissue preconditioning may explain concentric lesions in Baló's type of multiple sclerosis. *Brain,* 128**,** 979-87.
STADELMANN, C., TIMMLER, S., BARRANTES-FREER, A. & SIMONS, M. 2019. Myelin in the Central Nervous System: Structure, Function, and Pathology. *Physiol Rev,* 99**,** 1381-1431.
STANKIEWICZ, J., PANTER, S. S., NEEMA, M., ARORA, A., BATT, C. E. & BAKSHI, R. 2007. Iron in chronic brain disorders: imaging and neurotherapeutic implications. *Neurotherapeutics,* 4**,** 371-386.
STARKE, R. M., CHALOUHI, N., DING, D., RAPER, D. M. S., MCKISIC, M. S., OWENS, G. K., HASAN, D. M., MEDEL, R. & DUMONT, A. S. 2014. Vascular Smooth Muscle Cells in Cerebral Aneurysm Pathogenesis. *Translational Stroke Research,* 5**,** 338-346.
STEEN, C., D'HAESELEER, M., HOOGDUIN, J. M., FIERENS, Y., CAMBRON, M., MOSTERT, J. P., HEERSEMA, D. J., KOCH, M. W. & DE KEYSER, J. 2013. Cerebral white matter blood flow and energy metabolism in multiple sclerosis. *Mult Scler,* 19**,** 1282-9.
STONE, N. L., ENGLAND, T. J. & O'SULLIVAN, S. E. 2019. A Novel Transwell Blood Brain Barrier Model Using Primary Human Cells. *Front Cell Neurosci,* 13**,** 230.
STUART, T., BUTLER, A., HOFFMAN, P., HAFEMEISTER, C., PAPALEXI, E., MAUCK, W. M., 3RD, HAO, Y., STOECKIUS, M., SMIBERT, P. & SATIJA, R. 2019. Comprehensive Integration of Single-Cell Data. *Cell,* 177**,** 1888-1902.e21.
SU, K. G., BANKER, G., BOURDETTE, D. & FORTE, M. 2009. Axonal degeneration in multiple sclerosis: the mitochondrial hypothesis. *Current neurology and neuroscience reports,* 9**,** 411.
SUDARSHAN, S., SOURBIER, C., KONG, H. S., BLOCK, K., VALERA ROMERO, V. A., YANG, Y., GALINDO, C., MOLLAPOUR, M., SCROGGINS, B., GOODE, N., LEE, M. J., GOURLAY, C. W., TREPEL, J., LINEHAN, W. M. & NECKERS, L. 2009. Fumarate hydratase deficiency in renal cancer induces glycolytic addiction and hypoxia-inducible transcription factor 1alpha stabilization by glucose-dependent generation of reactive oxygen species. *Mol Cell Biol,* 29**,** 4080-90.
SUN, Q., CIBAS, E. S., HUANG, H., HODGSON, L. & OVERHOLTZER, M. 2014. Induction of entosis by epithelial cadherin expression. *Cell Res,* 24**,** 1288-98.
SUN, X., TANAKA, M., KONDO, S., OKAMOTO, K. & HIRAI, S. 1998. Clinical significance of reduced cerebral metabolism in multiple sclerosis: a combined PET and MRI study. *Ann Nucl Med,* 12**,** 89-94.
SUTTON, V. R., DAVIS, J. E., CANCILLA, M., JOHNSTONE, R. W., RUEFLI, A. A., SEDELIES, K., BROWNE, K. A. & TRAPANI, J. A. 2000. Initiation of apoptosis by granzyme B requires direct cleavage of bid, but not direct granzyme B-mediated caspase activation. *J Exp Med,* 192**,** 1403-14.
SWANK, R. L., ROTH, J. G. & WOODY, D. C., JR. 1983. Cerebral blood flow and red cell delivery in normal subjects and in multiple sclerosis. *Neurol Res,* 5**,** 37-59.
SWEENEY, M. D., KISLER, K., MONTAGNE, A., TOGA, A. W. & ZLOKOVIC, B. V. 2018. The role of brain vasculature in neurodegenerative disorders. *Nat Neurosci,* 21**,** 1318-1331.
SZABÓ, C. & DAWSON, V. L. 1998. Role of poly(ADP-ribose) synthetase in inflammation and ischaemia-reperfusion. *Trends Pharmacol Sci,* 19**,** 287-98.
TANG, D., KANG, R., BERGHE, T. V., VANDENABEELE, P. & KROEMER, G. 2019. The molecular machinery of regulated cell death. *Cell Res,* 29**,** 347-364.
TEPAVČEVIĆ, V. 2021. Oligodendroglial Energy Metabolism and (re)Myelination. *Life (Basel),* 11.

THIEL, M., CALDWELL, C. C., KRETH, S., KUBOKI, S., CHEN, P., SMITH, P., OHTA, A., LENTSCH, A. B., LUKASHEV, D. & SITKOVSKY, M. V. 2007. Targeted deletion of HIF-1alpha gene in T cells prevents their inhibition in hypoxic inflamed tissues and improves septic mice survival. *PLoS One,* 2**,** e853.

TOMPKINS, S. M., PADILLA, J., DAL CANTO, M. C., TING, J. P., VAN KAER, L. & MILLER, S. D. 2002. De novo central nervous system processing of myelin antigen is required for the initiation of experimental autoimmune encephalomyelitis. *J Immunol,* 168**,** 4173-83.

TOUSSAINT, M., JACKSON, D. J., SWIEBODA, D., GUEDÁN, A., TSOUROUKTSOGLOU, T. D., CHING, Y. M., RADERMECKER, C., MAKRINIOTI, H., ANISCENKO, J., BARTLETT, N. W., EDWARDS, M. R., SOLARI, R., FARNIR, F., PAPAYANNOPOULOS, V., BUREAU, F., MARICHAL, T. & JOHNSTON, S. L. 2017. Host DNA released by NETosis promotes rhinovirus-induced type-2 allergic asthma exacerbation. *Nat Med,* 23**,** 681-691.

TRAPP, B. D. & STYS, P. K. 2009. Virtual hypoxia and chronic necrosis of demyelinated axons in multiple sclerosis. *The Lancet Neurology,* 8**,** 280-291.

TRESS, O., MAGLIONE, M., MAY, D., PIVNEVA, T., RICHTER, N., SEYFARTH, J., BINDER, S., ZLOMUZICA, A., SEIFERT, G., THEIS, M., DERE, E., KETTENMANN, H. & WILLECKE, K. 2012. Panglial gap junctional communication is essential for maintenance of myelin in the CNS. *J Neurosci,* 32**,** 7499-518.

TROMPOUKI, E., HATZIVASSILIOU, E., TSICHRITZIS, T., FARMER, H., ASHWORTH, A. & MOSIALOS, G. 2003. CYLD is a deubiquitinating enzyme that negatively regulates NF-kappaB activation by TNFR family members. *Nature,* 424**,** 793-6.

TSUNEDA, T. 2020. Fenton reaction mechanism generating no OH radicals in Nafion membrane decomposition. *Scientific Reports,* 10**,** 18144.

TSUNODA, I. & FUJINAMI, R. S. 2010. Neuropathogenesis of Theiler's murine encephalomyelitis virus infection, an animal model for multiple sclerosis. *J Neuroimmune Pharmacol,* 5**,** 355-69.

TSUNODA, I., KUANG, L. Q., LIBBEY, J. E. & FUJINAMI, R. S. 2003. Axonal injury heralds virus-induced demyelination. *Am J Pathol,* 162**,** 1259-69.

TUMMERS, B. & GREEN, D. R. 2017. Caspase-8: regulating life and death. *Immunol Rev,* 277**,** 76-89.

TUMMERS, B. & GREEN, D. R. 2022. The evolution of regulated cell death pathways in animals and their evasion by pathogens. *Physiol Rev,* 102**,** 411-454.

TUOHY, V. K., LU, Z., SOBEL, R. A., LAURSEN, R. A. & LEES, M. B. 1989. Identification of an encephalitogenic determinant of myelin proteolipid protein for SJL mice. *J Immunol,* 142**,** 1523-7.

TURRENS, J. F. 2003. Mitochondrial formation of reactive oxygen species. *J Physiol,* 552**,** 335-44.

TWAYANA, K. S. & RAVANAN, P. 2018. Eukaryotic cell survival mechanisms: Disease relevance and therapeutic intervention. *Life Sciences,* 205**,** 73-90.

TZARTOS, J. S., FRIESE, M. A., CRANER, M. J., PALACE, J., NEWCOMBE, J., ESIRI, M. M. & FUGGER, L. 2008. Interleukin-17 production in central nervous system-infiltrating T cells and glial cells is associated with active disease in multiple sclerosis. *Am J Pathol,* 172**,** 146-55.

UDDIN, M., WATZ, H., MALMGREN, A. & PEDERSEN, F. 2019. NETopathic Inflammation in Chronic Obstructive Pulmonary Disease and Severe Asthma. *Front Immunol,* 10**,** 47.

VACCHELLI, E., MA, Y., BARACCO, E. E., SISTIGU, A., ENOT, D. P., PIETROCOLA, F., YANG, H., ADJEMIAN, S., CHABA, K., SEMERARO, M., SIGNORE, M., DE NINNO, A., LUCARINI, V., PESCHIAROLI, F., BUSINARO, L., GERARDINO, A., MANIC, G., ULAS, T., GÜNTHER, P., SCHULTZE, J. L., KEPP, O., STOLL, G., LEFEBVRE, C., MULOT, C., CASTOLDI, F., RUSAKIEWICZ, S., LADOIRE, S., APETOH, L., BRAVO-SAN PEDRO, J. M., LUCATTELLI, M., DELARASSE, C., BOIGE, V., DUCREUX, M., DELALOGE, S., BORG, C., ANDRÉ, F., SCHIAVONI, G., VITALE, I., LAURENT-PUIG, P., MATTEI, F., ZITVOGEL, L. & KROEMER, G. 2015. Chemotherapy-induced antitumor immunity requires formyl peptide receptor 1. *Science,* 350**,** 972-8.

VAN DEN BRINK, S. C., SAGE, F., VÉRTESY, Á., SPANJAARD, B., PETERSON-MADURO, J., BARON, C. S., ROBIN, C. & VAN OUDENAARDEN, A. 2017. Single-cell sequencing reveals dissociation-induced gene expression in tissue subpopulations. *Nat Methods,* 14**,** 935-936.

VARGA, A. W., JOHNSON, G., BABB, J. S., HERBERT, J., GROSSMAN, R. I. & INGLESE, M. 2009. White matter hemodynamic abnormalities precede sub-cortical gray matter changes in multiple sclerosis. *J Neurol Sci,* 282**,** 28-33.

VASEVA, A. V., MARCHENKO, N. D., JI, K., TSIRKA, S. E., HOLZMANN, S. & MOLL, U. M. 2012. p53 opens the mitochondrial permeability transition pore to trigger necrosis. *Cell,* 149**,** 1536-1548.

VASSALLO, A., WOOD, A. J., SUBBURAYALU, J., SUMMERS, C. & CHILVERS, E. R. 2019. The counter-intuitive role of the neutrophil in the acute respiratory distress syndrome. *Br Med Bull,* 131**,** 43-55.

VOLPE, J. J. 2012. Neonatal encephalopathy: an inadequate term for hypoxic-ischemic encephalopathy. *Ann Neurol,* 72**,** 156-66.

VOROBJEVA, N. V. & CHERNYAK, B. V. 2020. NETosis: Molecular Mechanisms, Role in Physiology and Pathology. *Biochemistry (Mosc),* 85**,** 1178-1190.

VOUSDEN, K. H. & PRIVES, C. 2009. Blinded by the light: the growing complexity of p53. *Cell,* 137**,** 413-431.

WADDELL, D. R. & DUFFY, K. T. 1986. Breakdown of self/nonself recognition in cannibalistic strains of the predatory slime mold, Dictyostelium caveatum. *J Cell Biol,* 102**,** 298-305.

WAJANT, H. 2002. The Fas signaling pathway: more than a paradigm. *Science,* 296**,** 1635-6.

WAKE, H., LEE, P. R. & FIELDS, R. D. 2011. Control of local protein synthesis and initial events in myelination by action potentials. *Science,* 333**,** 1647-51.

WANG, F., GÓMEZ-SINTES, R. & BOYA, P. 2018. Lysosomal membrane permeabilization and cell death. *Traffic,* 19**,** 918-931.

WANG, H., LU, Q., CHENG, S., WANG, X. & ZHANG, H. 2013. Autophagy activity contributes to programmed cell death in Caenorhabditis elegans. *Autophagy,* 9**,** 1975-82.

WANG, L., DU, F. & WANG, X. 2008. TNF-alpha induces two distinct caspase-8 activation pathways. *Cell,* 133**,** 693-703.

WANG, Y., DAWSON, V. L. & DAWSON, T. M. 2009. Poly(ADP-ribose) signals to mitochondrial AIF: a key event in parthanatos. *Exp Neurol,* 218**,** 193-202.

WARDLAW, J. M., SMITH, C. & DICHGANS, M. 2019. Small vessel disease: mechanisms and clinical implications. *Lancet Neurol,* 18**,** 684-696.

WEAVER, J. G., TARZE, A., MOFFAT, T. C., LEBRAS, M., DENIAUD, A., BRENNER, C., BREN, G. D., MORIN, M. Y., PHENIX, B. N. & DONG, L. 2005. Inhibition of adenine nucleotide translocator pore function and protection against apoptosis in vivo by an HIV protease inhibitor. *The Journal of clinical investigation,* 115**,** 1828-1838.

WEBB, J. D., MURÁNYI, A., PUGH, C. W., RATCLIFFE, P. J. & COLEMAN, M. L. 2009. MYPT1, the targeting subunit of smooth-muscle myosin phosphatase, is a substrate for the asparaginyl hydroxylase factor inhibiting hypoxia-inducible factor (FIH). *Biochem J,* 420**,** 327-33.

WEI, H. & YU, X. 2016. Functions of PARylation in DNA damage repair pathways. *Genomics, proteomics & bioinformatics,* 14**,** 131-139.

WEIDEMANN, A., KERDILES, Y. M., KNAUP, K. X., RAFIE, C. A., BOUTIN, A. T., STOCKMANN, C., TAKEDA, N., SCADENG, M., SHIH, A. Y., HAASE, V. H., SIMON, M. C., KLEINFELD, D. & JOHNSON, R. S. 2009. The glial cell response is an essential component of hypoxia-induced erythropoiesis in mice. *J Clin Invest,* 119**,** 3373-83.

WERNER, P., PITT, D. & RAINE, C. S. 2001. Multiple sclerosis: altered glutamate homeostasis in lesions correlates with oligodendrocyte and axonal damage. *Ann Neurol,* 50**,** 169-80.

WESTERHEIDE, S. D., ANCKAR, J., STEVENS, S. M., JR., SISTONEN, L. & MORIMOTO, R. I. 2009. Stress-inducible regulation of heat shock factor 1 by the deacetylase SIRT1. *Science,* 323**,** 1063-6.
WHITE, E., MEHNERT, J. M. & CHAN, C. S. 2015. Autophagy, Metabolism, and Cancer. *Clin Cancer Res,* 21**,** 5037-46.
WINTERBOURN, C. C. 1995. Toxicity of iron and hydrogen peroxide: the Fenton reaction. *Toxicol Lett,* 82-83**,** 969-74.
WITTE, M. E., GEURTS, J. J., DE VRIES, H. E., VAN DER VALK, P. & VAN HORSSEN, J. 2010. Mitochondrial dysfunction: a potential link between neuroinflammation and neurodegeneration? *Mitochondrion,* 10**,** 411-418.
WITTE, M. E., MAHAD, D. J., LASSMANN, H. & VAN HORSSEN, J. 2014. Mitochondrial dysfunction contributes to neurodegeneration in multiple sclerosis. *Trends in Molecular Medicine,* 20**,** 179-187.
WOLSWIJK, G. 1998. Chronic stage multiple sclerosis lesions contain a relatively quiescent population of oligodendrocyte precursor cells. *J Neurosci,* 18**,** 601-9.
WOOD, C. D., THORNTON, T. M., SABIO, G., DAVIS, R. A. & RINCON, M. 2009. Nuclear localization of p38 MAPK in response to DNA damage. *International journal of biological sciences,* 5**,** 428.
WOODRUFF, R. H., FRUTTIGER, M., RICHARDSON, W. D. & FRANKLIN, R. J. 2004. Platelet-derived growth factor regulates oligodendrocyte progenitor numbers in adult CNS and their response following CNS demyelination. *Mol Cell Neurosci,* 25**,** 252-62.
WRAY, S. Modelling neurodegenerative disease using brain organoids. Seminars in Cell & Developmental Biology, 2021. Elsevier, 60-66.
WU, G., FANG, Y.-Z., YANG, S., LUPTON, J. R. & TURNER, N. D. 2004. Glutathione Metabolism and Its Implications for Health. *The Journal of Nutrition,* 134**,** 489-492.
WU, J., RUTKOWSKI, D. T., DUBOIS, M., SWATHIRAJAN, J., SAUNDERS, T., WANG, J., SONG, B., YAU, G. D. & KAUFMAN, R. J. 2007. ATF6alpha optimizes long-term endoplasmic reticulum function to protect cells from chronic stress. *Dev Cell,* 13**,** 351-64.
WU, Y., ZHANG, J., YU, S., LI, Y., ZHU, J., ZHANG, K. & ZHANG, R. 2022. Cell pyroptosis in health and inflammatory diseases. *Cell Death Discovery,* 8**,** 191.
WUERFEL, J., BELLMANN-STROBL, J., BRUNECKER, P., AKTAS, O., MCFARLAND, H., VILLRINGER, A. & ZIPP, F. 2004. Changes in cerebral perfusion precede plaque formation in multiple sclerosis: a longitudinal perfusion MRI study. *Brain,* 127**,** 111-9.
XIE, C., LIU, Y.-Q., GUAN, Y.-T. & ZHANG, G.-X. 2016. Induced stem cells as a novel multiple sclerosis therapy. *Current stem cell research & therapy,* 11**,** 313-320.
YAMAMOTO, H. & MATSUI, T. 2023. Molecular mechanisms of macroautophagy, microautophagy, and chaperone-mediated autophagy. *Journal of Nippon Medical School,* advpub.
YAMASHITA, T., MIYAMOTO, Y., BANDO, Y., ONO, T., KOBAYASHI, S., DOI, A., ARAKI, T., KATO, Y., SHIRAKAWA, T. & SUZUKI, Y. 2017. Differentiation of oligodendrocyte progenitor cells from dissociated monolayer and feeder-free cultured pluripotent stem cells. *PLoS One,* 12**,** e0171947.
YAN, X., ZHOU, R. & MA, Z. 2019. Autophagy-Cell Survival and Death. *Adv Exp Med Biol,* 1206**,** 667-696.
YANG, J., ZHOU, R. & MA, Z. 2019. Autophagy and Energy Metabolism. *Adv Exp Med Biol,* 1206**,** 329-357.
YANG, J. H., REMPE, T., WHITMIRE, N., DUNN-PIRIO, A. & GRAVES, J. S. 2022. Therapeutic Advances in Multiple Sclerosis. *Front Neurol,* 13**,** 824926.
YANG, W. S. & STOCKWELL, B. R. 2016. Ferroptosis: death by lipid peroxidation. *Trends in cell biology,* 26**,** 165-176.
YAQUBI, M., LUO, J. X. X., BAIG, S., CUI, Q. L., PETRECCA, K., DESU, H., LAROCHELLE, C., AFANASIEV, E., HALL, J. A., DUDLEY, R., SROUR, M., HAGLUND, L., OUELLET, J., GEORGIOPOULOS, M., SANTAGUIDA, C., SONNEN, J. A., HEALY, L. M., STRATTON, J. A., KENNEDY, T. E. & ANTEL, J. P.

2022. Regional and age-related diversity of human mature oligodendrocytes. *Glia,* 70**,** 1938-1949.
YERMAKOV, L. M., HONG, L. A., DROUET, D. E., GRIGGS, R. B. & SUSUKI, K. 2019. Functional Domains in Myelinated Axons. *Adv Exp Med Biol,* 1190**,** 65-83.
YEUNG, M. S., DJELLOUL, M., STEINER, E., BERNARD, S., SALEHPOUR, M., POSSNERT, G., BRUNDIN, L. & FRISÉN, J. 2019a. Oligodendrocyte generation dynamics in multiple sclerosis. *Nature,* 566**,** 538.
YEUNG, M. S. Y., DJELLOUL, M., STEINER, E., BERNARD, S., SALEHPOUR, M., POSSNERT, G., BRUNDIN, L. & FRISÉN, J. 2019b. Dynamics of oligodendrocyte generation in multiple sclerosis. *Nature,* 566**,** 538-542.
YIN, X., CRAWFORD, T. O., GRIFFIN, J. W., TU, P., LEE, V. M., LI, C., RODER, J. & TRAPP, B. D. 1998. Myelin-associated glycoprotein is a myelin signal that modulates the caliber of myelinated axons. *J Neurosci,* 18**,** 1953-62.
YOULE, R. J. & STRASSER, A. 2008. The BCL-2 protein family: opposing activities that mediate cell death. *Nature Reviews Molecular Cell Biology,* 9**,** 47-59.
YU, H., PARDOLL, D. & JOVE, R. 2009. STATs in cancer inflammation and immunity: a leading role for STAT3. *Nature reviews cancer,* 9**,** 798-809.
YU, L., CHEN, Y. & TOOZE, S. A. 2018. Autophagy pathway: Cellular and molecular mechanisms. *Autophagy,* 14**,** 207-215.
YU, S. W., WANG, H., DAWSON, T. M. & DAWSON, V. L. 2003. Poly(ADP-ribose) polymerase-1 and apoptosis inducing factor in neurotoxicity. *Neurobiol Dis,* 14**,** 303-17.
YU, X., JI, C. & SHAO, A. 2020. Neurovascular Unit Dysfunction and Neurodegenerative Disorders. *Front Neurosci,* 14**,** 334.
ZAMZAMI, N., HAMEL, C. E., MAISSE, C., BRENNER, C., MUÑOZ-PINEDO, C., BELZACQ, A.-S., COSTANTINI, P., VIEIRA, H., LOEFFLER, M. & MOLLE, G. 2000. Bid acts on the permeability transition pore complex to induce apoptosis. *Oncogene,* 19**,** 6342-6350.
ZANNINI, L., DELIA, D. & BUSCEMI, G. 2014. CHK2 kinase in the DNA damage response and beyond. *Journal of molecular cell biology,* 6**,** 442-457.
ZAPPIA, L. & OSHLACK, A. 2018. Clustering trees: a visualization for evaluating clusterings at multiple resolutions. *Gigascience,* 7.
ZAWADZKA, M., RIVERS, L. E., FANCY, S. P., ZHAO, C., TRIPATHI, R., JAMEN, F., YOUNG, K., GONCHAREVICH, A., POHL, H. & RIZZI, M. 2010a. CNS-resident glial progenitor/stem cells produce Schwann cells as well as oligodendrocytes during repair of CNS demyelination. *Cell stem cell,* 6**,** 578-590.
ZAWADZKA, M., RIVERS, L. E., FANCY, S. P., ZHAO, C., TRIPATHI, R., JAMEN, F., YOUNG, K., GONCHAREVICH, A., POHL, H., RIZZI, M., ROWITCH, D. H., KESSARIS, N., SUTER, U., RICHARDSON, W. D. & FRANKLIN, R. J. 2010b. CNS-resident glial progenitor/stem cells produce Schwann cells as well as oligodendrocytes during repair of CNS demyelination. *Cell Stem Cell,* 6**,** 578-90.
ZECCA, L., YOUDIM, M. B., RIEDERER, P., CONNOR, J. R. & CRICHTON, R. R. 2004. Iron, brain ageing and neurodegenerative disorders. *Nat Rev Neurosci,* 5**,** 863-73.
ZEINSTRA, E., WILCZAK, N. & DE KEYSER, J. 2000. [3H]dihydroalprenolol binding to beta adrenergic receptors in multiple sclerosis brain. *Neurosci Lett,* 289**,** 75-7.
ZEIS, T., GRAUMANN, U., REYNOLDS, R. & SCHAEREN-WIEMERS, N. 2008. Normal-appearing white matter in multiple sclerosis is in a subtle balance between inflammation and neuroprotection. *Brain,* 131**,** 288-303.
ZHANG, C., SUSUKI, K., ZOLLINGER, D. R., DUPREE, J. L. & RASBAND, M. N. 2013. Membrane domain organization of myelinated axons requires βII spectrin. *J Cell Biol,* 203**,** 437-43.

ZHANG, C. X., CHENG, Y., LIU, D. Z., LIU, M., CUI, H., ZHANG, B. L., MEI, Q. B. & ZHOU, S. Y. 2019a. Mitochondria-targeted cyclosporin A delivery system to treat myocardial ischemia reperfusion injury of rats. *J Nanobiotechnology,* 17**,** 18.

ZHANG, F., WU, Y. & TIAN, W. 2019b. A novel approach to remove the batch effect of single-cell data. *Cell Discov,* 5**,** 46.

ZHANG, G., WANG, X., ROTHERMEL, B. A., LAVANDERO, S. & WANG, Z. V. 2022. The integrated stress response in ischemic diseases. *Cell Death & Differentiation,* 29**,** 750-757.

ZHAO, C., LI, W. W. & FRANKLIN, R. J. 2006. Differences in the early inflammatory responses to toxin-induced demyelination are associated with the age-related decline in CNS remyelination. *Neurobiol Aging,* 27**,** 1298-307.

ZHAO, F., MANCUSO, A., BUI, T. V., TONG, X., GRUBER, J. J., SWIDER, C. R., SANCHEZ, P. V., LUM, J. J., SAYED, N., MELO, J. V., PERL, A. E., CARROLL, M., TUTTLE, S. W. & THOMPSON, C. B. 2010. Imatinib resistance associated with BCR-ABL upregulation is dependent on HIF-1alpha-induced metabolic reprograming. *Oncogene,* 29**,** 2962-72.

ZHAO, Y. G., CODOGNO, P. & ZHANG, H. 2021. Machinery, regulation and pathophysiological implications of autophagosome maturation. *Nat Rev Mol Cell Biol,* 22**,** 733-750.

ZHIVOTOVSKY, B. & ORRENIUS, S. 2011. Calcium and cell death mechanisms: A perspective from the cell death community. *Cell Calcium,* 50**,** 211-221.

ZHOU, H., WANG, B., SUN, H., XU, X. & WANG, Y. 2018. Epigenetic regulations in neural stem cells and neurological diseases. *Stem Cells International,* 2018.

ZHU, C., WANG, X., XU, F., BAHR, B. A., SHIBATA, M., UCHIYAMA, Y., HAGBERG, H. & BLOMGREN, K. 2005. The influence of age on apoptotic and other mechanisms of cell death after cerebral hypoxia-ischemia. *Cell Death Differ,* 12**,** 162-76.

ZONCU, R., EFEYAN, A. & SABATINI, D. M. 2011. mTOR: from growth signal integration to cancer, diabetes and ageing. *Nature Reviews Molecular Cell Biology,* 12**,** 21-35.